UNIVERSITA' DEGLI STUDI DI PAVIA

Dipartimento di Biologia e Biotecnologie "Lazzaro Spallanzani"

An RNA map of Nova2-regulated alternative splicing in endothelial cells

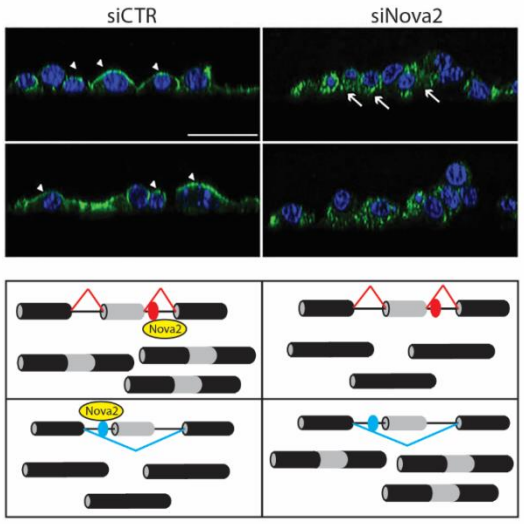

Tutors:
Dr. Claudia Ghigna
Prof. Antonio Torroni

Istituto di Genetica Molecolare-Consiglio Nazionale delle Ricerche (IGM-CNR)

Di Matteo Anna
Dottorato di Ricerca in
Genetica, Biologia Molecolare e Cellulare
XXIX Ciclo – A.A. 2013-2016

UNIVERSITA' DEGLI STUDI DI PAVIA

Dipartimento di Biologia e Biotecnologie "Lazzaro Spallanzani"

An RNA map of Nova2-regulated alternative splicing in endothelial cells

Tutors:
Dr. Claudia Ghigna
Prof. Antonio Torroni

Istituto di Genetica Molecolare-Consiglio Nazionale delle Ricerche (IGM-CNR)

Di Matteo Anna
Dottorato di Ricerca in
Genetica, Biologia Molecolare e Cellulare
XXIX Ciclo – A.A. 2013-2016

ABSTRACT

Alternative splicing (AS) generates different mRNAs leading to production of protein isoforms with different functional properties. Since more than 90% of the human genes undergo AS, it plays a major role in the generation of human proteomic diversity. There is now ample evidence that just as AS is important for normal physiology, so altered AS is important for cancer. Altered AS in tumors is frequently due to changes in the levels of AS regulators leading to combined disruption of tumor suppressor genes and activation of oncoproteins involved in tumor establishment, progression and in resistance to therapeutic treatments.

Angiogenesis, the growth of new blood vessels from pre-existing vasculature, plays a crucial role in tumor development by allowing oxygen and nutrients to reach proliferating cancer cells. In recent years, angiogenesis has been deeply investigated because its inhibition represents a promising anti-cancer therapeutic modality. However, all attempted strategies to date have shown modest therapeutic effects indicating that tumor angiogenesis is a more complex phenomenon than previously anticipated. Hence, a better understanding of the mechanisms sustaining growth of tumor vessels will be crucial to identify novel and effective anti-angiogenic therapies for cancer treatment.

Traditionally, the molecular pathways involved in angiogenesis have been suggested to act primarily through regulation of transcription. Recently, the emphasis on crucial events of gene expression is changing, as many post-transcriptional programs cooperate to promote vascular development. For the first time, our group found that the formation of vascular lumen during angiogenesis is controlled at post-transcriptional level by the AS factor Nova2, previously considered neural cell-specific. Through AS of target exons affecting the Par complex and its regulators, Nova2 controls the establishment of endothelial cell polarity, a prerequisite for vascular lumen organization. Consequently, Nova2 *in vivo* ablation causes vascular lumen formation defects, reminiscent of aberrant morphology of the tumor vasculature.

By performing RNA-Seq of Nova2 depleted or overexpressing endothelial cells (ECs), I identified novel Nova2-mediated AS exons belonging to factors involved in angiogenesis or vascular development suggesting that Nova2 controls an essential layer of vascular gene expression regulation.

Among the novel identified Nova2 targets in ECs there is *Ptbp2*, an AS factor until now considered restricted to brain and testis. Notably, I demonstrated that Nova2 functions to repress Ptbp2 expression in ECs by promoting skipping of *Ptbp2* exon 10 leading to the production of a *Ptbp2* transcript degraded by the NMD (Non-sense Mediated mRNA Decay) pathway. Importantly, I found that Nova2

dependent AS regulation of *Ptbp2* is specifically conserved in zebrafish endothelium. Collectively, my results reveal a hierarchy of splicing factors that integrate splicing decisions during angiogenesis.

ABBREVIATIONS

AJ: Adherens Junction
AS: Alternative Splicing
AS-NMD: AS -activated Nonsense-Mediated mRNA Decay
ASO: Antisense Oligonucleotide
BBB: Blood Brain Barrier
BM: Basement membrane
CHX: Cyclohexamide
CLIP: UV Cross-Linking and Immunoprecipitation
CNS: Central Nervous System
EC: Endothelial Cell
ECM: Extracellular Matrix
EJC: Exon Junction Complex
EMT: Epithelial-to-Mesenchymal Transition
GAP: GTPase Activating Protein
GEF: Guanine nucleotide Exchange Factor
hnRNP: heterogeneous nuclear ribonucleoprotein
iCLIP: individual-nucleotide resolution CLIP
NISE/NISS: Nova intronic splicing enhancer/silencer
NT: nucleotide
PAR-CLIP: photoactivatable ribonucleoside–enhanced crosslinking and immunoprecipitation
POMA: Paraneoplastic Opsoclonus-Myoclonus Ataxia
PTC: Premature Termination Codon
RBP: RNA Binding Protein
RBD: RNA Binding Domain
snRNA: small nuclear RNA
SR: serine-arginine rich protein
SRF: Splicing Regulatory Factor
TJ: Tight Junction
UTR: Untranslated Region
vSMC: vascular Smooth Muscle Cell

INTRODUCTION

1. Introduction

It was in 1977 that Richard J. Roberts and Phillip A. Sharp independently discover that eukaryotic genes have a "splitted nature", with several segments of coding DNA, called exons, interspersed in much longer non-coding sequences, named introns. This discovery led to identify a process (splicing or the removal of introns) fundamental for expressing the genetic information and that has changed our view on how genes in higher organisms develop during the course of evolution.
In general, in eukaryotic genes the size of introns varies from 100 to 100,000 nt, while the exon size is typically between 50-250 nt [1]. Notably, higher eukaryotes have a greater percentage of genes containing introns [1] than lower eukaryotes and their introns have a tendency to be larger [2]. The typical human gene contains an average of 8 exons. However, there are some exceptions such as the *Dystrophin* gene, which contains 70 introns (it generates the longest primary transcript with 2.4 million nt), and the *α-interferon* gene does not contain introns.
Eukaryotic protein-coding genes are transcribed in the nucleus by Polymerase II giving rise to heterogeneous nuclear RNAs, a subset of which consists of primary transcripts (pre-mRNAs), which are processed in mature messenger mRNAs then transported into the cytoplasm to be translated into proteins [3]. Unlike prokaryotic mRNAs, eukaryotic pre-mRNAs undergo extensive modifications after synthesis. In addition to splicing, this complex process of maturation includes: 5'-end capping and 3'-end cleavage/polyadenylation [4]. All these events take place within the nucleus either co-transcriptionally or immediately after transcription and have important roles for the correct localization, stability and translation of the mRNA [5].
The discovery of "split genes" has had fundamental consequences for basic research in biology as well as for applied research concerning several human diseases.

1.1 The splicing reaction

Splicing is the nuclear processing mechanism by which introns are removed from the primary pre-mRNA transcripts and exons are joined together in order to generate mature mRNAs and to reconstitute the correct reading frame of the resulting proteins [6]. This cut-and-paste reaction is directed by moderately conserved, short consensus sequences located at intron-exon boundaries [6]. These "core splicing signals", able to differentiate an exon from an intron and guide the "exon definition" process [7], are (Fig. 1):
- the 5' splice site (5' ss) or "donor site" that in mammals is AG|**GU**RAGU (R for purine, | for splice site and bold for the dinucleotide 5' intron boundary);
- the 3' splice site (3' ss) or "acceptor site" Y**AG**|G (Y for pyrimidine, | for splice site, bold for the dinucleotides 3' intron boundary);

- the branch point sequence (BPS) located 18-40 nt upstream of the 3' ss and with consensus sequence YNYUR**A**Y (N for any nucleotide, A for adenosine of the branch point),
- in higher organisms, a polypyrimidin tract (PPT) of variable length (10-30 nt) upstream of the 3' ss is also common.

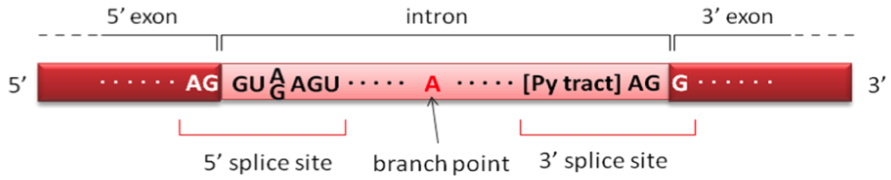

Fig. 1. Core splicing signals. *Cis*-acting consensus sequences at exon-intron boundaries are used by the spliceosome for the cut-and-paste reaction (two sequential trans-esterifications) that removes the intron. These short, poorly conserved elements of a typical eukaryotic gene are: the 5' splice site (5' ss or "donor site"), the 3' splice site (3' ss or "acceptor site"), the branch site and the polypyrimidine (Py) tract.

To ensure the specific properties of cells and tissues, splicing must be quick and accurate, a very challenging task considering that introns are typically much larger than exons. Splicing fidelity is achieved through pre-mRNAs *cis-acting* elements that discriminate exons from introns, direct the splicing machinery to the intron-exon boundaries and act as binding sites for the factors that regulate splicing ("splicing code").
The splicing reaction consists of two sequential transesterification reactions [6] (Fig. 2). In the first reaction, a nucleophilic attack of the 2' -OH group of the A residue within the branch point to the phosphate of the G within the 5' ss generates two intermediates: an exon (with a new free 3' -OH) and the intron connected to the second exon in a lariat-shaped structure (Fig. 2). In the second transesterification reaction, the newly released 3' -OH of the first exon attacks the phosphoryl group at the 3' ss of the second exon leading to ligation of the two exons, while the intervening intron in lariat configuration is released and then degraded [8] (Fig. 2).

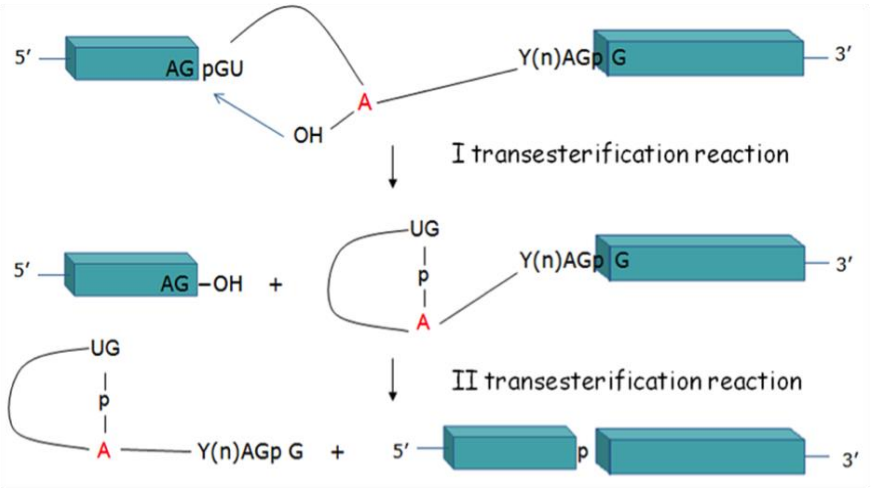

Fig. 2. Schematic representation of the splicing reaction. Two exons (blue boxes) are separated by an intron (line). The consensus sequences in metazoans at the 5' ss, branch point and splice site are indicated (Y is a pyrimidine). The cross-intron assembly and disassembly cycle of the major spliceosome catalyzes two transesterification reactions leading to the joining of the two exons and to the removal of the intron as a "lariat". See text for details.

Splicing reactions are catalyzed by a large ribonucleoprotein (RNP) complex known as spliceosome. The spliceosome, the most complex macromolecular machines so far described in the cells and containing many as 300 distinct proteins and five RNAs, is characterized by highly plasticity and flexibility of conformation and composition [8,9] (Fig. 3). It is generated by the assembly of small nuclear ribonucleoproteins particles (snRNPs, U1, U2, U5, and U4/U6) and several non-snRNP factors. Each snRNP consists of a uridine-rich small nuclear RNA (snRNA), a common set of seven Sm proteins (B/B′, D3, D2, D1, E, F, and G) and a variable number of complex-specific proteins [8]. According to the most accepted model [10], the spliceosome assembly occurs by the stepwise interaction of snRNP components with the pre-mRNA.

At first, the U1 snRNP binds to the 5' ss, followed by binding of splicing factor 1 (SF1) to the BPS and binding of the U2 auxiliary factor (U2AF) heterodimer at the PPT to form the E complex. This early or commitment complex defines the intron boundaries. Next, U2 snRNP replaces SF1 at the BPS leading to the formation of the complex A. The pre-catalytic complex B is then generated by the entry of the pre-assembled tri-snRNP consisting of U4, U5 and U6 snRNPs. The catalytic activation of the B complex is characterized by several conformational and compositional rearrangements, including the dissociation of U1 and U4 snRNPs that is required for carry out the first transesterification reaction. These changes generate the C complex, which undergoes additional rearrangements to complete the second catalytic reaction [8]. Finally, the mature mRNA is released, while the spliceosome dissociates and snRNPs enter in a new round of splicing.

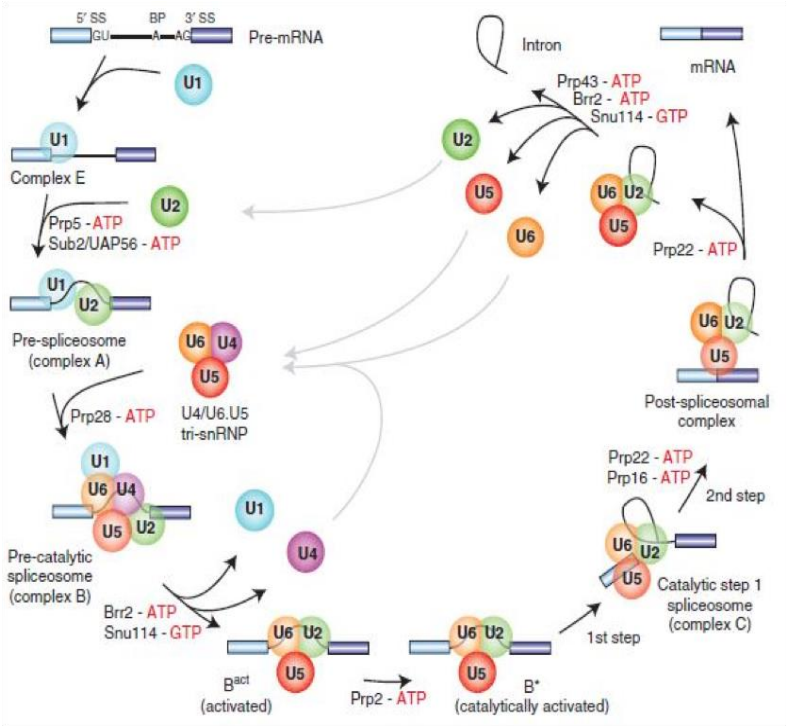

Fig. 3. The spliceosome cycle. The complex and sequential interactions of ribonucleoproteins and non-snRNP splicing factors that assemble in a step-wise manner on the nascent pre-mRNA is depicted. At the end of the catalysis these factors are released and are ready to start a new cycle of splicing. Other enzymes, such as RNA-dependent ATPases/helicases, which catalyze RNA-RNA rearrangements and ribonucleoproteins remodeling events at specific steps of the splicing cycle are also indicated. Modified from [10].

1.2 Alternative splicing

Alternative splicing (AS) is the molecular mechanism by which the removal of introns and the different inclusion or exclusion of exons generate multiple distinct mRNAs from a single gene [11]. This process produces functionally different proteins or, through AS of UTRs, different mRNAs with diverse localization, stability, as well as efficiency of translation.
The first example of AS was discovered in mammalian in the early 1980s, when membrane-bound and secreted forms of antibodies were demonstrated to be encoded by the same gene [12]. This observation has had a profound impact on biologists' thinking leading to the revision of the central dogma of modern molecular biology "one gene-one protein". However, since its discovery, a large number of genes that are alternatively spliced in tissue-specific, developmentally-regulated and signal-dependent manner has been reported [13] and this number is constantly increasing. More recently, microarrays and high-throughput sequencing analyses showed that AS is more prominent in complex tissues with several cell types, such as

testis and nervous system and among genes involved in regulatory functions [11].

The existence of AS process has evolutionary implications since it explains the discrepancy between the number of protein-coding genes and organism complexity. For example, our genome contains only 20.000 - 25.000 genes (International Human Genome Sequencing Consortium 2004 [14], a number similar to those of less complex organisms, such as the fruit fly *Drosophila melanogaster* (14.000 genes) [15] and the nematode *Caenorhabditis elegans* (19.000 genes) [16]. Importantly, the number of gene undergoing AS increases with the complexity of the organism. Thus, more than 90% of human multiexonic genes undergo AS, while the current estimate of AS is of about 13% in *C. elegans* and 40% in *D. melanogaster*, respectively [17,18]. These observations suggest that AS is one of the main sources of proteomic diversity in multicellular eukaryotes. In addition, it has been reported that AS and transcription predominantly regulate different subsets of genes [19,20]. AS thus provides a versatile, additional layer of regulation to generate the molecular and cellular complexity of different cell and tissue types.

At the molecular level, five distinct AS schemes have been reported [6] (Fig. 4).

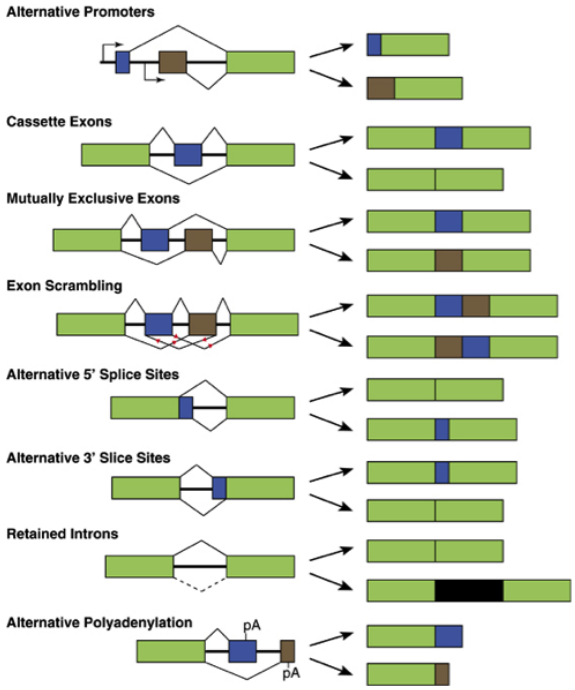

Fig. 4. Different schemes of AS mechanisms. While constitutive exons (green boxes) are always present in the mature transcript, AS exons (blue or brown boxes) frequently can be either included or skipped from the mature transcript (exon skipping). Intron retention, usage of alternative 3'- or 5' ss and selection of mutually exclusive exons are other possible mechanisms of AS. Alternative promoter usage and alternative polyadenylation are less frequent events. Modified from [21].

The most common type of AS in higher eukaryote (nearly the 40% of all AS events) [22], is the exon skipping, in which an "exon cassette" can be either included or excluded from the mRNA. The use of alternative 5' or 3' ss, in which exons can be extended or shortened in length, represents the 18,4% and 7,9% of all AS events in higher eukaryotes, respectively [22]. In rare case (5% in vertebrates and invertebrates (plants)), the excision of an intron is suppressed, (intron retention). Other less frequent events of AS are the so-called multiple cassette exons that are mutually exclusive (i.e. the mature mRNA always contains only one of several possible exon choices). Finally, alternative promoters and poly-adenylation sites contribute to the heterogeneity of transcripts generated from a single gene. In addition to modify protein features, AS can also affect the stability of transcripts through the Nonsense-Mediated mRNA Decay (NMD) pathway, a surveillance pathway that exists in all eukaryotes and that degrades transcripts containing premature stop codons.

1.3 Alternative splicing regulation

AS exons are characterized by short and degenerated splice site that are not sufficient to trigger exon definition. Thus, the main cause of AS is the intrinsic weakness of these sites that leads to reduced affinity for spliceosomal components. The recognition of AS exons is ensured by an additional layer of information provided by *cis*-acting sequences and *trans*-acting factors. *Cis*-acting sequences are non-splice site short sequences (around 10 nt) located in proximity of an AS exon. On the basis of their position and model of action, they have been classified in the exonic or intronic splicing enhancers (ESEs or ISEs) and the exonic or intronic splicing silencers (ESSs or ISSs) that, respectively, promote and inhibit exon recognition by the spliceosome [7,23] (Fig. 5).

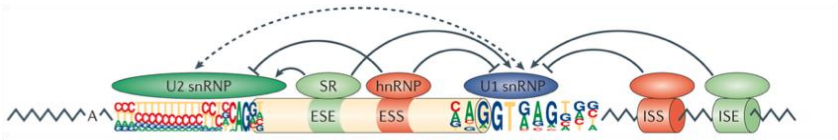

Fig. 5. *Cis*-acting sequences. Splicing enhancers and silencers can be located in exons (ESE and ESS) or in introns (ISE and ISE) and they are able to allow or inhibit the recognition of the splice sites by RNPs of the spliceosome (U2 snRNP and U1 snRNP). ESE elements are bound by splicing factors of the SR family. In addition, SR factors can counteract the inhibitory activity of hnRNP proteins bound to ESS or ISS elements. Modified from [24].

The best-characterized splicing enhancers are typically purine-rich and are the binding sites for serine-arginine (SR) factors, while silencers are mainly bound by hnRNP (heterogeneous nuclear ribonucleoprotein) factors. SR proteins are a family of RNA-binding proteins (RBPs) highly conserved in animal and plant cells [25]. These factors take their name from the characteristic C-terminal arginine-serine-rich domain (RS domain) involved in protein-protein interactions during constitutive and alternative

splicing reaction, as well as in other aspects of RNA metabolism [26], whereas the binding specificity is conferred by one or two N-terminal RNA-binding domains (RBDs or RRMs, RNA recognition motifs) [27]. The family comprises about 12 proteins, which range from 20 to 75 kDa in size, characterized by similar modular structure and recently classified with the new nomenclature SRSF (Serine/Arginine rich Splicing Factor) from 1 to 12 [27]. Two models have been proposed to explain the mechanism by which SR proteins promote exon inclusion during AS reactions. According to the "recruitment model", ESE-bound SR directly recruits components of the spliceosome machinery through specific protein-protein interactions mediated by the RS domain (for example stabilizing the binding of U1 snRNP at the 5' ss and U2AF65 at the 3' ss). Another model ("inhibitor model") suggests that SR proteins are able to antagonize the activity of an adjacent negative ESS element bound to an hnRNP repressor protein [28].
Unlike the enhancer sequence, splicing silencer elements identified to date seem remarkably diverse and they are the binding sites for factors that block access of the splicing machinery to a splice site. Among the RBPs interacting with the splicing silencer elements there are hnRNPs, the most abundant proteins in the nucleus of higher eukaryotes [29]. Structurally, similar to SR proteins, hnRNPs are characterized by a modular structure with one or more RBDs (usually at the N-terminus), connected through linker regions to one or more auxiliary domains that mediate protein-protein interactions or regulate their cellular localization [29]. Three types of RNA binding domains have been identified in hnRNP proteins: RRM (RNA recognition motif), hnRNP K homology domain (a protein domain that was first identified in the human hnRNP K) and RGG domain, a protein region rich in Arg-Gly-Gly repetitions [30]. In addition to a structural role, important to protect RNAs from degradation (similar to the model for the packaging of DNA by histones), hnRNPs have also specific (active) functions in several steps of RNA metabolism, such as mRNA nuclear export, stability and translation [31], and in a variety of biological processes (DNA maintenance and repair, chromatin remodeling and transcription) [32–34]. During splicing reaction, the mechanism of hnRNPs action depends on the position of their binding sites along the pre-mRNA [1,35]; hnRNPs can directly compete with the binding of SR factors on adjacent splicing regulatory elements ("inhibitory model") or multimerize on the pre-mRNA and displace ESE-bound SR factors ("multimerization and cooperative binding"). Also, hnRNPs bound to ISSs, flanking an alternative exon, lead to the formation of a loop that hides the exon and impairs its recognition by the spliceosome machinery ("looping out").

1.4 Nova proteins

In the vast majority of cases, splicing factors (SR and hnRNPs) are ubiquitously expressed and tissue-specific AS events are the result of differences in the concentration and/or activity of these proteins [36]. In line with this, large-scale computational analysis showed that changes in the

expression levels of splicing regulators ("splicing factor signatures") correlate with tissue-specific AS profiles [37].

Several cell- or tissue-specific AS regulators have been identified and most of them are enriched in nervous system and muscle tissues, including Nova1/2 proteins, Ptbp2, Fox1/2/3, Muscleblind proteins (Mbnl1, Mbnl2 and Mbnl3), Hu proteins, TIA1/TIAR, nSR100/SRRM4 and members of the CELF/BRUNOL and ELAVL families [38–40]. Interestingly, compared to other tissues, mammalian nervous system shows high levels of tissue-specific AS regulation and AS events detected in the brain are more highly conserved [41]. These observations suggest that AS plays fundamental roles during neural development [42]. Indeed, by increasing (rapidly and efficiently) proteome diversity, AS is a critical modulator of complex neuronal processes, such as synaptic plasticity [43].

The Nova (neuro-oncological ventral antigen) family consists of two RNA-binding proteins, Nova1 and Nova2, originally identified as factors recognized by antibodies produced in patients with paraneoplastic opsoclonus myoclonus ataxia (POMA), a type of diseases at the intersection of neurobiology, immunology, and oncology [44]. In particular, POMA patients are characterized by latent cancer (frequently gynecologic or lung tumor) and develop antibodies against antigens, expressed both by their tumors and by neurons of the central nervous system (CNS) ("onconeural antigens", i.e Nova proteins), which recognize and inhibit neuronal proteins, thus affecting the function of the motor nervous system [44]. However, Nova proteins show mutually exclusive expression within the CNS. Indeed, Nova2 is highly expressed in the neurons of neocortex and hippocampus of the postnatal mouse brain, whereas Nova1 is specifically expressed in hypothalamus, ventral midbrain, hindbrain and spinal cord [45,46]. In addition, cortical Nova2 expression level increases from neuronal progenitor cells to differentiated neurons [46].

Nova proteins share high sequence homology with 75% of amino acid identity [45]. Moreover, they are homologous to the RNA-binding protein hnRNP K, since they harbor three KH-type RNA binding domains with a higher aminoacidic identity (from 87% to 93%) [47]. In addition, these splicing factors are characterized by indistinguishable biochemical properties; indeed, through the third KH domain (KH3), they are able to contact pre-mRNAs in correspondence of YCAY motifs (or "YCAY cluster" in which Y= pyrimidine) and the final outcome of the splicing reaction depends on the position of these binding sites on the targets (defined as "RNA map") [48]. In particular, Nova proteins act as silencer of splicing when bind to YCAY clusters upstream or within an AS exon (within 200 nt of distance from the splice site); in this case exon skipping is achieved by preventing the association of U1 snRNP with the 5' ss. On the contrary, Nova proteins function as enhancer of splicing when bound to intronic sequences located downstream the AS exon by favoring spliceosome assembly and, as a consequence, exon inclusion [48].

Nova proteins are phylogenetically conserved among vertebrate species, with the aminoacid sequence of Nova2 KH domain 94% identical between zebrafish and mouse orthologues [49]. Moreover, the RNA-binding specificity

and regulatory activity of Nova orthologs apparently have been preserved throughout evolution [50,51]. *Nova1* null mice provided the first model for understanding the dysfunction of the motor nervous system in POMA patients [52]. They were born phenotypically identical to wild type littermates, but subsequently they appeared smaller, showing action-induced tremulousness and overt motor weakness associated to an increased apoptotic death of motor neurons in the spinal cord and brainstem and died an average of 7–10 days after birth [52]. Interestingly, *Nova1* null mice presented alterations in the AS profile of neuronal transcripts, for example glycine receptor α2 gene (GlyRα2) and neuronal ionotropic receptor, GABAA Rγ2, encoding for inhibitory receptors [52]. Recently, *Nova2* null mice were also generated (Saito et al. 2016). Similarly to *Nova1* null mice, *Nova2-/-* mice were born alive, but failed to thrive, demonstrating progressive motor dysfunction and overt motor weakness, and they died an average of 14-18 postnatal days [46]. Interestingly, *Nova2-/-* but not *Nova1-/-* displayed several peculiar phenotype, such as agenesis of the corpus callosum, alterations of the axon outgrowth of the ventral motoneurones and reduced efferent innervations of the cochlea [46] (see also below).

Finally, also *Nova1/Nova2* double knockout mice (DKO) were generated and characterized; due to motor–neuronal dysfunctions, these mice were paralyzed, failed to cluster acetylcholine receptors at the neuromascular junction (NMJ) and showed defective neuromuscular synapses [53]. Interestingly, Nova-dependent regulation of *Agrin* splicing was found to have important consequence on NMJ development [53].

The characterization of the functional role of Nova proteins during neural development was significantly facilitated by advances in biochemical (cross-linking and immunoprecipitation, CLIP) and bioinformatic approaches. In CLIP experiment, an RBP is immunoprecipitated after UV cross-linking from a cell lysate, followed by purification of associated RNA [48]. Additional adjustments of the original protocol were introduced in order to specifically improve its resolution [54,55]. In particular, when coupled with microarray or high-throughput sequencing (RNA-Seq) this technique allowed to identify transcriptome-wide binding sites associated with a specific AS factor [56]. Notably, by using splicing sensitive microarrays [57] and CLIP approach [57,58], Ule and colleagues found that Nova proteins modulate a significant fraction (around 7%) of all AS events in the brain; in particular, several of these pre-mRNAs encode for regulators of the synaptic development and/or activity (including neurotransmitter receptors, cation channels, adhesion and scaffold proteins) [57]. Remarkably, these proteins interact one to each other in the synapse suggesting that Nova control a multilayer network and that Nova-mediated AS plays an important role in affecting physical interactions between these factors during neural development [57,59] (Fig. 6).

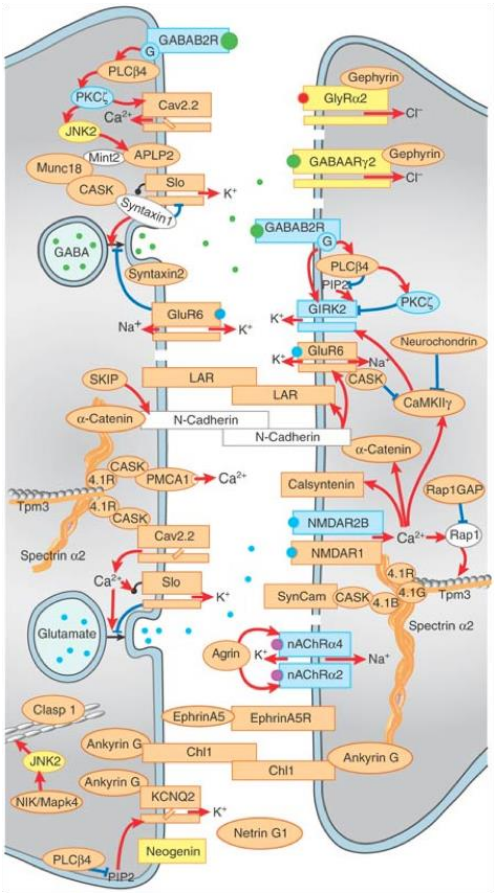

Fig. 6. Nova proteins regulate AS of pre-mRNAs encoding proteins interacting in the synapse. Pre-mRNA targets of Nova proteins were identified by different experimental approach. Validated targets identified by the microarray are shown in orange, proteins encoded by RNAs identified by Nova CLIP tags are shown in blue; targets identified by combined biochemical and genetic studies are shown in yellow. Positive (red arrow) or negative (blue bars) interactions among the different elements of the network are shown. Modified from [57].

Recently, by performing an *in vivo* RNAi screening, Nova proteins were identified as important regulators of neuronal migration and axon guidance in the spinal cord [60]. In particular, *Nova1/Nova2* DKO were found to show severe defects in the migration of the spinal cord interneurons and their progenitors and to disturb the axon outgrowth and guidance of the commissural interneurons [60]. Importantly, these phenotypic defects were similar to that observed in the knockout of *Dcc*, a receptor involved in guiding the axons to the correct location during developing of the nervous system [60]. Interestingly, AS of *Dcc* is controlled by Nova proteins that are able to promote the production of a longer isoform (DccL, containing exon 17). *Dcc* AS was disrupted in Nova DKO, whereas neural defects were rescued by specific over-expression of DccL, suggesting that Nova play crucial functions in the development of commissural neurons [60].

The RNA-binding properties of Nova proteins suggest that they could regulate common RNA targets. However, the recent detailed characterization of *Nova1* or *Nova2* null mice revealed that some actions are unique to Nova2 (but not to Nova1) and these proteins control different regulatory networks in developing cortical neurons [46]. In particular, high-throughput sequencing and crosslinking immunoprecipitation (HITS-CLIP) of total RNA extracted from cortex of *Nova1-/-* and *Nova2-/-* mice showed that Nova2 (but not Nova1) presented alteration of the AS profile of several guidance related genes, i.e *Dcc, Slit2, Robo2, Neo1* [46]. These findings suggested that Nova2 uniquely regulates AS of a coordinated set of pre-mRNAs encoding for essential components of the axon guidance pathway during neural differentiation and that neural defects of *Nova2-/-* are the consequence of aberrant processing of these gene transcripts [46].

Nova proteins shuttle between the nucleus and the cytoplasm, with two-thirds of Nova proteins detectable in the cytoplasmic fraction of the mouse brain [61]. Interestingly, HITS-CLIP experiment was used to identify 3′-untranslated region (3' UTR) element that mediates Nova-dependent localization, in dendritic spines and synaptic contacts, of specific mRNA targets whose splicing is instead regulated by Nova proteins in the nucleus [61]. Recently, it has been also reported that Nova proteins are able to indirectly regulate the mRNA stability of their targets through a post-transcriptional mechanism in which AS is associated to nonsense-mediated decay (AS-NMD) [62]. In this case, HITS-CLIP identified YCAY clusters in introns (rather than in 3′ UTRs) leading to discovery of cryptic exons whose splicing triggers NMD pathway. Notably, AS-NMD of these exons was regulated by seizures, a process that also modified Nova subcellular localization and determined changes in synaptic proteins, in particular in factors involved in familial epilepsy. In line with this, Nova haploinsufficient mice showed spontaneous epilepsy [62].

Despite the vast amount of data regarding the ability of Nova proteins to regulate AS during neural differentiation, little is known about the mechanisms that control their (protein or mRNA) expression levels [63]. The observation that the 3′ UTR of *Nova1* and *Nova2* genes are very different suggest that diverse post-transcriptional events are involved in regulating their differential expression within the CNS [64]. The 3′ UTR of *Nova1* is well conserved in mammals (97% identity between human and mouse) and enriched in regulatory AU-rich consensus elements (ARE), whereas the 3′ UTR of *Nova2* is shorter and more variable among orthologous genes [64]. Interestingly, the *Nova1* expression level is post-transcriptionally regulated through nELAV, a neuronal-specific RBP that directly binds to *Nova1* ARE, increasing *Nova1* mRNA stability and translation. In addition, protein kinase C-induced phosphorylation of nELAV is able to stimulate *Nova1* translation [64]

Also, Nova1 expression level is modulated by glucocorticoids, which induce Nova1 downregulation and, as a consequence, changes in the AS pattern of specific Nova1 pre-mRNA targets [65]. Curiously, exon 4 of the *Nova-1* pre-mRNA is itself a target of Nova-dependent splicing regulation. Indeed, Nova1 regulates its own splicing by suppressing exon 4 inclusion

[66]. Since the region encoded by *Nova1* exon 4 contains many putative phosphorylation sites for serine/threonine kinases, it has been proposed that Nova1 could autoregulate its splicing activity in response to different cellular stimuli [66]. Finally, Nova1 has been recently identified as a factor that affects microRNA (miRNA) functions in neurons [67]. Specifically, Nova1 directly interacts with Ago proteins (a key elements of the miRNA-induced silencing complex, miRISC) and, as a consequence, stimulates neuronal miRNA function [67]. These findings suggest that Nova1 is a component of the neuronal miRISC complex and it is able to inhibit mRNA expression independently by its (sequence-specific) RNA-binding activity.

1.5 Ptbp2 or nPTB protein

Ptbp2 (also known as neural- or brain-enriched nPTB/brPTB), initially identified as a tissue-restricted paralogue of the ubiquitously expressed splicing regulator polypyrimidine tract binding protein (PTB, Ptbp1 or hnRNP I) [68], is an RNA-binding protein enriched in the brain, where it is expressed in glia and neurons and thought to be involved in cell-specific AS regulation [69,70]. Subsequently, Ptbp2 was also found to be expressed at high levels in muscle and testis during spermatogenesis process [70–72].
The aminoacid sequence of Ptbp2 has 74% of identity with that of Ptbp1, mantaining the modular structure of four RRM motifs separated by flexible linkers [73,74]. The best-characterized function of the two Ptbp proteins is in the regulation of AS patterns. HITS-CLIP experiment defined CU- and UCU-rich sequences as the consensus sequences for Ptbp2 binding [75], in agreement with previously defined sequence elements required for RNA binding by Ptbp1 [76–78]. Recent global analyses demonstrated that Ptbp1 and Ptbp2 function as AS repressors able to inhibit exon inclusion by binding to sequences within or upstream of the regulated exon [75,79]. Moreover, it has been proposed that, similar to Ptbp1, Ptbp2 antagonizes the binding/activity of core splicing factors (such as U2AF) near the Ptb-repressed exons and prevents the spliceosome assembly at adjacent splice sites by interfering with the interactions between components of the spliceosome [80]. However, in some cases Ptbp proteins can also promote exon inclusion by binding to sequences downstream of the regulated exon [75,79,81]. These data indicated that Ptbp proteins act as position dependent AS factors that promote or repress exon inclusion depending on the locations of their binding sites in RNA targets in agree with observations initially made with several tissue-restricted RNA-binding proteins including Nova1/2, RbFox2, Mbnl1, TIA1/2, hnRNP C, hnRNP L and TDP-43 [56,82–85].
Despite the high homology in peptide sequence, genome wide analysis in cell cultures (such as neuroblastoma and HeLa cells) revealed that Ptbp proteins have different splicing regulatory properties [86–88]. Indeed, Ptbp proteins regulate AS of overlapping and distinct sets of pre-mRNA targets with several of the Ptbp2 targets implicated in neuronal differentiation or synapse activity [86–88] suggesting that the role(s) of these proteins may diverge in different cell types or developmental stages. Moreover, overlapping targets may also have a different sensitivity to Ptbp1 and Ptbp2,

with some AS exons more affected by Ptbp1, other more influenced by Ptbp2 and other equally responding to both proteins [89,90]. For example, Ptbp2 is able to repress *c-src* N1 exon inclusion weakly than Ptbp1 but it binds to the N1 downstream control sequence (DCS) with higher affinity than Ptbp1 [69], suggesting that the difference in exon sensitivity may also results from a different capacity of Ptbp proteins to interact with other splicing co-factors [91]. In line with this, it has been found that Ptbp2 antagonizes the ability of Nova proteins to regulate neuron-specific AS events such as the exon 3A of *GlyRα2* pre-mRNA in which the Ptbp2 binding motif is located near the Nova binding site [70].

As reported before, Ptbp1 is present in most mammalian tissues but is replaced by Ptbp2 in the nervous system [69,70]. In particular, during the early phases of neuronal development, Ptbp2 is expressed at low levels in neuronal progenitor cells, but is gradually upregulated when these cells are induced to differentiate into post-mitotic neurons [89,92,93]. In contrast, Ptbp1 is present at high levels in neural progenitor cells, glia and other non-neuronal tissues, but is repressed in differentiating neurons and this event is associated with an increased level of Ptbp2 protein [70,87,88,93]. Cell type-specific expression of Ptbp proteins can be controlled (in part) by a cross-regulation mechanism. Ptbp1 is able to bind to *Ptbp2* pre-mRNA and to promote skipping of *Ptbp2* exon10 (34 nt exon), an event that introduces a premature termination codon (PTC) and triggers degradation of *Ptbp2* mRNA by the NMD pathway [86,89]. In mammals, a PTC is recognized as premature when located >50–55 nt upstream of the exon-exon junction marked by the exon junction complex (EJC). EJCs downstream of PTCs are no longer removed during the "pioneer" round of translation and recruit essential NMD factors, including Upf1/Rent1, that in turn promotes mRNA degradation [94]. Initially, NMD was considered only a mechanism that eliminates aberrant mRNAs that would produce a truncated protein due to the presence of a PTC arising from nonsense codon containing alleles [94]. It is now evident that NMD is involved in quantitative post-transcriptional regulation of gene expression when it is coupled with AS in the process called AS-NMD (Alternative Splicing-activated NMD) or RUST (Regulated Unproductive Splicing and Translation) [95]. Alternative "poison" exons containing premature in-frame stop codons, or introns in the 3' UTR, are particularly frequent in mammalian genes for AS regulators, such as SR factors and hnRNP proteins [96,97] and for many core spliceosomal proteins [98]. Most of these proteins can regulate their own mRNA level by modulating AS-NMD in a feedback mechanism designed to maintain the protein homeostatic level [98]. Interestingly, in several genes for SR factors and hnRNPs, AS-NMD cassettes overlap highly conserved or ultraconserved elements (UCEs); [96,99] longer than 200 bp, with 100% identity among rat, mouse and human genomes. In the case of *Ptbp2* gene, exon 10 is located within a UCE element of the mammalian genome with the intronic region nearby exon 10 that is nearly 100% identical between human and mouse [100].

Interestingly, Ptbp2 protein itself is also able to repress exon 10 splicing, creating negative feedback loop that allows Ptbp2 to control its own

synthesis [89]. In addition, exon 10 of *Ptbp2* has also been identified as target of HuR protein [101], whereas Matrin3, an RNA- and DNA-binding nuclear matrix protein involved in neural and muscular degenerative diseases [102], is able to antagonize Ptbp1 and favor inclusion of exon 10 in the *Ptbp2* transcript [103].

By using splicing-sensitive exon junction microarrays and RNA-Seq experiments, it has been reported that the regulatory switch from Ptbp1 to Ptbp2 protein expression levels is sufficient to induce significant changes in the neuronal-specific AS program [87,104]. In particular, changes in the expression levels of Ptbp proteins control two transitions in splicing programs during neuronal differentiation (Fig. 7).

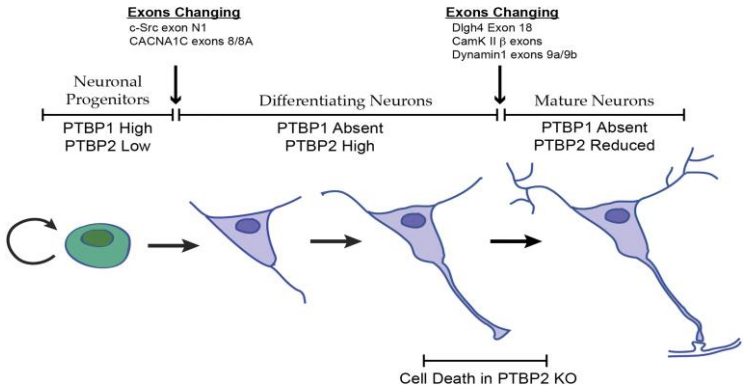

Fig. 7. PTB proteins expression levels changes during neuronal differentiation define three splicing regulatory states. The first Ptbp1/Ptbp2 switch occurs when neuronal progenitor cells are induced to differentiate, this defines the first stage of AS regulation that affects exons more sensitive to Ptbp1 (i.e *Cacna1c* calcium channel exon 8). During differentiation, neurons are characterized by high Ptbp2 levels while Ptbp1 is absent, therefore exon responding to both RBPs are repressed. A third switch in AS profile occurs when neurons definitely mature and establish synapses, at this stage Ptbp2 levels decrease while Ptbp1 continues to be absent, to guarantee adult brain-isoforms of genes such as *Dlg4, CamK II β and Dynamin1*. These specific isoforms, expressed in *Ptbp2* null neurons induce cell death and ihhibit neuronal maturation. Modified from [104].

In neuronal progenitor cells, Ptbp1 (but not Ptbp2) is present and able to repress many Ptb-dependent exons. When these cells initiate to differentiate, Ptbp1 is repressed, mainly through the action of miR-124 [88], whereas Ptbp2 is induced and this changes the AS profiles of transcripts that are more sensitive to Ptbp1 than Ptbp2 and maintains the embryonic splicing program during differentiation. High Ptbp2 expression persists in differentiating neurons, but after synaptogenesis Ptbp2 is reduced leading to another AS transition, where Ptb-dependent exons undergo changes in their splicing.

In order to understand the function of Ptbp2 in the nervous system, several mouse genetic models have been generated [75,104]. *Ptbp2*-null mice were paralysed and died soon after birth for respiratory failure, probably due to the lack of innervation of the diaphragm [75] indicating that Ptbp2 is essential

for postnatal survival. Interestingly, neuronal progenitors in the *Ptbp2*-null brain exhibited an aberrant polarity and were associated with regions of premature neurogenesis and a reduction of the neural progenitor pool [75]. Notably, by using HITS-CLIP experiments combined with results from splicing-sensitive microarrays, Licatalosi et al. demonstrated that the major action of Ptbp2 is to inhibit splicing of alternative exons present in genes encoding for proteins associated with control of cell fate, proliferation and the actin cytoskeleton, suggesting a role for Ptbp2 in neurogenesis [75]. Because of neonatal lethal phenotype, conditional gene targeting approaches were recently used by the laboratory of Prof. Douglas L. Black in order to study Ptbp2 function specifically in the nervous system [104]. Interestingly, depletion of Ptbp2 in developing mouse cortex caused extensive neuronal death and degeneration [104]. In addition, *Ptbp2* knockout brain showed substantial reduction in the expression levels of several synaptic proteins, whereas cultured neurons from *Ptbp2*-/- mice were unable to mature and characterized by a number of signs of neuronal death including neurite retraction, membrane blebbing, shrinkage and nuclear condensation. Importantly, transcriptome-wide analyses indicated that morphological changes in the mutant mice were associated to AS alternations of genes involved in postnatal brain development or affecting processes such as the growth of axons and dendrites or the formation of synapses. Moreover, these data showed that the major action of Ptbp2 is to inhibit the expression of protein isoforms normally found in adult brain, but precociously expressed in the developing mutant embryo. Collectively, all these findings reveal that Ptbp2, by inhibiting the expression of adult forms of proteins until neurons have matured, plays an essential role in controlling neuronal development.
Finally, Zagore and colleagues have recently demonstrated that Ptbp2 plays also important function in testis where it regulates spermatogenesis process [72]. In line with this, Ptbp2 ablation resulted in germ cell loss due to increased apoptosis of meiotic spermatocytes and postmeiotic arrest of spermatid differentiation [72].

2. Alternative splicing in cancer

Cancer is a heterogeneous and complex disease, in which the integrated circuits of epigenetic, transcriptional and post-transcriptional programs that operate in normal cells are deregulated and reprogrammed to confer hallmark capabilities to cancer cells [105].
In the recent years the importance of AS for tumor progression has become incredibly evident [106,107]. Indeed, AS is a very plastic mechanism that offers the possibility to modify the proteome of cancer cells thus contributing to the combined disruption of tumor suppressor genes and activation of oncogenes involved in tumor establishment, progression and in resistance to therapeutic treatments [106,108,109] In particular, several cancer-associated genes are controlled by AS and these genes encode for proteins implicated in all major aspects of cancer cell biology including cell cycle control, proliferation, apoptosis, metabolism, angiogenesis, differentiation, signal

transduction pathways, motility, invasion and metastasis [106,107,110].
Genome-wide analyses (RNA-Seq and splicing-sensitive microarrays) have revealed profound differences in the AS programs of cancer cells compared to normal cells [111]. Aberrant splicing profiles in tumors result from *cis*-acting mutations in cancer-relevant genes as well as altered expression or activity of *trans*-acting splicing factors [112]. It has been observed that cancer-associated genes, especially tumor suppressor genes, have a greater susceptibility to mutation-induced aberrant splicing than other genes [113]. Inherited or somatic mutations can generate or disrupt splice sites, splicing enhancer and silencer elements or create cryptic donor and acceptor sites [112]. Salient examples of these types of mutations are those occurring in tumor-associated genes including *BRCA1/2*, *p53*, *APC*, *MLH1*, *MDM2*, *MSH2*, *KLF6*, *CDH17*, *KIT* and *LKB1* [112,114]. For example, for the transcription factor Kruppel-like Factor 6 a germeline single nucleotide (G/A) polymorphism in intron 1 has been described to be associated with high risk of prostate cancer [115]. Interestingly, this polymorphism generates the binding site for the SRSF5 splicing factor thus favoring the utilization of a cryptic splicing site in exon 2 [115] and promoting the production of the dominant negative KLF-SV1 isoform implicated in prostatic cancer progression [116]. Notably, KLF-SV1 was found to be overexpressed in lung and ovarian cancers [117] and associated with poor survival in breast cancer patients [118]. Recent analysis also revealed that splicing factors represent a novel class of mutational targets in various hematopoietic malignancies, including myelodysplastic syndromes, myeloid neoplasms and chronic lymphocytic leukemia [119]. The most affected genes were *U2AF1 (U2AF35), SRSF2 (SC35), SF3B1 (SF3B155 or SAP155) and ZRSR2 (URP*) [120].
A common signature of cancer cells is a general loss of splicing fidelity caused by changes in expression levels (or activity) of specific splicing factors [112,121]. Indeed, the expression levels of SR and hnRNP proteins are frequently altered in different cancer types and several splicing factors behave as a *bona fide* proto-oncogene [110,122,123]. For example, SRSF1 is an oncogenic splicing protein upregulated in many human cancers [124]; it is able to transform human and mouse mammary epithelial cells *in vivo* and *in vitro* and induce tumor formation in nude mice [124,125]. Relevant to the oncogenic potential of SRSF1, its over-expression increases cell proliferation and delays apoptosis and these effects depend on SRSF1 activity in AS regulation [110,123]. Indeed, SRSF1, promotes the production of the Bcl-XL, a long anti-apoptotic isoform of *Bcl-X* gene [124]. In addition, SRSF1 stimulates the production of short protein isoforms of *S6K*1, which are overexpressed in breast cancers and able to increase cell transformation, motility and anchorage-independent growth of breast epithelial cells [124,126] Notably, these AS isoforms bind and increase mTORC1 activity [126] thus creating a signal loop that guarantees the activation of Akt/mTOR mitogenic pathway also in absence of external stimuli. Interestingly, the proto-oncogene Myc directly activates the transcription of *SRSF1* and as a consequence influences the AS profile of others SRSF1 targets among which the signaling kinase *Mknk2* and the transcription factor *Tead1* [127].
Fascinating from my point of view is the observation that cancer cells are

able to re-express embryonic splicing isoforms (down-regulated in adult normal tissues) with important roles in development thus recapitulating the AS profiles of undifferentiated cells [121,128]. Moreover, a number of AS transcripts are generated *de novo* in cancer cells with some cancer-specific variants peculiar of specific cancer types [121,129,130]. In line with this, it has been reported that there are as many as 15.000 cancer-specific AS events, a great number of which generates novel proteins [121,129,130]. All these findings indicate that cancer-related AS isoforms could play a direct and causative role in tumor progression [106,112]. Moreover, they might represent potential sources for novel diagnosis and classification of cancers and, more importantly, could be the targets for innovative therapeutic interventions based on highly selective splicing correction approaches [106,131,132].
On the basis of what has been described in this section it is clear that deciphering the mechanisms underlying alternation of AS splicing in tumors may prove crucial to understand how splicing machinery is controlled and integrated with other cellular processes involved in cancer progression in order to obtain a better comprehension of the neoplastic process. In the next sections, I will focus on examples of altered splicing pattern of genes relevant for apoptosis, tumor metabolism, invasion and metastasis.

2.1 Tumor cell escape from apoptosis

One of the hallmark of cancer cells is their ability to bypass apoptosis, a programmed form of cell death [105]. In particular, to survive to apoptotic signals present in the tumor microenvironment, cancer cells activate anti-apoptotic "stratagems", such as modulation of specific AS patterns [133]. Several genes encoding for apoptotic regulators are regulated by AS, which is able to produce isoforms with opposite function (pro-apoptotic or anti-apoptotic). Notably, in tumors AS of these genes is generally dysregulated toward the production of the pro-survival variant[106,107,128]. Below, I discuss some examples for which well-characterized splicing regulatory mechanisms have been proposed.
Bcl-x. One of the earliest discovered examples of genes involved in apoptosis with an AS profile altered in tumor cells, is *Bcl-x*, a member of the Bcl-2 family [134]. Selection of the proximal 5′ ss in exon 2 of *Bcl-x* pre-mRNA causes the production of the anti-apoptotic long Bcl-xL variant, while the pro-apoptotic short Bcl-xS variant is produced by the use of the distal alternative 5′ ss. In several cancer types, the Bcl-xL splicing isoform is upregulated thus increasing resistance to chemotherapeutic agents [135]. Due to its relevance in cancer, *Bcl-x* splicing has been extensively investigated in the past years and several RBPs were shown to regulate this specific AS event, including Sam68, hnRNP A1, SRSF1, SRSF9, hnRNP F/H, RBM25 and SF3B1/SAP15 [136–139]. In addition, a number of works have demonstrated that *Bcl-x* provides a potential target for the development of new therapeutic strategies able to prevent the production of the aberrant Bcl-xL variant [140,141]. For example, Bauman and colleagues have used a modified antisense oligonucleotide (ASO), complementary to

the downstream 5′ ss of exon 2 in *Bcl-x* pre-mRNA, to correct AS in a mouse model of melanoma [141]. Interestingly, this oligo was able to efficiently redirected splicing machinery to the upstream 5′ ss, decreasing the anti-apoptotic Bcl-xL isoform, while increasing the pro-apoptotic Bcl-xS variant. Significantly, this treatment reduced the tumor growth and the incidence of metastasis to the lung [141].

Fas. The interaction between the FAS death receptor, codified by *Tnr6* gene, and its ligand FASL encoded by *Tnfs6*, mediates one of the best characterized extrinsic signaling pathways of apoptosis [142]. Several AS isoforms of FAS have been described, including an anti-apoptotic soluble isoform (sFAS), lacking of the transmembrane domain encoded by exon 6 [143]. Interestingly, this sFAS variant, which probably exert its anti-apoptotic function competing with FAS ligand binding [144], has been detected in the sera of patients with solid and haemopoietic tumors [145,146]. Positive regulator of *Fas* exon 6 inclusion are: TIA-1, TIAR-1 (TIA-1 related), and EWS (Ewing sarcoma protein) [21,147]. On the contrary, RBM5, HuR, hnRNP A1, Ptbp1, hnRNP C1/C2 negatively regulate exon 6 promoting the production of the anti-apoptotic isoform [148,149]. Recently, an automatized genome-wide siRNA screening, has identified 200 genes whose knockdown modulates the FAS/sFAS ratio [150]. These genes include classical splicing regulators, core spliceosome components, as well as factors implicated in transcription and chromatin remodeling, RNA transport and intracellular signaling [150].

Mcl-1. Mcl-1 (myeloid cell leukemia-1) is another member of the Bcl-2 family whose AS produces pro- and anti-apoptotic isoforms. In particular, the full length Mcl-1L isoform, generated by inclusion of exon 2, is able to antagonize apoptosis by sequestering pro-apoptotic factors in mitochondria, thus inhibiting mitochondrial outer membrane permeabilization, whereas the pro-apoptotic short isoform Mcl-1S, lacking of exon 2, is able to dimerize with Mcl-1L and direct it to proteosomal degradation [151]. Interestingly, Mcl-1L was found upregulated in several cancer tissues and cell lines, associated with poor prognosis in breast and oral cancers and implicated in resistance to anti-cancer therapies [152–154]. As in the case of *Bcl-x*, ASOs have been successfully used to prevent the production of the aberrant anti-apoptotic Mcl-1 [155]. More importantly, siRNA-mediated *Mcl-1L* knockdown has been also shown to be sufficient to induce apoptosis in a tumor xenograft model and, as consequence, to cause a complete loss of tumorigenic capacity [156].

Caspase-9. Caspases are important regulators of the apoptotic process [157]. In particular, Caspase-9, a protease activated after the release of cytochrome c from mitochondria, is a member of this family implicated in the execution phase of apoptosis [158]. Inclusion of exons 3, 4, 5, and 6 in *casp-9* mRNA generates the caspase-9a pro-apoptotic isoform, whereas skipping of these exons produces the anti-apoptotic isoform caspase-9b [159]. Significantly, Caspase 9a/9b ratio is altered in non-small cell lung cancer (NSCLC) and involved in resistance to a number of chemotherapeutic agents [160,161]. It has been shown that SRSF1, by binding to a splicing enhancer element located in intron 6, is able to promote the simultaneous exclusion of exons 3, 4, 5

and 6, thus stimulating the production of Caspase 9b [161]. Interestingly, phosphoinositide 3-kinase/Akt pathway can regulate AS of *casp-9* via a coordinated mechanism involving the phosphorylation of SRSF1 at specific serine residues [160]. Similarly, to SRSF1, hnRNP L binds to a splicing regulatory element and regulates the AS profile of *casp-9* gene. Notably, down-regulation of hnRNP L has been found able to inhibit tumorigenesis process in xenograft mouse model [162].

2.2 Links between metabolism and cancer

Most cancer cells predominantly produce energy through aerobic glycolysis, rather than oxidative phosphorylation as normal tissues [163]. This switch (also known as the Warburg effect, named for its discoverer) gives proliferative advantages to cancer cells, which can utilize more efficiently the glycolytic intermediates and have glycolytic rates up to 200 times higher than those of their normal tissues of origin even if oxygen is plentiful.

Pyruvate Kinase. Aerobic glycolysis is in part achieved in mammals by regulated expression of AS isoforms of the Pyruvate kinase (PK), the enzyme involved in the catalysis of the final step of glycolysis [164]. Through mutually exclusive inclusion of exons 9 and 10, the *PKM* gene produces two different isoforms with opposite functions. The PKM1 isoform, expressed in most adult tissues where drives oxidative phosphorylation, is generated by inclusion of exon 9, whereas the PKM2 form, expressed in embryonic cells where elicits aerobic glycolysis, is produced by exon 10 inclusion [165]. Notably, in agree with the idea that aerobic glycolysis is essential and necessary for proliferation, replacing PKM2 with PKM1 in cancer cells increased oxidative phosphorylation, thus reducing tumor growth in nude mice [164]. Three hnRNP splicing repressors, hnRNP A1, hnRNP A2, and hnRNP I/Ptbp1, have been found to cooperate in promoting the production of PKM2 isoform by binding to sequences flanking *PKM* exon 9 [166,167]. Notably, all these factors are over-expressed in several cancers [168–170] and their expression can be activated by the oncogenic transcription factor c-Myc that binds to the promoters of all three genes [167]. In line with the effect on *PKM* splicing, depletion of hnRNP A1/A2 or Ptbp1 in a glioblastoma cell line was sufficient to decrease the production of lactate [166]. All these findings suggest that during neoplastic transformation upregulation of c-Myc might predispose tumor cells to alter their metabolism through modulation of *PKM* AS. Moreover, they identified a pathway that regulates an AS event required for tumour cell proliferation.

Recently, ASO technology was used to correct aberrant AS and induce specific down-regulation of PKM2 isoform [171]. Importantly, ASO treatment was also sufficient to induce apoptosis of glioblastoma cell lines [172]. Importantly, this approach potentially represents an effective therapeutic strategy in glioblastoma since these tumor cells are able to take up chemically modified ASOs *in vivo* without the support of delivery agents [172].

Max. Myc-associated factor X (Max) together with Myc is a member of the the basic helix-loop-helix leucine zipper (bHLHZ) family of transcription

factors [173]. It has been shown that hnRNP A1 promotes the inclusion of exon 5 in *Max* mRNA leading to the production of the Delta Max splice variant, a truncated protein implicated in Myc-driven transformation in glioblastoma since it is able to stimulate glioblastoma cell proliferation by stimulating the expression of glycolytic genes [174]. Interestingly, many glioblastoma express a constitutively activated form of the EGF receptor (EGFRvIII) [175], which induces upregulation of hnRNP A1 via mTOR signaling [174]. Interestingly, high hnRNP A1 expression was correlated with high EGFRvIII and glycolytic gene expression in primary glioblastoma samples and was associated with decreased overall survival of patients [174]. Moreover, Delta Max expression was sufficient to rescue the induction of the glycolytic genes in EGFRvIII-depleted cells, whereas knockdown of this AS variant inhibited aerobic glycolysis and impaired the growth of EGFRvIII-expressing xenografts [174].

2.3 Tumor cell invasion and metastasis

More than 90% of cancer-related deaths are due to the development of metastasis, a process by which of tumor cells invade adjacent tissues and disseminate toward distant organs [176]. This is a complex process that involves i) migration and invasion of tumor cells through the basement membrane and endothelial walls; ii) intravasation within the blood and the lymphatic systems; iii) extravasation into distant tissues, and iv) proliferation and growth of tumor cells allowing efficient metastatic colonization [176].

The first gene for which altered AS has been associated to metastasis formation is *CD44* [177]. CD44 is a cell-surface glycoproteins involved in cell-cell interactions, cell adhesion and migration [177]. Moreover, it functions as receptor for several components of the extracellular matrix (ECM) (i.e. matrix metalloproteases, collagen, laminin and fibronectin) [178]. *CD44* pre-mRNA is regulated by AS that affects 10 adjacent exons (v1–v10) and generates multiple CD44 high-molecular-weight isoforms with different extracellular domains [178].

Standard CD44 (CD44s), lacking all alternative exons, is predominantly expressed in normal tissues, whereas CD44 splicing isoforms, for example those containing exons v5, v6 and v7, are over-expressed in various tumors and involved in tumor cell invasion and metastasis [178–180]. Interestingly, the CD44v6 isoform, upregulated in adenocarcinomas [179], squamous cell carcinoma [180] and associated to poor prognosis in gastric cancers [181], is able to form a complex with c-Met and its ligand hepatocyte growth factor (HGF) and it is absolutely required to mediate the HGF-dependent activation of Ras signaling [182]. Importantly, several mAbs targeting CD44v6 have been evaluated in clinical trials [183]. Similarly, the CD44v5 variant is over-expressed in several cancer types and has a prognostic value for gastric and renal cancers [184]. CD44v5 production is regulated by Sam68 splicing factor; in particular Sam68 can promote inclusion of exon v5 by acting through different mechanisms: i) competing/displacing the antagonistic splicing repressor hnRNP A1 that binds a specific splicing silencer element

located within exon v5, ii) favoring the recruitment of spliceosomal factors and iii) interacting with the splicing co-activator SRm160 [139]. In addition to Sam68, other splicing factors (including hnRNPA1, SRp55, SF2/ASF, Tra-2 beta, ESRP1 and YB-1) have been shown to regulate specific CD44 variant exons [185–190]. Interestingly, depletion of the splicing regulator ESRP1 in metastatic 4T1 cells was found sufficient to shift the splicing CD44 pattern toward the production of CD44s leading to inhibition of metastatic lung lesions in mouse models [191]. One of the most important mechanisms through which cancer cells spread and form metastasis is the Epithelial-to-Mesenchymal transition (EMT) [192]. During EMT, differentiated epithelial cells undergo several molecular and morphological changes: they assume an elongated fibroblast-like shape, lose their intercellular junctions and acquire invasive properties (mesenchymal phenotype). Intriguingly, EMT is a transient process that characterize only a subset of cells at the invasive front of the metastasizing primary carcinomas and is reversed after the establishment of metastasis [193]. In particular, the reverse process of EMT, namely the Mesenchymal-to-Epithelial Transition (MET), is important for the re-differentiation of tumor cells to an epithelial phenotype and for clonal outgrowth at final metastatic sites [194]. Recent studies have demonstrated an important contribution of AS regulation in the cascade of events characterizing the morphological conversion of tumor cells during EMT [195]. The first demonstration of the importance of AS in EMT process derived from the analysis of *Ron* proto-oncogene, encoding a "scatter factor receptors" involved in the control of cell dissociation, migration, and matrix invasion" [196]. *Ron* pre-mRNA is regulated by AS that generates different isoforms with distinct biological activities [197]. In particular, ΔRon is a constitutively active isoform deleted of 49 amino acids in the extracellular domain that originates from skipping of *Ron* exon 11 [198]. Notably, ΔRon accumulates during tumor progression of epithelial cancers and confers increased motility to expressing cells [199,200]. In the past, our group found that SRSF1, a member of SR proteins that is often upregulated in several human tumors [124], directly binds to the enhancer and stimulates skipping of exon 11, thus promoting the production of ΔRon isoform that in turn triggers activation of the EMT program increasing the invasive properties of the cells. Moreover, we also found that hnRNP A1 is able to antagonize the binding of SRSF1, prevent the exon skipping event and activate the reversal MET program [201].

Interestingly, SRSF1 protein levels are modulated in mesenchymal and epithelial cells through AS-NMD [202]. In particular, the 3'UTR of *SRSF1* gene contains an intron that is normally retained in the mature transcript in mesenchymal cells. Splicing of this intron in epithelial cells produces a PTC-containing RNA molecule, substrate for NMD pathway. In line with these observations, mesenchymal cells are characterized by higher levels of SRSF1 and ΔRon, compared to epithelial cells [202]. Notably, EMT/MET programs are also controlled by Sam68 that processes the *SRSF1* 3'UTR-intron, favoring the production of NMD-prone isoform [202].

Since ΔRon is a cancer-specific isoform involved in EMT, its production could represent a potential target for the development of new anti-

metastatic therapeutic strategies [132,197]. In this regard, our group used bifunctional oligonucleotides TOES (Targeted Oligonucleotide Enhancers of Splicing) technology to correct altered *ΔRon* splicing in cancer cells. In particular, we have designed a TOES complementary to the first region of exon 11 and containing a tail of GGA repeats, known to function as a strong enhancer [132]. In addition, we also employed a new class of splicing inhibitors, namely indole-derived compounds (IDCs), that selectively block the ESE-dependent splicing activity of individual SR proteins, like SRSF1 [132]. Both treatments resulted in efficient correction of ΔRon splicing by increasing exon 11 inclusion. Notably, some IDCs molecules also affected the invasive phenotype of cells stably over-expressing SRSF1 [132].

Another important regulator of EMT process is Rac1, a small GTPase of the mammalian Rho family involved in actin cytoskeleton organization, cell growth, cell-cell adhesion, and migration [203–205]. The AS variant Rac1b is generated by inclusion of a highly conserved 57 nt cassette exon (exon 3b) that results in an in-frame insertion of 19 new amino acids in the domain involved in the interaction with regulator and effector molecules [205,206]. This insertion impairs the GTPase activity, making a constitutively active alternatively spliced isoform [207]. Interestingly, Rac1b is upregulated in breast cancers [208] as well as in colorectal tumors at various stages of neoplastic progression [209]. A pletheora of RBPs regulate exon 3b inclusion/skipping: SRSF1 increases full lenght isoform, while SRSF3, SRSF7 and hnRNP A1 promote the skipping of the exon [210–212]. Significantly, matrix metalloproteinases (MMPs), important family of proteinases of the tumor microenvironment upregulated in almost all types of human cancer and associated with poor survival [213], were found able to determine activation of EMT and tumorigenesis process in transgenic mice by promoting the expression of Rac1b [214].

Epithelial-specific alternative splicing factors ESRP1 and ESRP2 (Epithelial Splicing Regulatory Proteins 1 and 2), are two important regulators of the mesenchymal and epithelial splicing signatures [215]. During EMT, the ESRP1/2 expression levels regulate AS changes of *Fgfr2*, *Ctnnd1*, *CD44* and *ENAH* genes [216] involved in different aspects of the metastatic cascade, such as cell-cell and cell-matrix adhesion, actin cytoskeleton organization, and migration. Importantly, knockdown of ESRP1 and ESRP2 was found able to determine a complete switch from the epithelial to the mesenchymal AS variant of these genes leading to a drastic reorganization of actin cytoskeleton as well as morphology and a reduction of invasive properties of treated cells [216]. Conversely, ectopic expression of either ESRP1 or ESRP2 in mesenchymal cells switched splicing of these genes toward an epithelial pattern suggesting that extensive changes in AS play a profound role in shaping the changes in cell behavior that characterize the EMT [216].

3. Vasculogenesis and angiogenesis

Cells that form small organisms, such as the worm *C. elegans*, reach oxygen by simple diffusion, whereas other avascular species, such as *D.*

melanogaster, are characterized by an oxygen transport network through their entire body (even at the end of the legs). On the contrary, in order to supply oxygen and nutrients and to the remove carbon dioxide and metabolic wastes, larger sizes organisms, such as vertebrates, have devolved a complex and specialized apparatus, the vascular system. Since this system is critical for proper tissue development, homeostasis and function, therefore is not surprising that it is one of the first organ systems to form in the embryo [217].

The vertebrate vascular system is composed of: arteries, which distribute oxygen and nutrients from the heart to the rest of the organism, arterioles and capillaries, which allow efficient exchange within tissues, veins and small veins (venules) that collect waste molecules and carbon dioxide and finally return to the heart through the large axial cardinal veins [217]. Arteries, veins and capillaries share the same basal unit, the endothelial cell (EC), which directly contacts blood stream and has its apical surface of the front to the vascular lumen. However, ECs from arteries, veins and capillaries differ for their hemodynamic properties and their envelope [218]. Arteries, transporting blood at high pressure and speed, are covered by ECM, elastic fibers and multiple layers of specialized vascular smooth muscle cells (vSMCs), to ensure contractility [219]. On the contrary, veins contain low-pressure blood and have a thin layer of vSMCs, whereas capillaries are formed by one layer of ECs and basal lamina, supported by pericytes [219].

During embryogenesis, the vasculature is formed primarily through two main mechanisms (Fig. 8):

- vasculogenesis, the *de novo* formation of vessels; is a process starting at 7.5 days post coitum (dpc) from stem cells (angioblasts derived from mesodermal cells) that differentiate into ECs and organize the primitive vascular plexus with tubular like structures before the heart beats;
- angiogenesis (from the Greek word *Angêion*, meaning vessel), the growth of new vessels from pre-existing vessels, which expands and remodels the first vascular plexus [220].

Remodelling is characterized by different steps involving EC proliferation, migration, reshaping, pruning and fusion (see below) and this process is important to support blood flow and tissue perfusion. In addition, this process is associated to recruitment of pericytes and vSMCs that protect ECs from apoptosis and stabilize the vascular tone. Notably, a number of transcription factors regulate angioblast differentiation to ECs, whereas other factors are involved in the specification of the (anatomical and functional) features of arteries and veins [221].

In adulthood, vessels are quiescent and angiogenesis is present only in particular conditions, (such as the female cycle and pregnancy) but in conditions of active physiological tissue growth (such as tissue repair, inflammation, ischemia, infectious and immune disorders) ECs migrate and proliferate to form new vessels [222]. Moreover, angiogenesis is an important process to support cancer development and progression, by allowing oxygen and nutrients to reach proliferating tumor tissues and by providing cancer cells with the metastatic route to colonize distant organs [222].

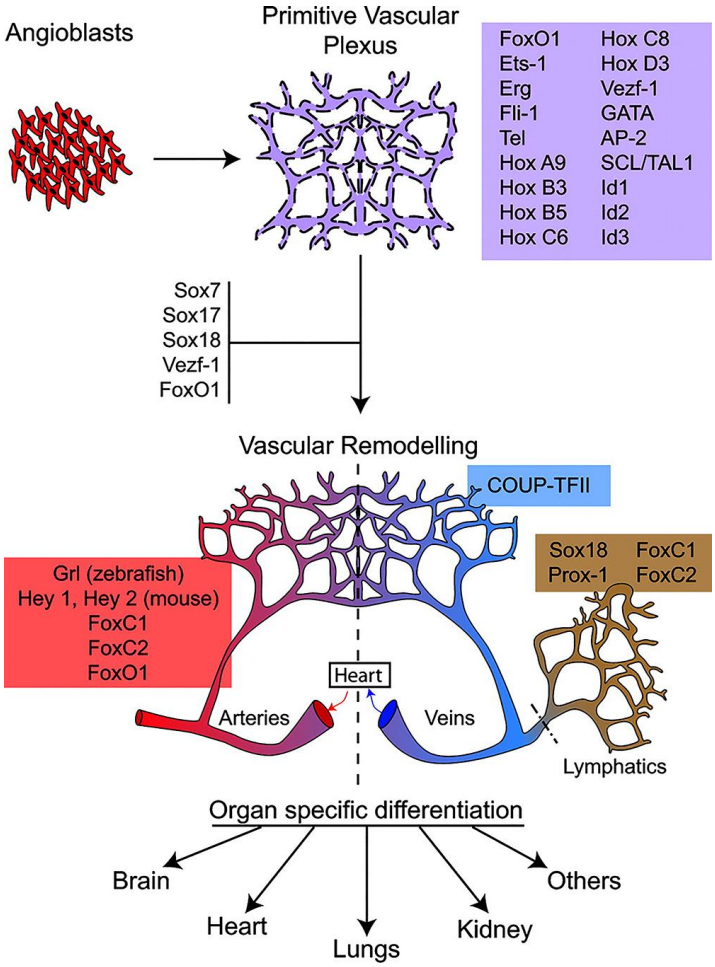

Fig. 8. Vascular network forms through vasculogensis and angiogenesis. Primitive vascular plexus is formed by vaculogenesis (upper part). Endothelial cells differentiate from mesodermal progenitors called angioblasts and acquire specific markers. The plexus undergoes further remodeling in large and small vessels (arteries, veins and capillaries) by angiogenesis (lower panel). Endothelial cells then acquire organ-specific characteristics that are induced by the crosstalk with cells of the surrounding tissues. Transcription factors specific for each type of vessels are shown in colored boxes. Modified from [223].

3.1 Sprouting angiogenesis

Two types of angiogenesis have been described in adults: sprouting angiogenesis and intussusceptive angiogenesis, in which capillary wall extends into the lumen to split a single vessel in two [224,225]. I will focus on sprouting angiogenesis since this process is better understood having been discovered nearly 200 years ago.

Sprouting angiogenesis is a highly regulated process characterized (as suggested by the name) by sprouts of ECs growing toward an angiogenic stimulus (for example VEGF, vascular endothelial growth factor, see

below). It can be schematized in the following steps: EC sprouting with enzymatic degradation of basement membrane, EC proliferation, migration of ECs, lumenogenesis and tubulogenesis (EC tube formation), vessel fusion (anastomosis), vessel pruning and pericyte stabilization [226] (Fig. 9).

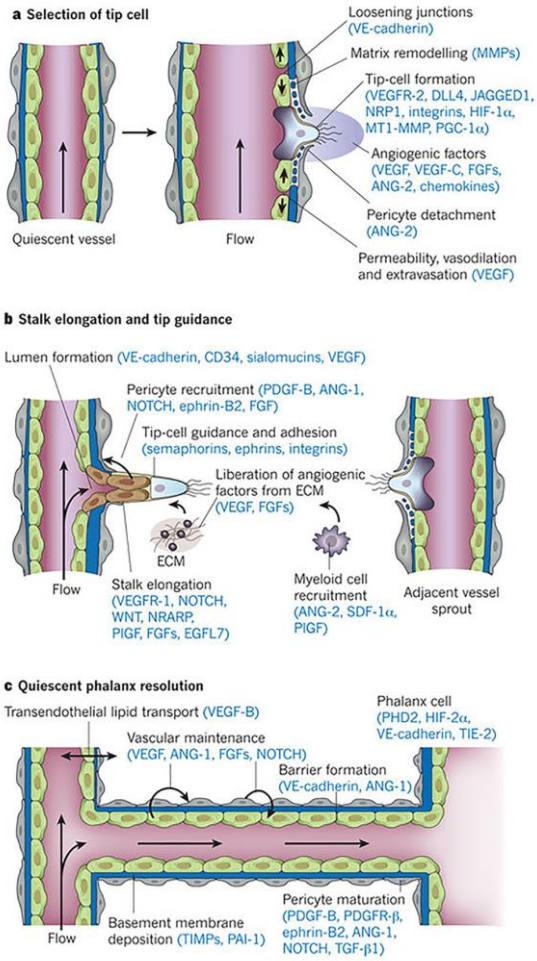

Fig. 9. The sequential steps of vessel sprouting. (A) After stimulation with angiogenic factors, the quiescent vessel dilates and an endothelial cell, tip cell, is selected to ensure branch formation. (**B**) Tip cell at the forefront of the sprout invades the surrounding tissue probing guidance molecules by extending cell protrusions. The stalk cells (behind the tip) proliferate ensuring the elongation of the new vessel branch and the lumen formation. (**C**) Newly formed branches fuse through tip cell–tip cell interactions. Finally, sprout maturation occurs by reconstitution of BM and pericyte/SMC recruitment and ECs acquire a quiescent phenotype (phalanx). Known key molecular players involved in different processes are indicated in parentheses. Modified from [227].

Endothelial cell sprouting. Quiescent ECs, in response to an angiogenic stimulus, are converted to an active phenotype characterized by a high

mitotic index and increased capacity to migrate and degrade the ECM [228]. Sprouting starts with the detachment of mural cells (such as SMCs and pericytes) from blood vessels and when the activated ECs disrupt the tight junctions (TJs, mainly composed by claudin5), adherents junctions (AJs, formed by homophilic interactions of vascular endothelial (VE)-cadherin) and gap junctions, which exist between neighbouring ECs and perivascular cells and invade into the basement membrane and surrounding ECM [220]. Activated ECs begin secreting matrix metalloproteinases, MMPs (especially MMP1, MMP2 and Membrane type 1 Metalloprotease MT1-MMP) to degrade the basal lamina and the surrounding matrix [229].

EC proliferation and directed migration. Initiation of sprouting requires the specification of ECs into tip or stalk cells [230]. The tip cell is an EC in a pre-existing vessel that is selected to become a migratory leading cell [231]. Tip cell is highly polarized and forms filopodia and lamellipodia, cellular protrusions that sense the microenvironment for guidance cues in order to direct navigation of the growing vessel [232]. Filopodia are thin, finger-like and highly dynamic actin-rich membrane protrusions that extend out from the cell edge [233]. Lamellipodia are short protrusions that contain a very branched actin network and are located at the front edge of the cell. In lamellipodia, the intracellular cytoskeleton is connected to the extracellular matrix via adhesion molecules, allowing stress fibers of actin/myosin filaments to pull the cell forward [233].

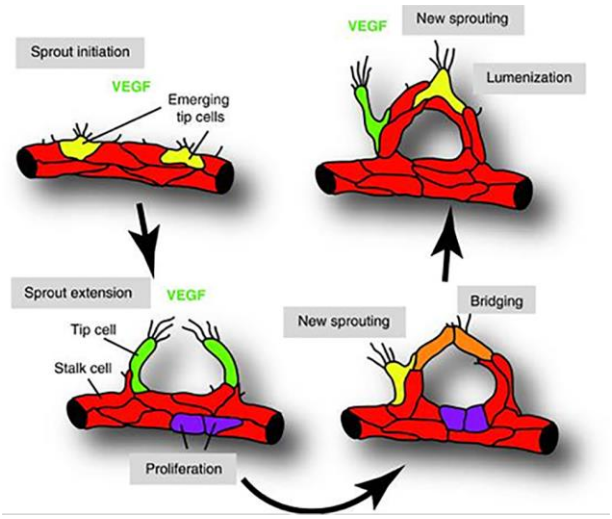

Fig. 10. New blood vessel formation by angiogenic sprouting. The initial step of angiogenesis is the sprouting of tip cells in response to external signalling cues, i.e. VEGF. Tip cells start to migrate followed by proliferative cells, called stalk cells. Migration finishes when other tip cells are encountered, resulting in the establishment of a new connection (anastomosis). Subsequently, lumen formation takes place to allow vessel perfusion by blood carrying nutrients and oxygen. Modified from [234].

While, tip cell does not proliferate and is not implicated in the formation of the vascular lumen [230] stalk cells follow the leading tip cell, proliferate and thereby elongate the growing branch [235]. In addition, stalk cells form the vessel lumen through the *lumenogenesis* process [236]. Together, the tip and stalk cells generate a vascular sprout growing toward an angiogenic stimulus (Fig. 10).

The gradient of VEGF causes the selection of a single EC to became the tip cell, whereas stalk cells differentiate under the influence of the tip cell [237]. It has been recently reported that tip cell controls adjacent ECs in a hierarchical manner through VEGF and Notch signaling pathways [238].

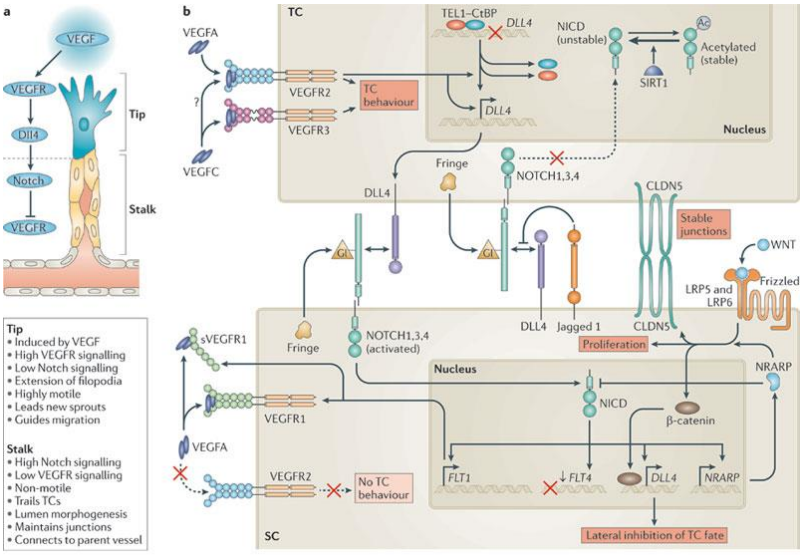

Fig. 11. Hierarchically organization of tip and stalk cells. (A) VEGF signalling induces selection of tip cell, high DLL4 represses VEGFR signalling through Notch by exercising lateral inhibition of stalk cell to become a tip. **(B)** Molecular mechanisms inducing tip cell and stalk cell definition are depicted: VEGF/VEGFR signalling pathway induce DLL4 transcription through disruption of the transcriptional repressor TEL/CtBP (translocation ETS leukaemia/ carboxy-terminal-binding protein). DLL4 activates Notch signalling in stalk cells which in turn inhibits the expression of VEGFR3 (encoded by FLT4) and upregulates the expression of VEGFR1 (encoded by FLT1) and soluble VEGFR1 (sVEGFR1), which represses VEGFR2 function and blocks TC behaviour. Active Notch also induces *DLL4* expression in stalk cell to propagate the DLL4–Notch-mediated lateral inhibition of VEGFR2 and VEGFR3 along developing vessels. Notch-induced Notch-regulated ankyrin repeat-containing protein (NRARP) expression enhances WNT signalling in stalk cells, which stabilizes EC-EC junctions, promotes proliferation and may increase *DLL4* expression via β-catenin. NRARP also promotes negative feedback loop to block Notch signalling in tip cell. Jagged 1 inhibits Notch signalling in ECs by counteracting DLL4–Notch interactions on tip cell when Notch is glycosylated (Gl) by Fringe family of glycosyltransferases. Deacetylation of the Notch intracellular domain (NICD) by sirtuin 1 (SIRT1) may also negatively influence tip cell Notch signalling. Modified from [239].

Binding of VEGF to VEGF Receptor 2 (VEGFR2), which is mediated by Nrp, activates in the tip cell a signaling cascade that blocks binding of a transcriptional repressive complex to *DLL4* promoter [240], thus inducing expression of DLL4 (a ligand for Notch), which activates Notch1 on adjacent stalk cells. In the (future) stalk cells, Notch1 is cleaved in the intracellular domain after DLL4 interaction [241].
This event produces a transcriptional factor that downregulates the expression of VEGFR3 and upregulates VEGFR1 and sVEGFR1, thus blocking VEGFR2 function, filopodia and lamellipodia formation and repressing the tip cell phenotype in stalk cells [241]. Moreover, Notch activation also induces DLL4 expression in stalk cells to propagate the DLL4/Notch-mediated lateral inhibition of VEGFR2 along developing vessels [238]. In addition, Notch upregulates the Notch-regulated ankyrin repeat-containing protein (NRARP) that, through Wnt signaling pathway, maintains EC-EC junctions and promotes proliferation of stalk cells [242] Finally, Notch signalling in tip cells is blocked by Jagged 1 (another Notch ligand), which is expressed in stalk cells and impedes DLL4–Notch interactions on tip cells when Notch is glycosylated (Gl) by Fringe family glycosyltransferases in the Golgi apparatus [243]. Deacetylation of the Notch intracellular domain (NICD) by sirtuin 1 (SIRT1) in stalk cells influence the duration and amplitude of cell Notch signalling [244] (Fig. 11).
Lumen formation and tubulogenesis. In addition to their role in elongating the sprout, stalk cells play also important functions in the vascular lumen formation. Several studies have shown that lumen formation occurs through two major mechanisms: i) cell hollowing, if lumen forms intracellularly by coalescence of vacuoles [245] or extracellularly by exocytosis of vacuoles [246] and ii) cord hollowing, when lumen initiates extracellularly by active repulsion of adjacent ECs and is expanded by active cell shape change [247]. Recently other two models have been proposed as alternative way to form vascular lumen [248]: iii) transcellular lumen formation or membrane invagination, when a non-lumenized EC is fused to an angiogenic sprout, containing a lumen already perfused [249], and iv) lumen ensheathment, observed during cardinal veins development in zebrafish [250].
Even if the mechanisms of lumenogenesis are not completely understood, a critical step is the polarization of the stalk cells, which will be extensively discussed in the next section since this process is controlled at the post-transcriptional level by the AS factor Nova2 [251].
Anastomosis, vessel pruning and maturation. Anastomosis is the fusion process of two tip cells. Even if anastomosis is a EC-autonomous process, it has been shown that macrophages and phagocytic cells of the immune system, serve both as 'bridge cells' and as "guidance posts" in order to precisely orientate tip cells during their fusion [252,253]. Once new connections have been established the newly network undergo to several remodelling processes, including vessel stabilization or regression. This vessel maturation is strongly dependent on the Ang/Tie and DLL4/Notch signalling pathways [239]: Angiopoietin-1 (Ang1), produced by stalk cells, contacts Tie2 receptor and this interaction stabilizes vasculature, mainly by upregulation of *DLL4* expression in ECs and activation of Notch signalling

[254]. As previously mentioned, Notch prevents sprouting by inhibiting VEGFR2 expression and by inducing the expression of NRARP, which in turn activates Wnt signalling leading to increased proliferation and TJ stabilisation [242]. The final step of maturation requires pericytes recruitment for vessel stabilization and its perfusion by blood [255]. Oxygen reduces VEGF signalling and, as a consequence, blocks migration and proliferation of ECs and stimulates AJs formation [256]. These events contribute to the alignment of ECs to generate what are called "phalanx cells" (from the Greek word *phálanx*, meaning military formation) [257].

3.2 Mediators of sprouting angiogenesis

One of the main stimulus for blood vessels formation is the hypoxia, a condition that enhances the protein level of the transcription factor hypoxia inducible factor-1 (HIF-1), which in the nucleus binds to hypoxia response elements (HRE) in the promoters of target genes leading to their activation [258].

The most important HIF-1 target is the VEGF [259]. VEGF was isolated for the first time from the medium of a tumor cell line [260] and subsequently described as one of the most important EC specific cytokine that promotes blood vessel growth [261]. VEGF plays a central role in promoting physiological and pathological (tumor) angiogenesis [262]. VEGF is produced by many cell types (such as macrophages, platelets, keratinocytes and renal mesangial cells) [263–265] and several embryonic tissues during development [266]. Notably, VEGF is upregulated in many cancers and it contributes to tumor angiogenesis [267].

VEGF belongs to a family of glycoproteins comprising VEGFA,B,C,D and E and placenta growth factor PIGF-1 and -2 [268]. VEGF molecules interact with three receptors (VEGF receptors (VEGFR) 1–3, also known as Flt1, Flk1 and Flt4, respectively) [237], characterized by the presence of seven immunoglobulin homology domains in their extracellular region involved in the ligand recognition and receptor dimerization [269]. The intracellular domains of these receptors display a tyrosine kinase activity, which causes receptor autophosphorylation and, subsequently, activation of several signalling pathways, in particular the Raf-Mek-Erk1/2 cascade (for VEGFR2) and the Raf-Mek-Erk1/2 and the PI3-kinase-Akt pathways (for VEGFR3) [270]. In addition, a number of non-tyrosine kinase co-receptors (that mediate VEGF-VEGFR interaction) have been also described, for example the Neurophilins (NRP1 and NRP2) [271]. The most studied family member is VEGFA that plays critical roles in EC migration and proliferation, EC sprouting and tube formation [237]. Moreover, VEGFA induces vasodilation, promotes vascular permeability and EC survival [272].

AS play an important role in controlling VEGFA activity, since this process is responsible for the production of pro- and anti- angiogenic variants. AS occurs extensively within VEGF pre-mRNA, generating various isoforms with different C-terminal domains and distinct affinity for its receptors and with a non-redundant role in angiogenesis [273]. AS of the C-terminal end by using proximal splice sites generates VEGFxxx (pro-angiogenic) isoforms,

whereas the use of distal splice sites promotes VEGFxxxb (anti-angiogenic) isoforms (xxx indicates the position of the amino acid residue in the mature protein). Notably, since VEGFxxx isoforms activate the downstream signaling pathways and stimulate angiogenesis, while VEGFxxxb inhibit this process [274], it is not surprising that VEGFxxxb is preferentially expressed in normal tissues and it is downregulated in cancer [275].

Fibroblast Growth Factor (FGF). Other pro-angiogenic cytokines are the Fibroblast Growth Factors (FGFs). The FGF is a complex family composed of 22 members [276]. Interestingly, FGF-1 and FGF-2 are able to mediate angiogenesis by inducing EC proliferation and migration *in vitro* and *in vivo* [277]. FGF signalling is also important for the maintenance of vascular integrity [278].

Transforming growth factor-beta (TGF-β). Transforming growth factor beta (TGF-β) is a multifunctional cytokine belonging to the transforming growth factor superfamily with critical roles in regulating EC biology [279,280]. TGF-β signal induces the formation of a heteromeric complex, composed of receptor serine kinases (type I and type II receptors), which phosphorylates cytoplasmic receptor-associated Smad proteins (R-Smads) leading to their dissociation from the receptor and their interaction with the common mediator Smad4 to form the active SMAD complex [281]. The active complex accumulates in the nucleus where it directly regulates gene transcription in conjunction with transcription factors [282]. ECs express two TGF- β receptors type II: ALK1 (EC-specific) and ALK5 [283]. Signalling by TGF-β is cellular context-dependent, since it is able to achieve contrasting functions depending by the stage of the angiogenesis process [284] and by the type of receptor bound on ECs. This is particularly evident in cultured ECs, where TGF-β can either promote or suppress EC migration, proliferation, permeability and sprouting [284]. Moreover TGF-β, in synergy with the Platelet-derived growth factor (PDGF), is involved in recruitment of pericytes and vSMCs, allowing the stabilization of the capillary sprouting [228]. Finally, TGF-β promotes the expression of angiogenic signals and ECM-degrading proteases [228], TGF-β upregulates EC-specific expression of VEGF and induces VEGF/VEGFR2-mediated EC apoptosis [285].

Angiopoietins. The angiopoietins family comprises secreted factors angiopoietin-1 and-2 (Ang1 and Ang2) with a variety of function in endothelium mediated by interaction with the EC-restricted Tie2 receptor. Ang1 has strong vascular protective effects, since it is able to suppress plasma leakage, inhibit vascular inflammation and prevent EC death [286]. Moreover, Ang-1 is also known to reduce VEGFA-stimulated vascular permeability [287]. Finally, Ang2 antagonizes Ang1 in the vasculature, preventing branching and sprouting of blood vessels [288].

Other angiogenesis regulators are shown in Table 1.

Table 1. List of other angiogenesis mediators

ANGOGENESIS MEDIATOR	FUNCTION
TNF-α (Tumor Necrosis Factor-alfa)	Inflammatory cytokine, secreted primarily by activated macrophages during inflammation and immune response. Generally it is pro-angiogenic *in vivo*, it mediates angiogenesis directly, by inducing cell differentiation, and indirectly, by stimulating the production of angiogenic factors from other cells [289].
EGF (Epidermal Growth Factor) and HB-EGF (Heparin-binding EGF-like growth factor)	Both induce angiogenesis via activation of PI3K, MAPK (mitogen-activated protein kinase) and eNOS (endothelial Nitric Oxhyde Synthase) in a VEGF-independent fashion [290].
HGF (Hepathocyte Growth Factor)	Mesenchyme-derived cytokine that stimulates the proliferation and the migration of ECs *in vitro* and has angiogenic properties *in vivo*, including stimulation of cell migration, proliferation, protease production, invasion, and organization into capillary-like tubes [291,292].
PDGF-BB (Platelet-Derived Growth Factor)	It is one growth factor that regulates cell growth and division. It contributes to angiogenesis *in vitro* by binding to PDGFR-beta and mediating endothelial proliferation and cord/tube formation, and it may have a paracrine effect on ECs. It is required for the recruitment and differentiation of pericytes during vessel maturation [293,294].
Chemokines	Small heparin-binding proteins, mostly known for their role in inflammation and immune surveillance, recently emerged as important regulators of angiogenesis. They can act either directly via direct regulation of endothelial function downstream of activation of G-protein coupled chemokine receptors or indirectly by recruiting pro-angiogenic immune cells and endothelial progenitors to the neo-vascular niche [295].
G-CSF (Granulocyte Colony-Stimulating Factor)	Modulates angiogenesis by increasing myelomonocytic cells (VEGFR1+ neutrophils) and their release of VEGF. Administration of G-CSF into ischemic tissue provides a novel and safe therapeutic strategy to improve neovascularization [296].
Leptin	Adipose tissue secreted factor that activates the signalling cascades including PI3K/Akt-STAT3 able to activate transcription factor [MCP-1, TNF-*α*, IL-6/-2, and endothelin-1] involved in proatherogenic/angiogenic and inflammatory effects, potentiating endothelial proliferation [297].
Pleiotropin (PTN) or Heparin-Binding Growth Factor-8 (HBGF8)	Regulates the pro-angiogenetic renin-angiotensin pathway. It stimulates new capillary and arteriolar growth in injured tissues [298,299] .
Follistatin (FS)	Inhibiting the negative regulator of angiogenesis activin induces ECs proliferation and angiogenesis [300].

3.3. EC junctions and EC polarization

The mechanisms underlying the establishment of cell polarity and lumen formation have been extensively investigated in epithelial tissues of mammals, where they have crucial roles in several processes, including axon guidance, asymmetrical distribution of cell organelles, membrane trafficking events, asymmetric cell division, differentiation and activation of the immune response [301]. Notably, the importance of the cell polarity is highlighted by the observation that its alteration is linked to several disorders, including cancer progression [302,303]. Only recently it has been shown that the acquisition of apical-basal polarity by ECs is a crucial event for the organization of the vascular lumen during angiogenesis [236]. Indeed, during angiogenesis ECs need to distinguish the apical surface, which faces the lumen of the vessel, from the basal side that remains in contact to the ECM.

As in epithelial tissues and nervous system, a key determinant for the acquisition of the EC polarity is the Par (partitioning defective) polarity complex [304]. This is a quaternary complex that includes: two scaffold proteins (Par3 and Par6), the small GTPases Cdc42 and the atypical protein kinase C (aPKC or PKCξ) [304]. In addition, the small GTPases Rac1 and Rap1 are important regulators of the Par complex during organization of the vascular lumen [305].

The correct localization and activity of the Par complex depend on Par3 (and in particular on its phosphorylated status), which is the major player in promoting the assembly of the whole complex. The first phase of blood vessel lumen morphogenesis involves Par3 binding to JAM (junction adhesion molecule) proteins, an event that will localize the Par complex to the TJs of ECs [306] and causes the redistribution of junctional proteins (including ZO-1, claudin 5, CD99 and VE-cadherin) from the apical EC surface to the vascular cord periphery. Subsequently, Par-3 recruits other components of the Par complex, PKCζ and Par-6, the latter able to recruit Cdc42, which (when bound to GTP) activates aPKC by relieving it from Par6-mediated inhibition. Activated aPKC also phosphorylates Par3 that, as a consequence, dissociates from the complex allowing to aPKC to interact with other substrates in a signaling cascade that determines the segregation of different molecules and different membrane domains [307]. Finally, Par3, through its PDZ domains, remains localized in the TJ seal, whereas the remaining complex Cdc42/Par6/ PKCξ shiftes in the apical and sub-apical region of the EC [308]. Once EC polarity is established, lumen formation is induced by the redistribution of β1 integrin, CD34 and podocalyxin (Podxl), initially located at the cell-cell boundaries [309]. Following its redistribution, Podxl recruits the apical protein moesin, whose accumulation may control lumen morphogenesis by recruiting actin and microtubule cytoskeletons [247] (Fig. 12).

Cdc42 and Rac1 are small GTPase belonging to the Rho GTPase family, which cycle between an inactive (GDP-bound) and an active (GTP-bound) conformational state [310]. The association of both Rac1 and Cdc42 with the Par complex is induced during EC lumen formation [311]. Notably, in their

activated form, they are able to bind downstream effectors (for example p21-activated kinases, Paks) and to stimulate signal transduction pathways modulating the organization of the cytoskeleton [312]. In particular, Pak2 (activated by both Rac1 and Cdc42) and Pak4 (activated only by Cdc42) were found to be required for ECs luminogenesis [312]. In line with this, Pak4 and Pak2 phosphorylation correlates with EC lumen formation and RNA interference-mediated suppression of these kinases strongly inhibits these processes [312].

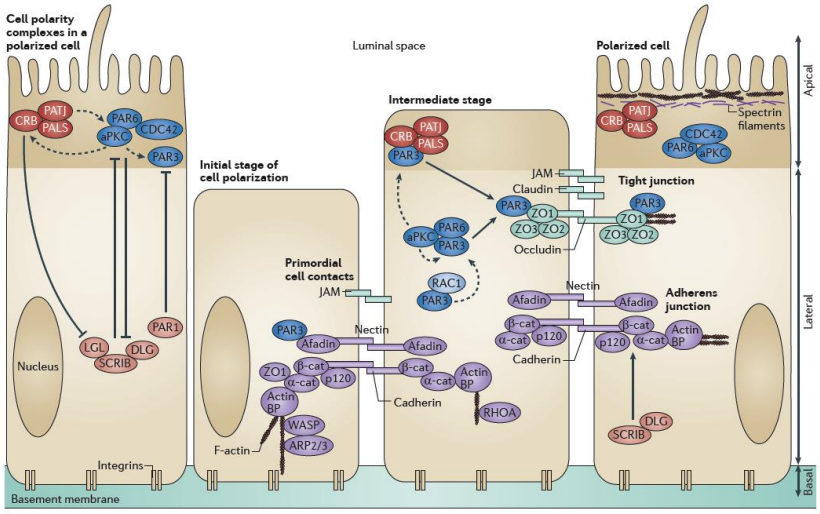

Fig. 12. Par polarity complex is essential for establishment of apical-basal cell polarity. The Par complex (composed of Par3, Par6 and Pkcξ) is shown as blue figures in epithelial cells. Other complexes (Crb/Palsj/Patj,in red and Scrib/Lgl/Dlg in orange) involved in apical-basal polarity are also represented. At early stages of cell polarization Par3 binds to afadin and localizes at the apical-basal membrane of the cell. When Par6 recruits active Cdc42, Pkcξ is activated and phosphorylates Par3, which in turn exit from the complex and remains localized at TJs, defining the apical-lateral side of the cell, while Par6, Pkcξ and Cdc42 define the apical membrane. Dotted arrows represent the different subcellular translocations. Modified from [307].

Recent studies have shown that also the cerebral cavernous malformation (CCMs) signaling proteins (in particular CCM2 and CCM1) are required for the correct localization and to promote activation of the Par polarity complex [305,313,314]. Interestingly, CCM1 stabilizes the AJs (primarily through a direct binding with the vascular endothelial-cadherin, VEC) and stimulates the recruitment of the Par complex at the cell-cell junctions [305]. In addition, the endothelial-restricted Ras interacting protein 1 (Rasip1) and its binding partner RhoA GTPase-activating protein 29 (Arhgap29) were also found to influence EC lumen morphogenesis [315]. Remarkably, depletion of either Rasip1 or Arhgap29 has been shown to impair endothelial tube morphogenesis by altering EC polarity and adhesion and by affecting the organization of cytoskeletal and the structure of the

junctional EC complexes. Notably, these defects resulted from inhibition of Cdc42 and Rac1 signalling pathways [315].
In epithelial tissues, cell polarity is also regulated by Discs large/Scribble/Lgl proteins and Crumbs/PALS1/PATJ complexes, which localize, respectively, to the AJs and TJs and separate apical and basolateral domains to further regulate apical/basolateral polarity [316,317]; yet, the role of these complexes in EC function and polarity are poorly understood. Interestingly, it has been recently found that Scribble is highly expressed in ECs and involved in directional EC migration [318], a process that depends by the establishment of cell polarity [319]. Notably, Scribble depletion in zebrafish was reported to impair angiogenic processes, delay the formation of intersegmental vessels and cause several malformations of the vessels (especially in the brain), in particular a strong haemorrhagic phenotype [319].

4. The neurovascular link

To perform more complex functions, during evolution vertebrates have evolved two highly specialized systems consisting of ordered networks of branched structures: the nervous system, with neurons characterized by long fibers (axons) that connect the CNS to every other part of the body, and the vascular system, with arteries to supply oxygen and nutrients to the organs, and veins to deprive them of waste and toxic compounds [320].
In 16th century the Belgian anatomist Andreas Vesalius (the founder of the modern human anatomy), by performing dissections on cadavers, observed that vessels and nerves display similar patterning [Vesalius, A De Humani Corporis Facrica (The fabric of the Human Body) (Oporinus, Basel, 15439] (Fig. 13).

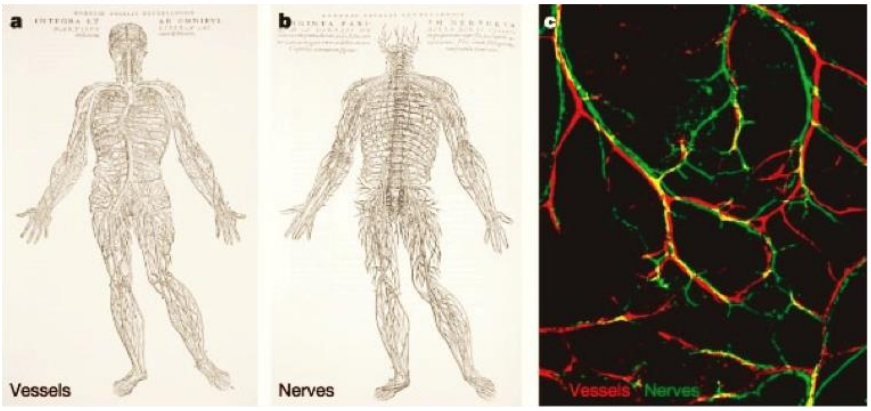

Fig. 13. The neurovascular link. Andrea Vesalius drawing of the anatomical parallelism of vascular and nervous systems (left). Nerves (green) and blood vessels (red) alignment to reach their tissue targets. Modified from [321].

Indeed, he reported that, although the nervous and vascular system are functionally different, they proceed alongside each other and share a high degree of anatomic parallelism in several regions of the body. However, it

has only recently emerged that, in addition to anatomical similarities, these systems also present several cellular and molecular analogies and common functional organization than previously expected [322,323].
During their growth vessels and nerves possess similar specialized structures able to select the right trajectory in the surrounding tissues: the tip cell and the axonal growth cone. The tip cell is a highly polarized and specialized subtype of EC at the forefront of endothelial sprouts that, through the extension of numerous filopodia, explores the environment and guides the new blood vessel towards the angiogenic stimulus in order to reach its distant target tissues [321] (Fig. 14). Analogously, the growth cone is a highly mobile and sensory structure located at the end of the growing axon that, through dynamic cycles of extension and retraction of filopodia, constantly probes the environment to guide the axon to its final target in a process called "axon guidance" [321] (Fig. 14).

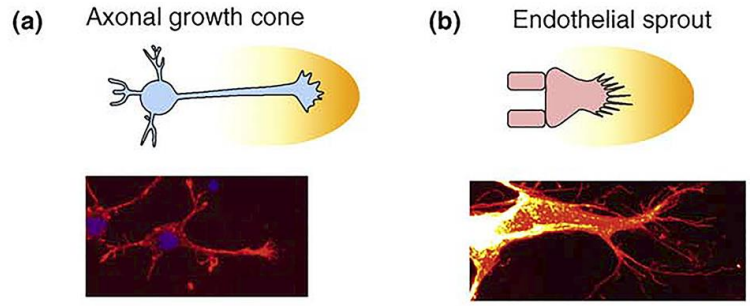

Fig. 14. Similarities between axonal growth cone and endothelial tip cell. (**A**) Schematic representations (upper panels) and real images (lower panels) of a mouse cortical neuron stained for actin (red) and DAPI (blue) and a mouse retinal endothelial tip cell stained for the endothelial-specific marker CD31 (red) following attractive guidance cues (**B**). Modified from [321].

Since the vascular system developed later than nerves during evolution, it has been proposed that the explanations for their similar functional organization is that neurons and ECs are able to respond to common classes of signals. Indeed, neuronal signals that control axon guidance (such as netrin/DCC/UNC, Slit/Robo, semaphorin/NRP/plexin and Eph/ephrin families) are also recently linked to vessel patterning [234]. Interestingly, to emphasize the similarity between vascular and nervous systems, molecules regulating development of both systems have been recently termed "angioneurins" [324]. For example, the ephrin protein family of class A and class B by binding to Eph A and B subfamilies of cell-surface receptors, are able to mediate axon guidance as well as synapse formation in nervous system, whereas they are essential for arterial-venous specification during vascular development [323]. Notably, the prototypic angioneurin is the vascular endothelial growth factor (VEGF), originally discovered as a key angiogenic factor that stimulates EC survival, proliferation, migration, differentiation and permeability [230], but recently found to have important roles also during development (and disease) of the nervous system, where it acts as a neuroprotective, neurotrofic and neuroprolifertive factor [325].

Recent studies further provide evidence that the "neurovascular link" (term used to describe the strong connections - anatomical, cellular and molecular - between the vascular and the nervous systems) [322], is more important for understanding the molecular basis of several vascular and neuronal disorders [322]. Indeed, blood vessels and nerves cross-talk, are functionally interdependent and influence their mutual development [322–324]. Accordingly, axons have the ability to guide vessels during their path, and vice versa [321], whereas ECs support normal functioning, ensure maintenance, and promote reparative regeneration of the CNS [326]. Moreover, the CNS is characterized by a peculiar "neurovascular unit", which plays important role to mantain neuronal homeostasis, the blood-brain barrier (BBB), composed of ECs, pericytes (e.g., mural cells of the vascular smooth muscle lineage surrounding capillaries), astrocytic endfeet and neurons [327]. Given the clinical importance of the BBB as a critical barrier for several drugs, a further characterization of the molecular basis of the neurovascular unit will be crucial to improve our understanding of several human disorders and to identify new therapeuthic strategies.
It is noteworthy that malfunctioning or an imbalance in angioneurin signaling has been observed to contribute to various neurological disorders indicating that these diseases do not result exclusively from neuronal defects [324]. In line with this, vascular abnormalities have also been identifies in several neurodegenerative disorders, including Alzheimer's disease (AD), Parkinson's disease (PD) and amyotrophic lateral sclerosis (ALS). Notably, vascular dysfunction observed in AD can be observed before disease onset, suggesting that these vascular alterations might causally contribute to disease initiation or progression [328]. Since angioneurins (especially VEGF) have both vascular and neuronal effects, their pharmacological targeting might offer novel opportunities to develop innovative therapeutic strategies for neurological diseases. In line with this, VEGF gene therapy was successfully used to delay the onset of paralysis and extend overall survival in preclinical models of ALS [329,330].

4.1 The angioneurins family

Angioneurins family comprises classical axon-guidance cues, such as netrin/DCC/UNC, Slit/Robo, semaphorin/NRP/plexin and Eph/ephrin families, which also regulate vascular development [323]. The observation that several neuronal diseases have also vascular abnormalities [324] quickly led to the identification of several other members of the angioneurins family (see Table 2). In this paragraph, I will discuss canonical neurotrophic factors that have been shown to act on ECs and have angiogenic properties.
Netrins. In mammals, netrin family is composed by secreted laminin-related molecules (Netrin-1, -3, and -4) and proteins tethered to the cellular membrane by a glycophosphatidylinositol Glycophosphatidylinositol (GPI) anchor (Netrin-G1 and -G2) [331]. Netrin-1, -3, and -4 interact with specific receptors: the DCC (deleted in colorectal cancer) family (consisting of DCC and neogenin) and the uncoordinated (UNC) 5 subfamily (UNC5A, B, C and D and Down syndrome cell adhesion molecule, DSCAM) [332]. On the

contrary, Netrin-G proteins do not bind any of the known netrin receptors, but specifically interact with NGL-1 (netrin-G1 ligand) and NGL-2 (netrin-G2 ligand) [333].

Netrins function as attractants or repellent signals for neurons and ECs and these effects are dependent on the type of receptor they contact [332]. In particular, attractive signals are elicited through activation of the DCC or DSCAM signalling pathways [334], whereas repulsion is dependent on the UNC5 receptors, either as homodimers or heterodimers with DCC [335].

Interestingly, the Netrin receptor Unc5b is predominantly expressed in ECs and functions as a repulsive guidance receptor during vessel patterning [336]. Since Unc5b induces retraction of the tip cell filopodia and vessel regression (antiangiogenic effects), its depletion in mouse and zebrafish embryos has been shown to cause ectopic filopodial extension from endothelial tip cells and extra-branching of blood vessels [337]. On the contrary, inactivation of Netrin-1 is associated with a loss of vessels during zebrafish development suggesting a pro-angiogenic effect of Netrin-1 [338]. Recently, Unc5b has been described as a "dependence receptor" [339]. The cytoplasmic portion of the Unc5b receptor contains a death domain able to induce apoptosis of receptor expressing cells in the absence of its ligand Netrin-1, whereas ligand binding triggers survival signaling [339] by blocking the death-associated protein kinase (DAPK) pathway [340]. The observation that Netrin-1 acts as a survival factor for ECs, by blocking the proapoptotic effect of the dependence receptor Unc5b [339], reconciles the initial apparently contradictory conclusions that Netrin-1 is either a pro- or an antiangiogenic factor [337,338].

Finally, the EC-specific axon guidance receptor Robo4 was also described as novel Unc5b interaction partner. Notably, by binding to Robo4, Unc5b maintains vascular integrity by counteracting VEGF signaling [341].

Semaphorins. Semaphorins (about twenty) are both membrane-bound and soluble molecules that function mainly as repulsive guidance factors during axonal pathfinding [342]. They are classified in eight groups and function through two types of receptors: plexins (divided into four subclasses A, B, C, and D) and neurophilins (Nrp1 and Nrp2) [343].

Semaphorin-3A and Semaphorin-3E are the best studied in vasculature [343]. Semaphorin-3E and its receptor Plexin-D1 negatively regulate angiogenesis in zebrafish by modulation of VEGF signalling [344]. In line with this, depletion of Plexin-D1 in zebrafish has been shown to cause increased intersomitic vessel branching [345].

Semaphorin-3E plays important role in vascular development where it functions as a repulsive cue for Plexin-D1 expressing ECs [346]. At a molecular level, Semaphorin-3E/Plexin-D1 induces the cytoskeleton collapse by activation of Arf6, which triggers integrin-β1 internalization, and by negative regulation of the cell-ECM adhesion interactions [347].

During embryogenesis, Nrp1 and Nrp2 are initially co-expressed in the ECs, but as development proceeds, Nrp1 becomes restricted to arteries, whereas Nrp2 to veins and lymphatic vessels [348]. Interestingly, Nrp1 plays a role in tip cell selection since ECs with higher Nrp1 levels have a higher chance to become a tip cell rather than a stalk cell during sprouting

angiogenesis [349]. Remarkably, Nrp1 has also been implicated in the arterial-vein specification [350].

Ephrins. Ephrin receptors (Eph) and ephrin ligands are not secreted molecules initially identified in the CNS where they are involved in several processes including cell movement, adhesion, shape, proliferation, survival and differentiation [351]. In particular, Eph receptors are tyrosine kinases characterized by the presence of a single cytoplasmic kinase domain that becomes activated after binding of their ephrin ligands. In mammals 14 Ephs have been identified [352]. Ephrin B2 and its known receptor Ephb4 are the most studied members of this family in ECs due to their strikingly restricted expression in arteries and veins, respectively [353]. Ephrin B2 and Ephb4 act during blood vessel morphogenesis and, in particular, this signaling pathway functions by sorting arterial and venous ECs into their respective vessels [354]. In line with this, depletion of ephrin B2 or its receptor EphB4 in mouse has been shown to cause several vascular defects, including expanded aortae, underdeveloped cardinal veins and ECs with venous identity that were mislocalized in the aorta [354]. Notably, Ephrin B2 is also able to directly interact with VEGFRs and regulates VEGF signalling [355].

Slits. The Slit proteins form another family of secreted molecules involved in axon guidance in CNS where they repel axon growth cones upon binding of Roundabout (Robo) receptors [356]. Of the four known mammalian *Robo* genes (*Robo1*, *Robo2*, *Robo3* and *Robo4*), *Robo4* is selectively expressed in ECs and has been implicated in vessel permeability [357,358]. In particular, studies in mice and in zebrafish indicate that Robo4 maintains vascular integrity and inhibits angiogenesis by counteracting VEGF-mediated signalling [359,360]. However, Slit-Robo signalling also induce neovascolarization, cooperating with VEGF-A by means of scaffold proteins Nck1/2 and Rac1 [361].

ECs also express Robo1/2 receptors and Slits (in particular Slit2) which promote EC migration and modulate EC polarity during angiogenesis [362]. Finally, splicing plays important role in controlling Slit signalling. Indeed, AS of *Slit2* pre-mRNA produces a transcript lacking exon 15 and encoding for a molecule (Slit2-ΔE15) with higher capacity, compared to the full length protein, to induce vessels stabilization [363], suggesting that Slit2-ΔE15 could play important role to increase efficacy of chemotherapy and radiotherapy.

Table 2. The angioneurins family

ANGIONEURIN	FUNCTION
BDNF (Brain-Derived Neurotrophic Factor)	It is required for the maintenance of cardiac vessel-wall stability during development. Interestingly, in the adult, BDNF stimulates angiogenesis in the heart, skeletal muscle and skin by binding to its receptor, TrkB, on ECs. It also stimulates revascularization of ischaemic limbs by recruiting proangiogenic bone marrow cells [364,365].
IGF-I (Insulin-like Growth Factor-1)	Modulates the basal brain angiogenesis taking part in vessels development. Promotes neurovascular regeneration in stroke, repairs the decline of vascular density that accompanies brain aging [366].
EPO (Erythropoietin)	Prevents vascular degeneration; stimulates angiogenesis. Decrease vascular permeability by preservation of the BBB by restoring expression of the tight junction proteins [367].
NGF (Nerve Growth Factor)	It stimulates angiogenesis, either indirectly, by increasing the expression of VEGF, or directly, by promoting vascular cell growth [368].
PDGF (Platelet Derived Growth Factor)	It is produced by capillary ECs and signaled to neighboring vSMC/perycites) progenitors to promote their migration along angiogenic sprouts and to recruit them to newly formed vessels [369].
PGRN or GRN (Granulin)	It is a member of the granulin/epithelin family of growth factors. PGRN stimulates cancer progression and tumor angiogenesis, at least in part by affecting EC directly (although it also affects them indirectly by upregulating VEGF expression). PGRN also has direct neurotrophic effects on motor and cortical neurons [370].
NT3 (Neurotrophin 3) and NT4 (Neurotrophin 4)	Members of Neurothrophins family. NT3 is required for proprioceptive neuron survival and induces angiogenesis by activating the PI3K-Akt-eNOS signalling pathway. NT4 could promote angiogenic activities in adult mice and it is necessary for the successful growth of regenerating axons in peripheral nerves [371,372].

5. Tumor angiogenesis and anti-angiogenic therapies

As reported before, angiogenesis is the physiological process through which new blood vessels form from pre-existing vessels [217]. This process is also critical for the pathogenesis of several disorders and to support cancer development and progression [373]. Indeed, in order to grow beyond 2-3 mm in size, the tumor mass needs to develop an own vasculature to obtain oxygen and nutrients [374,375]. In addition, angiogenesis also provides tumor tissues with the metastatic route to colonize distant organ [376]. For all these reasons, angiogenesis is a hallmark of cancer.

Sprouting angiogenesis is the most commonly studied modality of new vessel formation in tumors and hypoxia is the major stimulus to induce tumor angiogenesis [258]. In the early stages of tumor growth, the increased

metabolism of tumor cells causes localized hypoxia, a condition that induces expression of HIF-1 [377]. The HIF-1 mediated response to hypoxia determines the secretion, by multiple cell types within the hypoxic tumor microenvironment, of a number of angiogenic growth factors such as VEGF and FGF that activate sprouting angiogenesis from neighboring vessels [378].

ECs respond to hypoxic conditions by proliferating and migrating into the hypoxic area [258]. Furthermore, blood vessels support cell recruitment leading to stabilization of the newly formed vessel; in particular, they continuously recruit leukocytes from the circulation that in turn can stimulate neo-vascularization [379].

In addition to sprouting angiogenesis, it has to be mentioned that tumors are able to build their vasculature through other mechanisms: i) vasculogenesis (when endothelial progenitor from the bone marrow differentiates to ECs); ii) vessel co-option (when tumor cells co-opt pre-existing vessels); iii) vascular-mimicry (when tumor cells line tumor vessels mimicking a real vascular endothelium) and iv) cancer stem-like cells differentiate to ECs [380]. However, several analyses showed that tumour vasculature presents specific functional characteristic and it is morphologically and structurally aberrant compared to normal resting vessels in the organism. This is the consequence of the fact that an altered balance of pro- and anti-angiogenic cytokines triggers EC proliferation and migration [381]. In contrast to physiological angiogenesis, in tumor the levels of angiogenesis stimulators overcome that of inhibitors, thus promoting vessel neo-formation. In contrast to physiological angiogenesis, in particular, tumor vessels show high fragility, they are poorly organized, hyperpermeable and characterized by hemorrhagic phenotype; the cellular junctions are weak and this causes fenestrations between ECs and offers to cancer cells the opportunity to escape from primary tumor and form metastasis. In addition, tumor blood vessels are characterized by high heterogeneity with a severely altered lumen (defined as "mosaic"): they are enlarged, tortuous in some regions, whereas they are very thin in other parts. Finally, tumor ECs in the tumour vasculature show aberrant EC polarity, they can detach from the basement membrane and at the same time they can form protrusions in the lumen [382].

The idea of blocking angiogenesis as a strategy to arrest tumor growth arose in 1971 when Prof. Judah Folkman proposed that tumor growth is angiogenesis dependent [383]. He hypothesized that the destruction of tumor blood vessels can lead to cancer regression since tumor cells rely on blood vessels to obtain nutrients and oxygen and satisfy their metabolic needs ("anti-angiogenic therapy"). Successively, an increase of interest in angiogenesis research has provided evidence that inhibition of angiogenesis could reduce tumor growth [384,385] and has generated the indispensable understandings to develop the first clinically approved anti-angiogenic agents [227]. Indeed, tumor vascular ECs are interesting for a number of reasons: *i)* they are readily accessible for drugs *via* the blood circulation; *ii)* they are genetically stable and therefore would respond in a consistent and predictable way to drugs; *iii)* inhibition or regression of tumor vessels leads,

in most cases, to cancer cell death and it is estimated that more than 100 tumor cells rely on a single EC for their survival.

Today, the study of anti-angiogenic therapies has yielded several anti-cancer treatments approved by the U.S. Food and Drug Administration (FDA) [386]. The main categories of anti-angiogenic therapies are monoclonal antibodies, directed against endothelium specific growth factors and its receptors and small molecule tyrosine kinase inhibitors (TKIs) of pro-angiogenic growth factor receptors [387]. Several of those drugs are being tested in pre-clinical studies also as therapeutic targets in other diseases (various ischaemic and inflammatory diseases) since increasing evidence showed that pathological angiogenesis is an important process to support their development [373].

The first FDA approved anti-angiogenesis inhibitor was the Bevacizumab (Avastin Roche/Genentech, commercial name), a humanized monoclonal antibody that, by binding to active VEGF, is able to block its interaction with VEGFRs and the down-stream signalling pathway. It has been approved for colorectal cancer [388], non-small cell lung cancer [389], renal cancers [390], ovarian cancer [391], glioblastoma multiforme of the brain [392] and in combination with other drugs (paclitaxel) in metastatic breast cancer [393]. Other FDA approved drugs are the Sorafenib (Nexavar; Bayer) and the Sunitinib (Sutent; Pfizer), small molecules inhibiting VEGFR1, 2 and 3 signaling used in the treatment of patients with advanced hepatocellular carcinoma [394] and advanced renal cell carcinoma [395]. Another important class of anti-angiogenic agents is represented by the inhibitors of mTOR, a regulator of PI3 kinase/AKT pathway relevant for angiogenesis and cancer progression [396]. Recent evidence indicated that rapamycin and related mTOR inhibitors also inhibit VEGF expression and limit VEGF-dependent EC proliferation in treatment of human eye diseases with ocular neovascularization [397].

VEGF-targeted therapies (such as Avastin) have shown to be efficacious in a number of cancers, particularly when combined with conventional chemotherapeutics [398]. However, in most cases these therapies prolong disease-free survival of the patients of just a few months [386]. Notably, it has been reported that, so far, the benefits of anti-angiogenic agents are transient and these therapies have showed modest therapeutic effects for a number of reasons: 1) inhibition of a single target leads to the upregulation of additional angiogenic factors (such as angiopoietin 1) [399]; 2) VEGF blocking is applicable only on new vessel growth but not on pre-existing vessels [399]; 3) the primary response of the patients is often followed by the establishment of resistance mechanisms and they acquire an established vasculature [399]; 4) in several cases, tumors activate escape or evasion process in response to VEGF inhibition leading to acquisition of more aggressive features, which promotes invasion and metastasis formation [399].

A promising novel paradigm that might complement current anti-angiogenic strategies is based on the so called hypothesis of "tumor vessel normalization" [400]. Indeed, several studies performed in the '90s, have shown that drugs that inhibit VEGF signaling can briefly restore ("transient window") several of the abnormal aspects (in structure and function) of

tumor vasculature [401,402]. It was postulated that transient vessel normalization can decrease the tortuosity of tumor vessels and stimulate vessel maturation through the recruitment of pericytes and the normalization of vascular basement membrane [227]. In addition, it has been reported that vessel normalization is able to reduce the interstitial fluid pressure, the oedema and, more importantly, to increase in a transient manner perfusion, oxygenation and drug delivery [227]. Based on these observations, vessel normalization is currently emerging as a novel opportunity to improve the responsiveness to chemotherapy, immunotherapy and radiation therapy [227,403].

Recently, it has become clear that the "angiogenic switch" is not only driven by pro-angiogenic growth factors but is also the result of several alterations in the metabolism of ECs [404]. Thus, the "angiogenic switch" also needs an "angiogenic metabolic switch" in which ECs adapt their metabolism to generate additional energy to sustain their growth, proliferation and migration [405]. Similar to cancer cells, tumor ECs are highly glycolytic and, even if oxygen is available for oxidative glucose metabolism, they use aerobic glycolysis. Interestingly, pro-angiogenic factors regulate EC metabolism: for example, VEGF induces the expression of the glucose transporter GLUT1 [406], the lactate dehydrogenase B [407] and the glicolysis activator PFKFB3 (6-phosphofructo-2-kinase/fructose-2,6-bisphosphatase 3) [408]. The dependence of ECs on glycolysis suggest that this signalling pathway could be a possible target for anti-angiogenic therapy. In line with this hypothesis, EC-specific depletion of *PFKFB3* or its inhibition with small molecules was found able to impair glycolysis and angiogenesis and, more importantly, inhibit tumor growth *in vivo* [409].

Although the anti-angiogenic therapy is considered, worldwide, a promising anti-cancer approach, these findings indicate that tumor angiogenesis is a much more complex phenomenon than previously anticipated. Hence, a better understanding of the molecular mechanisms sustaining growth of tumor vessels could help to overcome these problems; moreover, it will be crucial to identify novel and more efficient anti-angiogenic therapies for cancer treatment.

BACKGROUND AND AIM OF THE THESIS

Until now, molecular pathways regulating angiogenesis have been suggested to act primarily through the regulation of transcription [410]. Instead, our recent data indicate that post-transcriptional programs play important roles to regulate endothelial cells (ECs) biology. In particular, for the first time, our group demonstrated that AS regulation orchestrates some important features of the vascular development [251]. We found that the AS factor Nova2, previously considered to be neural cell-specific [57], is also expressed in ECs of the blood vessels and regulated during angiogenesis [251].
As amply discussed in the introduction, Nova2 is one of the best characterized mammalian tissue specific AS regulators, which is involved in establishing the appropriate spatio-temporal generation of splicing variants during neuronal differentiation [46,60]. In particular, Nova2 controls AS of pre-mRNAs encoding for molecules involved in synaptic development, synaptic transmission, cell-cell signalling, axon guidance, and dynamic organization of the actin cytoskeleton [46,57,60].
Several studies have highlighted significant similarities between the nervous and vascular systems and molecules affecting both neural and vascular functions were recently termed "angioneurins" [324]. An important functional similarity in the development of the vascular and nervous systems is the establishment of the apical-basal cell polarity; indeed, it is a crucial event for the organization of the vascular lumen, a fundamental step during angiogenesis occurring concomitantly with invasion and growth of the incipient vascular sprout [236], and for axon guidance [411], respectively. Notably, the Par polarity complex is a key element of cell polarity in both systems [236,411]. The specific localization and activity of the Par polarity complex involve the association of four key components: Par3, Par6, the small GTPase Cdc42 and the atypical protein kinase C (PKCz) [236]. In addition, the small GTPases Rac1 and Rap1 are important regulators of the Par complex during organization of the vascular lumen [236,305].
Through gain- and loss-of function approaches, we found that Nova2 depletion in cultured ECs impairs the apical distribution and the downstream signaling of the Par polarity complex, resulting in altered EC polarity. These defects are linked to AS changes of Nova2 target exons affecting the Par complex and its regulators. To study the biological role of Nova2 *in vivo*, in collaboration with Prof. Elisabetta Dejana (IFOM, Milan-Italy), we used *nova2* morpholino-mediated knockdown in the embryos and larvae of zebrafish, which constitutes a unique and powerful model to study vertebrate vascular development [412]. To independently validate our findings, we have also used clustered regularly interspaced short palindromic repeat (CRISPR)-induced genetic mutation to generate *nova2* mutant fish. By using these approaches, we demonstrated that Nova2 controls the development of the vascular system *in vivo* by modulating endothelial polarity and lumen formation [251].
On the basis of the fact that Nova2 affects both neural and vascular cell processes, we suggest that Nova2 is a novel member of the "angioneurins" family. Interestingly, Nova2 is the only member of the "angioneurins" family defined so far that functions as post-transcriptional regulator.

Our results highlight the importance of using high-throughput strategies to identify new AS isoforms regulated during angiogenesis. Since AS and transcription predominantly regulate independent sets of genes [19,413], our main goal is to characterize AS regulation of angiogenesis and to identify novel Nova2-regulated AS isoforms that are responsible for this process.
The specific aims of my PhD project were:

1) to identify novel Nova2 targets in ECs (*Chapter I; III and IV of the Results*);
2) to characterize the functional role(s) of selected Nova2-mediated AS variants in ECs (*Chapter II of the Results*).

In order to identify genes with an AS modulated by Nova2 in ECs, *Nova2* gain- and loss-of-function ECs were analyzed by RNA-Seq (high-throughput sequencing of RNA). Moreover, to identify direct Nova2 mRNA targets, I have also used CLIP-Seq (UV-induced crosslinking, immunoprecipitation and sequencing), a technique already performed successfully to identify Nova2 targets in the brain [82]. In collaboration with Dr. Markus Landthaler (Max Delbrück Center for Molecular Medicine, Berlin-German), I already completed the CLIP experiment and sequencing and I am currently waiting for the bioinformatic analysis of the results.

RESULTS

CHAPTER I
Identification of novel genes modulated by Nova2 in endothelium by RNA-Seq of *Nova2* knockdown ECs

In order to identify novel genes with an AS pattern modulated by Nova2 in ECs, *Nova2* loss-of-function ECs were analyzed by RNA-Seq, which was performed on two replicates of RNA extracted from *Nova2* knockdown ECs compared to control ECs [251]. In particular, to generate stable *Nova2* knockdown cells, in collaboration with Prof. Dejana we used lentiviral vectors carrying the shRNA specific for mouse *Nova2* gene and VE100 cells, an immortalized mouse EC line generated and extensively characterized by our collaborator [414]. To build a complete map of the Nova2-regulated AS events in endothelium, bioinformatic analysis was performed in collaboration with Dr. Manuel Irimia (EMBL/CRG, Barcelona) and Prof. Benjamin J. Blencowe (University of Toronto, Canada) and *vast-tools* (Vertebrate Alternative Splicing and Transcription Tools) was used to identify and quantify all major types of AS events (including single and multiple cassette exons and microexons, alternative 5' and 3' ss and alternatively retained introns) from each RNA-Seq sample [415]. In particular, *vast-tools* map reads to comprehensive sets of exon-exon junctions (EEJs) and exon-intron junctions (EIJs) to derive alternative sequence inclusion levels (PSIs, "Percent Spliced In", for exons; PIR, 'Percent Intron Retention', for introns) [39]. Differentially regulated AS events were defined as those showing an absolute $\Delta PSI \geq 15$ between *Nova2* knockdown and control means and a $\Delta PSI \geq 15$ between the ranges of the two groups. *vast-tools* program identified 365 AS events differentially regulated upon *Nova2* depletion with respect to control ECs, including 188 (51,5%) cassette exons (Fig. 15A and Table 3 in Appendix). The AS events were subdivided on the basis of the predicted impact on the coding sequence of the affected genes in (Fig. 15B):

i) 41% (150) AS events predicted to generate protein isoforms both when Nova2 is present or depleted (Prot. Isoforms);
ii) 37% (135) AS events predicted to trigger non-sense mediated decay (NMD) or create a truncated protein when Nova2 is present (Dysf. with Nova2);
iii) 9.0% (33) AS events predicted to trigger NMD or create a truncated protein when Nova2 is absent (Dysf w/o Nova2);
iv) 11.0% (40) AS events in non-coding regions (UTR);
v) 2% (7) AS not able to be catalogued into the previous categories.

Using ClueGo software, we performed a Gene Ontology (GO) enrichment analysis of AS events predicted to generate alternative protein isoforms (41% of all AS events and 64% of cassette exons, Fig. 15B). Interestingly, we found a significant enrichment for genes involved in cytoskeleton organization. In addition, the strongest enriched functional terms corresponded to chromatin remodeling and regulation, suggesting a multilayered impact of Nova2 regulation on ECs biology. Finally, we also observed multiple GO terms related to neuronal differentiation and function

(e.g. positive regulation of neurogenesis and nervous system development), similar to those reported for Nova-regulated genes in neuronal cells [57] (Fig. 15C).

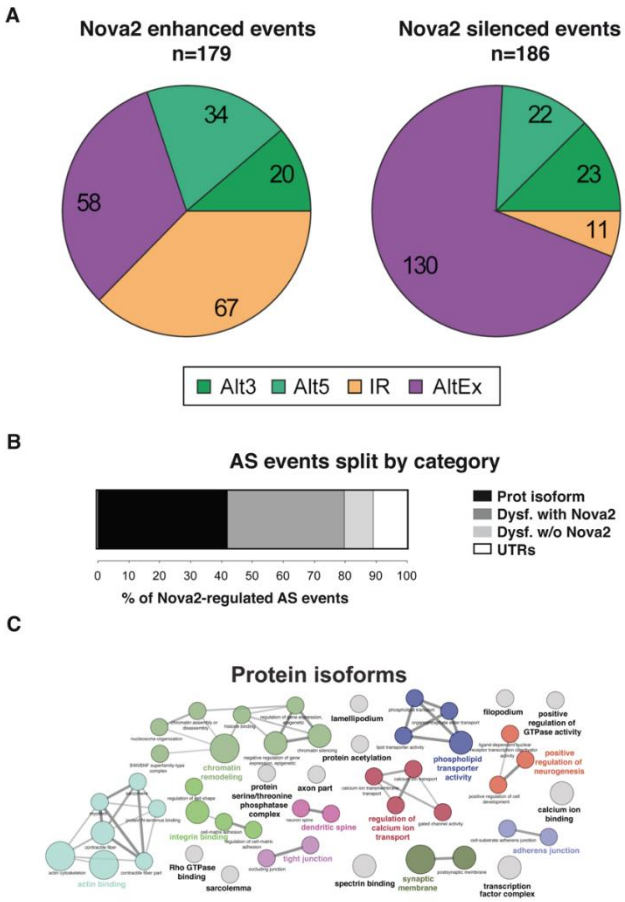

Fig. 15. Nova2 regulated AS events in ECs. (**A**) By performing RNA-Seq of *Nova2* knockdown and control ECs, we identified 365 AS events affected by Nova2 depletion classified as: alternative use of an internal cassette exon (AltEx), intron retention (IR), alternative 5' ss (Alt5) and alternative 3' ss (Alt3). (**B**) The 365 AS events were also subdivided on the basis of the predicted impact on the coding sequence of the affected genes in: (i) AS events predicted to generate protein isoforms both when Nova2 is present or depleted (Prot. isoforms); (ii) AS events predicted to trigger non-sense mediated decay (NMD) or create a truncated protein when Nova2 is present (Dysf. with Nova2); (iii) AS events predicted to trigger NMD or create a truncated protein when Nova2 is absent (Dysf. w/o Nova2) and (iv) AS events in non-coding regions (UTRs). (**C**) Gene Ontology (GO) enrichment analysis with ClueGo software. GO terms are represented as nodes based on their kappa score level (>0.4). The node size represents the term enrichment significance. Figure modified from [251].

Since Nova2 is expressed in both brain and ECs, we analyzed the overlap between alternative exons predicted to be regulated by Nova proteins in the brain (325 cassette exons identified by [416]) and those showing changes in

inclusion levels upon *Nova2* knockdown in the endothelium. Nearly all (319/325) exons could be matched to *vast-tools*. Of these, 61% (195/319) had enough read coverage to derive inclusion estimates (PSIs) in all four EC RNA-Seq samples. From these, 28/195 (14.4%) exons showed a difference in PSI (ΔPSI) ≥10 upon *Nova2* knockdown in ECs in the same direction as previously predicted for Nova proteins in the brain, revealing a highly significant overlap (p value<0.05) between alternative exons predicted to be regulated by Nova proteins in the brain and those showing changes in inclusion levels upon *Nova2* knockdown in endothelium. Only 2/195 (1%) changes go in the opposite direction (Fig. 16). Interestingly, the significant overlap between alternative exons predicted to be regulated by Nova proteins in the brain and those showing changes in inclusion levels upon *Nova2* knockdown in the ECs (p=1.93e-11, hypergeometric test) could be even higher since very different approaches were used in our and Zhang et al. studies [416].

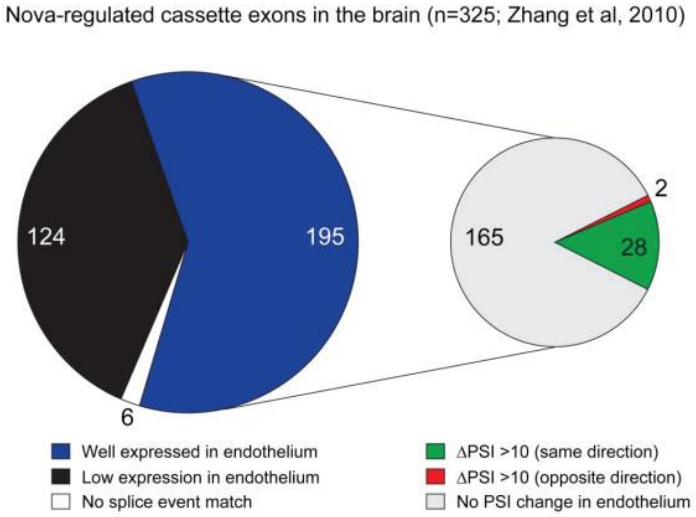

Fig. 16. Comparison between Nova-regulated cassette exons in neural and ECs. Left: of the 325 predicted Nova-regulated cassette exons by Zhang C. et al. 2010 [416], 195 exons have enough read coverage to confidently estimate PSI ("Percent Spliced Inclusion", for exons) in our samples compared to 124 that do not; a further 6 exons could not be matched to our data. Right: Out of the 195 exons with enough read coverage, 28 show a change in PSI>10 upon *Nova2* knockdown in ECs in the expected direction, 2 in the opposite and 165 did not show a significant PSI change. Figure modified from [251].

During the first year of my PhD course, I have contributed to the bioinformatics analysis of data generated from RNA-Seq of *Nova2* knockdown ECs compared to control ECs; moreover, I have also validated by RT-PCR the AS profile of selected genes in different *in vitro* systems. These results are summarized on a recently published paper, in which I am one of the authors (Giampietro C, Deflorian G, Gallo S, **Di Matteo A**, Pradella D, Bonomi S, Belloni E, Nyqvist D, Quaranta V, Confalonieri S,

Bertalot G, Orsenigo F, Pisati F, Ferrero E, Biamonti G, Fredrickx E, Taveggia C, Wyatt CD, Irimia M, Di Fiore PP, Blencowe BJ, Dejana E, Ghigna C. The alternative splicing factor Nova2 regulates vascular development and lumen formation. *Nat Commun*. 2015; **6:** 8479).

Among the novel identified Nova2 targets in ECs, I found several genes encoding for regulators of the activity of the small GTPases Cdc42, Rac1 (members of the Rho GTPase family) and Rap1. As discussed in the introduction, these small GTPase are important regulators of the Par complex during organization of the vascular lumen [236,305]

Small G proteins (20-25 kDa in size) are able to cycle between an inactive GDP-bound state and an active GTP-bound conformation, which induces downstream signaling events. Moreover, their activity is controlled by activators (Guanine nucleotide exchange factors, GEFs), which catalyze the exchange from G-protein-bound GDP to GTP, and inhibitors (GTPase-activating proteins, GAPs) that catalyze the hydrolysis of GTP to GDP, thereby inactivating small G proteins [417].

To confirm a possible molecular link between these AS events and the phenotypes described above, I analyzed AS changes in selected targets:

- ***Dock9/Zizimin1*** exon 38 (44 nt). Dock9 is an activator (or GEF) of Cdc42, a component of the Par polarity complex [418]. Notably, depletion of *Dock9* in ECs blocks VEGF-driven Cdc42 activation and inhibits filopodia formation [419].
- ***Ktn1*** exon 23 (69 nt). Ktn1 is involved in a wide variety of cellular processes, including vesicle transport, cell migration, regulation of cytoskeletal dynamics and axonal transport [420]. Ktn1 interacts with RhoG, a member of the Rho family of small GTPases that activates Rac1 and Cdc42 through a microtubule-dependent pathway [420]. Ktn1 plays also important roles in the formation of focal adhesions and in controlling cell shape and motility [421].
- ***Cd97*** exon 5 (135 nt). Cd97 is an adhesion G protein-coupled receptor involved in EC migration and invasion during angiogenesis [422]. It is able to activate a signal cascade that increases Rho-GTP levels [423].
- ***Lrch3*** exon 17 (107 nt). Lrch3 is a cytoskeletal scaffolding factor involved in a number of cellular processes such as the control of cell shape under environmental variations [424]. It interacts with several Cdc42 activators such as Dock6, Dock7 and Dock8 [425].
- ***Sorbs1*** exon 21A (60 nt). Sorbs1 is a member of the SoHo (sorbin-homology) family of adaptor proteins that play roles in cell adhesion and cytoskeletal organization [426]. It localizes at zonula adherens in epithelial cells and at cell-cell AJ [427].
- ***Abi1*** (Abl interactor 1) exon 3A (15 nt). Abi1 regulates actin polymerization and cytoskeletal architecture/remodeling [428]. It is essential for the formation of membrane protrusions where it specifically localizes [429,430].
- ***Phldb2*** (Pleckstrin homology like domain family B member 2) exon 10 (144 nt). Phldb2 is involved in the appropriate organization of microtubule networks for maintaining cell polarity [431].

- ***Magi1*** exon 16A (166 nt). Magi1 is a scaffold protein that recruits Rap1 at junctions. Interestingly, Darnell and colleagues [416] reported Nova2-dependent AS regulation of *Magi1* exon 13A. Our RNA-Seq identified exon 16A of *Magi1* as additional Nova2-regulated AS exon in ECs.
- ***Dysf*** exon 17A (42 nt). Dysf is transmembrane protein involved in EC adhesion and angiogenesis through poly-ubiquitination and degradation of platelet endothelial cellular adhesion molecule-1 (PECAM-1/CD31) [432].

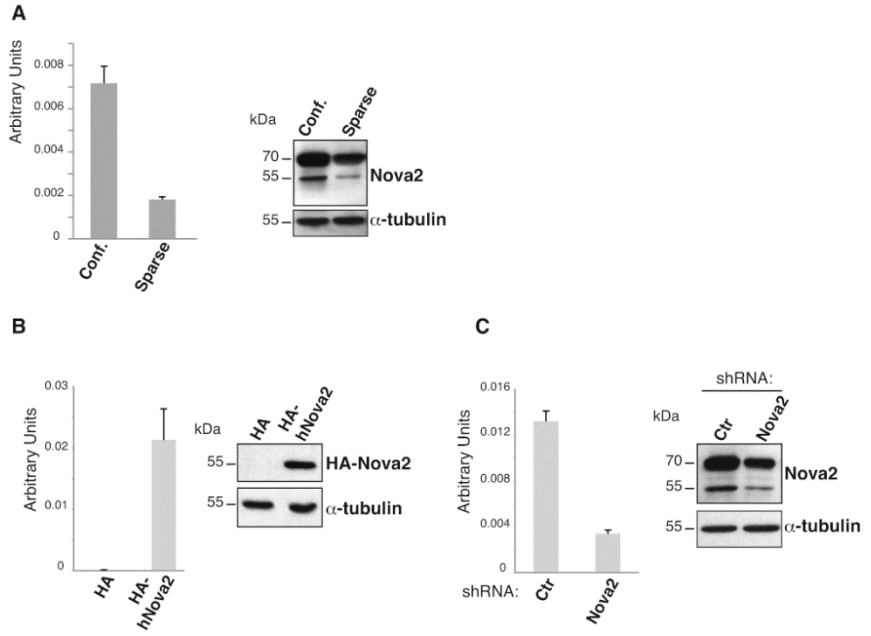

Fig. 17. Nova2 depleted and overexpressing ECs. (**A**) RT–qPCR analysis of *Nova2* mRNA expression levels in mouse VE100 ECs grown as confluent or sparse. The Nova2 protein level was also analyzed by immunoblotting using an anti-Nova2 antibody (α-tubulin as the loading control). (**B**) Nova2 mRNA and protein levels in sparse ECs overexpressing HA-tagged Nova2 and (**C**) confluent *Nova2* knockdown VE100 ECs. Error bars indicate mean ±s.d. calculated from three independent experiments (n= 3). Figure modified from [251].

To confirm the RNA-Seq results and validate selected genes as novel Nova2 targets in ECs, I analyzed by RT-PCR their AS:

1) during *in vitro* angiogenesis. It is important to know that signal-transduction pathways that modulate endothelial growth can be analyzed in culture by growing ECs at different density [433]. In particular, at low density (sparse) ECs assume an angiogenic-like phenotype, while at high density (confluent) they switch to a non-angiogenic phenotype. Notably, my group has recently shown that Nova2 is upregulated in confluent versus sparse ECs [251] (Fig. 17A);
2) in *Nova2* overexpressing ECs (Fig. 17B);
3) in *Nova2* knockdown ECs (Fig. 17C).

By performing RT-PCR analysis, I confirmed that Nova2 expression levels

correlated with AS changes of these targets (Fig. 18). Moreover, it is known that Nova2 is a peculiar AS factor since regulates the final outcome of the splicing reaction on the basis of the position of its binding sites (YCAY cluster, Y=pyrimidine) on the pre-mRNA target [48]. Indeed, Nova2 usually inhibits exon inclusion when bound to the exonic or upstream intronic region, while stimulates it when bound to downstream intronic regions [48]. Interestingly, with the exception of Abi1, I found that AS pattern of all these selected genes is consistent with the position of Nova2 binding sites, suggesting that they may be direct Nova2 target genes in ECs (Fig. 18).
These newly identified Nova2 targets expanded the list of previously known targets involved in apical-basal polarity, actin polymerization dynamics and cytoskeletal remodeling [416], important processes associated with cell polarity, cell shape, motility and adhesion.

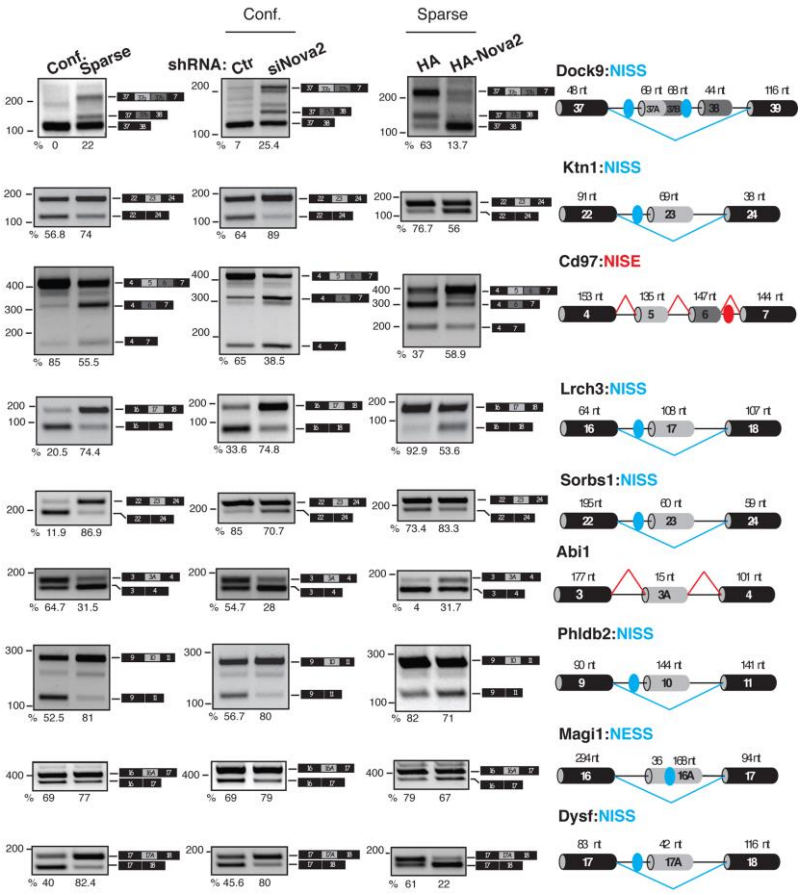

Fig. 18. Validation of novel Nova2 target exons in ECs. RT-PCR analysis of selected novel Nova2 targets encoding for cell polarity, cell shape, motility and adhesion regulators in: confluent and sparse mouse VE100 ECs (left), in confluent Nova2 knockdown ECs (middle) and in sparse ECs overexpressing HA-tagged Nova2 (right). For each gene, the schematic representations of the genomic region containing the AS exon, the transcripts generated from skipping or inclusion of the AS exon and the percentage of exon inclusion (calculated by ImageJ software) are indicated. Grey boxes, AS exons; black boxes, constitutive exons; blue/red dots indicate YCAY clusters predicted to function as Nova2 silencer/enhancer. Blue/red bars indicate Nova2-silenced/enhanced exon inclusion. NISS, Nova2 intronic splicing silencer; NISE, Nova2 intronic splicing enhancer. For *Dock9* the percentage is the ratio between the isoform containing exon 37a plus 37b and total, whereas for *Cd97* the percentage indicates the ratio between the isoform containing exons 5 plus 6 and total. Figure modified from [251].

CHAPTER II
Characterization of the functional role(s) of selected Nova2-mediated AS variants in ECs

1. Ptbp2 is expressed in ECs and inversely correlated with Nova2

Among the novel Nova2 targets identified by RNA-Seq in *Nova2* knockdown ECs, I found *Ptbp2*. In particular, RNA-Seq indicated that Nova2 promotes skipping of *Ptbp2* exon 10 leading to the production of an mRNA molecule known to be degraded by the Non-sense Mediated mRNA Decay (NMD) pathway [89]. Accordingly, by RNA-Seq I found an increased *Ptbp2* steady state transcript level in *Nova2* knockdown compared to control ECs (not shown).

The above results are surprising and drew my attention since *Ptbp2* expression was considered, until now, to be restricted to brain and testis [69,72]. However, by using GENEVESTIGATOR®, a search engine for gene expression, which integrates thousands of published microarray and RNA-Seq experiments across different biological contexts such as diseases, drugs, tissues, cancers progression, cell lines or genotypes, I found that *Ptbp2* expression is detected in 9 samples of primary human umbilical artery endothelium cells (HUAEC) and 52 samples of internal mammary artery (https://genevisible.com/tissues/HS/Gene%20Symbol/PTBP2).

It is important to note that several recent works demonstrated that Ptbp2 controls AS of genes encoding for regulators of cellular polarity including cytoskeleton organization, GTP binding and membrane-associated regulators of cellular projections [434]. Consequently, neuronal progenitors in the *Ptbp2*-null brain exhibited an aberrant polarity and premature neurogenesis [75,104]. Since an important functional similarity in the development of the vascular and nervous systems is the establishment of the apical-basal polarity, as this is crucial for the organization of the vascular lumen and for axon guidance [236,411], I hypothesized that at least a fraction of transcripts encoding for polarity regulators with an AS profile altered in Nova2 knockdown ECs, could be indirect Nova2 targets *via* upregulation of Ptbp2.

Validating the RNA-Seq results, I first confirmed Ptbp2 protein expression by western blot in embryonic (VE100) and adult (JAM) ECs generated and extensively characterized in the laboratory of Prof. Dejana [435,436] (Fig. 19A). Notably, as in the case of mouse brain (E18.5) and human neuroblastoma SH-SY5Y cells, in ECs the anti-Ptbp2 specific antibody recognized one immunoreactive band around 58 kDa, as previously reported [69] (Fig. 19A). In addition, immunofluorescence (IF) analysis confirmed Ptbp2 expression in ECs with the protein mainly localized in the nucleus but excluded from nucleoli (Fig. 19B) as observed for embryonic neocortex [75].

Since AS-NMD is a mechanism to finely tune protein expression [437], I analyzed by qRT-PCR and western blotting the Ptbp2 expression in stable *Nova2* knockdown or *Nova2* overexpressing ECs (compared to control ECs) previously generated from my laboratory [251]. I found that both mRNA and protein levels of Ptbp2 were upregulated in *Nova2* depleted ECs (Fig. 19C). Conversely, overexpression of Nova2 correlated with down-regulation of

Ptbp2 (Fig. 19D). Moreover, my group has recently shown that Nova2 is upregulated in confluent versus sparse ECs [251]. Interestingly, I found that Nova2 and Ptbp2 expression levels inversely correlated in sparse versus confluent ECs, whereas Ptbp1, a well-known repressor of *Ptbp2* exon 10 splicing that promotes *Ptbp2* downregulation [89], increased in sparse ECs compared to confluent ECs (Fig. 19E).

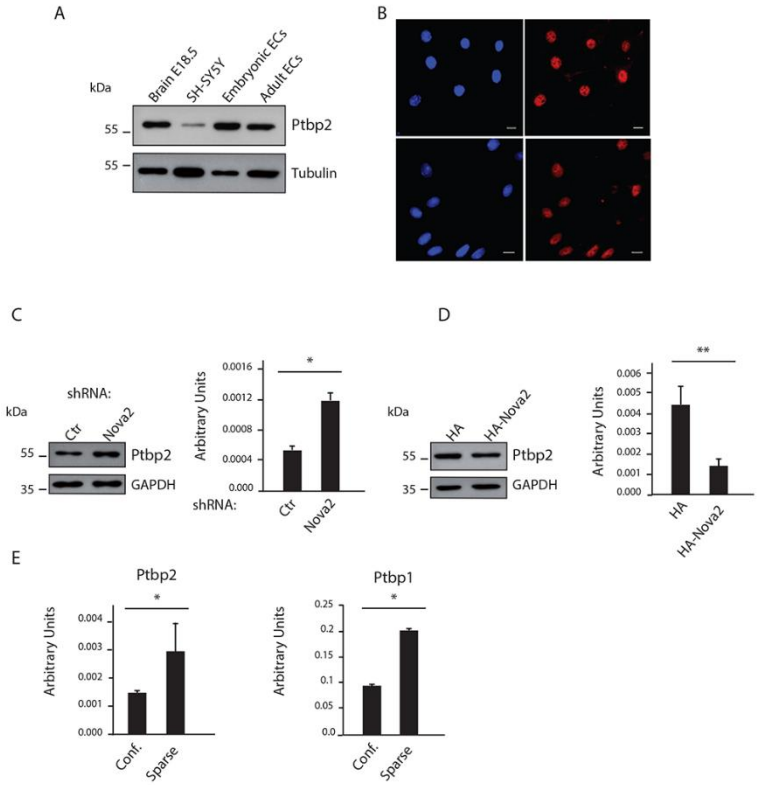

Fig. 19. Ptbp2 is expressed in ECs and inversely correlated with Nova2. (**A**) Immunoblotting analysis of Ptbp2 in whole mouse brain E18.5, in human neuroblastotma SH-SY5Y cells and in mouse embryonic (VE100) and adult (JAM) EC (α-tubulin as the loading control). (**B**) Immunofluorescence analysis of Ptbp2 (red) and DAPI (blue) in embryonic (upper panels) and adult ECs (lower panels) (magnification 60x; scale bar 10 μm). (**C**) Ptbp2 protein (left) and mRNA expression (right) levels in *Nova2* knockdown ECs (grown as confluent) and (**D**) in overepressing ECs (grown as sparse). (**E**) qRT-PCR analysis of *Ptbp2* and *Ptbp1* expression levels in ECs grown at different densities (confluent or sparse). Error bars indicate ±s.d. calculated from three independent experiments (n= 3). * p-value < 0.05 calculated by two tailed, unpaired, t-test (n=3); ** p-value < 0.01 calculated by two tailed, unpaired, t-test (n=3).

Collectively, these data indicate that Ptbp2, in addition to nervous system and testis [72,75], is also expressed in endothelium where its expression is inversely correlated with Nova2.

2. Nova2 regulates the splicing pattern of *Ptbp2* exon 10

RNA-Seq showed that *Ptbp2* exon 10 is a novel Nova2-regulated AS target

in ECs. By using RT-PCR analysis with RNA extracted from *Nova2* overexpressing ECs [251], I found that high Nova2 expression level increased skipping of *Ptbp2* exon 10, whereas the opposite effect was observed in ECs depleted of Nova2 (Fig. 20A). Moreover, I found that Nova2 expression and skipping of *Ptbp2* exon 10 were correlated in confluent and sparse ECs (Fig. 20A).

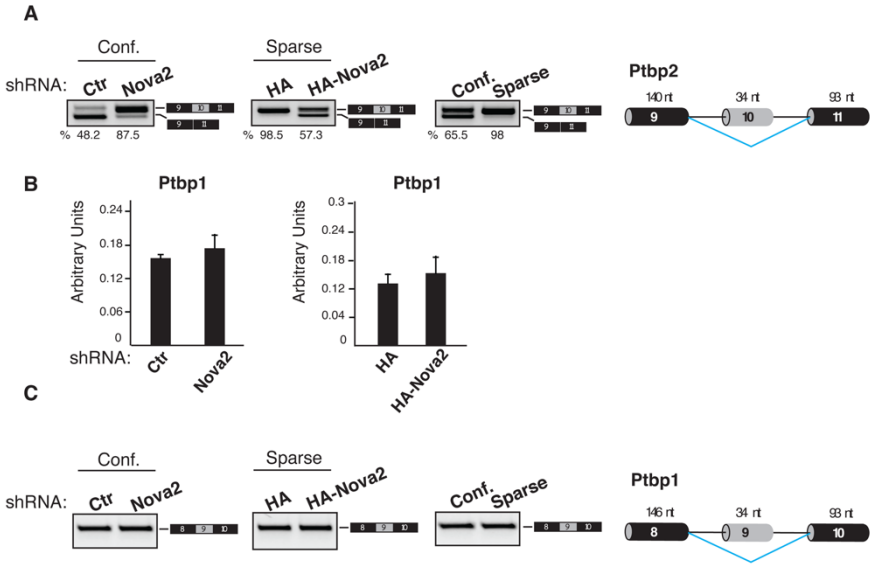

Fig. 20. AS of *Ptbp2* is regulated by Nova2 in ECs. (**A**) RT-PCR analysis of the AS profile of exon 10 of *Ptbp* in confluent *Nova2* knockdown ECs (left), in sparse Nova2 overexpressing ECs (middle) and in confluent and sparse ECs (right). (**B**) *Ptbp1* mRNA *e*xpression levels in *Nova2* knockdown (left) and Nova2 overexpressing ECs (right). (**C**) AS profile of *Ptbp1* exon 9, whose skipping produce a NMD-sensitive isoform, in *Nova2* knockdown ECs (left), *Nova2* overexpressing ECs (middle) and in confluent and sparse mouse ECs (right). The schematic representations of the genomic region containing the AS exons of *Ptbp1* and *Ptbp2* (AS exon in grey; constitutive exon in black), the transcripts generated from skipping or inclusion of the AS exon and the percentage of exon inclusion (calculated by ImageJ software) are indicated. Error bars indicate ±s.d. calculated from three independent experiments (n= 3).

Splicing of *Ptbp2* exon 10 has been shown to be regulated by several AS factor, mainly by its paralog Ptbp1 [89]. Thus, to rule out the possibility that splicing of *Ptbp2* exon 10 was an indirect effect due to Ptbp1 contribution, I analyzed Ptbp1 expression upon modification of Nova2 expression in ECs. Importantly, as shown in Fig. 20B and 20C, I found that both expression levels and AS of *Ptbp1* exon 9, whose skipping produce a NMD-sensitive isoform, were not affected by variation of Nova2 expression in ECs (Fig. 20B and C).

As reported above, Nova2 is able to promote or repress exon inclusion depending on the location of its binding sites (YCAY cluster elements) in its pre-mRNA targets [48]. In particular, Nova2 usually supports exon

skipping when bound upstream of exonic or intronic regions, while it stimulates exon inclusion when bound to downstream intronic regions [48]. In line with this, I found that two YCAY clusters are localized in intron 9 of *Ptbp2* pre-mRNA respectively 129 and 215 nt upstream of exon 10 (Fig. 21). Moreover, the position of these putative Nova2-binding sites is consistent with direction of the observed AS changes in *Ptbp2* pre-mRNA (Fig. 20A) suggesting that *Ptbp2* is a direct Nova2 AS target.
To determine if Nova2 directly binds to the *Ptbp2* pre-mRNA *in vivo*, in collaboration with the laboratory of Prof. Paronetto (Department of Movement, Human and Health Sciences University of Rome "Foro Italico"), I performed iCLIP (UV crosslinking followed by immunoprecipitation), a method to identify direct protein-RNA interactions [438] (see also below). RNA of *in vivo* cross-linked ECs was immunoprecipitated by using a commercial anti-Nova2 antibody or control IgG. RNAs bound by Nova2 were analyzed by qRT-PCR with primers A (spanning the YCAY clusters) or primers B (mapping to intron 10 as negative control) (Fig. 21). Importantly, as shown in Fig. 21, I found that Nova2 specifically binds to the endogenous *Ptbp2* transcript at the level of intron 9, upstream to exon 10.

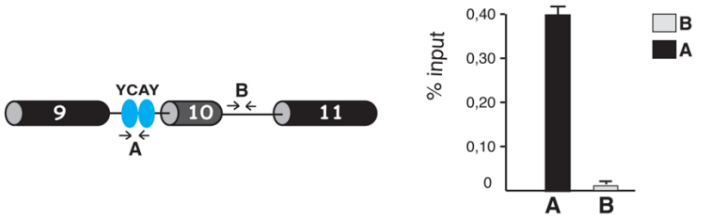

Fig. 21. Nova2 CLIP using *in vivo* crosslinked ECs. Immunoprecipitation of the *Ptbp2* pre-mRNA from *in vivo* cross-linked ECs (VE100) using anti- Nova2 or IgG antibodies. The immunoprecipitated RNAs were analyzed by qRT-PCR with primers A (annealing to the YCAY cluster in intron 9) or primers B (annealing to the intron 10 as negative control). Error bars indicate ±s.d. calculated from two independent experiments. Blue dots represent the YCAY clusters (129 and 215 nt upstream of exon 10) that function as Nova2 splicing silencer.

To further investigate the role of Nova2 in regulating splicing of *Ptbp2* exon 10, I performed an *in vivo* splicing assay in HeLa cells with a *Ptbp2* minigene (p-Ptbp2) that I generated by cloning, in the mammalian expression vector pCDNA 3.1+ (Invitrogen), the region of the mouse *Ptbp2* gene spanning the exons 9, 10, 11 with the flanking introns (Fig. 22A). This minigene was co-transfected in HeLa cells with plasmids sustaining the overexpression of HA-tagged Nova2 [251], T7-tagged SRSF1 [200] or with the empty vector as negative control. To specifically amplify transcripts derived from p-Ptbp2 minigene and avoid interference from the endogenous *Ptbp2* transcripts, I used primers Ptbp2-for and BGHrev,

mapping on the exon 9 and pCDNA 3.1+, respectively. Moreover, the expression of the HA-tagged Nova2 and T7-tagged SRSF1 was also verified by western blotting. As shown in Fig. 22B, while splicing of the transcripts generated from p-Ptbp2 co-transfected with the empty vector showed both FL (inclusion of exon 10) and exon 10 skipped bands, overexpression of Nova2 was sufficient to switch the splicing pattern of p-Ptbp2 transcripts increasing skipping of exon 10 (Fig. 22B, lane 2). Notably, this effect was specific of Nova2 since overexpression of SRSF1 was unable to increase skipping of *Ptbp2* exon 10.

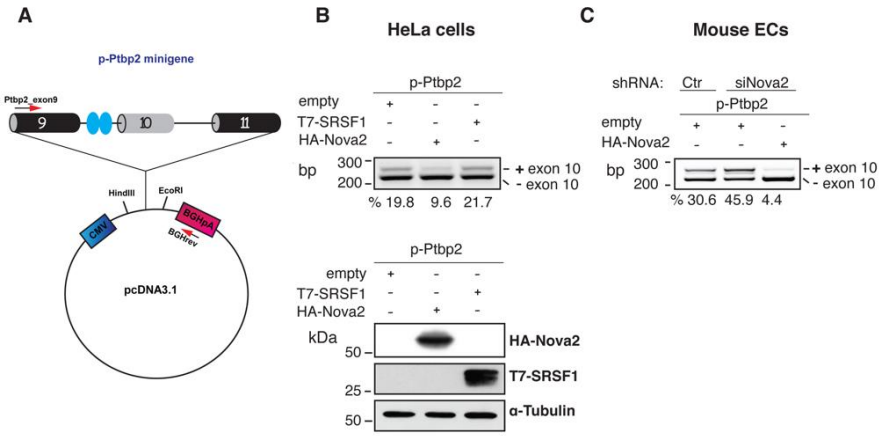

Fig. 22. *in vivo* splicing assay with *Ptbp2* minigene. (**A**) Schematic representation of *Ptbp2* minigene (p-Ptbp2) generated by cloning, in the mammalian expression vector pCDNA 3.1+ (Invitrogen), the region of *Ptbp2* gene spanning the exons 9, 10, 11 with the flanking introns. Arrows indicate Ptbp2-for and BGHrev primers used to analyze the splicing of p-Ptbp2 minigene. Blue dots represent the YCAY clusters that function as Nova2 silencer. (**B**) RT-PCR analysis of p-Ptbp2 splicing in HeLa cells co-transfected with the indicated expression vectors (upper panel). HA-Nova2 and T7-SRSF1 upregulation was confirmed by western blotting by using anti-HA and anti-T7 antibodies, respectively; α-tubulin as loading control (lower panel). (**C**) RT-PCR analysis of p-Ptbp2 splicing in control ECs and *Nova2* knockdown ECs co-transfected with the indicated expression vectors. Agarose gel quantification of exon inclusion by ImageJ is also reported.

To further confirm Nova2-mediated splicing of *Ptbp2* exon 10, I also performed an *in vivo* splicing assay in *Nova2* knockdown and control ECs. As shown in Fig. 22C, splicing of p-Ptbp2 minigene was affected by Nova2 expression levels, since in Nova2 depleted ECs the AS pattern was shifted toward inclusion of exon 10 (compared to control ECs). Importantly, co-transfection of p-Ptbp2 minigene in *Nova2* knockdown ECs with the plasmid for the overexpression of HA-Nova2 increased skipping of exon 10 (Fig. 22C, lane 3).
Collectively, my results demonstrated that Nova2 promotes skipping of

Ptbp2 exon 10 by directly binding to *Ptbp2* pre-mRNA.

3. Nova2 mediated AS-NMD of *Ptbp2*

As predicted by the AS-NMD model [439] (Fig. 23A), my results suggested that Nova2-mediated AS switch of *Ptbp2* exon 10 could be responsible for the different expression of *Ptbp2* observed in stable *Nova2* knockdown or *Nova2* overexpressing ECs (Fig. 19C and D). NMD occurs during the pioneer round of translation and NMD substrates are stabilized by the translation inhibitor cycloheximide (CHX) [439].

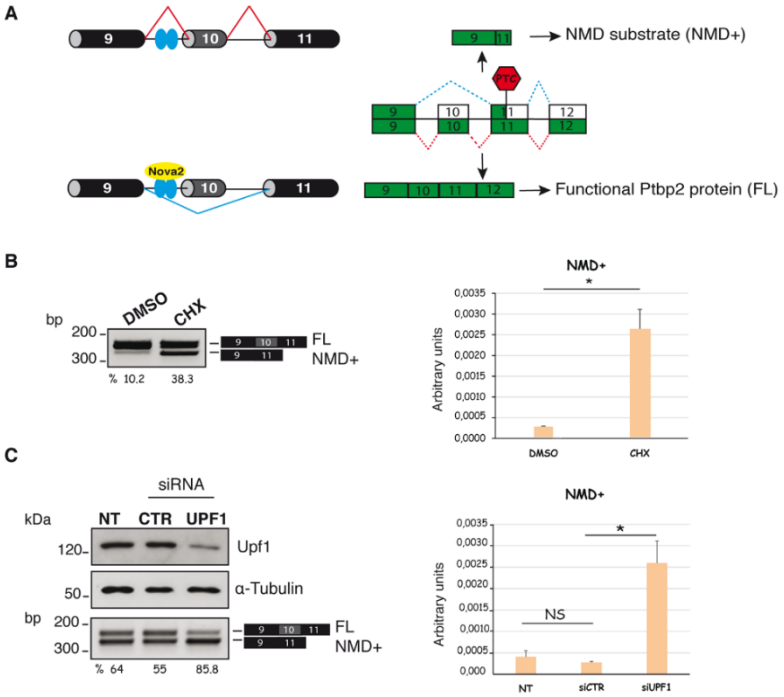

Fig. 23. Nova2 controls AS-NMD of *Ptbp2* pre-mRNA. (**A**) Schematic representation of the Nova2-mediated AS-NMD of *Ptbp2*. Nova2 promotes skipping of *Ptbp2* exon 10 (left) leading to PTC (premature translation termination codon) introduction in exon 11 (red hexagon), (right). Dotted lines indicate the different ORFs generated by inclusion or skipping of exon 10. NMD-sensitive splicing isoform (NMD+) is shown above the exons, whereas the functional *Ptbp2* ORF (FL) is shown below the exons. (**B**) *Ptbp2* splicing was analyzed by RT-PCR in *Nova2* knockdown ECs treated for 4 h with cycohexamide (CHX) or with DMSO as control (left). The histogram shows the relative quantification of the NMD+ transcript by qRT-PCR (right). (**C**) Left: mouse ECs (VE100) were transfected with *Upf1* siRNA or with control siRNA (siCTR) or untreated (NT). These cells were analyzed in western blot with anti-Upf1 and anti-α-Tubulin antibodies (upper panels on the right) and in RT-PCR to analyze *Ptbp2* splicing (lower panel on the lefft). Right: mouse ECs treated with the indicated siRNA oligos were also analyzed in qRT-PCR with primers specific for the NMD+ transcript of *Ptbp2* as in panel B. In all histograms, error bars indicate ±s.d. calculated from three independent experiments (n= 3). * p-value < 0.05 calculated by two tailed, unpaired t-test n=3. NS: not significant.

Hence, to verify the involvement of the NMD pathway in the regulation of *Ptbp2* expression levels in ECs, I treated ECs knockdown for *Nova2* with CHX or DMSO (as a control). As shown in Fig. 23B, CHX specifically increased the level of NMD+ transcripts (skipping of exon 10). Moreover, the effect of CHX was also confirmed by qRT-PCR in which I used a specific set of primers detecting only the NMD+ isoform (Fig. 23B). To rule out that this result could be due to pleiotropic effects of CHX rather than specific stabilization of NMD+ transcripts, I inhibited the NMD pathway by siRNA-mediated knockdown of the key NMD factor Upf1 [439]. Similarly to CHX treatment, down-regulation of *Upf1* led to increase in *Ptbp2* NMD+ transcript, as quantified by qRT-PCR. However, in contrast with CHX, depletion of *Upf1* slightly changed the ratio between the two *Ptbp2* splicing products, as already reported by Boutz et al [89] (Fig. 23C).
Altogether, these results support the conclusion that Nova2 directly reduces the expression level of the splicing factor Ptbp2 in ECs by activating an AS-NMD program.

4. Splicing of *Ptbp2* exon 10 is conserved in zebrafish and regulated by Nova2 expression levels

By performing *nova2* morpholino-mediated knockdown and CRISPR-induced genetic mutation in collaboration with Prof. Elisabetta Dejana my laboratory has recently demonstrated that depletion of *nova2* in zebrafish impairs EC polarity and, as a consequence, alters the organization of the vascular lumen [251]. To specifically visualize the developing blood vessels, transgenic embryos expressing the enhanced green fluorescent protein (EGFP) gene under the control of the endothelial-specific promoters *Tg(fli1a:EGFP)y1)* and *Tg(kdrl:EGFP)* were used [440]. Notably, vascular defects were associated with modifications of the AS of pre-mRNAs encoding for regulators of the activity/localization of Par polarity complex [251].

Since *Ptbp2* gene, identified as novel Nova2 target in ECs, has putative orthologs in zebrafish, I have decided to investigate their AS in this organism that constitutes a unique and powerful model to study vertebrate vascular development [412]. In particular, zebrafish has two duplicated orthologs of the mouse *Ptbp2* gene called *Ptbp2a* and *Ptbp2b*. By using Blast tool, I found that *Ptbp2b* (exon 11) has a slightly higher percentage of sequence identity with the *Ptbp2* mouse gene if compared to *Ptbp2a* (exon 5) (86% of nucleotide identity for *Ptbp2b* compared to 80% of *Ptbp2a*) resulting in a higher amino acid sequence identity of Ptbp2b zebrafish protein (78%) with the Ptbp2 mouse protein compared to Ptbp2a (76%) (Fig. 24A). Therefore, I analyzed AS of *Ptbp2b* exon 11 and *Ptbp2a* exon 5 by RT-PCR in *nova2* CRISPR-mutated zebrafish, compared to wild type fishes. For both genes, I cannot see significant differences between the AS patterns of *nova2* mutant versus control zebrafish (Fig. 24B, left). This result could be due to the fact that non-vascular tissues had mask the effect of Nova2 in ECs. Thus, to investigate *Ptbp2* splicing specifically in endothelium, I analyzed the AS profile of two zebrafish genes in ECs freshly purified from *nova2* mutant and control zebrafish embryos. As depicted in Fig. 24B

(right), I found that *Ptbp2b* exon 11 and *Ptbp2a* exon 5 were spliced in endothelium in nova2-dependent manner (although the effect was greater for *Ptbp2b* gene). Notably, in line with this result, I found that nova2 binding sites (YCAY clusters) are conserved between mouse and two zebrafish *Ptbp2* genes and localized upstream of exon 11 for *Ptbp2b* and exon 5 for *Ptbp2a*.
However, in control zebrafish embryos, *Ptbp2b* exon 11 and *Ptbp2a* exon 5 were spliced in opposite way suggesting the presence of additional AS factors involved in their regulation.

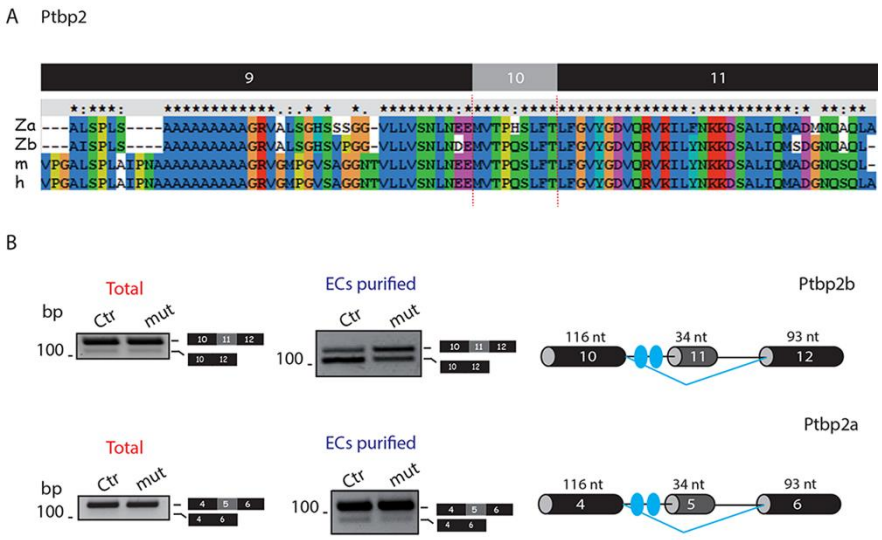

Fig. 24. Splicing of *Ptbp2* is regulated by Nova2 in zebrafish. (**A**). Zebrafish (Za) has two duplicated orthologs of the mouse *Ptbp2* gene called *Ptbp2a* and P*tbp2b*. Zebrafish Ptbp2a and Ptbp2b, mouse (m) and human (h) Ptbp2 protein sequences were analyzed by ClustalX 2.1. * indicated fully conserved residue; "strong" fully conserved group; ° "weaker" fully conserved group. (**B**) On the left, splicing of *Ptbp2b* exon 11 (upper panel) and *Ptbp2*a exon 5 (lower panel) analyzed by RT-PCR with RNA extracted from total control (Ctr) and total *nova2* mutant (mut) zebrafish embryo 4 days postfertilization (dpf). On the right, RT-PCR of RNA extracted from freshly purified ECs of control (Ctr) and *nova2* mutant (mut) zebrafish embryo at 4 dpf of *Ptbp2b* exon 11 (upper panel) and *Ptbp2*a exon 5 (lower panel). The zebrafish genomic regions of *Ptbp2a* and *Ptbp2b* (with the AS exon in grey) are also indicated. Blue dot, YCAY clusters that function as Nova2 intronic silencer. Blue bars, nova-silenced exon inclusion.

CHAPTER III

Identification of novel genes modulated by Nova2 in endothelium by RNA-Seq of *Nova2* overexpressing ECs

In order to extend RNA map of Nova2-regulated exons in endothelium, Nova2 gain-of-function ECs were also analyzed by RNA-Seq. In particular, RNA-Seq was performed on two replicates of RNA extracted from stable *Nova2* overexpressing ECs versus control ECs. These stable *Nova2* overexpressing ECs were generated in collaboration with Prof. Elisabetta Dejana by using mouse VE100 ECs and lentiviral vectors carrying the cDNA specific for mouse *Nova2* gene as described in [251]. Moreover, RNAs extracted from these ECs were also previously used in RT-PCR experiments for the validation of AS changes identified by RNA-Seq in *Nova2* depleted ECs (Fig. 18).

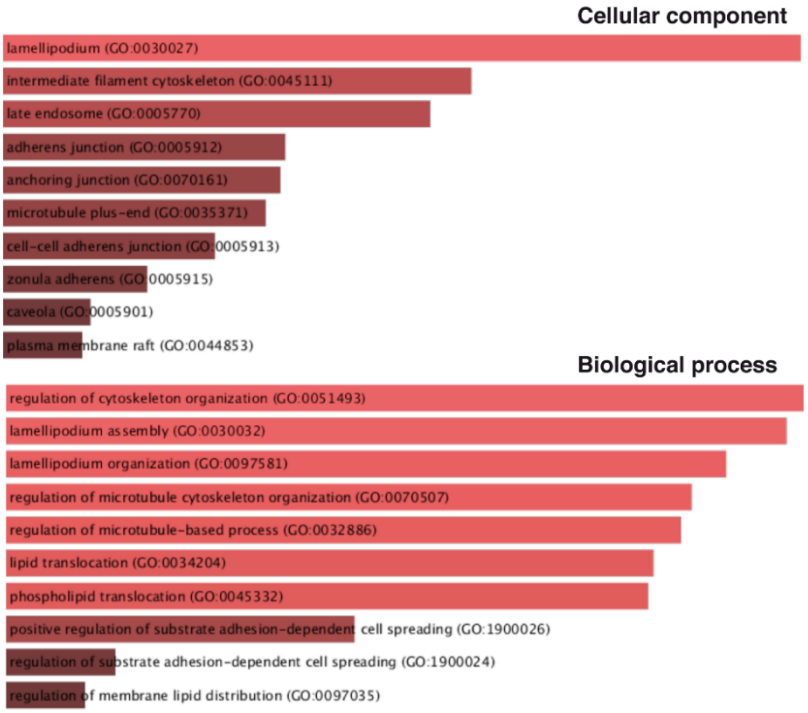

Fig. 25. Gene Ontology (GO) enrichment analysis of Nova2 regulated AS in ECs. Gene Ontology (GO) enrichment analysis with EnrichR database of the 172 AS cassette exons differentially regulated upon Nova2 overexpression in ECs (with respect to control cells). Bar graph showed the top 10 enriched terms for the GO of Cellular component (upper panel) and Biological process (lower panel) gene-set libraries. The longer bars and lighter colored bars mean that the term is more significant.

By using *vast-tools* in collaboration with Dr. Irimia and Prof. Blencowe, we identified 172 AS cassette exons differentially regulated upon Nova2 overexpression with respect to control ECs, (Table 4 in Appendix).

Successively, by using Enrichr database (http://amp.pharm.mssm.edu/Enrichr/) [441], I performed a GO enrichment analysis that showed a significant enrichment for genes involved in cytoskeleton organization, cell-cell adhesion (including anchoring and adherens junctions) and formation of lamellipodia and intermediate filaments, similar to the multiple GO terms identified by RNA-Seq in *Nova2* depleted ECs (Fig. 15C).
I have focused my analysis on AS changes in the following selected genes:
- ***Myo9a*** (or *Myo-IXa*) exon 6 (57 nt). Myo-IXa is a member of class IX single-headed actin motors with a conserved RhoGAP domain. It is a negative regulator of Rho GTPase able to promote localized reorganization of the actin cytoskeleton, a central process during migration and acquisition of apical-basal polarity [442];
- ***Rapgef6*** exon 21A (24 nt). Rapgef6 is a well-known upstream activator of Rap1 in ECs. Interestingly, it plays important functions during maturation of the adherens junction [443];
- ***Fmnl2*** (*formin-related protein 2*) exon 26 (47 nt). Fmnl2 is a member of formin-related proteins, a family of molecules implicated in cell polarity [444]. Fmnl2 has been identified as the first Cdc42 downstream effector promoting cell migration, actin polymerization at the leading edge of lamellipodia and filopodia [445,446];
- ***Srgap1*** exon 12A (34 nt). Srgap1 is a GAP involved in selective inactivation of Cdc42 [447]. It is crucial regulator of number, size and morphology of lamellipodia and cell migration [447];
- ***Pix-beta*** (or *Arhgef7*) exon 15 (225 nt). Pix-beta is a GEF with well-known Cdc42 specificity [448].

As previously showed for Nova2-mediated AS changes identified by RNA-Seq in *Nova2* depleted ECs (Fig. 18), AS for also these genes was validated by RT-PCR (Fig. 26) in:

i) *in vitro* angiogenesis (Fig. 17A);
ii) *Nova2* overexpressing ECs (Fig. 17B);
iii) *Nova2* knockdown ECs (Fig. 17C).

As shown in Fig. 26, I found that all analyzed genes are spliced in a Nova2- and a YCAY clusters dependent manner suggesting that Nova2 plays a critical role in the control of networks and signaling pathways that mediate the ECs biology.

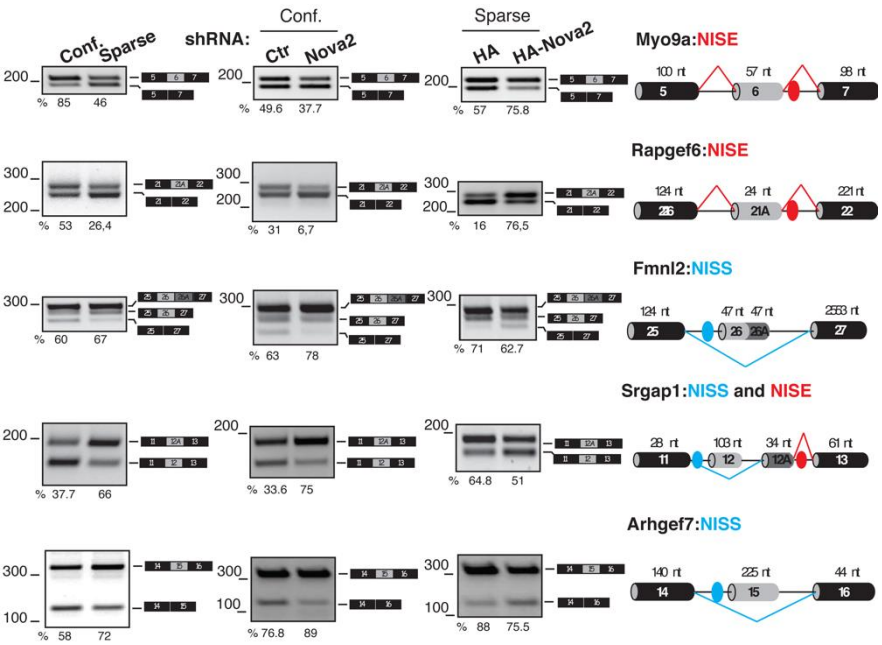

Fig. 26. Validation of novel Nova2 target exons identified upon *Nova2* overexpression in ECs. Splicing analysis of novel Nova2 target exons identified by RNA-Seq in *Nova2* overexpressing ECs versus control ECs. These exons belong to genes involved in cytoskeleton organization, cell-cell adhesion (including anchoring and adherens junctions) and in formation of lamellipodia and intermediate filaments. RT-PCR was performed in: confluent and sparse mouse VE100 ECs (left), in confluent *Nova2* knockdown ECs (middle) and in sparse ECs overexpressing HA-tagged Nova2 (right). For each gene, the schematic representations of the genomic region containing the AS exon, the transcripts generated from skipping or inclusion of the AS exon and the percentage of exon inclusion (calculated by ImageJ software) are indicated. Grey boxes, AS exons; black boxes, constitutive exons; blue/red dots indicate YCAY clusters predicted to function as Nova2 silencer/enhancer. Blue/red bars indicate Nova2-silenced/enhanced exon inclusion. NISS, Nova2 intronic splicing silencer; NISE, Nova2 intronic splicing enhancer. For *Fmnl2* the percentage is the ratio between the isoform containing exon 26 plus 26A and total.

CHAPTER IV

Identification of direct Nova2 targets in ECs

RNA-Seq potentially could have identified AS changes indirectly regulated by Nova2 in ECs and ascribable to other splicing factors (i.e. Ptbp2). Thus, in order to identify direct Nova2 targets and define a complete (genome-wide) RNA map of Nova2 regulated AS exons in endothelium I have performed iCLIP-Seq (individual-nucleotide resolution UV-induced crosslinking, immunoprecipitation and sequencing) [54]. Notably, CLIP-Seq has been already performed successfully to identify Nova2 targets in the brain using commercially available Nova2 antibodies [46].

iCLIP-Seq has significant advantages over previous methods. First, UV cross-linking is performed on live cells or tissues; in this way the results should reflect an unperturbed *in vivo* situation in particular regarding the significant intermolecular interactions, salt and ion concentration. Second, because the covalent bond formed by UV crosslinking is irreversible, the target RNA can be partially digested to short RNA tags facilitating the subsequent sequencing-based target identification techniques. Third, a number of purification steps following the initial immunoprecipitation greatly help to improve the signal-to-noise of RNA tags encoding the direct protein-binding site. The RNA bound with nonspecific co-immunoprecipitated proteins is removed during SDS-PAGE separation of protein-RNA complexes and free RNA is removed during transfer to nitrocellulose membrane. RNA specifically associated to the target protein is ligated to RNA-linkers, which allows PCR-based amplification of iCLIP tags and deep-sequencing (see scheme in Fig. 27A).

To identify direct Nova2 targets, in collaboration with Dr. Maria Paola Paronetto (University of Rome "Foro Italico"), I performed iCLIP-Seq in which *in vivo* UV RNA-protein crosslinking (at UV 254 nm) and immunoprecipitation are followed by the isolation of crosslinked segments and sequencing.

Unfortunately, by sequencing the immunoprecipitated RNAs, we obtained reads that were extremely enriched in 3' adapters and, in particular, with insufficient coverage to perform bioinformatic analysis. For this reason, we decided to perform PAR-CLIP (Photoactivatable-Ribonucleoside-Enhanced Crosslinking and Immunoprecipitation). This technique, developed by Dr. Landthaler and colleagues [55] is a modification of the original CLIP protocol that overcomes some of its problems and limitations. For example, recovery of CLIP material is limited by low efficiency of the crosslinking reaction. Moreover, position of the crosslink is not readily identifiable in target RNAs making it difficult to distinguish real direct targets from the background of non-crosslinked RNAs. Thanks to the "Mobility Program" of the University of Pavia, I spent one month in the

laboratory of Dr. Landthaler (Max-Delbrück-Centrum für Molekulare Medizin, Berlin) in order to perform PAR-CLIP experiment.

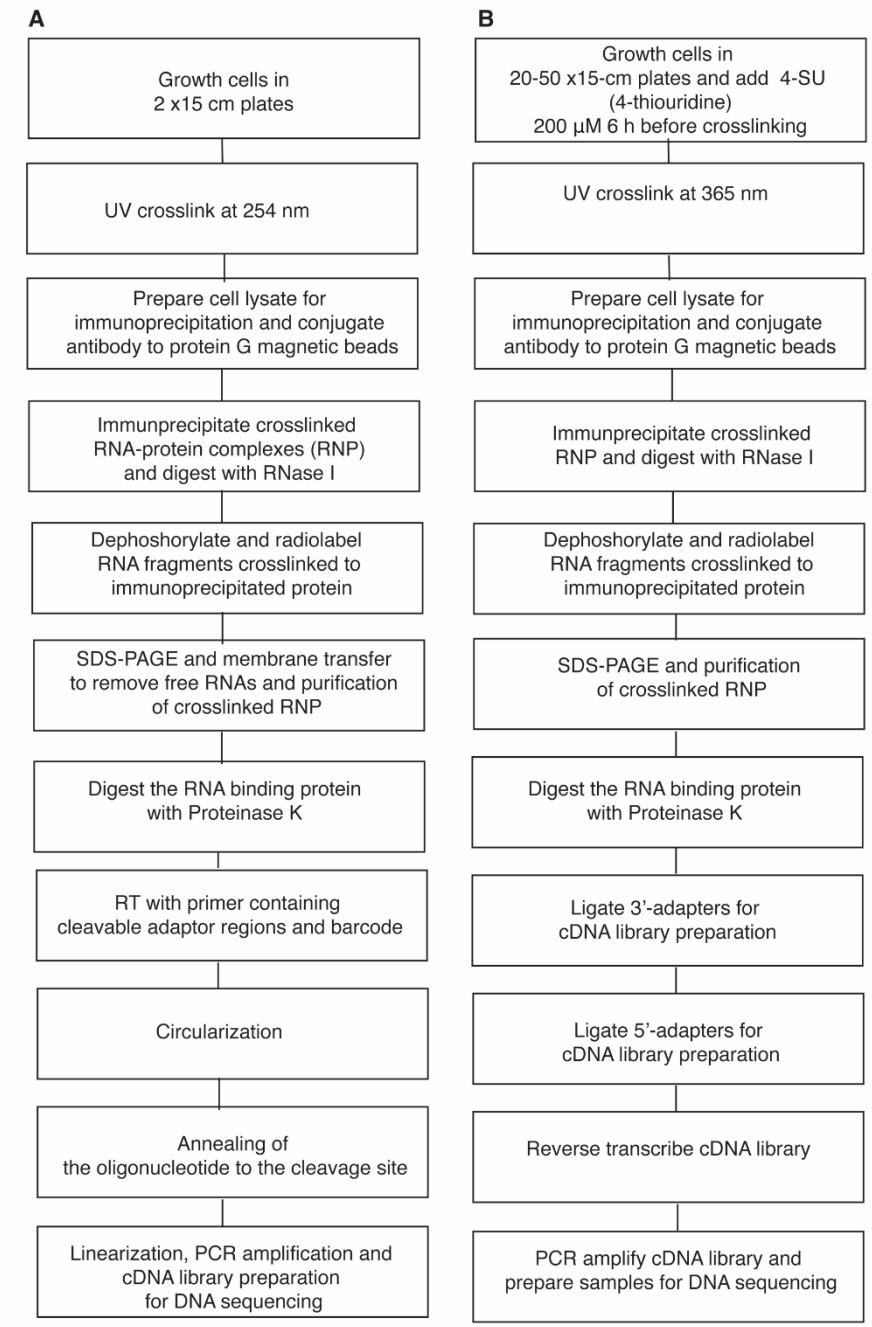

Fig. 27. Schematic representation of the (**A**) iCLIP and (**B**) PAR-CLIP experiments.

PAR-CLIP is based on the incorporation of photoreactive ribonucleoside analogs into nascent RNA transcripts. This modification allows irradiation

of the cells by UV light of 365 nm to induce efficient crosslinking of photoreactive nucleoside-labeled cellular RNAs interacting with a specific RNA-binding protein. After immunoprecipitation with a specific antibody, the isolated RNAs are converted into a cDNA library and deep sequenced. Importantly, the exact position of crosslinking can be identified by mutation of analogs incorporated in the RNAs (usually T to C mutation) facilitating their separation from the background fragments present in the sample (see scheme in Fig. 27B).

To this purpose, I used adult mouse ECs (JAM) that showed higher level of Nova2 compared to embryonic ECs (VE100) [251] and I followed the established protocol [55] depicted in Fig. 27B. In this way, I was able to visualize the Nova2-RNAs complexes as a band corresponding to the 75 kDa Nova2 isoform, whereas radioactive signal was absent when no UV crosslinking was used (Fig. 28A). Importantly, I managed to obtain RNA molecules crosslinked to Nova2 protein, purified and ligated to 5'-adapter and 3'-adapter (Fig. 28B), which have been sent for sequencing. Currently, I am waiting for the bioinformatic analysis of the results.

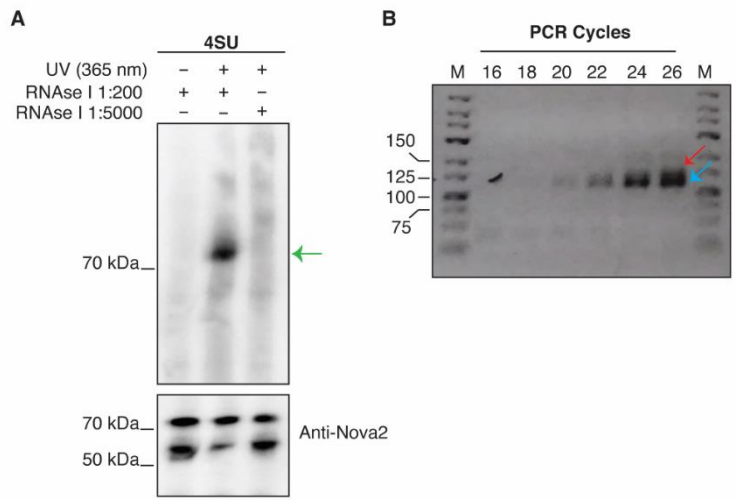

Fig. 28. Nova2 PAR-CLIP experiments in adult mouse ECs (JAM). (A) Visualization of RNA-Nova2 complexes in the upper panel: SDS-PAGE gel of the crosslinked and 5'-radiolabeled RNA-protein complexes immunoprecipitated (IP) with a commercially available Nova2 antibody (Santa Cruz). Lane 1: negative control with no UV crosslinking; lane 2: high RNase I concentration; lane 3: low RNase I concentration. A radioactive band corresponding to the expected size of Nova2 protein (green arrow) is detectable only in the sample crosslinked at 365 nm of UV. Immunoblotting of control and crosslinked ECs identified the typical Nova2 isoforms at 70kDa and ~55 kDa (lower panel). **(B)** Adaptor ligation analysis. With the increase of PCR cycles two bands are detectable on agarose gel: the lower one (light blue arrow) is the adapter-only PCR product, whereas the upper one (red arrow) is the PCR product containing the Nova2 RNA tags linked to 5'- and 3'-adapters. The number of PCR cycles and the size of the 25 bp ladder loaded at both sides of the gel are indicated.

DISCUSSION AND CONCLUSIONS

Alternative splicing (AS) is a post-transcriptional process by which a single gene generates multiple protein isoforms with different functional and structural properties [449]. Since than 90% of the human genes undergoes AS, this process provides the primary source to expand the human proteome encoded by a limited repertoire of genes [7,20]. Notably, a causative role of aberrant AS in cancer progression has been provided [112]. It is now clear that the major cause of inappropriate AS in tumors is the altered expression level of specific AS regulators [106]. The great plasticity offered by AS to modify the tumor proteome makes it precious tool used by cancer cells to inhibit suppressor genes and generate oncoproteins involved in tumor establishment, progression and in resistance to therapeutic treatments [109,139,195].

The main interest of our laboratory is to investigate the role of AS in tumor progression. Recently, we have started to study the functional implication of AS during angiogenesis in collaboration with the group of Prof. Elisabetta Dejana.

Angiogenesis is the growth of new vessels from pre-existing vasculature and this process is responsible for blood vessels growth in the developing embryo [322]. In adulthood, angiogenesis is also critical for the pathogenesis of several disorders and to support cancer development and progression, by allowing oxygen and nutrients to reach proliferating tumor tissues and by providing cancer cells with the metastatic route to colonize distant organs [450]. Notably, anti-angiogenic therapies have been exploited as anticancer approach [451]. However, these treatments have showed only modest therapeutic effects underlining the urgent need for a better understanding of the molecular mechanisms sustaining growth of tumor blood vessels.

Until now, molecular pathways regulating angiogenesis have been suggested to act primarily through the regulation of transcription. However, our recent data indicate that several post-transcriptional mechanisms regulate ECs biology [251,452]. In line with this, for the first time, our group demonstrated that AS regulation orchestrates vascular development [251]. We found that the AS factor Nova2, previously considered to be neural cell-specific [57], it is also expressed in vascular endothelium and regulated during angiogenesis. Through gain- and loss-of-function approaches in cultured ECs, we found that Nova2 regulates the establishment of EC apical-basal polarity, a prerequisite for correct vascular lumen organization, through controlled AS of mRNAs encoding for Par complex components and its regulators. Importantly, depletion of *nova2* caused vascular lumen formation defects in zebrafish [251]. In particular, we found that the large vessels of the trunk and the head displayed regions of restriction and enlargement; this type of morphology, with a severely altered lumen, is somehow reminiscent of the morphology of tumor vasculature.

On the basis of the fact that Nova2 affects both neural and vascular cell processes, we suggest that Nova2 is a novel member of the “angioneurins” family. Interestingly, Nova2 is the only “angioneurin” that functions as post-transcriptional regulator.

During my PhD I have used high-throughput technologies to identify novel Nova2 targets in ECs. My results demonstrate that Nova2 modulates AS of transcripts encoding for factors involved in cytoskeletal organization, cell adhesion and polarity (Fig. 18 and 25) consistent with the phenotypes described above. Due to the fact that many of Nova2-regulated AS events generate novel protein with unknown function(s), it is difficult to achieve a comprehensive insight of phenotypic consequences of *Nova2* overexpression or knockdown in ECs and to interpret the global impact of the AS changes we have identified. However, as already observed for the brain [57], Nova2-regulated target genes in ECs encode proteins that interact with each other, suggesting that Nova2-mediated AS plays an important role in affecting physical interactions between these factors during vascular development. This is the case of Abi1 and Arhgef7, whose association is important for PDGF-induced actin cytoskeleton organization [453]. Hence, the phenotypic changes that we observed on *Nova2* knockdown are likely the integrated effects of several AS changes that may act in a coordinated and non-redundant manner.

To identify novel and direct Nova2 targets in ECs, I performed PAR-CLIP and I am waiting for the bioinformatic analysis of the results. In this way, I will be able to construct the "RNA map" of Nova2 regulated AS exons in ECs.

Among Nova2 novel identified targets in ECs, I focused on *Ptbp2*, an AS factor until now considered restricted to brain and testis [69,72]. It is well known that Ptbp2, by binding to CU-rich sequences within or near the AS exons, is able to repress their splicing [79,81,91,454]. Here, I report that Ptbp2 is also expressed in endothelium and that Ptbp2 expression levels in ECs are controlled by a Nova2-mediated AS-NMD event. Indeed, I found that Nova2 promotes skipping of *Ptbp2* exon 10 leading to the production of an mRNA molecule degraded by the NMD pathway (Fig. 20 and 23) indicating that Nova2 functions to repress Ptbp2 expression in ECs (Fig. 19C and D). Importantly, I found that Nova2 dependent AS regulation of *Ptbp2* is specifically conserved in zebrafish endothelium (Fig. 24). It is tempting to speculate that this switch in RNA binding proteins during vascular development could cause changes in the splicing profile of exons that are sensitive to Ptbp2 similarly to the previously described Ptbp1/Ptbp2 interplay during neuronal differentiation [104] (Fig. 7). Collectively, my results reveal a hierarchy of splicing factors that integrate splicing decisions during vascular development.

It is important to note that Ptbp2 interacts with Nova proteins in the brain and that it is able to antagonize the stimulatory effect of Nova proteins on the splicing of exon E3A in *GlyRα2* transcripts [70]. Interestingly, even if Ptbp2 expression in the brain was observed in the nuclei of diverse cell types, including Nova2-positive cortical neurons [70], Ptbp2 and Nova2 showed reciprocal pattern of expression in E14.5 spinal cord [75]. Thus, my findings of Nova2-mediated AS-NMD of *Ptbp2* transcripts could explain the reduced expression of Ptbp2 in mature neurons in which Ptbp1 is absent [104]. It would be of great interest to investigate if Nova2-dependent *Ptbp2*

regulation is restricted to endothelium or if it takes place also in other tissues (i.e. brain).

Recent works have reported that Ptbp2 regulates AS of genes involved in cellular polarity and cytoskeleton organization [434]. Consequently, neuronal progenitors in the *Ptbp2*-null brain exhibited an aberrant polarity and premature neurogenesis [75,104]. Since an important functional similarity in the development of the vascular and nervous systems is the establishment of the apical-basal polarity, as this is crucial for the organization of the vascular lumen and for axon guidance [411,455], I hypothesized that at least a fraction of transcripts encoding for polarity regulators with an AS profile altered in *Nova2* knockdown ECs could be indirect Nova2 targets *via* upregulation of Ptbp2.

In the future it will be interesting to investigate if:

1) common AS exons were present in our RNA-Seq data (*Nova2* depleted or overexpressing ECs) and published data sets of Ptbp2-regulated AS events;

2) these exons affected proteins involved in the establishment of cell polarity or in the organization of cytoskeleton;

3) mis-regulated AS of these exons is observed upon modification of *Nova2* expression levels in ECs *in vitro* or in *nova2* mutant zebrafish *in vivo*;

4) if changes in expression of Ptbp2 in ECs (gain- and loss-of-function experiments) affects the establishment of EC polarity and the organization of vascular lumen *in vitro*;

5) if downregulation of Ptbp2 is able to rescue the altered polarity of *Nova2* depleted ECs or vascular defects of *nova2* mutant zebrafish *in vivo*.

MATERIALS AND METHODS

Cell culture

Mouse endothelial cells VE100 and JAM, immortalized endothelial cell lines generated and extensively characterized by our collaborators [414,435,436] were cultured in DMEM (GIBCO) medium with 10% fetal bovine serum (FBS; EuroClone), glutamine (2 mM, Sigma-Aldrich), penicillin/streptomycin (100 U l^{-1}, Sigma-Aldrich), sodium pyruvate (1 mM, Sigma-Aldrich), heparin (100 µg ml^{-1}, from porcine intestinal mucosa; Sigma-Aldrich) and EC growth supplement (5 µg ml^{-1}, made from calf brain; complete culture medium).VE100 were grown as sparse or confluent by placing 500,000 cells in 100 mm and 35 mm Petri dishes, respectively. The same medium, additioned with puromycin 3 µg ml^{-1} (InvivoGen), was used for stable VE100 cells knockdown or overexpressing *Nova2* (Giampietro et al., 2015).
Human cervix carcinoma HeLa cells (ATCC, CCL-2) were grown in Dulbecco's modified Eagle's medium (DMEM) media supplemented with 10% fetal bovine serum (FBS) and 4mM L-glutamine.

Immunofluorescence

Mouse ECs were seeded in 35 mm Petri dishes coated with Gelatin (Difco) 0.1% and cultured for 48 h. ECs were fixed with 4% paraformaldehyde (PFA) and then permeabilized with 0.5% Triton X-100 for 10 min. Blocking (1 h), primary (overnight) and secondary (1 h) antibodies were diluted in PBS with 2% BSA. Primary antibody: anti-Ptbp2 (EPR9890, Abcam). Secondary antibody: anti-rabbit antibody conjugated with Alexa Fluor 555. Nuclei were stained with 0.1 g ml^{-1} DAPI (Sigma-Aldrich).
For imaging, epifluorescence microscope (Optical Microscope Olympus IX71) equipped with 60X objective was used. Photomicrographs were taken with digital camera Cool SNAPES (Photometrics). Data acquisition was done using the MetaMorph 7.7.5 software (Universal Imaging Corporation). Images were exported to Photoshop (Adobe). No manipulations were performed other than adjustments in brightness and contrast.

Cycloheximide (CHX) treatment

To study the sensitivity of splicing isoforms to NMD, mouse VE100 ECs transduced with lentiviral vectors carrying shRNA for *Nova2* [251] were seeded in 35 mm Petri dishes to reach 80% of confluence after 24h. Cells were treated with CHX (Sigma-Aldrich) at a final concentration of 50 µg ml^{-1} or with DMSO as negative control for 4h before analysis.

Plasmid transfection

Plasmids were transfected in HeLa cells and in mouse ECs transduced with lentiviral vectors carrying shRNA for *Nova2* [251] or control ECs by using Lipofectamine 3000 (Invitrogen) as recommended by the provider. Briefly, cells were seeded in 35 mm

Petri dishes to reach 80% of confluence after 24h. Cells were then transfected and assayed after 24 h.

RNA interference with siRNA oligonucleotides
RNA interference was carried out as described [456]. Briefly, VE100 ECs were seeded in 35 mm Petri dishes to reach 80% of confluence after 24h. Cells were then transfected two times with 24 h intervals by using Lipofectamine 3000 (Invitrogen) according to the manufacturer's instructions. Cells were assayed 24 h after the second transfection. I used the following RNA interference siRNA oligonucleotides: ON-TARGETplus Upf1 siRNA (pool of four siRNA) and ON-TARGETplus non-targeting pool (as a negative control) (Dharmacon).

RNA extraction, RT-PCR and qRT-PCR
Total RNA was isolated using the RNeasy Mini Kit (QIAGEN) according to the manufacturer's instructions.
For freshly purified zebrafish ECs RNA was extracted with RNeasy Micro Kit (QIAGEN) according to the manufacturer's instructions.
After treatment with DNase I (Ambion), 2–3 μg of RNA were retro-transcribed with a mix of oligos $d(T)_{18}$ and random hexamers and Superscript III RT (Invitrogen). An aliquot (1/20) of RT was then PCR-amplified with the Taq Polymerase GoTaq (Promega). For qRT-PCR, an aliquot of the RT reaction was analyzed with QuantiTect SYBR Green PCR (QIAGEN) by using LyghtCycler 480 (Roche). Target transcript levels were normalized to those of reference genes (Ubiquitin). The expression of each gene was measured in at least three independent experiments. All PCR primers were listed in Table 5 and Table 6. All PCR products were sequenced and the bands intensity on agarose gel was quantified with the NIH Image J program (version 1.45).

Western blot analysis
Cells were lysed in Laemmli buffer and proteins were separated using SDS–PAGE and analyzed by western blotting by standard procedures. The following primary antibodies were used: anti-Nova2 (1:200 Santa Cruz Biotechnology, C-16), anti-Ptbp2 (EPR9890, Abcam; 1:5,000), anti-GAPDH (1:5,000 Abcam; 1:50,000 AbFrontier), anti-Tubulin (1:100,000 Sigma-Aldrich), anti-haemagglutinin (HA; 1:1,000 Roche). The following secondary antibodies linked to horseradish peroxidase (Jackson ImmunoResearch) were used: anti-Mouse (1:10,000), anti-Goat (1:5,000) and anti-Rabbit (1:10,000). Immunostained bands were detected using the chemiluminescent method (Pierce).

Plasmids
Mouse p-Ptbp2 minigene encompassing exons 9, 10 and 11 with the flanking introns

was amplified with primers Ptbp2-exon9-HindIII and Ptbp2-exon 11-EcoRI (Table 7); Ptbp2 cassette was cloned in pcDNA3.1(+) vector (Invitrogen) into the HindIII and EcoRI sites. These construct was verified by sequencing. HA-Nova2 and T7-SRSF1 expression vectors were already generated in our laboratory [200,251].

RNA- Seq and splicing analysis

RNA-Seq was conducted on two control and two *Nova2*-depleted ECs and on two control and two *Nova2*-overexpressing ECs. Samples were sequenced on Illumina HiSeq2500 (average of ~93 million, 100 nt paired-end reads for each run). In collaboration with Prof. Blencowe and Dr. Irimia we employed *vast-tools* to identify and quantify all major types of AS events. Only AS events with a minimum read coverage in all four samples were compared, which was defined as:

- For cassette exons (except for those quantified using the microexon pipeline, see Irimia *et al*. for details): (i) ⩾10 reads mapping to the sum of exclusion EEJs or (ii) ⩾10 reads mapping to one of the two inclusion EEJs and ⩾5 to the other inclusion EEJ.
- For microexons: (i) ⩾10 reads mapping to the sum of exclusion EEJs or (ii) ⩾10 reads mapping to the sum of inclusion EEJs.
- For intron retention: (i) ⩾10 reads mapping to the sum of skipping EEJs or (ii) ⩾10 reads mapping to one of the two inclusion EIJs and ⩾5 to the other inclusion EIJ.
- For alternative 3′ and 5′ splice sites: ⩾10 reads mapping to the sum of all EEJs involved in the specific event.

Additional filtering was used to remove intron retention events with a binomial *P* value score above 0.05 in any of the four samples.
Cassette exons events identified by RNA-Seq are listed in Table 3 (*Nova2* depleted ECs) and Table 4 (*Nova2* overexpressing ECs) of the Appendix.

Zebrafish strains and ECs purification form Zebrafish embryos

Zerafish experiments were carried out in the facility of IFOM (Milan) in collaboration with Dr. De Florian. Zebrafish from wild type AB and transgenic Tg(fli1a:eGFP) or Tg(Kdrl:GFP) strains were maintained and bred according with standard procedures and national guidelines (Italian decree "4th March 2014, n.26"), under IACUC (Institutional Animal Care and Use Committee) approval.
For ECs purification experiment 50-60 zebrafish embryos of 4 days post-fertilization from transgenic line Tg(fli1a:eGFP) or Tg(Kdrl:GFP) of control or *nova2* CRISPR-mutated zebrafish were used. GFP negative fish (from AB lines) were used as negative control.
Embryos were washed with PBS, treated with deyolking solution. Deyolked embryos were dissociated by using protease solution at 28°C for around 50 min. [Protease solution: 1 ml of PBS 10X, 20 µl of EDTA 0.5M, pH 8, 1 ml Trypsin 2.5%,

7.98 ml sterile water] Dissociation was monitored with stereomicroscope.
The reaction was stopped with 1 ml of stop solution [1 ml PBS 10X, 3 ml FBS, 30 µl $CaCl_2$ 2M, 5.97 ml sterile water] and the final solution containing cells was centrifuged at 3.000 rpm for 3 min. Cells were resuspended in suspension media ($5x10^6$ cells ml^{-1}) [5 ml PBS 10X, 20 µl $CaCl_2$ 2M, 1 ml FBS, 4.48 ml sterile water (GIBCO ultra-pure)] and transferred in a "sorter/facs tube" by passing the cells through a cell strainer of 70 µm in ice. Cells were analyzed by IFOM Sorter Facility with the MoFlo Astrios (Beckman Coulter Inc.) cell sorter. GFP+ cells were centrifuged at 5.000 rpm for 10 min, the supernatant was discarded and TRIZOL reagent (500-750 µl) was added for subsequent RNA extraction.

iCLIP
iCLIP was carried out as described [54]. Mouse ECs (VE100) were seeded in two 150 mm Petri dishes coated with Gelatin (Difco) 0.1% and after 72 h were UV cross-linked on ice with 150 mJ cm^{-2} in a Stratlinker 2400 at 254 nm. Cells were then lysed in Lysis buffer (with protease inhibitors) and sonicated with 10 s bursts at 5 decibels. Samples were treated with RNAse I (Ambion, AM2295) 3min at 37°C. After centrifuging 10 min at 15000 rpm at 4°C, the supernatant was used in RNA-IP. For each RNA-IP, 25 µl of Dynabeads Protein G (Life Technologies) were conjugated with 2 µg of anti-Nova2 (Santa Cruz Biotechnology, C-16) or IgG (Jackson ImmunoResearch Laboratories) as control and incubate for 1h at 4°C. Beads were washed with high salt buffer and PNK buffer. 3' end RNA phosphorylation was performed in PNK buffer pH 6.5 and beads were washed again with high salt buffer and PNK buffer. Linker ligation was performed in ligation buffer overnight at 16°C. The beads were washed with PNK buffer, high salt buffer and again PNK buffer. Pre-adenylated linker L3-App was linked to the RNAs with RNA ligase (NEB) overnight. at 16°C. Beads were washed with PNK buffer, high salt buffer and again PNK buffer. ^{32}P-γ-ATP was used to label 5' end of RNAs 5 min at 37°C. RNA was eluted from the beads with NuPAGE loading buffer (Invitrogen), beads were precipitated on magnet and the eluate was collected and loaded on a 4-12% NuPAGE Bis-Tris gel (Invitrogen) according to the manufacturer's instructions. The protein-RNA complexes were transferred from the gel to a Protan BA85 Nitrocellulose Membrane (Whatman) and exposed O.N. at -80°C to a Fuji film. Protein-RNA complexes were cutted out of the nitrocellulose membrane by using autoradiograph as a mask. Protein was digested with Proteinase K (Roche) 20 min at 37°C in PNK buffer in presence of 7 M urea and incubated for further 20 min at 37°C. RNA was precipitated by addition of 0.5 µl glycoblue (Ambion) and 40 µl 3 M Sodium Acetate. Then RNA was precipitated overnight at -20°C in 100% ethanol. cDNA was retro-transcribed using Suprscript III (Invitrogen). cDNA was precipiteted with ethanol 100% overnight. The precipitated pellet was resuspended in water and runned in a 6% TBE-urea gel for 40 min at 180 V. A band corresponding to 100-150 nt was cutted

out from the gel and precipitated overnight. Subsequently the primer containing two cleavable adaptor regions and the barcode was ligated to the 5' end of the cDNA with CircLigase II (Epicentre). Circularyzed cDNA was then digested with BamHI (Fast Fermentas) for linearization. cDNA library was prepared by PCR amplification. For buffers composition see the original protocol [54].

PAR-CLIP

PAR-CLIP was carried out as described [55]. Mouse ECs (JAM) were expanded in the appropriate medium in 20 150 mm Petri dishes at 80% of confluence. 4-thiouridine (4SU) was added 6 h before crosslinking to a final concentration of 200 μM. Cells were UV crosslinked at 365 nm in a Spectrolinker XL-1500 (Spectronics Corporation). 20 150-mm dishes were used as a negative control. Cells were scraped and the pellet was collected by centrifugation at 500 g at 4°C for 5 min. Cell pellets were lysed in 1× NP40 lysis buffer and cleared by centrifugation at 13,000 g at 4°C for 15 min. RNA digestion was performed with RNase I diluted 1:200 (high RNAse concentration) or RNase I diluted 1:5000 10 min at 37 °C. Protein G Dynabeads (Invitrogen) were resuspended in twice the volume of citrate-phosphate buffer relative to the original volume of bead suspension. Beads were coupled to Nova2 antibody (Santa Cruz Biotechnology, C-16) (5 μg of antibody per 40 μl bead suspension) and incubated on a rotating wheel for 40 min at room temperature. Antibody-conjugated magnetic beads were washed twice in citrate-phosphate buffer to remove unbound antibody and the treated cell lysate was added; incubation was performed on a rotating wheel for 1 h at 4°C. After 3 washes with high salt wash buffer, 3' end of digested RNAs were phosphorylated with PNK enzyme and radiolabeled with ^{32}P-γ-ATP to a final concentration of 0.5 μCi μl^{-1} (1.6 μM ATP) 40 min at 37 °C. Non-radioactive ATP was added to obtain a final concentration of 100 μM and incubate for another 5 min at 37°C. Beads were washed and resuspended in PNK buffer without DTT, then SDS-PAGE loading buffer was added and the radiolabeled suspension was incubated 5 min in a heat block at 95°C to denature and release the immunoprecipitated Nova2 proteins with crosslinked RNA (RNA-RBP complexes). The supernatant was loaded on precast Novex Bis-Tris 4-12% polyacrylamide gel (Invitrogen), runned for 55 min at 200 V. The gel was exposed to a blanked phosphorimager screen overnight and visualized on a phosphorimager. The band that correspond to the expected size of Nova2 (70 kDa) was cutted out fom the gel and the crosslinked RNA-RBP complexes were electroeluted in 1× SDS running buffer at 100 V for 2 h. The recovered RNA underwent a standard cDNA library preparation protocol originally described for cloning of small regulatory RNAs, consisting of the following steps: 3' adapter ligation, 5’ adapter ligation, RT with Superscript III (Invitrogen) and PCR amplification. For buffers composition see the original protocol [55].

Primer lists

Table 5. Primers for RT-PCR

PRIMER NAME	SEQUENCE 5'- TO 3'-DIRECTION
Mouse-Magi1-for	CAAGGCAGCCAGAACTCTCT
Mouse-Magi1-rev	GGTGATGGTGGCAATCTTCT
Mouse-Dock9-for	TTCCAGTACATGGGGAAGCG
Mouse-Dock9 rev	ACCTCAGTAGCGATGTTGGC
Mouse-Abi1-for	ATCGCACCCGCAAATATGGA
Mouse-Abi1-rev	TGGGAGGGTTTGTTCTCGAC
Mouse-Dysf-for	ACCGCCTCACTCACAATGAC
Mouse-Dysf-rev	AACTCTCGGGGACTGCCATA
Mouse-Phldb2-for	AGTCTCACTGGTGGGAAAGG
Mouse-Phldb2-rev	TCTTTCGAGGCAGAGTGTCA
Mouse-Srgap1-for	ATGACTTGCTGCAGAGGACT
Mouse-Srgap1-rev	AATCGGATGCAGCTTTCCAC
Mouse-Fmnl2-for	TGCGGAATTAAGAAGGCGACA
Mouse-Fmnl2-rev	TGAAGGTGGTCTCCAGTCAC
Mouse- Myo9a-for	GCAGGAGCAAGTGAGGAAGA
Mouse- Myo9a-rev	CGTGTCTTGGGAAGAAATCC
Mouse- Rapgef6-for	TGACTTCTGCCAACATGGAC
Mouse- Rapgef6-rev	TGACTTCTGCCAACATGGAC
Mouse- Arhgef7-for	TTACACGAGTGGGTGGAACA
Mouse- Arhgef7-rev	TGGTCTTGGGGCTCTTACTG
Mouse-Ktn1-for	TGGACAGATCAAGTCTGTGGAA
Mouse-Ktn1-rev	GTTCTGCAGCTCCTGGACTT
Mouse-Cd97-for	ACACCTGCGTCTGTAACCTG
Mouse-Cd97-rev	TGCAGACGGTGGAATTGTGA

PRIMER NAME	SEQUENCE 5'- TO 3'-DIRECTION
Mouse-Lrch3-for	GATGTCACCTCAAGCTTTCCT
Mouse-Lrch3-rev	GTTGCAGGTGCAGATGACAG
Mouse-Ptbp2-for	CAGGGGCTCTCAGTCCTTTG
Mouse-Ptbp2-rev	CTGGGACTGGTTCCCATCAG
Mouse-Ptbp1-for	AGGTGCTGGGAATTCTGTCC
Mouse-Ptbp1-rev	CCATCTGCACAAGTGCGTTC
Zebrafish-Ptbp2a-for	GCGGCTGCTGGAAGAGTG
Zebrafish-Ptbp2a-rev	AAAAAGGATCTTCACGCGCT
Zebrafish-Ptbp2b-for	GGTAGCGTTGTCCGGTCATT
Zebrafish-Ptbp2b-rev	GGCCTGGTTTCCATCAGACA
BGHrev	CTAGAAGGCACAGTCGAGGCTGATCAGCGG

Table 6. Primers for qPCR

PRIMER NAME	SEQUENCE 5'- TO 3'-DIRECTION
Mouse-Ubiquitin-for	TCTTCGTGAAGACCCTGACC
Mouse-Ubiquitin-rev	CAGGTGCAGGGTTGACTCTT
Mouse-Nova2-for	AGGACTGATCATCGGTAAGG
Mouse-Nova2-rev	GGGTCTTCCTGTACCTTCTG
Human-Nova2-for	CAGCTTTATTGCCGAGAAGG
Human-Nova2-rev	ACCCATGCTCCTGACTGTTC
Mouse-Ptbp2-for	CTCCAGCCCAGAGTCCAGTA
Mouse-Ptbp2-rev	GCAAAGCCTGAAACTGGTTGT
Mouse-Ptbp1-for	GCACCGCTTCAAGAAACCAG
Mouse-Ptbp1-rev	TGAAGCCTTTGACCACACCA
Mouse-Ptbp2 NMD+-for	TAAATGAAGAGGTGTTTATGGA
Mouse-Ptbp2 NMD+-rev	TAAATGAAGAGGTGTTTATGGA

Table 7. Primers for cloning experiment

PRIMER NAME	**SEQUENCE 5'- TO 3'-DIRECTION**
Ptbp2-exon9-HindIII	CCCAAGCTTCTGTTCCAGGGGCTC TCAGT
Ptbp2-exon 11-EcoRI	CGGAATTCCGAGCTGGGACTGGT TCCCA

REFERENCES

1. Chen, M. & Manley, J. L. Mechanisms of alternative splicing regulation: insights from molecular and genomics approaches. *Nat. Rev. Mol. Cell Biol.* **10,** 741–54 (2009).
2. JiaYan, W. *et al.* Systematic analysis of intron size and abundance parameters in diverse lineages. *Sci. China Life Sci.* **56,** 968–974 (2013).
3. Maniatis, T. & Reed, R. An extensive network of coupling among gene expression machines. *Nature* **416,** 499–506 (2002).
4. Moore, M. J. *et al.* Pre-mRNA processing reaches back to transcription and ahead to translation. *Cell* **136,** 688–700 (2009).
5. Hocine, S., Singer, R. H. & Grünwald, D. RNA processing and export. *Cold Spring Harbor perspectives in biology* **2,** a000752 (2010).
6. Black, D. L. Mechanisms of Alternative Pre-Messenger RNA Splicing. *Annu. Rev. Biochem.* **72,** 291–336 (2003).
7. Wang, Z. & Burge, C. B. Splicing regulation: from a parts list of regulatory elements to an integrated splicing code. *RNA* **14,** 802–13 (2008).
8. Wahl, M. C. *et al.* The Spliceosome: design principles of a dynamic RNP machine. *Cell* **136,** 701–718 (2009).
9. Hoskins, A. A. *et al.* The spliceosome: a flexible, reversible macromolecular machine. *Trends Biochem. Sci.* **37,** 179–88 (2012).
10. Will, C. L. & Lührmann, R. Spliceosome structure and function. *Cold Spring Harb. Perspect. Biol.* **3,** 1–2 (2011).
11. Blencowe, B. J. Alternative Splicing: New Insights from Global Analyses. *Cell* **126,** 37–47 (2006).
12. Early, P. *et al.* Two mRNAs can be produced from a single immunoglobulin mu gene by alternative RNA processing pathways. *Cell* **20,** 313–319 (1980).
13. Fu, X.-D. & Ares, M. Context-dependent control of alternative splicing by RNA-binding proteins. *Nat. Rev. Genet.* **15,** 689–701 (2014).
14. Human Genome Sequencing Consortium, I. Finishing the euchromatic sequence of the human genome. *Nature* **431,** 931–945 (2004).
15. Pandey, U. B. & Nichols, C. D. Human disease models in Drosophila melanogaster and the role of the fly in therapeutic drug discovery. *Pharmacol. Rev.* **63,** 411–36 (2011).
16. Stein, L. D. *et al.* The genome sequence of Caenorhabditis briggsae: a platform for comparative genomics. *PLoS Biol.* **1,** E45 (2003).
17. Ramani, A. K. *et al.* Genome-wide analysis of alternative splicing in Caenorhabditis elegans. *Genome Res.* **21,** 342–8 (2011).
18. Graveley, B. R. *et al.* The developmental transcriptome of Drosophila melanogaster. *Nature* **471,** 473–9 (2011).
19. Le, K. *et al.* Detecting tissue-specific regulation of alternative splicing as a qualitative change in microarray data. *Nucleic Acids Res.* **32,** e180 (2004).
20. Pan, Q., Shai, O., Lee, L. J., Frey, B. J. & Blencowe, B. J. Deep surveying of alternative splicing complexity in the human transcriptome by high-throughput sequencing. *Nat. Genet.* **40,** 1413–1415 (2008).
21. Paronetto, M. P. *et al.* Regulation of FAS exon definition and apoptosis by the ewing sarcoma protein. *Cell Rep.* **7,** 1211–1226 (2014).
22. Keren, H., Lev-Maor, G. & Ast, G. Alternative splicing and evolution: diversification, exon definition and function. *Nat. Rev. Genet.* **11,** 345–355 (2010).
23. Wang, Y. *et al.* Mechanism of alternative splicing and its regulation. *Biomed. reports* **3,** 152–158 (2015).
24. Matera, A. G. & Wang, Z. A day in the life of the spliceosome. *Nat. Rev.*

Mol. Cell Biol. **15,** 108–121 (2014).
25. Long, J. C. & Caceres, J. F. The SR protein family of splicing factors: master regulators of gene expression. *Biochem. J.* **417,** 15–27 (2009).
26. Shepard, P. J. & Hertel, K. J. The SR protein family. *Genome Biol.* **10,** 242 (2009).
27. Manley, J. L. & Krainer, A. R. A rational nomenclature for serine/arginine-rich protein splicing factors (SR proteins). *Genes and Development* **24,** 1073–1074 (2010).
28. Zhu, J. *et al.* Exon identity established through differential antagonism between exonic splicing silencer-bound hnRNP A1 and enhancer-bound SR proteins. *Mol. Cell* **8,** 1351–61 (2001).
29. Dreyfuss, G., Matunis, M. J., Piñol-Roma, S. & Burd, C. G. hnRNP proteins and the biogenesis of mRNA. *Annu. Rev. Biochem.* **62,** 289–321 (1993).
30. Han, S. P., Tang, Y. H. & Smith, R. Functional diversity of the hnRNPs: past, present and perspectives. *Biochem. J.* **430,** 379–92 (2010).
31. Chaudhury, A., Chander, P. & Howe, P. H. Heterogeneous nuclear ribonucleoproteins (hnRNPs) in cellular processes: Focus on hnRNP E1's multifunctional regulatory roles. *RNA* **16,** 1449–1462 (2010).
32. Hnilicová, J. & Staněk, D. Where splicing joins chromatin. *Nucleus* **2,** 182–8 (2011).
33. Vautier, D. *et al.* Transcription-dependent nucleocytoplasmic distribution of hnRNP A1 protein in early mouse embryos. *J. Cell Sci.* **114,** 1521–31 (2001).
34. Dutertre, M. *et al.* DNA damage: RNA-binding proteins protect from near and far. *Trends Biochem. Sci.* **39,** 141–9 (2014).
35. Chen, H.-C. & Cheng, S.-C. Functional roles of protein splicing factors. *Biosci. Rep.* **32,** 345–59 (2012).
36. Nilsen, T. W. & Graveley, B. R. Expansion of the eukaryotic proteome by alternative splicing. *Nature* **463,** 457–63 (2010).
37. Grosso, A. R. *et al.* Tissue-specific splicing factor gene expression signatures. *Nucleic Acids Res.* **36,** 4823–4832 (2008).
38. Barbosa-Morais, N. L. *et al.* The evolutionary landscape of alternative splicing in vertebrate species. *Science (80-.).* **338,** 1587–1593 (2012).
39. Braunschweig, U. *et al.* Widespread intron retention in mammals functionally tunes transcriptomes. *Genome Res.* **24,** 1774–1786 (2014).
40. Merkin, J., Russell, C., Chen, P. & Burge, C. B. Evolutionary Dynamics of Gene and Isoform Regulation in Mammalian Tissues. *Science (80-.).* **338,** 1593–1599 (2012).
41. Lipscombe, D. Neuronal proteins custom designed by alternative splicing. *Current Opinion in Neurobiology* **15,** 358–363 (2005).
42. Li, Q., Lee, J.-A. & Black, D. L. Neuronal regulation of alternative pre-mRNA splicing. *Nat. Rev. Neurosci.* **8,** 819–831 (2007).
43. Zheng, S. *et al.* Alternative pre-mRNA splicing in neurons: growing up and extending its reach. *Trends Genet.* **29,** 442–448 (2013).
44. Buckanovich, R. J., Yang, Y. Y. & Darnell, R. B. The onconeural antigen Nova-1 is a neuron-specific RNA-binding protein, the activity of which is inhibited by paraneoplastic antibodies. *J. Neurosci.* **16,** 1114–1122 (1996).
45. Yang, Y. Y., Yin, G. L. & Darnell, R. B. The neuronal RNA-binding protein Nova-2 is implicated as the autoantigen targeted in POMA patients with dementia. *Proc. Natl. Acad. Sci. U. S. A.* **95,** 13254–9 (1998).
46. Saito, Y. *et al.* NOVA2-mediated RNA regulation is required for axonal pathfinding during development. *Elife* **e14371,** (2016).

47. Lewis, H. A. *et al.* Sequence-specific RNA binding by a Nova KH domain: implications for paraneoplastic disease and the fragile X syndrome. *Cell* **100,** 323–32 (2000).
48. Ule, J. *et al.* An RNA map predicting Nova-dependent splicing regulation. *Nature* **444,** 580–586 (2006).
49. Jelen, N., Ule, J., Živin, M. & Darnell, R. B. Evolution of Nova-Dependent Splicing Regulation in the Brain. *PLOS Genet* **3,** 236–243 (2007).
50. Brooks, A. N. *et al.* Conservation of an RNA regulatory map between Drosophila and mammals. *Genome Res.* **21,** 193–202 (2011).
51. Irimia, M. *et al.* Stepwise assembly of the Nova-regulated alternative splicing network in the vertebrate brain. *Proc. Natl. Acad. Sci. U. S. A.* **108,** 5319–24 (2011).
52. Jensen, K. B. *et al.* Nova-1 Regulates Neuron-Specific Alternative Splicing and Is Essential for Neuronal Viability. *Neuron* **25,** 359–371 (2000).
53. Ruggiu, M. *et al.* Rescuing Z+ agrin splicing in Nova null mice restores synapse formation and unmasks a physiologic defect in motor neuron firing. *Proc. Natl. Acad. Sci. U. S. A.* **106,** 3513–3518 (2009).
54. Konig, J. *et al.* iCLIP--transcriptome-wide mapping of protein-RNA interactions with individual nucleotide resolution. *J. Vis. Exp.* (2011). doi:10.3791/2638
55. Hafner, M. *et al.* Transcriptome-wide identification of RNA-binding protein and microRNA target sites by PAR-CLIP. *Cell* **141,** 129–41 (2010).
56. Licatalosi, D. D. & Darnell, R. B. RNA processing and its regulation: global insights into biological networks. *Nat. Rev. Genet.* **11,** 75–87 (2010).
57. Ule, J. *et al.* Nova regulates brain-specific splicing to shape the synapse. *Nat. Genet.* **37,** 844–852 (2005).
58. Ule, J. *et al.* CLIP identifies Nova-regulated RNA networks in the brain. *Science* **302,** 1212–5 (2003).
59. Darnell, R. B. RNA Protein Interaction in Neurons. *Annu. Rev. Neurosci.* **36,** 243–270 (2013).
60. Leggere, J. C. *et al.* NOVA regulate alternative splicing during neuronal migration and axon guidance in the spinal cord. *Elife* **5,** 1–25 (2016).
61. Racca, C. *et al.* The Neuronal Splicing Factor Nova Co-Localizes with Target RNAs in the Dendrite. *Front. Neural Circuits* **4,** 5 (2010).
62. Eom, T. *et al.* NOVA-dependent regulation of cryptic NMD exons controls synaptic protein levels after seizure. *Elife* **2,** e00178 (2013).
63. Chen, H.-H., Lin, J.-C. & Tar, W.-Y. in *RNA Processing* (InTech, 2011). doi:10.5772/22477
64. Ratti, A. *et al.* Post-transcriptional regulation of neuro-oncological ventral antigen 1 by the neuronal RNA-binding proteins ELAV. *J. Biol. Chem.* **283,** 7531–7541 (2008).
65. Park, E. *et al.* Nova-1 mediates glucocorticoid-induced inhibition of Pre-mRNA splicing of gonadotropin-releasing hormone transcripts. *J. Biol. Chem.* **284,** 12792–12800 (2009).
66. Dredge, B. K., Stefani, G., Engelhard, C. C. & Darnell, R. B. Nova autoregulation reveals dual functions in neuronal splicing. *EMBO J.* **24,** 1608–20 (2005).
67. Storchel, P. H. *et al.* A large-scale functional screen identifies Nova1 and Ncoa3 as regulators of neuronal miRNA function. *EMBO J.* **34,** 2237–2254 (2015).
68. Ashiya, M. & Grabowski, P. J. A neuron-specific splicing switch mediated by an array of pre-mRNA repressor sites: evidence of a regulatory role for the polypyrimidine tract binding protein and a brain-specific PTB

counterpart. *RNA* **3,** 996–1015 (1997).
69. Markovtsov, V. *et al.* Cooperative assembly of an hnRNP complex induced by a tissue-specific homolog of polypyrimidine tract binding protein. *Mol. Cell. Biol.* **20,** 7463–7479 (2000).
70. Polydorides, A. D., Okano, H. J., Yang, Y. Y., Stefani, G. & Darnell, R. B. A brain-enriched polypyrimidine tract-binding protein antagonizes the ability of Nova to regulate neuron-specific alternative splicing. *Proc. Natl. Acad. Sci. U. S. A.* **97,** 6350–5 (2000).
71. Romanelli, M. G., Lorenzi, P. & Morandi, C. Identification and analysis of the human neural polypyrimidine tract binding protein (nPTB) gene promoter region. *Gene* **356,** 11–8 (2005).
72. Zagore, L. L. *et al.* RNA Binding Protein Ptbp2 Is Essential for Male Germ Cell Development. *Mol. Cell. Biol.* **35,** 4030–42 (2015).
73. Oberstrass, F. C. *et al.* Structure of PTB bound to RNA: specific binding and implications for splicing regulation. *Science* **309,** 2054–7 (2005).
74. Romanelli, M. G., Diani, E. & Lievens, P. M.-J. New insights into functional roles of the polypyrimidine tract-binding protein. *Int. J. Mol. Sci.* **14,** 22906–32 (2013).
75. Licatalosi, D. D. *et al.* Ptbp2 represses adult-specific splicing to regulate the generation of neuronal precursors in the embryonic brain. *Genes Dev.* **26,** 1626–1642 (2012).
76. Chan, R. C. & Black, D. L. The polypyrimidine tract binding protein binds upstream of neural cell-specific c-src exon N1 to repress the splicing of the intron downstream. *Mol. Cell. Biol.* **17,** 4667–76 (1997).
77. Pérez, I., Lin, C. H., McAfee, J. G. & Patton, J. G. Mutation of PTB binding sites causes misregulation of alternative 3' splice site selection in vivo. *RNA* **3,** 764–78 (1997).
78. Reid, D. C. *et al.* Next-generation SELEX identifies sequence and structural determinants of splicing factor binding in human pre-mRNA sequence. *RNA* **15,** 2385–97 (2009).
79. Llorian, M. *et al.* Position-dependent alternative splicing activity revealed by global profiling of alternative splicing events regulated by PTB. *Nat. Struct. Mol. Biol.* **17,** 1114–23 (2010).
80. Sharma, S., Kohlstaedt, L. A., Damianov, A., Rio, D. C. & Black, D. L. Polypyrimidine tract binding protein controls the transition from exon definition to an intron defined spliceosome. *Nat. Struct. Mol. Biol.* **15,** 183–91 (2008).
81. Xue, Y. *et al.* Genome-wide analysis of PTB-RNA interactions reveals a strategy used by the general splicing repressor to modulate exon inclusion or skipping. *Mol. Cell* **36,** 996–1006 (2009).
82. Licatalosi, D. D. *et al.* HITS-CLIP yields genome-wide insights into brain alternative RNA processing. *Nature* **456,** 464–9 (2008).
83. Zhang, C. *et al.* Defining the regulatory network of the tissue-specific splicing factors Fox-1 and Fox-2. *Genes Dev.* **22,** 2550–2563 (2008).
84. Tollervey, J. R. *et al.* Analysis of alternative splicing associated with aging and neurodegeneration in the human brain. *Genome Res.* **21,** 1572–82 (2011).
85. Witten, J. T. & Ule, J. Understanding splicing regulation through RNA splicing maps. *Trends Genet.* **27,** 89–97 (2011).
86. Spellman, R., Llorian, M. & Smith, C. W. J. Crossregulation and functional redundancy between the splicing regulator PTB and its paralogs nPTB and ROD1. *Mol. Cell* **27,** 420–34 (2007).
87. Boutz, P. L., Chawla, G., Stoilov, P. & Black, D. L. MicroRNAs regulate

the expression of the alternative splicing factor nPTB during muscle development. *Genes Dev.* **21,** 71–84 (2007).
88. Makeyev, E. V, Zhang, J., Carrasco, M. A. & Maniatis, T. The MicroRNA miR-124 promotes neuronal differentiation by triggering brain-specific alternative pre-mRNA splicing. *Mol. Cell* **27,** 435–48 (2007).
89. Boutz, P. L. *et al.* A post-transcriptional regulatory switch in polypyrimidine tract-binding proteins reprograms alternative splicing in developing neurons. *Genes Dev.* **21,** 1636–1652 (2007).
90. Keppetipola, N. M. *et al.* Multiple determinants of splicing repression activity in the polypyrimidine tract binding proteins, PTBP1 and PTBP2. *RNA* **22,** 1172–80 (2016).
91. Keppetipola, N., Sharma, S., Li, Q. & Black, D. L. Neuronal regulation of pre-mRNA splicing by polypyrimidine tract binding proteins, PTBP1 and PTBP2. *Crit. Rev. Biochem. Mol. Biol.* **47,** 360–78 (2012).
92. Tang, Z. Z. *et al.* Regulation of the mutually exclusive exons 8a and 8 in the CaV1.2 calcium channel transcript by polypyrimidine tract-binding protein. *J. Biol. Chem.* **286,** 10007–16 (2011).
93. Zheng, S. *et al.* PSD-95 is post-transcriptionally repressed during early neural development by PTBP1 and PTBP2. *Nat. Neurosci.* **15,** 381–8, S1 (2012).
94. Popp, M. W.-L. & Maquat, L. E. Organizing principles of mammalian nonsense-mediated mRNA decay. *Annu. Rev. Genet.* **47,** 139–65 (2013).
95. McGlincy, N. J. & Smith, C. W. J. Alternative splicing resulting in nonsense-mediated mRNA decay: what is the meaning of nonsense? *Trends in Biochemical Sciences* **33,** 385–393 (2008).
96. Ni, J. Z. *et al.* Ultraconserved elements are associated with homeostatic control of splicing regulators by alternative splicing and nonsense-mediated decay. *Genes Dev.* **21,** 708–18 (2007).
97. Lareau, L. F. & Brenner, S. E. Regulation of Splicing Factors by Alternative Splicing and NMD Is Conserved between Kingdoms Yet Evolutionarily Flexible. *Mol. Biol. Evol.* **32,** 1072–1079 (2015).
98. Saltzman, A. L. *et al.* Regulation of Multiple Core Spliceosomal Proteins by Alternative Splicing-Coupled Nonsense-Mediated mRNA Decay. *Mol. Cell. Biol.* **28,** 4320–4330 (2008).
99. Lareau, L. F., Brooks, A. N., Soergel, D. A. W., Meng, Q. & Brenner, S. E. The coupling of alternative splicing and nonsense-mediated mRNA decay. *Adv. Exp. Med. Biol.* **623,** 190–211 (2007).
100. Rahman, L., Bliskovski, V., Kaye, F. J. & Zajac-Kaye, M. Evolutionary conservation of a 2-kb intronic sequence flanking a tissue-specific alternative exon in the PTBP2 gene. *Genomics* **83,** 76–84 (2004).
101. Lebedeva, S. *et al.* Transcriptome-wide Analysis of Regulatory Interactions of the RNA-Binding Protein HuR. *Mol. Cell* **43,** 340–352 (2011).
102. Johnson, J. O. *et al.* Mutations in the Matrin 3 gene cause familial amyotrophic lateral sclerosis. *Nat. Neurosci.* **17,** 664–666 (2014).
103. Coelho, M. B. *et al.* Nuclear matrix protein Matrin3 regulates alternative splicing and forms overlapping regulatory networks with PTB. *EMBO J.* **34,** 653–668 (2015).
104. Li, Q. *et al.* The splicing regulator PTBP2 controls a program of embryonic splicing required for neuronal maturation. *Elife* **3,** e01201 (2014).
105. Hanahan, D. & Weinberg, R. A. Hallmarks of cancer: The next generation. *Cell* **144,** 646–674 (2011).
106. Bonomi, S. *et al.* Oncogenic alternative splicing switches: Role in cancer

progression and prospects for therapy. *International Journal of Cell Biology* **2013,** 1–17 (2013).
107. Chen, J. & Weiss, W. A. Alternative splicing in cancer: implications for biology and therapy. *Oncogene* **34,** 1–14 (2014).
108. Ladomery, M. Aberrant alternative splicing is another hallmark of cancer. *International Journal of Cell Biology* **2013,** 1–6 (2013).
109. Oltean, S. & Bates, D. O. Hallmarks of alternative splicing in cancer. *Oncogene* **33,** 1–8 (2013).
110. Liu, S. & Cheng, C. Alternative RNA splicing and cancer. *Wiley Interdiscip. Rev. RNA* **4,** 547–566 (2013).
111. Germann, S., Gratadou, L., Dutertre, M. & Auboeuf, D. Splicing programs and cancer. *Journal of Nucleic Acids* **2012,** 269570 (2012).
112. Ghigna, C., Valacca, C. & Biamonti, G. Alternative splicing and tumor progression. *Curr. Genomics* **9,** 556–70 (2008).
113. Sterne-Weiler, T. & Sanford, J. R. Exon identity crisis: disease-causing mutations that disrupt the splicing code. *Genome Biol.* **15,** 201 (2014).
114. Srebrow, A. & Kornblihtt, A. The connection between splicing and cancer. *J. Cell Sci.* **119,** 2635–2641 (2006).
115. Narla, G. *et al.* A germline DNA polymorphism enhances alternative splicing of the KLF6 tumor suppressor gene and is associated with increased prostate cancer risk. *Cancer Res.* **65,** 1213–1222 (2005).
116. Narla, G. *et al.* KLF6-SV1 overexpression accelerates human and mouse prostate cancer progression and metastasis. *J. Clin. Invest.* **118,** 2711–2721 (2008).
117. DiFeo, A., Martignetti, J. A. & Narla, G. The role of KLF6 and its splice variants in cancer therapy. *Drug Resist. Updat.* **12,** 1–7 (2009).
118. Hatami, R. *et al.* KLF6-SV1 drives breast cancer metastasis and is associated with poor survival. *Sci. Transl. Med.* **5,** 169ra12 (2013).
119. Hahn, C. N., Venugopal, P., Scott, H. S. & Hiwase, D. K. Splice factor mutations and alternative splicing as drivers of hematopoietic malignancy. *Immunol. Rev.* **263,** 257–78 (2015).
120. Yoshida, K. & Ogawa, S. Splicing factor mutations and cancer. *Wiley Interdiscip. Rev. RNA* **5,** 445–459 (2014).
121. Sebestyen, E., Zawisza, M. & Eyras, E. Detection of recurrent alternative splicing switches in tumor samples reveals novel signatures of cancer. *Nucleic Acids Res.* **43,** 1345–56 (2015).
122. Shilo, A. *et al.* Splicing factor hnRNP A2 activates the Ras-MAPK-ERK pathway by controlling A-Raf splicing in hepatocellular carcinoma development. *RNA* **20,** 505–515 (2014).
123. Dvinge, H., Kim, E., Abdel-Wahab, O. & Bradley, R. K. RNA splicing factors as oncoproteins and tumour suppressors. *Nat. Rev. Cancer* **16,** 413–430 (2016).
124. Karni, R. *et al.* The gene encoding the splicing factor SF2/ASF is a proto-oncogene. *Nat. Struct. Mol. Biol.* **14,** 185–93 (2007).
125. Anczuków, O. *et al.* The splicing factor SRSF1 regulates apoptosis and proliferation to promote mammary epithelial cell transformation. *Nat. Struct. Mol. Biol.* **19,** 220–228 (2012).
126. Ben-Hur, V. *et al.* S6K1 Alternative Splicing Modulates Its Oncogenic Activity and Regulates mTORC1. *Cell Rep.* **3,** 103–115 (2013).
127. Das, S., Anczuków, O., Akerman, M. & Krainer, A. R. Oncogenic Splicing Factor SRSF1 Is a Critical Transcriptional Target of MYC. *Cell Rep.* **1,** 110–117 (2012).
128. David, C. J. & Manley, J. L. Alternative pre-mRNA splicing regulation in

cancer: Pathways and programs unhinged. *Genes and Development* **24,** 2343–2364 (2010).
129. Eswaran, J. *et al.* RNA sequencing of cancer reveals novel splicing alterations. *Sci. Rep.* **3,** 1689 (2013).
130. He, C., Zhou, F., Zuo, Z., Cheng, H. & Zhou, R. A global view of cancer-specific transcript variants by subtractive transcriptome-wide analysis. *PLoS One* **4,** e4732 (2009).
131. Pajares, M. J. *et al.* Alternative splicing: an emerging topic in molecular and clinical oncology. *Lancet Oncol.* **8,** 349–357 (2007).
132. Ghigna, C. *et al.* Pro-metastatic splicing of Ron proto-oncogene mRNA can be reversed: Therapeutic potential of bifunctional oligonucleotides and indole derivatives. *RNA Biol.* **7,** 495–503 (2010).
133. Letai, A. G. Diagnosing and exploiting cancer's addiction to blocks in apoptosis. *Nat. Rev. Cancer* **8,** 121–132 (2008).
134. Tomek, M., Akiyama, T. & Dass, C. R. Role of Bcl-2 in tumour cell survival and implications for pharmacotherapy. *J. Pharm. Pharmacol.* **64,** 1695–702 (2012).
135. Mercatante, D. R., Mohler, J. L. & Kole, R. Cellular response to an antisense-mediated shift of Bcl-x pre-mRNA splicing and antineoplastic agents. *J. Biol. Chem.* **277,** 49374–49382 (2002).
136. Garneau, D., Revil, T., Fisette, J.-F. & Chabot, B. Heterogeneous Nuclear Ribonucleoprotein F/H Proteins Modulate the Alternative Splicing of the Apoptotic Mediator Bcl-x. *J. Biol. Chem.* **280,** 22641–22650 (2005).
137. Massiello, A., Roesser, J. R. & Chalfant, C. E. SAP155 Binds to ceramide-responsive RNA cis-element 1 and regulates the alternative 5' splice site selection of Bcl-x pre-mRNA. *FASEB J.* **20,** 1680–1682 (2006).
138. Revil, T., Pelletier, J., Toutant, J., Cloutier, A. & Chabot, B. Heterogeneous Nuclear Ribonucleoprotein K Represses the Production of Pro-apoptotic Bcl-xS Splice Isoform. *J. Biol. Chem.* **284,** 21458–21467 (2009).
139. Frisone, P. *et al.* SAM68: Signal Transduction and RNA Metabolism in Human Cancer. *Biomed Res. Int.* **2015,** 1–14 (2015).
140. Heere-Ress, E. *et al.* BCL-XL is a chemoresistance factor in human melanoma cells that can be inhibited by antisense therapy. *Int. J. Cancer* **99,** 29–34 (2002).
141. Bauman, J. A., Li, S.-D., Yang, A., Huang, L. & Kole, R. Anti-tumor activity of splice-switching oligonucleotides. *Nucleic Acids Res.* **38,** 8348–56 (2010).
142. Elmore, S. Apoptosis: a review of programmed cell death. *Toxicol. Pathol.* **35,** 495–516 (2007).
143. Cascino, I., Fiucci, G., Papoff, G. & Ruberti, G. Three functional soluble forms of the human apoptosis-inducing Fas molecule are produced by alternative splicing. *J. Immunol.* **154,** 2706–13 (1995).
144. Cheng, J. *et al.* Protection from Fas-mediated apoptosis by a soluble form of the Fas molecule. *Science* **263,** 1759–62 (1994).
145. Ueno, T., Toi, M. & Tominaga, T. Circulating soluble Fas concentration in breast cancer patients. *Clin. Cancer Res.* **5,** 3529–3533 (1999).
146. Kavathia, N., Jain, A., Walston, J., Beamer, B. A. & Fedarko, N. S. Serum markers of apoptosis decrease with age and cancer stage. *Aging (Albany. NY).* **1,** 652–663 (2009).
147. Izquierdo, J. M. *et al.* Regulation of fas alternative splicing by antagonistic effects of TIA-1 and PTB on exon definition. *Mol. Cell* **19,** 475–484 (2005).
148. Pagliarini, V., Naro, C. & Sette, C. Splicing Regulation: A Molecular

Device to Enhance Cancer Cell Adaptation. *Biomed Res. Int.* **2015,** 543067 (2015).
149. Mickleburgh, I. *et al.* The organization of RNA contacts by PTB for regulation of FAS splicing. *Nucleic Acids Res.* **42,** 8605–8620 (2014).
150. Tejedor, J. R., Papasaikas, P. & Valcárcel, J. Genome-wide identification of Fas/CD95 alternative splicing regulators reveals links with iron homeostasis. *Mol. Cell* **57,** 23–38 (2015).
151. Clohessy, J. G., Zhuang, J., De Boer, J., Gil-Gómez, G. & Brady, H. J. M. Mcl-1 interacts with truncated bid and inhibits its induction of cytochrome c release and its role in receptor-mediated apoptosis. *J. Biol. Chem.* **281,** 5750–5759 (2006).
152. Ding, Q. *et al.* Myeloid cell leukemia-1 inversely correlates with glycogen synthase kinase-3beta activity and associates with poor prognosis in human breast cancer. *Cancer Res.* **67,** 4564–71 (2007).
153. Palve, V. C. & Teni, T. R. Association of anti-apoptotic Mcl-1L isoform expression with radioresistance of oral squamous carcinoma cells. *Radiat. Oncol.* **7,** 135 (2012).
154. Palve, V., Mallick, S., Ghaisas, G., Kannan, S. & Teni, T. Overexpression of Mcl-1L splice variant is associated with poor prognosis and chemoresistance in oral cancers. *PLoS One* **9,** e111927 (2014).
155. Shieh, J.-J., Liu, K.-T., Huang, S.-W., Chen, Y.-J. & Hsieh, T.-Y. Modification of alternative splicing of Mcl-1 pre-mRNA using antisense morpholino oligonucleotides induces apoptosis in basal cell carcinoma cells. *J. Invest. Dermatol.* **129,** 2497–506 (2009).
156. Ryou, S.-M. *et al.* Inhibition of xenograft tumor growth in mice by gold nanoparticle-assisted delivery of short hairpin RNAs against Mcl-1L. *J. Biotechnol.* **156,** 89–94 (2011).
157. McIlwain, D. R., Berger, T. & Mak, T. W. Caspase functions in cell death and disease. *Cold Spring Harbor perspectives in biology* **5,** a008656 (2013).
158. Wu, H. *et al.* Caspases: a molecular switch node in the crosstalk between autophagy and apoptosis. *Int. J. Biol. Sci.* **10,** 1072–83 (2014).
159. Schwerk, C. & Schulze-Osthoff, K. Regulation of apoptosis by alternative pre-mRNA splicing. *Mol. Cell* **19,** 1–13 (2005).
160. Shultz, J. C. *et al.* Alternative splicing of caspase 9 is modulated by the phosphoinositide 3-kinase/Akt pathway via phosphorylation of SRp30a. *Cancer Res.* **70,** 9185–96 (2010).
161. Shultz, J. C. *et al.* SRSF1 regulates the alternative splicing of caspase 9 via a novel intronic splicing enhancer affecting the chemotherapeutic sensitivity of non-small cell lung cancer cells. *Mol. Cancer Res.* **9,** 889–900 (2011).
162. Goehe, R. W. *et al.* hnRNP L regulates the tumorigenic capacity of lung cancer xenografts in mice via caspase-9 pre-mRNA processing. *J. Clin. Invest.* **120,** 3923–3939 (2010).
163. Jose, C., Bellance, N. & Rossignol, R. Choosing between glycolysis and oxidative phosphorylation: A tumor's dilemma? *Biochimica et Biophysica Acta - Bioenergetics* **1807,** 552–561 (2011).
164. Christofk, H. R. *et al.* The M2 splice isoform of pyruvate kinase is important for cancer metabolism and tumour growth. *Nature* **452,** 230–233 (2008).
165. Gupta, V. & Bamezai, R. N. K. Human pyruvate kinase M2: a multifunctional protein. *Protein Sci.* **19,** 2031–44 (2010).
166. Clower, C. V *et al.* The alternative splicing repressors hnRNP A1/A2 and

PTB influence pyruvate kinase isoform expression and cell metabolism. *Proc. Natl. Acad. Sci. U. S. A.* **107,** 1894–1899 (2010).
167. David, C. J., Chen, M., Assanah, M., Canoll, P. & Manley, J. L. HnRNP proteins controlled by c-Myc deregulate pyruvate kinase mRNA splicing in cancer. *Nature* **463,** 364–8 (2010).
168. Zhou, J. *et al.* Differential expression of the early lung cancer detection marker, heterogeneous nuclear ribonucleoprotein-A2/B1 (hnRNP-A2/B1) in normal breast and neoplastic breast cancer. *Breast Cancer Res. Treat.* **66,** 217–224 (2001).
169. Zhou, Z. J. *et al.* Overexpression of HnRNP A1 promotes tumor invasion through regulating CD44v6 and indicates poor prognosis for hepatocellular carcinoma. *Int. J. Cancer* **132,** 1080–1089 (2013).
170. He, X. *et al.* Involvement of polypyrimidine tract-binding protein (PTBP1) in maintaining breast cancer cell growth and malignant properties. *Oncogenesis* **3,** e84 (2014).
171. Gupta, V., Wellen, K., Mazurek, S. & Bamezai, R. N. Pyruvate Kinase M2: Regulatory Circuits and Potential for Therapeutic Intervention. *Curr. Pharm. Des.* **20,** 2595–2606 (2014).
172. Wang, Z., Jeon, H. Y., Rigo, F., Bennett, C. F. & Krainer, A. R. Manipulation of PK-M mutually exclusive alternative splicing by antisense oligonucleotides. *Open Biol.* **2,** 120133 (2012).
173. Diolaiti, D., McFerrin, L., Carroll, P. A. & Eisenman, R. N. Functional interactions among members of the MAX and MLX transcriptional network during oncogenesis. *Biochimica et Biophysica Acta - Gene Regulatory Mechanisms* **1849,** 484–500 (2015).
174. Babic, I. *et al.* EGFR mutation-induced alternative splicing of max contributes to growth of glycolytic tumors in brain cancer. *Cell Metab.* **17,** 1000–1008 (2013).
175. Montano, N. *et al.* Expression of EGFRvIII in glioblastoma: prognostic significance revisited. *Neoplasia* **13,** 1113–21 (2011).
176. Gupta, G. P. & Massagué, J. Cancer Metastasis: Building a Framework. *Cell* **127,** 679–695 (2006).
177. Goodison, S., Urquidi, V. & Tarin, D. CD44 cell adhesion molecules. *Mol. Pathol.* **52,** 189–196 (1999).
178. Xu, H. *et al.* The role of CD44 in epithelial-mesenchymal transition and cancer development. *Onco. Targets. Ther.* **8,** 3783–92 (2015).
179. Bánky, B. *et al.* Characteristics of CD44 alternative splice pattern in the course of human colorectal adenocarcinoma progression. *Mol. Cancer* **11,** 83 (2012).
180. Yang, H. *et al.* Expression and association of CD44v6 with prognosis in T2-3N0M0 esophageal squamous cell carcinoma. *J. Thorac. Dis.* **6,** 91–98 (2014).
181. Wu, Y. *et al.* CD44 family proteins in gastric cancer: a meta-analysis and narrative review. *Int. J. Clin. Exp. Med.* **8,** 3595–606 (2015).
182. Orian-Rousseau, V. *et al.* Hepatocyte growth factor-induced Ras activation requires ERM proteins linked to both CD44v6 and F-actin. *Mol. Biol. Cell* **18,** 76–83 (2007).
183. Weidle, U. H., Maisel, D., Klostermann, S., Weiss, E. H. & Schmitt, M. Differential splicing generates new transmembrane receptor and extracellular matrix-related targets for antibody-based therapy of cancer. *Cancer Genomics and Proteomics* **8,** 211–226 (2011).
184. Li, X. *et al.* Prognostic value of CD44 expression in renal cell carcinoma: a systematic review and meta-analysis. *Sci. Rep.* **5,** 13157 (2015).

185. Loh, T. J. *et al.* CD44 alternative splicing and hnRNP A1 expression are associated with the metastasis of breast cancer. *Oncol. Rep.* **34,** 1231–1238 (2015).
186. Filippov, V., Filippova, M. & Duerksen-Hughes, P. J. The early response to DNA damage can lead to activation of alternative splicing activity resulting in CD44 splice pattern changes. *Cancer Res.* **67,** 7621–30 (2007).
187. Galiana-Arnoux, D. *et al.* The CD44 alternative v9 exon contains a splicing enhancer responsive to the SR proteins 9G8, ASF/SF2, and SRp20. *J. Biol. Chem.* **278,** 32943–53 (2003).
188. Watermann, D. O. *et al.* Splicing factor Tra2-beta1 is specifically induced in breast cancer and regulates alternative splicing of the CD44 gene. *Cancer Res.* **66,** 4774–80 (2006).
189. Yae, T. *et al.* Alternative splicing of CD44 mRNA by ESRP1 enhances lung colonization of metastatic cancer cell. *Nat. Commun.* **3,** 883 (2012).
190. Stickeler, E. *et al.* The RNA binding protein YB-1 binds A/C-rich exon enhancers and stimulates splicing of the CD44 alternative exon v4. *EMBO J.* **20,** 3821–30 (2001).
191. Yoshikawa, M. *et al.* xCT Inhibition Depletes CD44v-Expressing Tumor Cells That Are Resistant to EGFR-Targeted Therapy in Head and Neck Squamous Cell Carcinoma. *Cancer Res.* **73,** 1855–1866 (2013).
192. Heerboth, S. *et al.* EMT and tumor metastasis. *Clin. Transl. Med.* **4,** 6 (2015).
193. Brabletz, T. To differentiate or not — routes towards metastasis. *Nat. Rev. Cancer* **12,** 425–436 (2012).
194. Polyak, K. & Weinberg, R. A. Transitions between epithelial and mesenchymal states: acquisition of malignant and stem cell traits. *Nat. Rev. Cancer* **9,** 265–73 (2009).
195. Biamonti, G., Bonomi, S., Gallo, S. & Ghigna, C. Making alternative splicing decisions during epithelial-to-mesenchymal transition (EMT). *Cell. Mol. Life Sci.* **69,** 2515–26 (2012).
196. Trusolino, L. & Comoglio, P. M. Scatter-factor and semaphorin receptors: cell signalling for invasive growth. *Nat. Rev. Cancer* **2,** 289–300 (2002).
197. Yao, H.-P., Zhou, Y.-Q., Zhang, R. & Wang, M.-H. MSP–RON signalling in cancer: pathogenesis and therapeutic potential. *Nat. Rev. Cancer* **13,** 466–481 (2013).
198. Collesi, C., Santoro, M. M., Gaudino, G. & Comoglio, P. M. A splicing variant of the RON transcript induces constitutive tyrosine kinase activity and an invasive phenotype. *Mol. Cell. Biol.* **16,** 5518–26 (1996).
199. Zhou, Y. Q., He, C., Chen, Y. Q., Wang, D. & Wang, M. H. Altered expression of the RON receptor tyrosine kinase in primary human colorectal adenocarcinomas: generation of different splicing RON variants and their oncogenic potential. *Oncogene* **22,** 186–197 (2003).
200. Ghigna, C. *et al.* Cell motility is controlled by SF2/ASF through alternative splicing of the Ron protooncogene. *Mol. Cell* **20,** 881–890 (2005).
201. Bonomi, S. *et al.* HnRNP A1 controls a splicing regulatory circuit promoting mesenchymal-to-epithelial transition. *Nucleic Acids Res.* **41,** (2013).
202. Valacca, C. *et al.* Sam68 regulates EMT through alternative splicing-activated nonsense-mediated mRNA decay of the SF2/ASF proto-oncogene. *J. Cell Biol.* **191,** 87–99 (2010).
203. Bosco, E. E., Mulloy, J. C. & Zheng, Y. Rac1 GTPase: a "Rac" of all trades. *Cell. Mol. Life Sci.* **66,** 370–4 (2009).
204. Ridley, A. J. Rho GTPases and cell migration. *J. Cell Sci.* **114,** 2713–22

(2001).
205. Jordan, P., Brazåo, R., Boavida, M. G., Gespach, C. & Chastre, E. Cloning of a novel human Rac1b splice variant with increased expression in colorectal tumors. *Oncogene* **18,** 6835–9 (1999).
206. Orlichenko, L. S. & Radisky, D. C. Matrix metalloproteinases stimulate epithelial-mesenchymal transition during tumor development. *Clin. Exp. Metastasis* **25,** 593–600 (2008).
207. Fiegen, D. Alternative Splicing of Rac1 Generates Rac1b, a Self-activating GTPase. *J. Biol. Chem.* **279,** 4743–4749 (2003).
208. Schnelzer, A. *et al.* Rac1 in human breast cancer: overexpression, mutation analysis, and characterization of a new isoform, Rac1b. *Oncogene* **19,** 3013–20 (2000).
209. Matos, P. & Jordan, P. Increased Rac1b expression sustains colorectal tumor cell survival. *Mol. Cancer Res.* **6,** 1178–84 (2008).
210. Goncalves, V., Matos, P. & Jordan, P. Antagonistic SR proteins regulate alternative splicing of tumor-related Rac1b downstream of the PI3-kinase and Wnt pathways. *Hum. Mol. Genet.* **18,** 3696–3707 (2009).
211. Pelisch, F. *et al.* Involvement of hnRNP A1 in the matrix metalloprotease-3-dependent regulation of Rac1 pre-mRNA splicing. *J. Cell. Biochem.* **113,** 2319–2329 (2012).
212. Goncalves, V. *et al.* Phosphorylation of SRSF1 by SRPK1 regulates alternative splicing of tumor-related Rac1b in colorectal cells. *RNA* **20,** 474–482 (2014).
213. Egeblad, M. & Werb, Z. New functions for the matrix metalloproteinases in cancer progression. *Nat Rev Cancer* **2,** 161–174 (2002).
214. Radisky, D. C. *et al.* Rac1b and reactive oxygen species mediate MMP-3-induced EMT and genomic instability. *Nature* **436,** 123–127 (2005).
215. Tavanez, J. P. & Valcárcel, J. A splicing mastermind for EMT. *EMBO J.* **29,** 3217–8 (2010).
216. Warzecha, C. C. & Carstens, R. P. Complex changes in alternative pre-mRNA splicing play a central role in the epithelial-to-mesenchymal transition (EMT). *Seminars in Cancer Biology* **22,** 417–427 (2012).
217. Lammert, E. & Axnick, J. Vascular lumen formation. *Cold Spring Harb. Perspect. Med.* **2,** a006619 (2012).
218. Alberts, B. *et al.* Blood Vessels and Endothelial Cells. (2002).
219. Adams, R. H. & Alitalo, K. Molecular regulation of angiogenesis and lymphangiogenesis. *Nat Rev Mol Cell Biol* **8,** 464–478 (2007).
220. Patel-Hett, S. & D'Amore, P. A. Signal transduction in vasculogenesis and developmental angiogenesis. *Int. J. Dev. Biol.* **55,** 353–63 (2011).
221. Corada, M., Morini, M. F. & Dejana, E. Signaling pathways in the specification of arteries and veins. *Arterioscler. Thromb. Vasc. Biol.* **34,** 2372–7 (2014).
222. Potente, M. *et al.* Basic and Therapeutic Aspects of Angiogenesis. *Cell* **146,** 873–887 (2011).
223. Dejana, E. & Kühl, M. The role of wnt signaling in physiological and pathological angiogenesis. *Circulation Research* **107,** 943–952 (2010).
224. Burri, P. H. & Tarek, M. R. A novel mechanism of capillary growth in the rat pulmonary microcirculation. *Anat. Rec.* **228,** 35–45 (1990).
225. Caduff, J. H., Fischer, L. C. & Burri, P. H. Scanning electron microscope study of the developing microvasculature in the postnatal rat lung. *Anat. Rec.* **216,** 154–64 (1986).
226. Logsdon, E. A., Finley, S. D., Popel, A. S. & MacGabhann, F. A systems biology view of blood vessel growth and remodelling. *J. Cell. Mol. Med.*

18, 1491–1508 (2014).
227. Carmeliet, P. & Jain, R. K. Molecular mechanisms and clinical applications of angiogenesis. *Nature* **473,** 298–307 (2011).
228. Ucuzian, A. A., Gassman, A. A., East, A. T. & Greisler, H. P. Molecular mediators of angiogenesis. *J. Burn Care Res.* **31,** 158–75 (2010).
229. Van Hinsbergh, V. W. M. & Koolwijk, P. Endothelial sprouting and angiogenesis: Matrix metalloproteinases in the lead. *Cardiovascular Research* **78,** 203–212 (2008).
230. Gerhardt, H. *et al.* VEGF guides angiogenic sprouting utilizing endothelial tip cell filopodia. *J. Cell Biol.* **161,** 1163–77 (2003).
231. Siekmann, A. F., Affolter, M. & Belting, H. G. The tip cell concept 10 years after: New players tune in for a common theme. *Experimental Cell Research* **319,** 1255–1263 (2013).
232. De Smet, F., Segura, I., De Bock, K., Hohensinner, P. J. & Carmeliet, P. Mechanisms of vessel branching: Filopodia on endothelial tip cells lead the way. *Arteriosclerosis, Thrombosis, and Vascular Biology* **29,** 639–649 (2009).
233. Mattila, P. K. & Lappalainen, P. Filopodia: molecular architecture and cellular functions. *Nat. Rev. Mol. Cell Biol.* **9,** 446–454 (2008).
234. Adams, R. H. & Eichmann, A. Axon guidance molecules in vascular patterning. *Cold Spring Harbor perspectives in biology* **2,** a001875–a001875 (2010).
235. Betz, C. *et al.* Cell behaviors and dynamics during angiogenesis. *Development* **143,** 2249–60 (2016).
236. Iruela-Arispe, M. L. & Davis, G. E. Cellular and Molecular Mechanisms of Vascular Lumen Formation. *Developmental Cell* **16,** 222–231 (2009).
237. Koch, S. & Claesson-Welsh, L. Signal transduction by vascular endothelial growth factor receptors. *Cold Spring Harbor Perspectives in Medicine* **2,** a006502 (2012).
238. Geudens, I. *et al.* Coordinating cell behaviour during blood vessel formation. *Development* **138,** 4569–83 (2011).
239. Herbert, S. P. & Stainier, D. Y. R. Molecular control of endothelial cell behaviour during blood vessel morphogenesis. *Nat. Rev. Mol. Cell Biol.* **12,** 551–64 (2011).
240. Roukens, M. G. *et al.* Control of endothelial sprouting by a Tel-CtBP complex. *Nat. Cell Biol.* **12,** 933–42 (2010).
241. Blanco, R. & Gerhardt, H. VEGF and Notch in tip and stalk cell selection. *Cold Spring Harb. Perspect. Med.* **3,** a006569 (2013).
242. Phng, L. K. *et al.* Nrarp Coordinates Endothelial Notch and Wnt Signaling to Control Vessel Density in Angiogenesis. *Dev. Cell* **16,** 70–82 (2009).
243. Andersson, E. R. & Lendahl, U. Therapeutic modulation of Notch signalling — are we there yet? *Nat. Rev. Drug Discov.* **13,** 357–378 (2014).
244. Guarani, V. *et al.* Acetylation-dependent regulation of endothelial Notch signalling by the SIRT1 deacetylase. *Nature* **473,** 234–8 (2011).
245. Kamei, M. *et al.* Endothelial tubes assemble from intracellular vacuoles in vivo. *Nature* **442,** 453–456 (2006).
246. Blum, Y. *et al.* Complex cell rearrangements during intersegmental vessel sprouting and vessel fusion in the zebrafish embryo. *Dev. Biol.* **316,** 312–322 (2008).
247. Strilić, B. *et al.* Electrostatic Cell-Surface Repulsion Initiates Lumen Formation in Developing Blood Vessels. *Curr. Biol.* **20,** 2003–2009 (2010).
248. Charpentier, M. S. & Conlon, F. L. Cellular and molecular mechanisms underlying blood vessel lumen formation. *BioEssays* **36,** 251–259 (2014).

249. Herwig, L. *et al. Distinct Cellular Mechanisms of Blood Vessel Fusion in the Zebrafish Embryo*. *Current Biology* **21,** (2011).
250. Helker, C. S. M. *et al.* The zebrafish common cardinal veins develop by a novel mechanism: lumen ensheathment. *Development* **140,** 2776–86 (2013).
251. Giampietro, C. *et al.* The alternative splicing factor Nova2 regulates vascular development and lumen formation. *Nat. Commun.* **6,** (2015).
252. Fantin, A. *et al.* Tissue macrophages act as cellular chaperones for vascular anastomosis downstream of VEGF-mediated endothelial tip cell induction. *Blood* **116,** 829–40 (2010).
253. Rymo, S. F. *et al.* A Two-Way Communication between Microglial Cells and Angiogenic Sprouts Regulates Angiogenesis in Aortic Ring Cultures. *PLoS One* **6,** e15846 (2011).
254. Zhang, J. *et al.* Angiopoietin-1/Tie2 signal augments basal notch signal controlling vascular quiescence by inducing delta-like 4 expression through AKT-mediated activation of ??-catenin. *J. Biol. Chem.* **286,** 8055–8066 (2011).
255. Simonavicius, N. *et al.* Pericytes promote selective vessel regression to regulate vascular patterning. *Blood* **120,** 1516–1527 (2012).
256. Krock, B. L., Skuli, N. & Simon, M. C. Hypoxia-induced angiogenesis: good and evil. *Genes Cancer* **2,** 1117–33 (2011).
257. De Smet, F., Segura, I., De Bock, K., Hohensinner, P. J. & Carmeliet, P. Mechanisms of vessel branching: Filopodia on endothelial tip cells lead the way. *Arteriosclerosis, Thrombosis, and Vascular Biology* **29,** 639–649 (2009).
258. Krock, B. L., Skuli, N. & Simon, M. C. Hypoxia-induced angiogenesis: good and evil. *Genes Cancer* **2,** 1117–33 (2011).
259. Ramakrishnan, S., Anand, V. & Roy, S. Vascular endothelial growth factor signaling in hypoxia and inflammation. *J. Neuroimmune Pharmacol.* **9,** 142–60 (2014).
260. Senger, D. R. *et al.* Tumor cells secrete a vascular permeability factor that promotes accumulation of ascites fluid. *Science* **219,** 983–5 (1983).
261. Ferrara, N. Binding to the extracellular matrix and proteolytic processing: two key mechanisms regulating vascular endothelial growth factor action. *Mol. Biol. Cell* **21,** 687–90 (2010).
262. Shibuya, M. Vascular endothelial growth factor and its receptor system: Physiological functions in angiogenesis and pathological roles in various diseases. *Journal of Biochemistry* **153,** 13–19 (2013).
263. Sunderkötter, C., Steinbrink, K., Goebeler, M., Bhardwaj, R. & Sorg, C. Macrophages and angiogenesis. *J. Leukoc. Biol.* **55,** 410–422 (1994).
264. Frank, S. *et al.* Regulation of vascular endothelial growth factor expression in cultured keratinocytes. Implications for normal and impaired wound healing. *J. Biol. Chem.* **270,** 12607–13 (1995).
265. Verheul, H. M. *et al.* Platelet: transporter of vascular endothelial growth factor. *Clin. Cancer Res.* **3,** 2187–90 (1997).
266. Nezhad, M. A. Vascular endothelial growth factor from embryonic status to cardiovascular pathology. *Reports Biochem. Mol. Biol.* **2,** 1–10 (2016).
267. Goel, H. L. & Mercurio, A. M. VEGF targets the tumour cell. *Nat. Rev. Cancer* **13,** 871–82 (2013).
268. Shibuya, M. Vascular Endothelial Growth Factor (VEGF) and Its Receptor (VEGFR) Signaling in Angiogenesis: A Crucial Target for Anti- and Pro-Angiogenic Therapies. *Genes Cancer* **2,** 1097–1105 (2011).
269. Stuttfeld, E. & Ballmer-Hofer, K. Structure and function of VEGF

receptors. *IUBMB Life* **61,** 915–922 (2009).
270. Tan, W. H., Popel, A. S. & Mac Gabhann, F. Computational model of VEGFR2 pathway to ERK activation and modulation through receptor trafficking. *Cell. Signal.* **25,** 2496–2510 (2013).
271. Lanahan, A. *et al.* The Neuropilin 1 Cytoplasmic Domain Is Required for VEGF-A-Dependent Arteriogenesis. *Dev. Cell* **25,** 156–168 (2013).
272. Brkovic, A. & Sirois, M. G. Vascular permeability induced by VEGF family members in vivo: Role of endogenous PAF and NO synthesis. *J. Cell. Biochem.* **100,** 727–737 (2007).
273. Giacca, M. Non-redundant functions of the protein isoforms arising from alternative splicing of the VEGF-A pre-mRNA. *Transcription* **1,** 149–153 (2010).
274. Biselli-Chicote, P. M., Oliveira, A. R. C. P., Pavarino, E. C. & Goloni-Bertollo, E. M. VEGF gene alternative splicing: Pro- and anti-angiogenic isoforms in cancer. *Journal of Cancer Research and Clinical Oncology* **138,** 363–370 (2012).
275. Pritchard-Jones, R. O. *et al.* Expression of VEGF(xxx)b, the inhibitory isoforms of VEGF, in malignant melanoma. *Br. J. Cancer* **97,** 223–30 (2007).
276. Ornitz, D. M. & Itoh, N. Fibroblast growth factors. *Genome Biol.* **2,** REVIEWS3005 (2001).
277. Turner, N. & Grose, R. Fibroblast growth factor signalling: from development to cancer. *Nat. Rev. Cancer* **10,** 116–129 (2010).
278. Murakami, M. *et al.* The FGF system has a key role in regulating vascular integrity. *J. Clin. Invest.* **118,** 3355–3366 (2008).
279. Viñals, F. & Pouysségur, J. Transforming growth factor beta1 (TGF-beta1) promotes endothelial cell survival during in vitro angiogenesis via an autocrine mechanism implicating TGF-alpha signaling. *Molecular and cellular biology* **21,** 7218–30 (2001).
280. Ferrari, G., Cook, B. D., Terushkin, V., Pintucci, G. & Mignatti, P. Transforming growth factor-beta 1 (TGF-beta1) induces angiogenesis through vascular endothelial growth factor (VEGF)-mediated apoptosis. *J. Cell. Physiol.* **219,** 449–58 (2009).
281. Zi, Z., Chapnick, D. A. & Liu, X. Dynamics of TG-β/Smad signaling. *FEBS Letters* **586,** 1921–1928 (2012).
282. Schmierer, B. & Hill, C. S. TGFbeta-SMAD signal transduction: molecular specificity and functional flexibility. *Nat. Rev. Mol. Cell Biol.* **8,** 970–982 (2007).
283. Oh, S. P. *et al.* Activin receptor-like kinase 1 modulates transforming growth factor-beta 1 signaling in the regulation of angiogenesis. *Proc. Natl. Acad. Sci. U. S. A.* **97,** 2626–31 (2000).
284. Van Meeteren, L. A., Goumans, M.-J. J. & Ten Dijke, P. TGF-β Receptor Signaling Pathways in Angiogenesis; Emerging Targets for Anti-Angiogenesis Therapy. *Curr. Pharm. Biotechnol.* **12,** 2108–20 (2011).
285. Ferrari, G. *et al.* VEGF, a prosurvival factor, acts in concert with TG-beta1 to induce endothelial cell apoptosis. *Proc. Natl. Acad. Sci. U. S. A.* **103,** 17260–17265 (2006).
286. Brindle, N. P. J., Saharinen, P. & Alitalo, K. Signaling and functions of angiopoietin-1 in vascular protection. *Circulation Research* **98,** 1014–1023 (2006).
287. Gavard, J., Patel, V. & Gutkind, J. S. Angiopoietin-1 Prevents VEGF-Induced Endothelial Permeability by Sequestering Src through mDia. *Dev. Cell* **14,** 25–36 (2008).

288. Maisonpierre, P. C. *et al.* Angiopoietin-2, a Natural Antagonist for Tie2 That Disrupts in vivo Angiogenesis. *Science (80-.).* **277,** 55–60 (1997).
289. Sainson, R. C. A. *et al.* TNF primes endothelial cells for angiogenic sprouting by inducing a tip cell phenotype. *Blood* **111,** 4997–5007 (2008).
290. Mehta, V. B., Besner, G. E., Mehta, V. B. & Besner, G. E. HB-EGF promotes angiogenesis in endothelial cells via PI3-kinase and MAPK signaling pathways. *Growth Factors* **25,** 253–263 (2007).
291. Bussolino, F. *et al.* Hepatocyte growth factor is a potent angiogenic factor which stimulates endothelial cell motility and growth. *J. Cell Biol.* **119,** 629–41 (1992).
292. Rosen, E. M. *et al.* HGF/SF in angiogenesis. *Ciba Found. Symp.* **212,** 215-26–9 (1997).
293. Battegay, E. J., Rupp, J., Iruela-Arispe, L., Sage, E. H. & Pech, M. PDGF-BB modulates endothelial proliferation and angiogenesis in vitro via PDGF beta-receptors. *J. Cell Biol.* **125,** 917–28 (1994).
294. Hellberg, C., Östman, A. & Heldin, C.-H. in 103–114 (2010). doi:10.1007/978-3-540-78281-0_7
295. Dimberg, A. in 59–80 (2010). doi:10.1007/82_2010_21
296. Ohki, Y. Granulocyte colony-stimulating factor promotes neovascularization by releasing vascular endothelial growth factor from neutrophils. *FASEB J.* (2005). doi:10.1096/fj.04-3496fje
297. Adya, R., Tan, B. K. & Randeva, H. S. Differential Effects of Leptin and Adiponectin in Endothelial Angiogenesis. *J. Diabetes Res.* **2015,** 1–12 (2015).
298. Herradon, G. *et al.* Pleiotrophin is an important regulator of the renin–angiotensin system in mouse aorta. *Biochem. Biophys. Res. Commun.* **324,** 1041–1047 (2004).
299. Koutsioumpa, M. *et al.* Pleiotrophin expression and role in physiological angiogenesis in vivo: potential involvement of nucleolin. *Vasc. Cell* **4,** 4 (2012).
300. Kozian, D. H., Ziche, M. & Augustin, H. G. The activin-binding protein follistatin regulates autocrine endothelial cell activity and induces angiogenesis. *Lab. Invest.* **76,** 267–76 (1997).
301. McCaffrey, L. M. & Macara, I. G. Epithelial organization, cell polarity and tumorigenesis. *Trends Cell Biol.* **21,** 727–35 (2011).
302. Huang, L. & Muthuswamy, S. K. Polarity protein alterations in carcinoma: a focus on emerging roles for polarity regulators. *Curr. Opin. Genet. Dev.* **20,** 41–50 (2010).
303. Chatterjee, S. J. & McCaffrey, L. Emerging role of cell polarity proteins in breast cancer progression and metastasis. *Breast cancer (Dove Med. Press.* **6,** 15–27 (2014).
304. Goldstein, B. & Macara, I. G. The PAR proteins: fundamental players in animal cell polarization. *Dev. Cell* **13,** 609–22 (2007).
305. Lampugnani, M. G. *et al.* CCM1 regulates vascular-lumen organization by inducing endothelial polarity. *J. Cell Sci.* **123,** 1073–80 (2010).
306. Itoh, M. *et al.* Junctional adhesion molecule (JAM) binds to PAR-3: A possible mechanism for the recruitment of PAR-3 to tight junctions. *J. Cell Biol.* **154,** 491–497 (2001).
307. Martin-Belmonte, F. & Mostov, K. Regulation of cell polarity during epithelial morphogenesis. *Curr. Opin. Cell Biol.* **20,** 227–234 (2008).
308. Morais-de-Sá, E., Mirouse, V. & St Johnston, D. aPKC phosphorylation of Bazooka defines the apical/lateral border in Drosophila epithelial cells. *Cell* **141,** 509–23 (2010).

309. Galvagni, F., Baldari, C. T., Oliviero, S. & Orlandini, M. An apical actin-rich domain drives the establishment of cell polarity during cell adhesion. *Histochem. Cell Biol.* **138,** 419–33 (2012).
310. Bustelo, X. R., Sauzeau, V. & Berenjeno, I. M. GTP-binding proteins of the Rho/Rac family: regulation, effectors and functions in vivo. *Bioessays* **29,** 356–70 (2007).
311. Koh, W., Mahan, R. D. & Davis, G. E. Cdc42- and Rac1-mediated endothelial lumen formation requires Pak2, Pak4 and Par3, and PKC-dependent signaling. *J. Cell Sci.* **121,** 989–1001 (2008).
312. Koh, W. *et al.* Formation of endothelial lumens requires a coordinated PKCepsilon-, Src-, Pak- and Raf-kinase-dependent signaling cascade downstream of Cdc42 activation. *J. Cell Sci.* **122,** 1812–22 (2009).
313. Kleaveland, B. *et al.* Regulation of cardiovascular development and integrity by the heart of glass–cerebral cavernous malformation protein pathway. *Nat. Med.* **15,** 169–176 (2009).
314. Whitehead, K. J. *et al.* The cerebral cavernous malformation signaling pathway promotes vascular integrity via Rho GTPases. *Nat. Med.* **15,** 177–184 (2009).
315. Xu, K. *et al.* Blood Vessel Tubulogenesis Requires Rasip1 Regulation of GTPase Signaling. *Dev. Cell* **20,** 526–539 (2011).
316. Bryant, D. M. & Mostov, K. E. From cells to organs: building polarized tissue. *Nat. Rev. Mol. Cell Biol.* **9,** 887–901 (2008).
317. Macara, I. G. Par proteins: partners in polarization. *Curr. Biol.* **14,** R160-2 (2004).
318. Michaelis, U. R. *et al.* The polarity protein Scrib is essential for directed endothelial cell migration. *Circ. Res.* **112,** 924–34 (2013).
319. Oubaha, M. *et al.* Formation of a PKC / -catenin complex in endothelial cells promotes angiopoietin-1-induced collective directional migration and angiogenic sprouting. *Blood* **120,** 3371–3381 (2012).
320. Carmeliet, P. Blood vessels and nerves: common signals, pathways and diseases. *Nat. Rev. Genet.* **4,** 710–720 (2003).
321. Carmeliet, P. & Tessier-Lavigne, M. Common mechanisms of nerve and blood vessel wiring. *Nature* **436,** 193–200 (2005).
322. Quaegebeur, A., Lange, C. & Carmeliet, P. The neurovascular link in health and disease: molecular mechanisms and therapeutic implications. *Neuron* **71,** 406–24 (2011).
323. Segura, I., De Smet, F., Hohensinner, P. J., Almodovar, C. R. de & Carmeliet, P. The neurovascular link in health and disease: an update. *Trends in Molecular Medicine* **15,** 439–451 (2009).
324. Zacchigna, S., Lambrechts, D. & Carmeliet, P. Neurovascular signalling defects in neurodegeneration. *Nat. Rev. Neurosci.* **9,** 169–181 (2008).
325. Ruiz de Almodovar, C., Lambrechts, D., Mazzone, M. & Carmeliet, P. Role and therapeutic potential of VEGF in the nervous system. *Physiol. Rev.* **89,** 607–48 (2009).
326. Butler, J. M., Kobayashi, H. & Rafii, S. Instructive role of the vascular niche in promoting tumour growth and tissue repair by angiocrine factors. *Nat. Rev. Cancer* **10,** 138–46 (2010).
327. Ballabh, P., Braun, A. & Nedergaard, M. The blood–brain barrier: an overview: Structure, regulation, and clinical implications. *Neurobiol. Dis.* **16,** 1–13 (2004).
328. Zlokovic, B. V. Neurovascular pathways to neurodegeneration in Alzheimer's disease and other disorders. *Nat. Rev. Neurosci.* **12,** 723 (2011).

329. Storkebaum, E. *et al.* Treatment of motoneuron degeneration by intracerebroventricular delivery of VEGF in a rat model of ALS. *Nat. Neurosci.* **8,** 85–92 (2005).
330. Azzouz, M. *et al.* VEGF delivery with retrogradely transported lentivector prolongs survival in a mouse ALS model. *Nature* **429,** 413–417 (2004).
331. Lai Wing Sun, K. *et al.* Netrins: versatile extracellular cues with diverse functions. *Development* **138,** 2153–69 (2011).
332. Moore, S. W., Tessier-Lavigne, M. & Kennedy, T. E. Netrins and their receptors. *Adv. Exp. Med. Biol.* **621,** 17–31 (2007).
333. Nakashiba, T. *et al.* Netrin-G1: a novel glycosyl phosphatidylinositol-linked mammalian netrin that is functionally divergent from classical netrins. *J. Neurosci.* **20,** 6540–50 (2000).
334. Ly, A. *et al.* DSCAM Is a Netrin Receptor that Collaborates with DCC in Mediating Turning Responses to Netrin-1. *Cell* **133,** 1241–1254 (2008).
335. Norris, A. D. & Lundquist, E. A. UNC-6/netrin and its receptors UNC-5 and UNC-40/DCC modulate growth cone protrusion in vivo in C. elegans. *Development* **138,** 4433–42 (2011).
336. Larrivée, B. *et al.* Activation of the UNC5B receptor by Netrin-1 inhibits sprouting angiogenesis. *Genes Dev.* **21,** 2433–2447 (2007).
337. Lu, X. *et al.* The netrin receptor UNC5B mediates guidance events controlling morphogenesis of the vascular system. *Nature* **432,** 179–86 (2004).
338. Wilson, B. D. *et al.* Netrins promote developmental and therapeutic angiogenesis. *Science* **313,** 640–4 (2006).
339. Castets, M. *et al.* Inhibition of endothelial cell apoptosis by netrin-1 during angiogenesis. *Dev. Cell* **16,** 614–20 (2009).
340. Guenebeaud, C. *et al.* The Dependence Receptor UNC5H2/B Triggers Apoptosis via PP2A-Mediated Dephosphorylation of DAP Kinase. *Mol. Cell* **40,** 863–876 (2010).
341. Koch, A. W. *et al.* Robo4 maintains vessel integrity and inhibits angiogenesis by interacting with UNC5B. *Dev. Cell* **20,** 33–46 (2011).
342. Negishi, M., Oinuma, I. & Katoh, H. Plexins: axon guidance and signal transduction. *C. Cell. Mol. Life Sci* **6205,** 1363–1371 (2005).
343. Wä Lchli, T. *et al.* Wiring the Vascular Network with Neural Cues: A CNS Perspective. (2015). doi:10.1016/j.neuron.2015.06.038
344. Kim, J., Oh, W.-J., Gaiano, N., Yoshida, Y. & Gu, C. Semaphorin 3E-Plexin-D1 signaling regulates VEGF function in developmental angiogenesis via a feedback mechanism. *Genes Dev.* **25,** 1399–411 (2011).
345. Torres-Vázquez, J. *et al.* Semaphorin-plexin signaling guides patterning of the developing vasculature. *Dev. Cell* **7,** 117–23 (2004).
346. Gu, C. *et al.* Semaphorin 3E and plexin-D1 control vascular pattern independently of neuropilins. *Science* **307,** 265–8 (2005).
347. Sakurai, A. *et al.* Semaphorin 3E initiates antiangiogenic signaling through plexin D1 by regulating Arf6 and R-Ras. *Mol. Cell. Biol.* **30,** 3086–98 (2010).
348. Herzog, Y., Kalcheim, C., Kahane, N., Reshef, R. & Neufeld, G. Differential expression of neuropilin-1 and neuropilin-2 in arteries and veins. *Mech. Dev.* **109,** 115–9 (2001).
349. Fantin, A. *et al.* NRP1 acts cell autonomously in endothelium to promote tip cell function during sprouting angiogenesis. *Blood* **121,** 2352–2362 (2013).
350. Fantin, A. *et al.* The cytoplasmic domain of neuropilin 1 is dispensable for angiogenesis, but promotes the spatial separation of retinal arteries and

veins. *Development* **138,** 4185–4191 (2011).
351. Lisabeth, E. M., Falivelli, G. & Pasquale, E. B. Eph receptor signaling and ephrins. *Cold Spring Harb. Perspect. Biol.* **5,** (2013).
352. Murai, K. K. & Pasquale, E. B. `Eph'ective signaling: forward, reverse and crosstalk. *J. Cell Sci.* **116,** (2003).
353. Hamada, K. *et al.* Distinct roles of ephrin-B2 forward and EphB4 reverse signaling in endothelial cells. *Arterioscler. Thromb. Vasc. Biol.* **23,** 190–7 (2003).
354. Kim, Y. H. *et al.* Artery and vein size is balanced by Notch and ephrin B2/EphB4 during angiogenesis. *Development* **135,** 3755–64 (2008).
355. Sawamiphak, S. *et al.* Ephrin-B2 regulates VEGFR2 function in developmental and tumour angiogenesis. *Nature* **465,** 487–91 (2010).
356. Blockus, H. & Chédotal, A. Slit-Robo signaling. *Development* **143,** 3037–44 (2016).
357. Huminiecki, L., Gorn, M., Suchting, S., Poulsom, R. & Bicknell, R. Magic roundabout is a new member of the roundabout receptor family that is endothelial specific and expressed at sites of active angiogenesis. *Genomics* **79,** 547–52 (2002).
358. Cai, H. *et al.* Roundabout 4 regulates blood-tumor barrier permeability through the modulation of ZO-1, Occludin, and Claudin-5 expression. *J. Neuropathol. Exp. Neurol.* **74,** 25–37 (2015).
359. Koch, A. W. *et al.* Robo4 Maintains Vessel Integrity and Inhibits Angiogenesis by Interacting with UNC5B. *Dev. Cell* **20,** 33–46 (2011).
360. Marlow, R. *et al.* Vascular Robo4 restricts proangiogenic VEGF signaling in breast. *Proc. Natl. Acad. Sci. U. S. A.* **107,** 10520–5 (2010).
361. Dubrac, A. *et al.* Targeting NCK-Mediated Endothelial Cell Front-Rear Polarity Inhibits Neovascularization. *Circulation* **133,** 409–421 (2016).
362. Fujiwara, M., Ghazizadeh, M. & Kawanami, O. Potential role of the Slit/Robo signal pathway in angiogenesis. *Vasc. Med.* **11,** 115–21 (2006).
363. Yang, Y. C. *et al.* The differential roles of Slit2-exon 15 splicing variants in angiogenesis and HUVEC permeability. *Angiogenesis* **18,** 301–312 (2015).
364. Kermani, P. & Hempstead, B. Brain-Derived Neurotrophic Factor: A Newly Described Mediator of Angiogenesis. *Trends Cardiovasc. Med.* **17,** 140–143 (2007).
365. Kermani, P. *et al.* Neurotrophins promote revascularization by local recruitment of TrkB+ endothelial cells and systemic mobilization of hematopoietic progenitors. *J. Clin. Invest.* **115,** 653–663 (2005).
366. Shigematsu, S. *et al.* IGF-1 regulates migration and angiogenesis of human endothelial cells. *Endocr. J.* **46 Suppl,** S59-62 (1999).
367. Kertesz, N., Wu, J., Chen, T. H.-P., Sucov, H. M. & Wu, H. The role of erythropoietin in regulating angiogenesis. *Dev. Biol.* **276,** 101–110 (2004).
368. Lazarovici, P., Gazit, A., Staniszewska, I., Marcinkiewicz, C. & Lelkes, P. I. Nerve Growth Factor (NGF) Promotes Angiogenesis in the Quail Chorioallantoic Membrane. *Endothelium* **13,** 51–59 (2006).
369. Sato, N. *et al.* Platelet-derived growth factor indirectly stimulates angiogenesis in vitro. *Am. J. Pathol.* **142,** 1119–30 (1993).
370. Yang, D. *et al.* Progranulin promotes colorectal cancer proliferation and angiogenesis through TNFR2/Akt and ERK signaling pathways. *Am. J. Cancer Res.* **5,** 3085–97 (2015).
371. Cristofaro, B. *et al.* Neurotrophin-3 Is a Novel Angiogenic Factor Capable of Therapeutic Neovascularization in a Mouse Model of Limb Ischemia. *Arterioscler. Thromb. Vasc. Biol.* **30,** 1143–1150 (2010).

372. Font, M. A., Arboix, A. & Krupinski, J. Angiogenesis, neurogenesis and neuroplasticity in ischemic stroke. *Curr. Cardiol. Rev.* **6,** 238–44 (2010).
373. Carmeliet, P. & Jain, R. K. Angiogenesis in cancer and other diseases. *Nature* **407,** 249–57 (2000).
374. Folkman, J., Long, D. M. & Becker, F. F. Growth and metastasis of tumor in organ culture. *Cancer* **16,** 453–467 (1963).
375. Ribatti, D. Judah Folkman, a pioneer in the study of angiogenesis. *Angiogenesis* **11,** 3–10 (2008).
376. Nguyen, D. X., Bos, P. D. & Massagué, J. Metastasis: from dissemination to organ-specific colonization. *Nat. Rev. Cancer* **9,** 274–284 (2009).
377. Kaur, B. *et al.* Hypoxia and the hypoxia-inducible-factor pathway in glioma growth and angiogenesis. *Neuro. Oncol.* **7,** 134–53 (2005).
378. Greijer, A. *et al.* Up-regulation of gene expression by hypoxia is mediated predominantly by hypoxia-inducible factor 1 (HIF-1). *J. Pathol.* **206,** 291–304 (2005).
379. Stenmark, K. R., Davie, N. J., Reeves, J. T. & Frid, M. G. Hypoxia, leukocytes, and the pulmonary circulation. *J. Appl. Physiol.* **98,** 715–21 (2005).
380. Döme, B., Hendrix, M. J. C., Paku, S., Tóvári, J. & Tímár, J. Alternative vascularization mechanisms in cancer: Pathology and therapeutic implications. *Am. J. Pathol.* **170,** 1–15 (2007).
381. Ziyad, S. & Iruela-Arispe, M. L. Molecular Mechanisms of Tumor Angiogenesis. *Genes Cancer* **2,** 1085–1096 (2011).
382. Bussolati, B., Deregibus, M. C. & Camussi, G. Characterization of molecular and functional alterations of tumor endothelial cells to design anti-angiogenic strategies. *Current vascular pharmacology* **8,** 220–232 (2010).
383. Folkman, J. Tumor angiogenesis: therapeutic implications. *N. Engl. J. Med.* **285,** 1182–6 (1971).
384. Ingber, D. *et al.* Synthetic analogues of fumagillin that inhibit angiogenesis and suppress tumour growth. *Nature* **348,** 555–557 (1990).
385. O'Reilly, M. S. *et al.* Angiostatin: a novel angiogenesis inhibitor that mediates the suppression of metastases by a Lewis lung carcinoma. *Cell* **79,** 315–28 (1994).
386. Vasudev, N. S. & Reynolds, A. R. Anti-angiogenic therapy for cancer: current progress, unresolved questions and future directions. *Angiogenesis* **17,** 471–94 (2014).
387. Samant, R. S. & Shevde, L. A. Recent Advances in Anti-Angiogenic Therapy of Cancer. *Oncotarget* **2,** 122–134 (2011).
388. Carrato, A., Gallego-Plazas, J. & Guillen-Ponce, C. Anti-VEGF therapy: a new approach to colorectal cancer therapy. *Expert Rev. Anticancer Ther.* **6,** 1385–1396 (2006).
389. Botrel, T. E. A., Clark, L. G. de O., Paladini, L. & Clark, O. A. C. Efficacy and safety of bevacizumab plus chemotherapy compared to chemotherapy alone in previously untreated advanced or metastatic colorectal cancer: a systematic review and meta-analysis. *BMC Cancer* **16,** 677 (2016).
390. Escudier, B., Cosaert, J. & Pisa, P. Bevacizumab: direct anti-VEGF therapy in renal cell carcinoma. *Expert Rev. Anticancer Ther.* **8,** 1545–1557 (2008).
391. Colombo, N., Conte, P. F., Pignata, S., Raspagliesi, F. & Scambia, G. Bevacizumab in ovarian cancer: Focus on clinical data and future perspectives. *Crit. Rev. Oncol. Hematol.* **97,** 335–348 (2016).
392. Reardon, D. A., Wen, P. Y., Desjardins, A., Batchelor, T. T. & Vredenburgh, J. J. Glioblastoma multiforme: an emerging paradigm of anti-VEGF

therapy. *Expert Opin. Biol. Ther.* **8,** 541–553 (2008).
393. Sachdev, J. C. & Jahanzeb, M. Evolution of bevacizumab-based therapy in the management of breast cancer. *Clin. Breast Cancer* **8,** 402–10 (2008).
394. Furuse, J. Sorafenib for the treatment of unresectable hepatocellular carcinoma. *Biologics* **2,** 779–88 (2008).
395. Jäger, D. *et al.* Sorafenib Treatment of Advanced Renal Cell Carcinoma Patients in Daily Practice: The Large International PREDICT Study. *Clin. Genitourin. Cancer* **13,** 156–164.e1 (2015).
396. Karar, J. & Maity, A. PI3K/AKT/mTOR Pathway in Angiogenesis. *Front. Mol. Neurosci.* **4,** 51 (2011).
397. Sasore, T. *et al.* Deciphering Combinations of PI3K/AKT/mTOR Pathway Drugs Augmenting Anti-Angiogenic Efficacy In Vivo. *PLoS One* **9,** e105280 (2014).
398. Dings, R. P. M. *et al.* Scheduling of radiation with angiogenesis inhibitors anginex and Avastin improves therapeutic outcome via vessel normalization. *Clin. Cancer Res.* **13,** 3395–402 (2007).
399. Carmeliet, P. Angiogenesis in life, disease and medicine. *Nature* **438,** 932–936 (2005).
400. Jain, R. K. Normalizing tumor vasculature with anti-angiogenic therapy: a new paradigm for combination therapy. *Nat. Med.* **7,** 987–9 (2001).
401. Goel, S., Wong, A. H.-K. & Jain, R. K. Vascular normalization as a therapeutic strategy for malignant and nonmalignant disease. *Cold Spring Harb. Perspect. Med.* **2,** a006486 (2012).
402. Jain, R. K. Normalizing Tumor Microenvironment to Treat Cancer: Bench to Bedside to Biomarkers. *J. Clin. Oncol.* **31,** 2205–2218 (2013).
403. Ma, J. & Waxman, D. J. Combination of antiangiogenesis with chemotherapy for more effective cancer treatment. *Mol. Cancer Ther.* **7,** 3670–84 (2008).
404. Eelen, G., de Zeeuw, P., Simons, M. & Carmeliet, P. Endothelial cell metabolism in normal and diseased vasculature. *Circ. Res.* **116,** 1231–44 (2015).
405. Verdegem, D., Moens, S., Stapor, P. & Carmeliet, P. Endothelial cell metabolism: parallels and divergences with cancer cell metabolism. *Cancer Metab.* **2,** 19 (2014).
406. Yeh, W.-L., Lin, C.-J. & Fu, W.-M. Enhancement of glucose transporter expression of brain endothelial cells by vascular endothelial growth factor derived from glioma exposed to hypoxia. *Mol. Pharmacol.* **73,** 170–7 (2008).
407. Goveia, J., Stapor, P. & Carmeliet, P. Principles of targeting endothelial cell metabolism to treat angiogenesis and endothelial cell dysfunction in disease. *EMBO Mol. Med.* **6,** 1–16 (2014).
408. De Bock, K. *et al.* Role of PFKFB3-driven glycolysis in vessel sprouting. *Cell* **154,** 651–63 (2013).
409. Xu, Y. *et al.* Endothelial PFKFB3 Plays a Critical Role in Angiogenesis. *Arterioscler. Thromb. Vasc. Biol.* **34,** 1231–1239 (2014).
410. Hamik, A., Wang, B. & Jain, M. K. Transcriptional regulators of angiogenesis. *Arterioscler. Thromb. Vasc. Biol.* **26,** 1936–47 (2006).
411. Solecki, D. J., Govek, E.-E., Tomoda, T. & Hatten, M. E. Neuronal polarity in CNS development. *Genes Dev.* **20,** 2639–47 (2006).
412. Montero-Balaguer, M. *et al.* Stable vascular connections and remodeling require full expression of VE-cadherin in zebrafish embryos. *PLoS One* **4,** e5772 (2009).
413. Pan, Q. *et al.* Revealing global regulatory features of mammalian

alternative splicing using a quantitative microarray platform. *Mol. Cell* **16,** 929–941 (2004).
414. Lampugnani, M. G., Orsenigo, F., Gagliani, M. C., Tacchetti, C. & Dejana, E. Vascular endothelial cadherin controls VEGFR-2 internalization and signaling from intracellular compartments. *J. Cell Biol.* **174,** 593–604 (2006).
415. Irimia, M. *et al.* A highly conserved program of neuronal microexons is misregulated in autistic brains. *Cell* **159,** 1511–23 (2014).
416. Zhang, C. *et al.* Integrative modeling defines the Nova splicing-regulatory network and its combinatorial controls. *Science* **329,** 439–43 (2010).
417. Stanley, R. J. & Thomas, G. M. H. Activation of G Proteins by Guanine Nucleotide Exchange Factors Relies on GTPase Activity. *PLoS One* **11,** e0151861 (2016).
418. Kuramoto, K., Negishi, M. & Katoh, H. Regulation of dendrite growth by the Cdc42 activator Zizimin1/Dock9 in hippocampal neurons. *J. Neurosci. Res.* **87,** 1794–805 (2009).
419. Abraham, S. *et al.* A Rac/Cdc42 exchange factor complex promotes formation of lateral filopodia and blood vessel lumen morphogenesis. *Nat. Commun.* **6,** 7286 (2015).
420. Vignal, E., Blangy, A., Martin, M., Gauthier-Rouvière, C. & Fort, P. Kinectin is a key effector of RhoG microtubule-dependent cellular activity. *Mol. Cell. Biol.* **21,** 8022–34 (2001).
421. Zhang, X. *et al.* Kinectin-mediated endoplasmic reticulum dynamics supports focal adhesion growth in the cellular lamella. *J. Cell Sci.* **123,** 3901–12 (2010).
422. Wang, T. *et al.* CD97, an adhesion receptor on inflammatory cells, stimulates angiogenesis through binding integrin counterreceptors on endothelial cells. *Blood* **105,** 2836–44 (2005).
423. Ward, Y. *et al.* LPA receptor heterodimerizes with CD97 to amplify LPA-initiated RHO-dependent signaling and invasion in prostate cancer cells. *Cancer Res.* **71,** 7301–11 (2011).
424. Foussard, H. *et al.* LRCH proteins: a novel family of cytoskeletal regulators. *PLoS One* **5,** e12257 (2010).
425. Couzens, A. L. *et al.* Protein interaction network of the mammalian Hippo pathway reveals mechanisms of kinase-phosphatase interactions. *Sci. Signal.* **6,** rs15 (2013).
426. Roignot, J. & Soubeyran, P. ArgBP2 and the SoHo family of adapter proteins in oncogenic diseases. *Cell Adhesion and Migration* **3,** 167–170 (2009).
427. Mandai, K. *et al.* Ponsin/SH3P12: An 1-afadin- and vinculin-binding protein localized at cell-cell and cell-matrix adherens junctions. *J. Cell Biol.* **144,** 1001–1017 (1999).
428. Kotula, L. Abi1, a critical molecule coordinating actin cytoskeleton reorganization with PI-3 kinase and growth signaling. *FEBS Lett.* **586,** 2790–4 (2012).
429. Innocenti, M. *et al.* Abi1 regulates the activity of N-WASP and WAVE in distinct actin-based processes. *Nat. Cell Biol.* **7,** 969–976 (2005).
430. Roffers-Agarwal, J., Xanthos, J. B. & Miller, J. R. Regulation of actin cytoskeleton architecture by Eps8 and Abi1. *BMC Cell Biol.* **6,** 36 (2005).
431. Hotta, A. *et al.* Laminin-based cell adhesion anchors microtubule plus ends to the epithelial cell basal cortex through LL5??/?? *J. Cell Biol.* **189,** 901–907 (2010).
432. Sharma, A. *et al.* A new role for the muscle repair protein dysferlin in

endothelial cell adhesion and angiogenesis. *Arterioscler. Thromb. Vasc. Biol.* **30,** 2196–2204 (2010).
433. Neri, D. & Bicknell, R. Tumour vascular targeting. *Nat Rev Cancer* **5,** 436–446 (2005).
434. Yap, K., Xiao, Y., Friedman, B. A., Je, H. S. & Makeyev, E. V. Polarizing the Neuron through Sustained Co-expression of Alternatively Spliced Isoforms. *Cell Rep.* **15,** 1316–1328 (2016).
435. Taddei, A. *et al.* Endothelial adherens junctions control tight junctions by VE-cadherin-mediated upregulation of claudin-5. *Nat. Cell Biol.* **10,** 923–934 (2008).
436. Antar, A. A. R. *et al.* Junctional Adhesion Molecule-A Is Required for Hematogenous Dissemination of Reovirus. *Cell Host Microbe* **5,** 59–71 (2009).
437. Smith, J. E. & Baker, K. E. Nonsense-mediated RNA decay - a switch and dial for regulating gene expression. *BioEssays* **37,** 612–623 (2015).
438. Jensen, K. B. & Darnell, R. B. in 85–98 (2008). doi:10.1007/978-1-60327-475-3_6
439. Isken, O. & Maquat, L. E. The multiple lives of NMD factors: balancing roles in gene and genome regulation. *Nat. Rev. Genet.* **9,** 699–712 (2008).
440. Lawson, N. D. & Weinstein, B. M. In vivo imaging of embryonic vascular development using transgenic zebrafish. *Dev Biol* **248,** 307–318 (2002).
441. Chen, E. Y. *et al.* Enrichr: interactive and collaborative HTML5 gene list enrichment analysis tool. *BMC Bioinformatics* **14,** 128 (2013).
442. Omelchenko, T. & Hall, A. Myosin-IXA Regulates Collective Epithelial Cell Migration by Targeting RhoGAP Activity to Cell-Cell Junctions. *Curr. Biol.* **22,** 278–288 (2012).
443. Dubé, N. *et al.* The RapGEF PDZ-GEF2 is required for maturation of cell–cell junctions. *Cell. Signal.* **20,** 1608–1615 (2008).
444. Wallar, B. J. & Alberts, A. S. The formins: active scaffolds that remodel the cytoskeleton. *Trends Cell Biol.* **13,** 435–46 (2003).
445. Block, J. *et al.* FMNL2 Drives Actin-Based Protrusion and Migration Downstream of Cdc42. *Curr. Biol.* **22,** 1005–1012 (2012).
446. Kühn, S. *et al.* The structure of FMNL2–Cdc42 yields insights into the mechanism of lamellipodia and filopodia formation. *Nat. Commun.* **6,** 7088 (2015).
447. Wong, K. *et al.* Signal transduction in neuronal migration: roles of GTPase activating proteins and the small GTPase Cdc42 in the Slit-Robo pathway. *Cell* **107,** 209–21 (2001).
448. Premont, R. T. *et al.* The GIT/PIX complex: An oligomeric assembly of GIT family ARF GTPase-activating proteins and PIX family Rac1/Cdc42 guanine nucleotide exchange factors. *Cell. Signal.* **16,** 1001–1011 (2004).
449. Kelemen, O. *et al.* Function of alternative splicing. *Gene* **514,** 1–30 (2013).
450. Potente, M., Gerhardt, H. & Carmeliet, P. Basic and Therapeutic Aspects of Angiogenesis. *Cell* **146,** 873–887 (2011).
451. Ferrara, N. & Kerbel, R. S. Angiogenesis as a therapeutic target. *Nature* **438,** 967–74 (2005).
452. Chen, L. J., Wei, S. Y. & Chiu, J. J. Mechanical regulation of epigenetics in vascular biology and pathobiology. *J. Cell. Mol. Med.* **17,** 437–448 (2013).
453. Campa, F., Machuy, N., Klein, A. & Rudel, T. A new interaction between Abi-1 and betaPIX involved in PDGF-activated actin cytoskeleton reorganisation. *Cell Res.* **16,** 759–70 (2006).
454. Kafasla, P. *et al.* Defining the roles and interactions of PTB. *Biochem. Soc.*

Trans. **40,** 815–820 (2012).
455. Iruela-Arispe, M. L. & Davis, G. E. Cellular and molecular mechanisms of vascular lumen formation. *Dev. Cell* **16,** 222–31 (2009).
456. Elbashir, S. M. *et al.* Duplexes of 21-nucleotide RNAs mediate RNA interference in cultured mammalian cells. *Nature* **411,** 494–498 (2001).

APPENDIX I
Tables

Table 3. RNA-Seq results for *Nova2* knockdown ECs, deposited as PRJNA293346.

GENE	EVENT	COORDINATES	LENGTH	dPSI
Scmh1	MmuEX0041243	chr4:120134618-120134760	143	18,54
Arfgap2	MmuEX0005709	chr2:91109227-91109268	42	14,29
Nutf2	MmuEX0032832	chr8:108390338-108390573	236	11,73
Zfp280d	MmuEX0053184	chr9:72199332-72199377	46	22,1
Bcl2l12	MmuEX0007843	chr7:52248114-52248401	288	12,44
Zbtb7c	MmuEX0052704	chr18:76255091-76255432	342	14,38
Slc25a40	MmuEX0042921	chr5:8427196-8427267	72	9,99
Mrps10	MmuEX0029715	chr17:47509525-47509594	70	17,46
Btbd10	MmuEX0008367	chr7:120495295-120495419	125	13,14
1700086O06Rik	MmuEX0000598	chr18:38400493-38400607	115	17,03
D4Wsu53e	MmuEX0013588	chr4:134481692-134481736	45	11,77
Ncor1	MmuEX0031185	chr11:62147165-62147658	494	11,68
Ntan1	MmuEX0032512	chr16:13826976-13827078	103	21,05
Ppp1r12a	MmuEX0036680	chr10:107689813-107689980	168	17,99
Phldb2	MmuEX0034878	chr16:45775081-45775200	120	28,25
Atp11c	MmuEX0006765	chrX:57482325-57482429	105	19,16
Mll3	MmuEX0029193	chr5:24800375-24800536	162	13,19
Rcor3	MmuEX0039316	chr1:193932525-193932582	58	13,83
Rims2	MmuEX0039868	chr15:39418080-39418331	252	11,85

GENE	EVENT	COORDINATES	LENGTH	dPSI
Fbrsl1	MmuEX0018757	chr5:110810620-110810665	46	7,08
Etl4	MmuEX0017446	chr2:20727402-20729000	1599	16,79
Phactr2	MmuEX0034669	chr10:12975116-12975127	12	8,59
Tsku	MmuEX0049313	chr7:105507868-105507977	110	15,92
Tacc1	MmuEX0046113	chr8:26310563-26310678	116	7,63
Dock9	MmuEX0015484	chr14:121991034-121991101	68	31,66
1700086O06Rik	MmuEX0000599	chr18:38399227-38399405	179	28,2
Btbd10	MmuEX0008366	chr7:120508419-120508483	65	11,91
Bub1	MmuEX0008425	chr2:127647678-127647730	53	9,46
Mpdz	MmuEX0029495	chr4:80963498-80963608	111	12,77
Atxn2l	MmuEX0007082	chr7:133635963-133636122	160	12,78
D19Ertd737e	MmuEX0013517	chr19:60296393-60296480	88	16,09
Msh5	MmuEX0029814	chr17:35170168-35170240	73	10,61
Fam190a	MmuEX0018203	chr6:61760625-61760702	78	16,66
Atp8a1	MmuEX0006941	chr5:68172227-68172300	74	19,58
Rims2	MmuEX0039869	chr15:39441610-39441687	78	9,84
Filip1l	MmuEX0019257	chr16:57506712-57506967	256	21,9
Srgap1	MmuEX0044896	chr10:121266283-121266385	103	10,5
Etl4	MmuEX0017445	chr2:20727212-20727289	78	9,87
Ccdc136	MmuEX0009562	chr6:29367932-29368153	222	34,13
Ccdc136	MmuEX0009561	chr6:29367072-29367578	507	26,49
Fmnl2	MmuEX0019399	chr2:52989446-52989492	47	13,22
Ccdc136	MmuEX0009560	chr6:29365431-29365655	225	18,51
Ccdc136	MmuEX0009559	chr6:29364786-29364980	195	14,5
Nfib	MmuEX0031610	chr4:81969449-81969614	166	14,25
Ubr2	MmuEX0050335	chr17:47117269-47117367	99	22,61
Itga7	MmuEX0024625	chr10:128378501-128378632	132	13,21
H2afy	MmuEX0022308	chr13:56191119-56191218	100	13,85
Pparg	MmuEX0036473	chr6:115372084-115372210	127	20,93
Tubgcp6	MmuEX0049915	chr15:88939651-88939726	76	14,85

GENE	EVENT	COORDINATES	LENGTH	dPSI
Wwox	MmuEX0052312	chr8:117203687-117203775	89	15,61
Ninl	MmuEX0031730	chr2:150795716-150795868	153	10,45
Slc12a8	MmuEX0042598	chr16:33617194-33617340	147	13,36
Soat2	MmuEX0044318	chr15:101991021-101991118	98	8,9
Zfp398	MmuEX0053291	chr6:47790251-47790646	396	9,96
Rabep2	MmuEX0038417	chr7:133588037-133588092	56	9,09
Ptbp2	MmuEX0037640	chr3:119427530-119427563	34	31,25
Zfp672	MmuEX0053547	chr11:58133369-58133456	88	7,56
Slc9a5	MmuEX0043617	chr8:107885461-107885538	78	12,76
Rnf38	MmuEX0040186	chr4:44171877-44171924	48	19,05
Trerf1	MmuEX0048821	chr17:47456301-47456567	267	17,49
Myo19	MmuEX0030471	chr11:84708980-84709056	77	5,28
Ahnak	MmuEX0004390	chr19:9076189-9081150	4962	16,25
Baz2a	MmuEX0007708	chr10:127533991-127534116	126	11,84
Pa2g4	MmuEX0033419	chr10:128000280-128000311	32	15,27
Ube2j2	MmuEX0050174	chr4:155329531-155329669	139	9,6
Asb7	MmuEX0006373	chr7:73823043-73823131	89	10,45
Fnip1	MmuEX0019507	chr11:54301214-54301297	84	12,14
BC024814	MmuEX0007398	chr16:8482220-8482260	41	24,71
Dcp1a	MmuEX0013926	chr14:31334776-31334841	66	9,81
Nadsyn1	MmuEX0030795	chr7:151007077-151007137	61	6,92
Guf1	MmuEX0022213	chr5:69954322-69954461	140	11,21
Armc9	MmuEX0006197	chr1:88148852-88148967	116	10,59
Narg2	MmuEX0030891	chr9:69269468-69269597	130	11,73
BC057079	MmuEX0007547	chr4:87842663-87842920	258	13,01
Phf8	MmuEX0034789	chrX:148006909-148007211	303	10,82
2310035C23Rik	MmuEX0000917	chr1:107588789-107588880	92	14,05
2010317E24Rik	MmuEX0000756	chr2:25228936-25229037	102	6,72
Dpy19l4	MmuEX0015657	chr4:11217538-11217669	132	13,96
Naa16	MmuEX0030728	chr14:79759263-79759335	73	13,83

GENE	EVENT	COORDINATES	LENGTH	dPSI
Trit1	MmuEX0049021	chr4:122726395-122726507	113	18,06
Trit1	MmuEX0049023	chr4:122729309-122729418	110	11,16
Ap1g2	MmuEX0005397	chr14:55723419-55723495	77	8,39
Rc3h2	MmuEX0039249	chr2:37232875-37232956	82	10,31
Ncoa1	MmuEX0031140	chr12:4249836-4249884	49	13,71
Iqcb1	MmuEX0024414	chr16:36851271-36851380	110	12,5
4930430F08Rik	MmuEX0001510	chr10:100044897-100044956	60	9,72
Spen	MmuEX0044633	chr4:141036661-141036729	69	11,17
AI848100	MmuEX0002765	chr1:163775691-163775711	21	19,38
Clcn3	MmuEX0011578	chr8:63454529-63454704	176	19,35
Sorbs2	MmuEX0044385	chr8:46826841-46826933	93	15,63
Hnrnpl	MmuEX0023118	chr7:29595691-29596187	497	11,98
Usp48	MmuEX0051064	chr4:137192849-137192902	54	19,14
Atrx	MmuEX0007049	chrX:103079646-103079759	114	14,32
2410002O22Rik	MmuEX0000992	chr13:104942245-104942262	18	10,96
Tcf12	MmuEX0046651	chr9:71716806-71716877	72	13,48
Magi1	MmuEX0027545	chr6:93644002-93644169	168	11,61
Ktn1	MmuEX0025961	chr14:48324095-48324163	69	27,48
Ppig	MmuEX0036568	chr2:69573925-69573954	30	7,61
Unc5b	MmuEX0050632	chr10:60239933-60239965	33	29,46
Fn1	MmuEX0019422	chr1:71650234-71650503	270	11,17
Ctnnd1	MmuEX0013079	chr2:84452689-84452706	18	11,76
Pja2	MmuEX0035334	chr17:64647065-64647250	186	12,96
Ppp3cb	MmuEX0036790	chr14:21322469-21322498	30	13,07
Fn1	MmuEX0019423	chr1:71660337-71660609	273	14,04
Nasp	MmuEX0030915	chr4:116283008-116283982	975	16,71
Baz1a	MmuEX0007699	chr12:56024372-56024467	96	9,22
Ubap2l	MmuEX0050122	chr3:89835233-89835292	60	15,6
Pitpnb	MmuEX0035275	chr5:111814540-111814624	85	11,26
Bag6	MmuEX0007608	chr17:35279505-35279550	46	13,82
Cobll1	MmuEX0012048	chr2:64943772-64943885	114	13,34

GENE	EVENT	COORDINATES	LENGTH	dPSI
Nfia	MmuEX0031607	chr4:97748416-97748507	92	6,88
Extl3	MmuEX0017658	chr14:65699217-65699312	96	8,1
Hsd17b7	MmuEX0023306	chr1:171889554-171889610	57	11,01
Dysf	MmuEX0016017	chr6:84046471-84046512	42	20,99
Atp9b	MmuEX0006987	chr18:81033094-81033170	77	14,66
Ccdc58	MmuEX0009830	chr16:36082777-36082902	126	12,91
Idh1	MmuEX0023577	chr1:65225564-65225986	423	15,04
3110009E18Rik	MmuEX0001293	chr1:122067978-122068055	78	9,77
Mpp2	MmuEX0029533	chr11:101941967-101942085	119	12,5
Mfsd8	MmuEX0028842	chr3:40626117-40626220	104	12,12
Zfp850	MmuEX0053660	chr7:28797355-28797469	115	13,71
Ttll3	MmuEX0049661	chr6:113351296-113351491	196	16,05
Evl	MmuEX0017508	chr12:109921558-109921620	63	17,17
Npr2	MmuEX0032213	chr4:43656207-43656281	75	12,29
Erbb2ip	MmuEX0017201	chr13:104617987-104618103	117	8,49
Lrch3	MmuEX0026798	chr16:32995892-32995999	108	44,16
Dennd5b	MmuEX0014303	chr6:149033393-149033458	66	18,24
Dock6	MmuEX0015442	chr9:21630227-21630319	93	14,23
Rims2	MmuEX0039873	chr15:39366384-39366563	180	8,18
Mical3	MmuEX0028987	chr6:120903652-120903702	51	20,71
Macf1	MmuEX0027478	chr4:123140781-123141014	234	20,78
Cyb561d1	MmuEX0013265	chr3:108003043-108003080	38	19,21
2210408F21Rik	MmuEX0000800	chr6:31278332-31278360	29	17,8
Atat1	MmuEX0006554	chr17:36035333-36035412	80	9,66
Macf1	MmuEX0027477	chr4:123142599-123142748	150	7,96
Epb4.1l2	MmuEX0016997	chr10:25215251-25215397	147	23,75
Epb4.1l2	MmuEX0016996	chr10:25213373-25213435	63	27,63
Galnt2	MmuEX0020016	chr8:126853613-126853700	88	11,88
Elmod3	MmuEX0016724	chr6:72547618-72547639	22	7,18
Srgap1	MmuEX0044897	chr10:121265785-121265818	34	5,67

GENE	EVENT	COORDINATES	LENGTH	dPSI
Apbb3	MmuEX0005541	chr18:36838048-36838124	77	17,23
Ccdc157	MmuEX0009654	chr11:4052912-4053059	148	12,81
Stxbp5	MmuEX0045642	chr10:9498712-9498765	54	13,31
Itga7	MmuEX0024626	chr10:128378878-128378997	120	14,11
Dock9	MmuEX0015485	chr14:121990533-121990576	44	37,45
H2afy	MmuEX0022309	chr13:56189617-56189703	87	15,37
Uqcc	MmuEX0050722	chr2:155735089-155735161	73	24,59
Abi1	MmuEX0003242	chr2:22818734-22818748	15	23
Idh3g	MmuEX0023592	chrX:71027637-71027648	12	15,11
Ralgapa1	MmuEX0038609	chr12:56822393-56822474	82	13,41
Mthfd2l	MmuEX0030013	chr5:91361938-91361971	34	17,57
Atxn1	MmuEX0007056	chr13:46051824-46051944	121	5,49
Slit2	MmuEX0043691	chr5:48612206-48612229	24	13,73
Trim46	MmuEX0048926	chr3:89040225-89040522	298	8,81
Zcwpw1	MmuEX0052857	chr5:138258121-138258204	84	19,72
Ralgps2	MmuEX0038672	chr1:158814664-158814756	93	11,9
Myl4	MmuEX0030395	chr11:104443308-104443343	36	18,58
Utrn	MmuEX0051174	chr10:12470263-12470340	78	8,17
Dclre1b	MmuEX0013911	chr3:103611995-103612021	27	12,04
Pikfyve	MmuEX0035194	chr1:65239108-65239140	33	8,57
Zfp251	MmuEX0053122	chr15:76700712-76700844	133	6,89
Rgs12	MmuEX0039621	chr5:35373117-35373270	154	10,39
Pctp	MmuEX0034087	chr11:89847407-89847474	68	15,67
Tfdp2	MmuEX0047063	chr9:96190999-96191046	48	22,12
Prss16	MmuEX0037439	chr13:22096960-22097101	142	10,35
Cbx5	MmuEX0009400	chr15:103045453-103045552	100	18,55
Ipo11	MmuEX0024350	chr13:107626292-107626506	215	41,24
Hmga1	MmuEX0023026	chr17:27693897-27694011	115	14,21
Flywch1	MmuEX0019365	chr17:23907202-23907295	94	21,14

GENE	EVENT	COORDINATES	LENGTH	dPSI
Prrc2b	MmuEX0037404	chr2:32068407-32070467	2061	16,66
Nbr1	MmuEX0031025	chr11:101433776-101433886	111	15,02
Palm	MmuEX0033522	chr10:79279537-79279668	132	12,88
Tmem44	MmuEX0047980	chr16:30549479-30549543	65	14,02
Dbp	MmuEX0013795	chr7:52961976-52962086	111	6,78
Trim46	MmuEX0048930	chr3:89042588-89042625	38	13,62
Taf4b	MmuEX0046215	chr18:14963226-14963348	123	9,99
Esco1	MmuEX0017371	chr18:10595674-10595873	200	10,82
Traf1	MmuEX0048684	chr2:34811716-34811800	85	8
Dixdc1	MmuEX0014761	chr9:50490642-50490731	90	16,88
Thbs3	MmuEX0047174	chr3:89020603-89020809	207	14,5
Ppfibp1	MmuEX0036531	chr6:146948184-146948216	33	34,84
Inpp4a	MmuEX0024183	chr1:37440184-37440216	33	10,55
Cd97	MmuEX0010283	chr8:86255802-86255936	135	33,17
Epb4.1l2	MmuEX0016999	chr10:25221384-25221437	54	31,71
Bin1	MmuEX0007975	chr18:32585878-32586006	129	19,41
Cask	MmuEX0009247	chrX:13128073-13128108	36	5,46
Magi1	MmuEX0027548	chr6:93654271-93654354	84	22,57
Spna2	MmuEX0044723	chr2:29869678-29869692	15	32,23

Table 4. RNA-Seq results for *Nova2* overexpressing ECs

GENE	EVENT	COORDINATES	LENGTH	dPSI
Lrch3	ENSMUSG00000022801	chr16:32995892-32995999	108	-35,48
Chi3l7	ENSMUSG00000043873	chr3:105822507-105822630	124	-33,85
AI987944	ENSMUSG00000056383	chr7:48643478-48643625	148	-31,67
Sorbs1	ENSMUSG00000025006	chr19:40374733-40374792	60	-30,73
Neo1	ENSMUSG00000032340	chr9:58732277-58732371	95	-30,62
Stoml1	ENSMUSG00000032333	chr9:58103341-58103620	280	-30,25
Atp11c	ENSMUSG00000062949	chrX:57482325-57482429	105	-29,09
Ccdc136	ENSMUSG00000029769	chr6:29361710-29361868	159	-28,92
Sh3pxd2a	ENSMUSG00000053617	chr19:47357511-47357594	84	-28,24
Bean1	ENSMUSG00000031872	chr8:106737816-106737926	111	-27,84
Dock11	ENSMUSG00000031093	chrX:33549938-33549976	39	-26,59
Zfyve26	ENSMUSG00000066440	chr12:80338160-80338342	183	-26,22
Phldb2	ENSMUSG00000033149	chr16:45775081-45775200	120	-25,29
Col13a1	ENSMUSG00000058806	chr10:61368002-61368028	27	-23,9
Mll5	ENSMUSG00000029004	chr5:23006269-23006394	126	-23,59
Macf1	ENSMUSG00000028649	chr4:123063792-123063800	9	-22,92
Myo5a	ENSMUSG00000034593	chr9:75040191-75040271	81	-22,91
Uchl3	ENSMUSG00000022111	chr14:102089789-102089864	76	-22,56

GENE	EVENT	COORDINATES	LENGTH	dPSI
D17H6S56E-3	ENSMUSG00000007030	chr17:35160795-35160887	93	-22,53
Usp40	ENSMUSG00000005501	chr1:89864971-89865024	54	-21,98
Ccno	ENSMUSG00000042417	chr13:113779099-113779284	186	-21,66
Ccdc136	ENSMUSG00000029769	chr6:29362364-29362534	171	-21,62
Gphn	ENSMUSG00000047454	chr12:79594937-79595044	108	-21,48
Eml2	ENSMUSG00000040811	chr7:19787179-19787276	98	-21,3
Tep1	ENSMUSG00000006281	chr14:51453589-51453752	164	-21,25
Adamts10	ENSMUSG00000024299	chr17:33680581-33680726	146	-20,93
Uap1	ENSMUSG00000026670	chr1:172078127-172078174	48	-20,88
Il3ra	ENSMUSG00000068758	chr14:15180428-15180582	155	-20,74
Unc5b	ENSMUSG00000020099	chr10:60239933-60239965	33	-20,45
Nbeal2	ENSMUSG00000056724	chr9:110543915-110543995	81	-20,3
F730043M19Rik	ENSMUSG00000052125	chr12:33823708-33823927	220	-20,08
Cln3	ENSMUSG00000030720	chr7:133724307-133724378	72	-19,85
Ceacam1	ENSMUSG00000074272	chr7:26259539-26259823	285	-19,82
Dnajc27	ENSMUSG00000020657	chr12:4107159-4107348	190	-19,76
Lrrcc1	ENSMUSG00000027550	chr3:14535999-14536204	206	-19,57
Pbrm1	ENSMUSG00000042323	chr14:31927035-31927190	156	-19,21
Tsc2	ENSMUSG00000002496	chr17:24743169-24743297	129	-19,07
Syne1	ENSMUSG00000019769	chr10:5153369-5153509	141	19,07

GENE	EVENT	COORDINATES	LENGTH	dPSI
Tsg101	ENSMUSG00000014402	chr7:54156397-54156488	92	-19
Wdfy3	ENSMUSG00000043940	chr5:102307025-102307078	54	-18,86
Sgce	ENSMUSG00000004631	chr6:4640469-4640495	27	-18,84
Huwe1	ENSMUSG00000025261	chrX:148240819-148240950	132	-18,79
Ccdc88a	ENSMUSG00000032740	chr11:29398409-29398612	204	-18,78
Txndc16	ENSMUSG00000021830	chr14:45792189-45792279	91	-18,52
Iffo1	ENSMUSG00000038271	chr6:125101813-125101821	9	-18,45
Crocc	ENSMUSG00000040860	chr4:140577569-140577732	164	-18,41
Hhat	ENSMUSG00000037375	chr1:194553478-194553672	195	-18,36
Fmnl2	ENSMUSG00000036053	chr2:52989446-52989492	47	-18,28
Crem	ENSMUSG00000063889	chr18:3295038-3295180	143	-18,24
Efcab5	ENSMUSG00000050944	chr11:76934598-76934887	290	-18,23
Slc22a17	ENSMUSG00000022199	chr14:55527660-55527700	41	-18,13
Atp8a1	ENSMUSG00000037685	chr5:68172227-68172300	74	-18,13
Lrrc61	ENSMUSG00000073096	chr6:48506954-48507093	140	-18,1
5730494N06Rik	ENSMUSG00000027341	chr2:132069755-132069789	35	-18,09
Ino80e	ENSMUSG00000030689	chr7:134000740-134000805	66	-17,96
Slc9a5	ENSMUSG00000014786	chr8:107885461-107885538	78	-17,86
1700020O03Rik	ENSMUSG00000021254	chr12:87609926-87610011	86	-17,83
Gpr19	ENSMUSG00000032641	chr6:134836909-134836954	46	-17,8
Phka1	ENSMUSG00000034055	chrX:99723406-99723456	51	-17,77
Kidins220	ENSMUSG00000036333	chr12:25725321-25725434	114	-17,74
Atp8b3	ENSMUSG00000003341	chr10:79986397-79986636	240	-17,68
Soat2	ENSMUSG00000023045	chr15:101991021-101991118	98	-17,67
Tle2	ENSMUSG00000034771	chr10:81048958-81049082	125	-17,65
Ranbp17	ENSMUSG00000040594	chr11:33237855-33237914	60	-17,63
Ube2l3	ENSMUSG00000038965	chr16:17173306-17173451	146	-17,62
Mtss1	ENSMUSG00000022353	chr15:58778881-58779075	195	-17,57
Ccdc136	ENSMUSG00000029769	chr6:29367072-29367578	507	-17,53
Dysf	ENSMUSG00000033788	chr6:84046471-84046512	42	-17,47
Dennd5b	ENSMUSG00000030313	chr6:149033393-149033458	66	-17,47
2610020H08Rik	ENSMUSG00000030924	chr7:126971606-126971720	115	-17,41
1700020O03Rik	ENSMUSG00000021254	chr12:87608094-87608133	40	-17,39

GENE	EVENT	COORDINATES	LENGTH	dPSI
Triobp	ENSMUSG00000033088	chr15:78791379-78791535	157	-17,39
Ctage5	ENSMUSG00000021000	chr12:60247323-60247349	27	-17,32
Ccdc136	ENSMUSG00000029769	chr6:29362902-29363087	186	-17,28
Neil1	ENSMUSG00000032298	chr9:56991565-56991626	62	-17,28
Epn1	ENSMUSG00000035203	chr7:5044914-5044988	75	-17,1
Crocc	ENSMUSG00000040860	chr4:140602687-140602770	84	-17,1
Slc26a11	ENSMUSG00000039908	chr11:119234425-119234485	61	-16,97
Gripap1	ENSMUSG00000031153	chrX:7377662-7377709	48	-16,96
Srr	ENSMUSG00000001323	chr11:74732939-74733164	226	-16,73
Rims2	ENSMUSG00000037386	chr15:39441610-39441687	78	-16,67
4931406P16Rik	ENSMUSG00000066571	chr7:35090804-35090941	138	-16,6
Cyp2ab1	ENSMUSG00000022818	chr16:20314271-20314431	161	-16,54
2210013O21Rik	ENSMUSG00000086316	chrX:150163405-150163482	78	-16,35
Ctns	ENSMUSG00000005949	chr11:72999791-72999961	171	-16,33
Raet1c	ENSMUSG00000053219	chr10:21891810-21891907	98	-16,27
Shc1	ENSMUSG00000042626	chr3:89228112-89228165	54	-15,96
Slc43a1	ENSMUSG00000027075	chr2:84700247-84700320	74	-15,9
Ccdc18	ENSMUSG00000056531	chr5:108625015-108625178	164	-15,87
Lrrc16a	ENSMUSG00000021338	chr13:24114365-24114505	141	-15,86
Thap2	ENSMUSG00000020137	chr10:114813408-114813603	196	-15,81
Atxn2	ENSMUSG00000042605	chr5:122231342-122231551	210	-15,77
Fggy	ENSMUSG00000028573	chr4:95510764-95510884	121	-15,69
Cd82	ENSMUSG00000027215	chr2:93283526-93283601	76	-15,68
Evl	ENSMUSG00000021262	chr12:109921558-109921620	63	-15,67
Arhgef7	ENSMUSG00000031511	chr8:11817660-11817884	225	-15,59
Lphn2	ENSMUSG00000028184	chr3:148512730-148512768	39	-15,58
Arfgap2	ENSMUSG00000027255	chr2:91109227-91109268	42	-15,54
Sh2b1	ENSMUSG00000030733	chr7:133611464-133611563	100	-15,53
Cyth1	ENSMUSG00000017132	chr11:118041516-118041518	3	-15,49
Carns1	ENSMUSG00000075289	chr19:4169899-4170071	173	-15,45
Syne1	ENSMUSG00000019769	chr10:5301207-5301275	69	-15,36
Slc43a1	ENSMUSG00000027075	chr2:84701533-84701656	124	-15,25
Rif1	ENSMUSG00000036202	chr2:51963960-51964111	152	-15,23

Appendix

GENE	EVENT	COORDINATES	LENGTH	dPSI
Prr3	ENSMUSG00000038500	chr17:36115656-36115726	71	-15,2
Zfp644	ENSMUSG00000049606	chr5:107110923-107111032	110	-15,18
Wbp1	ENSMUSG00000030035	chr6:83070766-83070867	102	-15,15
Lztfl1	ENSMUSG00000025245	chr9:123624418-123624538	121	-15,02
Ccdc122	ENSMUSG00000034795	chr14:77492577-77492693	117	15,06
Setd4	ENSMUSG00000022948	chr16:93593492-93593577	86	15,29
Serp2	ENSMUSG00000052584	chr14:76949789-76949861	73	15,38
Csgalnact1	ENSMUSG00000036356	chr8:71169698-71169834	137	15,45
Epb4.1l2	ENSMUSG00000019978	chr10:25221384-25221437	54	15,56
Ptprm	ENSMUSG00000033278	chr17:67046993-67047043	51	15,74
Srpk2	ENSMUSG00000062604	chr5:23122145-23122208	64	15,85
Il4i1	ENSMUSG00000074141	chr7:52093359-52093560	202	15,87
Insr	ENSMUSG00000005534	chr8:3181702-3181737	36	15,89
Cdk8	ENSMUSG00000029635	chr5:147104230-147104343	114	15,96
Atat1	ENSMUSG00000024426	chr17:36041053-36041121	69	16,03
Ewsr1	ENSMUSG00000009079	chr11:4978923-4978955	33	16,1
Ikbkg	ENSMUSG00000004221	chrX:71673101-71673241	141	16,12
Gm5595	ENSMUSG00000069727	chr7:49920388-49920514	127	16,26
Vdac3	ENSMUSG00000008892	chr8:23692555-23692607	53	16,33
Ccdc122	ENSMUSG00000034795	chr14:77491475-77491873	399	16,37
Lphn1	ENSMUSG00000013033	chr8:86448105-86448254	150	16,43
Parp11	ENSMUSG00000037997	chr6:127418050-127418170	121	16,51
Fancc	ENSMUSG00000021461	chr13:63501542-63501626	85	16,54
Rapgef6	ENSMUSG00000037533	chr11:54485157-54485180	24	16,66
Spice1	ENSMUSG00000043065	chr16:44355553-44355648	96	16,68
Ube2d3	ENSMUSG00000078578	chr3:135119565-135119608	44	16,71
Ppargc1b	ENSMUSG00000033871	chr18:61471808-61471924	117	16,89
Plcb4	ENSMUSG00000039943	chr2:135790788-135790823	36	16,93
Zfp53	ENSMUSG00000057409	chr17:21628190-21628280	91	16,98
Tmc8	ENSMUSG00000050106	chr11:117651530-117651653	124	17,07
Fnip2	ENSMUSG00000061175	chr3:79311761-79311850	90	17,37
Cast	ENSMUSG00000021585	chr13:74886253-74886309	57	17,38
Spice1	ENSMUSG00000043065	chr16:44356258-44356305	48	17,41

GENE	EVENT	COORDINATES	LENGTH	dPSI
Klf11	ENSMUSG00000020653	chr12:25339708-25340641	934	17,54
Cyld	ENSMUSG00000036712	chr8:91226211-91226337	127	17,58
Syne2	ENSMUSG00000063450	chr12:77201015-77201083	69	17,66
Mga	ENSMUSG00000033943	chr2:119747102-119747212	111	17,79
D630037F22Rik	ENSMUSG00000038122	chr10:55918241-55918366	126	17,82
Trerf1	ENSMUSG00000064043	chr17:47456301-47456567	267	17,85
Vps24	ENSMUSG00000053119	chr6:71502393-71502453	61	18,26
Srgap1	ENSMUSG00000020121	chr10:121265785-121265818	34	18,96
Amh	ENSMUSG00000035262	chr10:80269285-80269444	160	18,96
Stac2	ENSMUSG00000017400	chr11:97900933-97901070	138	19,05
2410127L17Rik	ENSMUSG00000024726	chr19:18768139-18768252	114	19,43
March7	ENSMUSG00000026977	chr2:60085545-60085569	25	19,49
Catsper2	ENSMUSG00000033486	chr2:121237886-121238026	141	19,94
Gm10348	ENSMUSG00000071793	chr8:19994879-19995046	168	19,96
Fam151b	ENSMUSG00000034334	chr13:93236932-93237067	136	20,12
Zbtb7c	ENSMUSG00000044646	chr18:76255091-76255432	342	20,2
St6galnac6	ENSMUSG00000026811	chr2:32463562-32463616	55	20,51
Ccdc142	ENSMUSG00000079511	chr6:83053396-83053526	131	20,89
N4bp2	ENSMUSG00000037795	chr5:66179292-66179380	89	20,91
Dimt1	ENSMUSG00000021692	chr13:107743514-107743578	65	20,91
Brca1	ENSMUSG00000017146	chr11:101385860-101387625	1766	21,06
Fam73a	ENSMUSG00000054942	chr3:151953755-151953873	119	22,22
Sipa1l2	ENSMUSG00000001995	chr8:127947093-127947146	54	22,33
Neto2	ENSMUSG00000036902	chr8:88214734-88214916	183	22,5
Myo9a	ENSMUSG00000039585	chr9:59637843-59637899	57	22,91
Plekha7	ENSMUSG00000045659	chr7:123291767-123291847	81	23,04
Luc7l2	ENSMUSG00000029823	chr6:38519502-38519534	33	24,74
Aff2	ENSMUSG00000031189	chrX:66776611-66776743	133	25
Dst	ENSMUSG00000026131	chr1:34252673-34252906	234	25,99
Anubl1	ENSMUSG00000042213	chr6:116235872-116235939	68	26,64
Magi1	ENSMUSG00000045095	chr6:93654271-93654354	84	28,19
Etl4	ENSMUSG00000036617	chr2:20681174-20681278	105	35,85
Eef1b2	ENSMUSG00000025967	chr1:63224441-63224450	10	38,89

APPENDIX II
Articles

Appendix

Hindawi Publishing Corporation
BioMed Research International
Volume 2015, Article ID 528954, 14 pages
http://dx.doi.org/10.1155/2015/528954

Review Article

SAM68: Signal Transduction and RNA Metabolism in Human Cancer

Paola Frisone,[1] Davide Pradella,[2] Anna Di Matteo,[2] Elisa Belloni,[2] Claudia Ghigna,[2] and Maria Paola Paronetto[1,3]

[1]*Laboratory of Cellular and Molecular Neurobiology, Santa Lucia Foundation, 00143 Rome, Italy*
[2]*Institute of Molecular Genetics-National Research Council (IGM-CNR), 27100 Pavia, Italy*
[3]*University of Rome "Foro Italico", Piazza Lauro de Bosis 15, 00135 Rome, Italy*

Correspondence should be addressed to Claudia Ghigna; arneri@igm.cnr.it
and Maria Paola Paronetto; mariapaola.paronetto@uniroma4.it

Received 12 January 2015; Accepted 24 February 2015

Academic Editor: Bo Zuo

Alterations in expression and/or activity of splicing factors as well as mutations in *cis*-acting splicing regulatory sequences contribute to cancer phenotypes. Genome-wide studies have revealed more than 15,000 tumor-associated splice variants derived from genes involved in almost every aspect of cancer cell biology, including proliferation, differentiation, cell cycle control, metabolism, apoptosis, motility, invasion, and angiogenesis. In the past decades, several RNA binding proteins (RBPs) have been implicated in tumorigenesis. SAM68 (SRC associated in mitosis of 68 kDa) belongs to the STAR (signal transduction and activation of RNA metabolism) family of RBPs. SAM68 is involved in several steps of mRNA metabolism, from transcription to alternative splicing and then to nuclear export. Moreover, SAM68 participates in signaling pathways associated with cell response to stimuli, cell cycle transitions, and viral infections. Recent evidence has linked this RBP to the onset and progression of different tumors, highlighting misregulation of SAM68-regulated splicing events as a key step in neoplastic transformation and tumor progression. Here we review recent studies on the role of SAM68 in splicing regulation and we discuss its contribution to aberrant pre-mRNA processing in cancer.

1. Introduction

SAM68 (SRC associated in mitosis of 68 kDa) was originally identified as a protein physically associated with and phosphorylated by the tyrosine kinase c-SRC during mitosis [1, 2], opening the interesting possibility of a signaling circuitry driven by c-SRC and affecting RNA processing and trafficking in a cell-cycle-dependent manner.

SAM68 belongs to the STAR (signal transduction and activation of RNA metabolism) family of RNA binding proteins (RBPs) that link signaling pathways to RNA processing [3, 4]. STAR proteins include *Artemia salina* GRP33 [5], *C. elegans* GLD-1 [6], mammalian QKI [7], SAM68 [8, 9], SLM-1 and SLM-2 [10, 11], *Drosophila* HOW [12], KEP1 and Sam50 [13], and the evolutionary conserved splicing factor SF1 [14]. All STAR proteins, from worms to mammals, share common architecture (Figure 1). They contain a GRP33/SAM68/GLD-1 (GSG) domain for RNA binding and homodimerization, flanked by regulatory regions harboring motifs for protein-protein interactions (Figure 1), often mediated by conserved amino acid residues targeted by posttranslational modifications [15]. SAM68 contains six proline-rich sequences and a tyrosine-rich region at the C-terminus, which form docking sites for signaling proteins containing SRC homology 3 (SH3) and 2 (SH2) domains (Figure 1) [1, 2, 9, 16]. Notably, tyrosine phosphorylation by SRC-related kinases impairs SAM68 homodimerization [17] as well as its affinity for RNA both *in vitro* [16, 18] and *in vivo* [19]. Additional posttranslational modifications were also reported to affect the functions of this RBP. SAM68 binds to and is methylated by the arginine methyltransferase PRMT1 [20], thus affecting SAM68 interaction with SH3 domains [21] and its nuclear localization [20]. SAM68 acetylation, described in tumorigenic breast cancer cell lines [22], by

Appendix

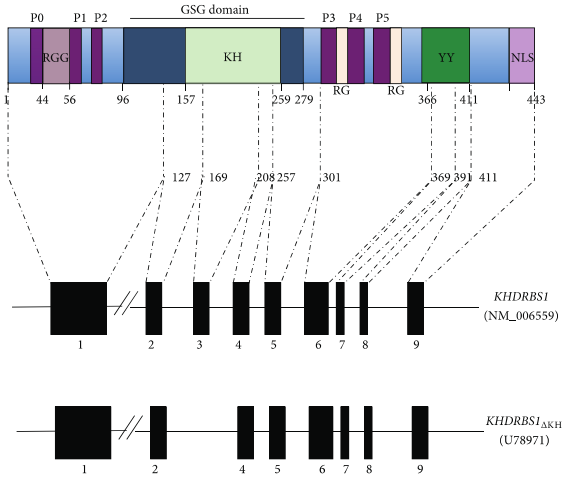

Figure 1: Schematic representation of SAM68 domains. In the upper part, schematic model representing the structural/functional domains of SAM68 protein as a prototype of a STAR protein. SAM68 protein is composed of the GRP33/SAM68/GLD-1 (GSG) domain, formed by a single heterogeneous nuclear ribonucleoprotein particle K (hnRNP K) homology domain (KH) embedded in two flanking regions, six consensus proline-rich motifs (P0–P5), arginine/glycine/glycine (RGG) and arginine/glycine (RG) boxes, C-terminal tyrosine-rich domain (YY), and a nuclear localization signal (NLS). In the lower part, the two protein coding mRNA isoforms of human *KHDRBS1* are represented. Black boxes indicate exons (numbered from 1 to 9). The sizes of exons and the protein domains encoded by each exon are indicated.

the acetyltransferase CBP increases SAM68 binding to RNA *in vitro*. Furthermore, SAM68 can be SUMOylated by the SUMO E3 ligase PIAS1, which enhances its transcriptional repression activity [23]. Thus, posttranslational modifications greatly influence the biochemical properties of SAM68 and finely tune its subcellular localization, interaction with signaling proteins, and RNA binding affinity.

Despite the growing interest in STAR proteins, their physiological role has not been completely elucidated yet. Nevertheless, recent mouse models of genetic ablation of STAR proteins are now greatly helping in pursuing this goal. In this review, we discuss the functional properties of SAM68 in signaling and RNA metabolism, with particular emphasis on malignant transformation. In particular, we highlight recent advances and new insights into SAM68-based signaling that have been made in the last two decades, which expand our understanding of STAR-mediated signaling in cancer cells.

2. SAM68 Biological Role(s): Lessons from Mouse Models

The first indication of the involvement of STAR proteins in tumorigenesis came from studies in *C. elegans*. Critical missense mutations in the *gld-1* gene caused germ-line tumors, thus suggesting an important role for *GLD-1* as a tumor suppressor [24]. These null mutations in hermaphrodites caused female germ cells to exit from the meiotic prophase and to start proliferating, thus leading to the formation of a germ-line tumor [3]. In this regard, it is important to notice that the function and localization of GLD-1 appear quite different from the SAM68 subfamily of STAR proteins. Indeed, GLD-1 is localized exclusively in the cytoplasm of germ cells and it does not contain the protein domains flanking the GSG of SAM68, which are involved in cell signaling [3]. Nevertheless, an initial observation seemed to suggest a similar tumor suppressor role also for SAM68.

Appendix

A random homozygous knockout (RHKO) screen in NIH3T3 murine fibroblasts indicated that functional inactivation of the *Sam68* gene induces tumorigenesis and allows NIH3T3 cells to form metastatic tumors in nude mice [25]. These studies suggested that SAM68 negatively affects neoplastic transformation, like its *C. elegans* ortholog *GLD-1*. However, in contrast to this proposed function, disruption of the *Sam68* gene in chicken DT40 cells showed reduced growth rate, indicating that SAM68 plays a positive role in cell proliferation [26]. Moreover, a natural alternative isoform of *SAM68* with deletion of the KH (RNA binding) domain ($SAM68_{\Delta KH}$) was specifically expressed during growth arrest in normal cells, but absent in SRC-transformed cells (Figure 1) [27]. Importantly, transfection of the $SAM68_{\Delta KH}$ isoform inhibited serum-induced DNA synthesis and Cyclin D1 expression, thus highlighting for the first time the involvement of SAM68 RNA binding activity in cell proliferation [27]. Thus, despite the initial putative role as a tumor suppressor gene, subsequent studies appeared to suggest a positive role of SAM68 in tumorigenesis. These findings were also supported by investigation of the *Sam68* knockout mouse model, which has recently unveiled the physiological processes in which SAM68 is involved.

Sam68-deficient mice displayed high lethality soon after birth [28]. Nevertheless, mice that survived beyond weaning showed a normal lifespan. Importantly, surviving *Sam68*–/– mice lived to old age (~2 years) and were not prone to tumor formation, clearly indicating that SAM68 is not a tumor suppressor *in vivo* [28]. Moreover, haploinsufficiency of SAM68 delayed mammary tumor onset and reduced metastasis [29]. Although the authors reported higher activation of SRC and FAK in the mammary gland of *Sam68* heterozygote females, indicating altered regulation of the SRC signal transduction pathway [29], whether or not this effect was related to the lower tumorigenicity of *Sam68* haploinsufficient cells was not investigated.

Additional phenotypes of the *Sam68*–/– mice revealed the important role played by this RBP in a number of physiological processes. Adult knockout females displayed defects in bone metabolism [28] and delayed development of sexual organs [29]. *Sam68*–/– mice were protected against age-induced osteoporosis and were characterized by preserved bone density. This phenotype was linked to the preferential differentiation of knockout mesenchymal stem cells toward osteoblasts instead of adipocytes [28]. Furthermore, *Sam68*–/– females displayed a reduction in the number of developing ovarian follicles, alteration of estrous cycles, and impaired fertility [30]. Similarly, spermatogenesis and fertility were impaired in *Sam68*–/– males, due to the involvement of both nuclear RNA processing events [31] and translational regulation of a subset of mRNAs during spermiogenesis [32]. Although almost exclusively nuclear in the majority of normal cells, SAM68 localized in the cytoplasm of secondary spermatocytes and associated with polysomes, thus playing a role in translational regulation of target mRNAs [32, 33]. Notably, this function in male germ cells closely resembles that of its orthologue in *C. elegans* GLD-1.

Aberrant regulation of splicing events also contributes to the phenotypes of *Sam68*–/– mice. For instance, stimulation of *Sam68*–/– cerebellar neurons was dramatically attenuated due to the impaired regulation of *Nrxn-1* alternative splicing [34]. *Nrxn-1* encodes a synaptic cell surface receptor that contributes to the assembly of functional presynaptic terminals, and a severe perturbation of *Nrxn-1* splice variants was observed in *Sam68*–/– brains [34]. Moreover, *Sam68*–/– mice exhibited a lean phenotype due to a dramatic reduction in adiposity. The decreased commitment to early adipocyte progenitors and defects in adipogenic differentiation were attributed to aberrant splicing of *mTOR* described in *Sam68*–/– mice [35].

Collectively, the defects documented in *Sam68* knockout mice reflect the multiple roles played by SAM68 in signal transduction and RNA processing and emphasize how aberrant regulation of SAM68 function(s) might contribute to oncogenic transformation [28, 29, 36]. Nevertheless, to what extent SAM68 RNA binding activity contributes to the mouse defects and to neoplastic transformation has not been unraveled yet, and, in this context, knock-in or transgenic mouse models displaying *Sam68* gene with mutations in the RNA binding domain would really help to answer this question.

3. SAM68 Signaling in Human Cancer

SAM68 acts as a scaffold protein in response to different signal transduction pathways [36, 41]. Through its proline-rich motifs, SAM68 interacts with the SH3 domains of different SRC kinases [1, 2], like BRK [42], FYN [18], and Itk/Tec/BTK [43], all involved in different aspects of cell transformation. Importantly, the interaction of SAM68 with the SRC SH3 domain enables SRC kinases to phosphorylate their substrates [9].

The interaction of SAM68 with FYN induces the assembly of a protein complex containing also PLCγ1 (phospholipase C gamma) [18], triggering its phosphorylation and activation [18, 44]. Interestingly, a truncated form of the tyrosine kinase receptor c-KIT, named tr-KIT, stimulates the formation of this complex [18]. Tr-KIT is aberrantly expressed in a subgroup of prostate cancer (PCa) patients and its expression correlates with enhanced activation of SRC and elevated expression and high tyrosine phosphorylation of SAM68 [45]. Moreover, SAM68 is frequently upregulated in PCa patients and promotes PCa cell proliferation and survival to chemotherapeutic agents [46], suggesting a role for this pathway in prostate cancer biology.

The breast tumor kinase BRK, a nonreceptor tyrosine kinase, is also responsible for the tyrosine phosphorylation of SAM68 in cancer cells, which has been associated with SAM68 increased nuclear localization and cell cycle promotion [47, 48]. Importantly, both SAM68 and BRK are upregulated in breast cancer cells and breast tumors [39, 48, 49]. In addition, in the transformed HT29 adenocarcinoma cell line, endogenous BRK colocalized in SAM68

Appendix

nuclear bodies (SNBs), and BRK-mediated phosphorylation of SAM68 impaired its ability to bind RNA molecules [50]. Consistent with these results, nuclear BRK was also detected in differentiated androgen-responsive LNCaP human PCa cell line, while it was mainly cytoplasmic in the undifferentiated and more aggressive androgen-unresponsive PC3 prostate cancer cell line [50]. Thus, relocalization of the BRK kinase during PCa development and progression may indicate disruption of a signaling pathway important for maintaining the normal phenotype of prostate epithelial cells.

Proteomic analyses revealed that SAM68 is able to form two (large and small) protein complexes, interacting with several RBPs and with regulators of cytoskeletal organization and signal transduction pathways [51, 52]. In accordance with this, *SAM68*-deficient fibroblasts displayed defects in cell migration [53] and an increase in SRC kinase activity [53]. These observations suggest that SAM68 is required for a negative feedback inhibition of SRC and that deregulated SRC activity could be responsible for the defects in actin cytoskeleton and cell migration observed in *SAM68*-deficient fibroblasts. Interestingly, epidermal growth factor (EGF) treatment induced a change in the size of the SAM68-containing complexes, from the large to the smaller one, the latter containing splicing activity [51]. Since EGF receptor (EGFR) stimulation triggers signaling cascades controlling cellular proliferation, migration, differentiation, and survival, and EGFR overexpression has been associated with poor prognosis in several types of epithelial cancers, such as lung, head and neck, colorectal, and breast cancer [54], EGFR-SAM68 signaling could be targeted to attenuate the oncogenic features of cancer cells.

In addition to PCa [46, 52], aberrant expression of SAM68 was detected in several other tumors. In particular, SAM68 was shown to be upregulated in colorectal cancer [55] and in patients with non-small cell lung cancer [56]. Moreover, in patients with renal cell carcinoma high SAM68 expression was inversely associated with overall survival while SAM68 cytoplasmic localization significantly correlated with pathologic grade and outcome of this tumor [57]. Furthermore, in breast cancer patients expression and cytoplasmic localization of SAM68 significantly correlated with clinical characteristics of patients, including clinical stage, tumour-nodule-metastasis classification, histological grade, and ER expression [39]. In line with an oncogenic role played by SAM68 in this tumor type, silencing of SAM68 inhibited proliferation and tumourigenicity of breast cancer cells [39]. Finally, SAM68 was shown to be significantly upregulated in cervical cancer at both mRNA and protein levels [58]. SAM68 upregulation and its cytoplasmic localization were significantly associated with risk factors and correlated with lymph node metastasis and poor prognosis in patients with early-stage cervical cancer [58]. Consistently, downregulation of SAM68 in cervical cancer cells inhibited cellular motility and invasion by the inhibition of the AKT/GSK-3 β/Snail pathway [58].

Collectively, these reports strongly suggest that high SAM68 expression and its cytoplasmic localization are associated with poor overall survival in different types of tumors. Moreover, the deregulation of SRC and AKT pathways could be involved in the oncogenic function of SAM68 in the cytoplasm.

4. SAM68 and Transcriptional Regulation in Human Cancer

The first evidence of the involvement of SAM68 in transcriptional regulation came out in 2002 when Hong and colleagues documented the repressive effect of SAM68 on different mammalian and viral promoter constructs [37]. Direct recruitment of SAM68 to a promoter region resulted in strong transcriptional repression and mutation of the SAM68 RNA binding domain had no influence on this effect, thus suggesting that SAM68 transcriptional activity occurs in a RNA-independent fashion [37]. Mechanistically, the authors described the functional association of SAM68 with the acetyl-transferase CBP, which caused modulation of CBP transcriptional activity (Figure 2(a)) [37].

Other reports confirmed the role of SAM68 as a transcriptional repressor. SAM68 was shown to interact with hnRNP K, leading to inhibition of the *trans*-activating effects of hnRNP K on c-myc target genes [59]. Moreover, overexpression of SAM68 in mouse fibroblasts inhibited accumulation of *Cyclin D1* and *E* transcripts [60], whereas SAM68 SUMOylation by PIAS1 further enhanced repression of Cyclin D1 expression (Figure 2(b)) [23].

In PCa cells, SAM68 was proposed to function as a transcriptional coregulator and to promote the transcriptional activity of the androgen receptor (Figure 2(c)) [38]. Furthermore, in hematopoietic stem cells SAM68 was shown to form an oncogenic transcriptional complex with mixed lineage leukaemia (MLL) and PRMT1 [61]. Chimeric fusion of MLL with PRMT1 or SAM68 enhanced self-renewal of primary hematopoietic cells; conversely, specific knockdown of PRMT1 or SAM68 suppressed MLL-mediated oncogenic transformation [61]. Similarly, SAM68 depletion in breast cancer cells impaired cell proliferation and their tumorigenic features through the upregulation of cyclin-dependent kinase inhibitors p21 (Cip1) and p27 (Kip1). Thus, in this context SAM68 depletion might lead to suppression of AKT phosphorylation and subsequent activation of FOXO factors, which in turn promote the upregulation of p21 (Cip1) and p27 (Kip1) (Figure 2(d)) [39].

In normal and transformed human T cells SAM68 was shown to bind the *CD25* promoter and facilitate p65 recruitment, thus suggesting a novel role for SAM68 in NF-κB regulation of gene expression in human T cell signaling (Figure 2(e)) [40]. In this context, *CD25* expression and aberrant NF-κB signaling led to increased proliferation, expression of antiapoptotic proteins, and drug resistance, while *SAM68* knockdown markedly impaired CD25 upregulation. Remarkably, elevated expression of CD25 has been detected in a large variety of hematopoietic malignancies and solid tumors [62]; thus the p65-SAM68 association might be strategically used to target CD25 expression in those particular tumors that depend on CD25 for survival [40].

Transcription and RNA processing machineries are tightly coupled. Temporal coupling not only provides efficient

Appendix

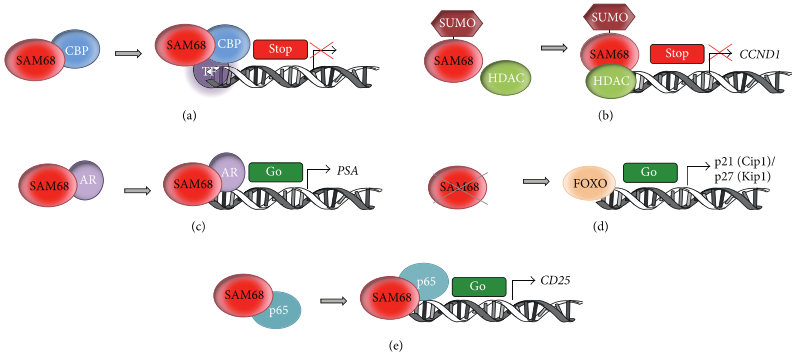

Figure 2: Transcriptional regulation by SAM68. (a) SAM68 forms a complex with CBP and transcriptional repressor factors (TF), thus negatively regulating CBP targets transcription [37]. (b) The PIAS1 complex SUMOylates SAM68, which interacts with a histone deacetylase (HDAC) and represses *CCDN1* transcription [23]. (c) SAM68 directly interacts with the androgen receptor (AR) and binds to androgen-responsive elements (AREs) leading to AR targets activation (i.e., *PSA* gene) [38]. (d) SAM68 depletion in breast cancer cells leads to activation of FOXO factors thus inhibiting cell proliferation and tumourigenicity through the upregulation of cyclin-dependent kinase inhibitors p21 (Cip1) and p27 (Kip1) [39]. (e) SAM68 binds the *CD25* promoter and facilitates p65 recruitment, thus contributing to NF-κB regulation of gene expression [40].

gene expression to accomplish rapid growth and proliferation, but also allows rapid response to diverse signaling events [63]. Many splicing regulators are recruited to nascent pre-mRNAs by their interaction with the phosphorylated carboxyl-terminal domain (CTD) of RNAPII thus affecting splicing decisions [64]. Interestingly, SAM68 was shown to interact directly with RNA polymerase II (RNAPII) in meiotic spermatocytes [31] and with the RNAPII associated Brahma (Brm) subunit of the SWI/SNF chromatin-remodeling complex [65]. These observations strongly suggest the involvement of SAM68 in cotranscriptional splicing. Thus, on one hand, SAM68 binding to transcription factors and to the RNAPII itself can affect transcriptional regulation of gene expression; on the other hand, through the cooperation with chromatin remodelers, SAM68 can impact cotranscriptional splicing events. In this regard, interaction of the protooncogenic transcription factor FBI-1 with SAM68 in PCa cells was shown to inhibit SAM68 recruitment on the *BCL-X* pre-mRNA, thus affecting apoptosis [66]. By contrast, binding of SAM68 to the transcriptional coactivator SND1 was required for the efficient association of SAM68 with RNAPII and for the recruitment of SAM68 on the *CD44* pre-mRNA [67]. Remarkably, *CD44* alternative splicing isoforms are associated with tumor progression and metastasis [68]. Thus, the SND1/SAM68 complex might be an important determinant of PCa progression and the concomitant upregulation of these proteins might provide an advantage for cancer cells to invade other tissues, consequently favoring the spreading of metastatic cells [67].

Hence, depending on the cellular partner, SAM68 displays different effects on target genes, modulating in this way different or even antagonistic functions within the cell.

In summary, growing evidence documents the involvement of SAM68 in the transcriptional regulation of gene expression of cancer related genes, both by direct binding to the chromatin and by recruitment of specific transcription factors, which in turn affect its splicing activity.

5. SAM68-Regulated Alternative Splicing Events in Cancer

SAM68 preferentially binds A/U-rich sequences in RNA [16]. SELEX experiments identified the UAAA consensus motif bound with Kd ~12–60 nM. Importantly, a single A to C mutation within this motif abolished SAM68 binding [69], indicating that this motif is involved in high affinity direct binding or in a specific RNA structure. Indeed, SAM68 was then shown to bind cellular RNAs enriched in such U/A-rich sequences [70] and to directly modulate alternative splicing events in target genes [71]. Interestingly, the UAAA motif matches with the last four bases of the mammalian polyadenylation signal AAUAAA, thus opening the hypothesis of SAM68 involvement in RNA stability.

During tumor progression, a variety of oncogenic signaling pathways induce modifications of the downstream effectors of key biological functions [76]. Notably, SAM68 was the first identified "hub factor" able to translate extracellular stimuli to pre-mRNA processing of specific target

Appendix

genes in the nucleus [71]. As mentioned above, several posttranslational modifications regulate the function and/or localization of SAM68. In particular, serine-threonine and tyrosine phosphorylation of SAM68, which often occurs in cancer cells, are important for SAM68 homodimerization and RNA affinity (Figure 3(a)) [2, 72, 73].

The *CD44* gene represents an interesting example of SAM68-mediated coupling between signal transduction cascades and alternative splicing. *CD44* pre-mRNA is affected by complex alternative splicing events occurring in 10 adjacent exons (v1–v10) to produce multifunctional transmembrane glycoprotein isoforms implicated in cell-cell and cell-matrix adhesion, migration, and invasion [77] and with crucial roles in cancer progression and metastasis [78]. By binding to A/U-rich enhancer element located within exon *v5*, SAM68 promotes the production of the oncogenic *CD44v5* variant (Figure 3(b), (A)) [71], which is upregulated in several cancers [78, 79] and bears prognostic value in gastric and renal carcinoma [80–82].

Several molecular mechanisms (not mutually exclusive) have been proposed to explain the ability of SAM68 to stimulate *CD44* exon *v5* inclusion: (i) SAM68 competes or displaces the antagonistic splicing repressor hnRNP A1 that binds a specific splicing silencer element located within exon *v5* [83]; (ii) SAM68 affects the dynamic recruitment of spliceosomal components, including U2AF65, an auxiliary factor involved in the recognition of the 3′ splice site during the splicing reaction [84]; upon SAM68 phosphorylation this interaction is disrupted and U2AF65 dissociates from pre-mRNA allowing the subsequent spliceosome remodeling and exon *v5* inclusion [85]; (iii) SAM68 interacts with the splicing coactivator SRm160 and they functionally cooperate to simulate *CD44* exon *v5* inclusion [86].

Aberrant regulation of alternative splicing is emerging as a key step in oncogenesis [87]. Recent data demonstrated that genotoxic stress widely modulates alternative splicing events in cancer cells [88, 89]. This regulation is exerted in part through reduced transcription elongation rates as a consequence of RNA polymerase II (RNAPII) phosphorylation [90] and in part through direct involvement of specific RBPs in the repair process or by specific regulation of DNA damage response gene expression [91], also accomplished by RBP relocalization [92]. *CD44* exon *v5* splicing is also influenced by genotoxic stress induced by chemotherapeutic drugs, such as the topoisomerase II inhibitor mitoxantrone (MTX) [93]. Specifically, MTX causes relocalization of SAM68 from nucleoplasm to transcriptionally active nuclear granules and this correlates with changes in alternative splicing of *CD44* exon *v5*. This effect is independent of signal transduction pathways activated by DNA damage [93]. Nevertheless, it appears to be functionally relevant for the cells, as SAM68 was found overexpressed in prostate carcinoma where it promotes resistance and survival to chemotherapeutic treatments [46].

In addition to *CD44*, changes in alternative splicing of other transcripts, including *Caspase 2* (*CASP2*) [94], *BCL-2* [90], the p53 negative modulators *MDM2* and *MDM4* [95], and *Cyclin D1* (*CCND1*), have been observed in cancer cells after treatment with chemotherapy drugs [96, 97]. Notably, *CCND1* pre-mRNA was also identified as a novel alternative splicing target of SAM68 [74]. *CCND1* is a protooncogene that is frequently deregulated in several human cancers through different mechanisms, such as chromosomal translocations, amplification of the *CCND1* locus, and intragenic mutations [97–99]. Alternative splicing also plays an important role in aberrant Cyclin D1 expression. The *CCND1* gene encodes two alternatively spliced transcripts: the canonical *Cyclin D1a* and the alternative *Cyclin D1b*, which results from the retention of intron 4 and premature termination of the transcript [100]. These isoforms display different biological properties and cellular localization [96]. In particular, Cyclin D1b is exclusively nuclear and displays stronger oncogenic potential than Cyclin D1a [74, 100, 101] and its upregulation correlates with poor prognosis in several tumor types [96]. At the molecular level, SAM68 was observed to bind to the proximal region of intron 4 and to interfere with the recruitment of the U1 snRNP, in this way promoting intron 4 retention (Figure 3(b), (B)) [74]. Signal transduction pathways affecting SAM68 phosphorylation status, such as those conveyed by ERK1/2 and SRC kinases, regulate alternative splicing of *CCND1* pre-mRNA by modulating SAM68 affinity for this target [74]. Notably, SAM68 expression positively correlates with levels of Cyclin D1b, but not D1a, in human PCa cells [97], suggesting that increased levels of SAM68 in human PCa contribute to tumorigenesis by elevating the expression of Cyclin D1b in this tumor type.

Recent studies have demonstrated an important contribution of alternative splicing regulation in the cascade of events characterizing the morphological conversion of tumor cells during epithelial-to-mesenchymal transition (EMT) [102], one of the major routes through which cancer cells acquire migratory and invasive potentials [103, 104]. SAM68 phosphorylation by ERK1/2 plays an important role during neoplastic progression of epithelial cells through activation of EMT. This is illustrated by the ability of SAM68 to repress alternative splicing-activated nonsense-mediated mRNA decay (AS-NMD) [105] of a splicing factor of the serine arginine (SR) family, SRSF1 [75]. AS-NMD of *SRSF1* pre-mRNA, which involves a cryptic intron in the 3′ UTR region of the gene, decreases *SRSF1* mRNA stability and protein levels (Figure 3(b), (C)) and, notably, this event is altered in colon cancer [75]. In mesenchymal cells, phosphorylation of SAM68 is controlled by soluble factors expressed by epithelial cells that act through the activation of ERK1/2 kinase [75]. SRSF1, an oncogenic splicing factor upregulated in many human cancers [106], severely impacts on cell physiology. For instance, its overexpression stimulates skipping of exon 11 of the *RON* protooncogene increasing the production of the constitutively active Δ*RON* isoform, which in turn promotes the acquisition of an invasive cellular phenotype [107]. Interestingly, inhibition of ERK activity by small molecules or by using conditioned medium from epithelial cells reverts SAM68 phosphorylation, decreases *SRSF1* mRNA and protein levels, promotes inclusion of *RON* exon 11, and induces the reversal program named mesenchymal-to-epithelial transition (MET) [75]. MET occurs at the final metastatic sites where redifferentiation of mesenchymal cells to an epithelial state is required for the colonization of distant organs [103, 104].

Appendix

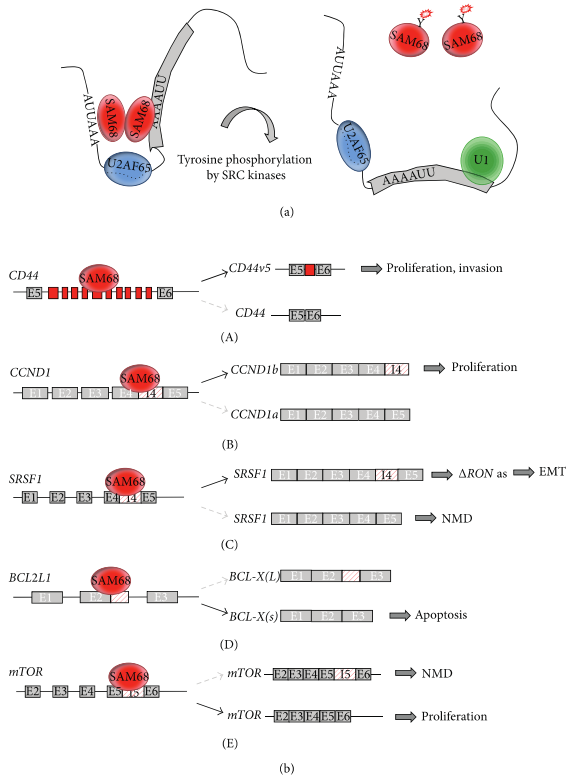

Figure 3: Model of SAM68 interaction with pre-mRNAs and splicing regulation. (a) SAM68 recognition of A/U-rich bipartite sequence in the pre-mRNA homodimerization allows simultaneous binding to the pre-mRNA and to U2AF65 [69–73]. Tyrosine phosphorylation of SAM68 reduces the RNA binding affinity and thus releases SAM68 from the pre-mRNA. (b) Model of alternative splicing events regulated by SAM68 in cancer cells. (A) SAM68 promotes inclusion of *CD44* variable exon *v5*. Inclusion of variable exons in the *CD44* pre-mRNA is specific to cancer cells and correlates with cancer progression and invasiveness [71]. (B) SAM68 promotes splicing events that regulate cell proliferation. Binding of SAM68 to *CCND1* intron 4 interferes with the correct recruitment of U1 snRNP at the exon 4 5′ splice sites, thus enhancing retention of intron 4 and generating the *Cyclin D1b* isoform. In prostate cancer, the expression of Cyclin D1b interrupts a negative feedback in the regulation of androgen receptor (AR) transcriptional activity, thereby promoting cell proliferation [74]. (C) As for *CCND1*, SAM68 promotes retention of *SRSF1* intron 4, thus stabilizing *SRSF1* pre-mRNA and inhibiting its degradation by nonsense-mediated decay (NMD) [75]. Accumulation of SRSF1 in turn favors the splicing of Δ*RON*, an oncogenic variant of *RON* that triggers epithelial-mesenchymal transition (EMT). (D) SAM68 regulates the alternative splicing of *BCL2L1* leading to the short (*BCL-X(s)*) proapoptotic isoform [19]. This activity can be reverted by tyrosine phosphorylation of SAM68 from SRC family kinases, thereby switching the role of SAM68 from being proapoptotic to being antiapoptotic and allowing cells to differentially react to external cues. (E) SAM68 regulates *mTOR* alternative splicing thus leading to the correct mRNA isoform and avoiding retention of intron 5 that generates a premature termination codon and the consequent reduction of mTOR protein levels [35]. Notably, mTOR is a critical effector in cell-signalling pathways commonly deregulated in human cancers and overexpression of the components involved in the PI3K/AKT/mTOR pathway has been shown to induce malignant transformation.

Appendix

A paradigmatic example of the central role of SAM68 in apoptosis is represented by the regulation of *BCL-X* (*BCL2L1*), a member of the *BCL-2* gene family. *BCL-X* pre-mRNA is alternatively spliced to generate two isoforms with opposite functions in promoting apoptosis. Selection of the proximal 5′ splice site (5′ SS) in exon 2 causes the production of the antiapoptotic long *BCL-X(L)* variant, while the proapoptotic short *BCL-X(s)* variant is produced by the use of the distal alternative 5′ SS [108]. In several cancer types, the *BCL-X(L)* isoform is upregulated thus increasing resistance to chemotherapeutic agents [109, 110]. Targeting this mechanism and switching the splicing of *BCL-X* gene toward the production of the proapoptotic variant thereby offer the opportunity to revert cancer cells resistance to chemotherapeutic drugs and to promote tumor cell death [111, 112]. Due to its relevance in cancer, *BCL-X* alternative splicing has been extensively investigated in the past years and several RBPs were shown to regulate this specific splicing event [19, 113–119]. Among these, SAM68 exerts a proapoptotic function, leading to production of *BCL-X(s)* variant [19]. In particular, SAM68-mediated splicing regulation of *BCL-X* depends on its specific binding to *BCL-X* pre-mRNA and on its ability to interact with the splicing repressor hnRNP A1, thus antagonizing SRSF1, a positive regulator of *BCL-X(L)* splicing (Figure 3(b), (D)) [19, 110]. However, in PCa cells, high levels of SAM68 do not correlate with high levels of *BCL-X(s)* [38, 46, 110]. This apparently contradictory observation can be explained by the fact that tyrosine phosphorylation of SAM68 by the SRC-related kinase FYN counteracts its splicing activity, promoting the antiapoptotic *BCL-X(L)* isoform [19, 120]. In tumors, SRC activity is often increased [121] and it correlates with SAM68 phosphorylation in different cancer types, including prostate cancer [45, 47, 122]. Recently, an additional layer of complexity to the regulation of SAM68-mediated *BCL-X* splicing in cancer has been revealed. This mechanism involves the direct interaction of the transcriptional factor FBI-1 with SAM68, reducing its binding to *BCL-X* pre-mRNA and therefore promoting the production of the antiapoptotic *BCL-X(L)* variant and cell survival [66]. Fascinatingly, FBI-1 function in *BCL-X* splicing regulation is dependent on the activity of histone deacetylases [66], suggesting an important link between this alternative splicing event and dynamic organization of chromatin structure.

The biological consequences and the possible contribution to tumor progression associated with the aberrant splicing in other relevant SAM68-regulated genes have also been recently described. For example, SAM68 is able to promote the production of the oncoprotein E6 of the human papilloma virus (HPV) type 16 [123], which is a known etiological agent for human cervical cancer [124]. *E6* alternative splicing is controlled by EGF through activation of ERK1/2-kinase that promotes SAM68 phosphorylation, suggesting a possible implication of SAM68 in HPV *E6* splicing during differentiation and the viral life cycle processes of cervical cancer.

More recently, SAM68 has been linked to regulation of alternative splicing of the mammalian target of rapamycin (mTOR) [35], which regulates cell size and cell proliferation in response to nutrients and various growth factors [125, 126]. SAM68-depleted cells display intron 5 retention in the *mTOR* mRNA, which generates a premature termination codon and the consequent reduction of mTOR protein levels (Figure 3(b), (E)) [35]. Notably, mTOR is a critical effector in cell-signaling pathways commonly deregulated in human cancers and overexpression of the components involved in the PI3K/AKT/mTOR pathway has been shown to induce malignant transformation [127]. Interestingly, loss of SAM68 reduces breast and PCa incidence [29, 46], suggesting that in cancer cells SAM68 activation may also regulate the expression of PI3K downstream kinases, such as mTOR.

Collectively, these findings indicate that an evaluation of SAM68-associated splicing signatures in diverse sets of tumors can be of medical relevance.

6. SAM68 and Noncoding RNAs

Recent reports have revealed the involvement of SAM68 in noncoding RNAs (ncRNAs) metabolism. ncRNAs are classified into small (18–200 nt) and long ncRNAs (lncRNAs; 200 nt to >100 kb) [128, 129] and play a role in a wide variety of biological processes, including almost all levels of gene expression regulation, from epigenetic to transcriptional and posttranscriptional control [130]. Coimmunoprecipitation studies documented the interaction between SAM68 and key proteins involved in microRNA (miRNA) biogenesis [131]. miRNA genes are transcribed by either RNA polymerase II or RNA polymerase III into long primary miRNA transcripts (pri-miRNAs) [132]. The cleavage of the pri-miRNAs into stem-loop precursors of ~70 nucleotides (pre-miRNAs) is mediated by DROSHA [133], whereas the cytoplasmic processing of pre-miRNAs into mature miRNAs is mediated by DICER [134]. Coimmunoprecipitation experiments performed in male germ cells indicated that SAM68 interacts with both DICER and DROSHA and that the knockout of *Sam68* leads to changes in expression of specific miRNAs in germ cells [131]. Remarkably, a similar functional interaction with components of the miRNA machinery was shown for Quaking (QKI), another member of the STAR family. In the U343 glioblastoma cell line and in primary rat oligodendrocytes QKI interacts with AGO2, a component of the RISC complex involved in miRNA-dependent translational repression, within stress granules [135]. Collectively, these findings suggest a general role for STAR proteins in the regulation of miRNAs.

Interaction between SAM68 and noncoding RNAs might also affect the splicing activity of this RBP. Recently, a long noncoding RNA (named *INXS*) has been described as a novel mediator of SAM68-dependent regulation of *BCL-X* splicing. *INXS* is transcribed from the antisense genomic strand of *BCL-X* gene and is downregulated in various tumor cell lines and in kidney tumor tissues, whereas its expression is induced by treatments that trigger apoptosis [136]. *INXS* interacts with SAM68 and favors its splicing activity, thus increasing the levels of *BCL-X(s)* isoform and enhancing apoptosis [136]. Notably, in favor of a possible role of *INXS* in anticancer therapy, *INXS* overexpression in a mouse xenograft model was sufficient to induce tumor regression and increase *BCL-X(s)* isoform [136].

Appendix

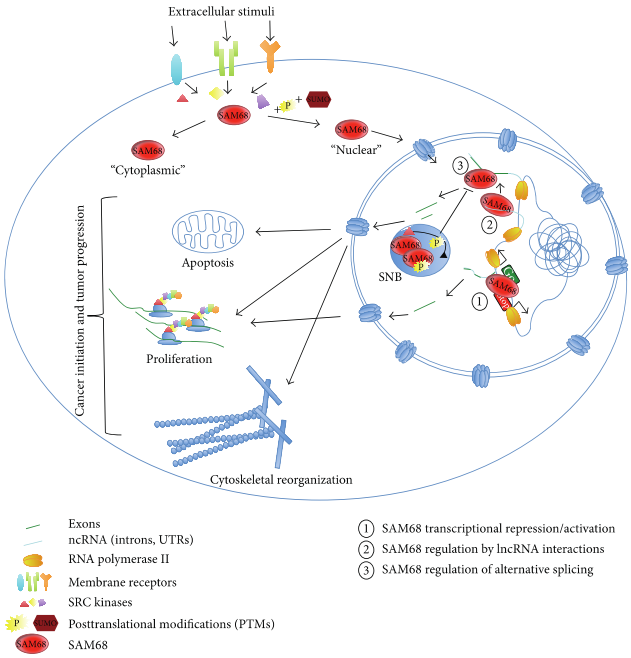

FIGURE 4: Role(s) of SAM68 in transcriptional and posttranscriptional regulation of gene expression in cancer cells. SAM68 and its regulatory networks contribute to important process involved in cancer initiation and progression, such as apoptosis, proliferation, and cytoskeletal reorganization, through different mechanisms. After posttranslational modifications (PTMs) induced by extracellular stimuli and mediated by SRC family kinases, SAM68 is committed to the nucleus where it is able to (1) promote or repress transcription of different targets (see Figure 2 for more details) and (2-3) regulate alternative splicing events through several molecular mechanisms, some of them mediated by lncRNAs (see Figure 3 for more details). In the nucleus, SAM68 can localize in specific bodies (SNB) and associate with other proteins (i.e., BRK kinase) that modify its phosphorylation status, thus affecting its RNA binding activity.

Thus, the complex regulatory network of proteins and ncRNAs orchestrated by SAM68 greatly contributes to the cellular signature in higher eukaryotes and plays a pivotal role in the regulation of gene expression in normal conditions and in oncogenic transformation.

7. Concluding Remarks

Misregulation of cancer-associated alternative splicing events is often correlated with unbalanced expression of splicing factors. SAM68 is a clear example of this concept, as it is upregulated in different types of tumors and it directly affects cancer initiation and progression. Transcriptional and posttranscriptional regulation of gene expression mastered by SAM68 chiefly contributes to changes in gene expression occurring in cancer cells. Moreover, SAM68 orchestrates transcript fate and function (Figure 4). Thus, depicting SAM68 signatures in normal and cancer cells would greatly help in understanding how SAM68 and its regulatory networks contribute to key features of tumor initiation and progression. Although the functional significance of SAM68-regulated alternative splicing events in human cancer has been clearly established, future studies unraveling the positional effect of SAM68 binding to pre-mRNAs would be instrumental for the development of new therapeutic approaches to target SAM68 activities in cancer.

Appendix

Conflict of Interests

The authors declare that there is no conflict of interests regarding the publication of this paper.

Acknowledgments

This work was supported by grants from the Associazione Italiana per la Ricerca sul Cancro (AIRC) (Project 11658 to Maria Paola Paronetto and Project 11913 to Claudia Ghigna), the Association for International Cancer Research (AICR), UK, (Project 14-0333 to Maria Paola Paronetto and Project 11-0622 to Claudia Ghigna), the University of Rome "Foro Italico" (RIC052013) to Maria Paola Paronetto, and Fondazione Banca del Monte di Lombardia to Claudia Ghigna.

References

[1] S. Fumagalli, N. F. Totty, J. J. Hsuan, and S. A. Courtneidge, "A target for Src in mitosis," *Nature*, vol. 368, no. 6474, pp. 871–874, 1994.

[2] S. J. Taylor and D. Shalloway, "An RNA-binding protein associated with Src through its SH2 and SH3 domains in mitosis," *Nature*, vol. 368, no. 6474, pp. 867–871, 1994.

[3] C. Vernet and K. Artzt, "STAR, a gene family involved in signal transduction and activation of RNA," *Trends in Genetics*, vol. 13, no. 12, pp. 479–484, 1997.

[4] K. E. Lukong and S. Richard, "Sam68, the KH domain-containing superSTAR," *Biochimica et Biophysica Acta: Reviews on Cancer*, vol. 1653, no. 2, pp. 73–86, 2003.

[5] M. Cruz-Alvarez and A. Pellicer, "Cloning of a full-length complementary DNA for an *Artemia salina* glycine-rich protein. Structural relationship with RNA binding proteins," *Journal of Biological Chemistry*, vol. 262, no. 28, pp. 13377–13380, 1987.

[6] A. R. Jones and T. Schedl, "Mutations in GLD-1, a female germ cell-specific tumor suppressor gene in *Caenorhabditis elegans*, affect a conserved domain also found in Src- associated protein Sam68," *Genes and Development*, vol. 9, no. 12, pp. 1491–1504, 1995.

[7] T. A. Ebersole, Q. Chen, M. J. Justice, and K. Artzt, "The *quaking* gene product necessary in embryogenesis and myelination combines features of RNA binding and signal transduction proteins," *Nature Genetics*, vol. 12, no. 3, pp. 260–265, 1996.

[8] P. Lock, S. Fumagalli, P. Polakis, F. McCormick, and S. A. Courtneidge, "The human p62 cDNA encodes Sam68 and not the RasGAP-associated p62 protein," *Cell*, vol. 84, no. 1, pp. 23–24, 1996.

[9] S. Richard, D. Yu, K. J. Blumer et al., "Association of p62, a multifunctional SH2- and SH3-domain-binding protein, with src family tyrosine kinases, Grb2, and phospholipase Cγ-1," *Molecular and Cellular Biology*, vol. 15, no. 1, pp. 186–197, 1995.

[10] M. di Fruscio, T. Chen, and S. Richard, "Characterization of Sam68-like mammalian proteins SLM-1 and SLM-2: SLM- 1 is a Src substrate during mitosis," *Proceedings of the National Academy of Sciences of the United States of America*, vol. 96, no. 6, pp. 2710–2715, 1999.

[11] J. P. Venables, C. Vernet, S. L. Chew et al., "T-STAR/ÉTOILE: a novel relative of SAM68 that interacts with an RNA-binding protein implicated in spermatogenesis," *Human Molecular Genetics*, vol. 8, no. 6, pp. 959–969, 1999.

[12] C. Fyrberg, J. Becker, P. Barthmaier, J. Mahaffey, and E. Fyrberg, "A *Drosophila* muscle-specific gene related to the mouse quaking locus," *Gene*, vol. 197, no. 1-2, pp. 315–323, 1997.

[13] M. Di Fruscio, T. Chen, S. Bonyadi, P. Lasko, and S. Richard, "The identification of two Drosophila K homology domain proteins: KEP1 and SAM are members of the Sam68 family of GSG domain proteins," *Journal of Biological Chemistry*, vol. 273, no. 46, pp. 30122–30130, 1998.

[14] S. Arning, P. Grüter, G. Bilbe, and A. Krämer, "Mammalian splicing factor SF1 is encoded by variant cDNAs and binds to RNA," *RNA*, vol. 2, no. 8, pp. 794–810, 1996.

[15] C. Sette, "Post-translational regulation of star proteins and effects on their biological functions," *Advances in Experimental Medicine and Biology*, vol. 693, pp. 54–66, 2010.

[16] S. J. Taylor, M. Anafi, T. Pawson, and D. Shalloway, "Functional interaction between c-Src and its mitotic target, Sam 68," *The Journal of Biological Chemistry*, vol. 270, no. 17, pp. 10120–10124, 1995.

[17] T. Chen, B. B. Damaj, C. Herrera, P. Lasko, and S. Richard, "Self-association of the single-KH-domain family members Sam68, GRP33, GLD-1, and Qk1: role of the KH domain," *Molecular and Cellular Biology*, vol. 17, no. 10, pp. 5707–5718, 1997.

[18] M. P. Paronetto, J. P. Venables, D. J. Elliott, R. Geremia, P. Rossi, and C. Sette, "tr-kit promotes the formation of a multimolecular complex composed by Fyn, PLCgamma1 and Sam68," *Oncogene*, vol. 22, no. 54, pp. 8707–8715, 2003.

[19] M. P. Paronetto, T. Achsel, A. Massiello, C. E. Chalfant, and C. Sette, "The RNA-binding protein Sam68 modulates the alternative splicing of Bcl-x," *Journal of Cell Biology*, vol. 176, no. 7, pp. 929–939, 2007.

[20] J. Côté, F.-M. Boisvert, M.-C. Boulanger, M. T. Bedford, and S. Richard, "Sam68 RNA binding protein is an in vivo substrate for protein arginine N-methyltransferase 1," *Molecular Biology of the Cell*, vol. 14, no. 1, pp. 274–287, 2003.

[21] M. T. Bedford, A. Frankel, M. B. Yaffe, S. Clarke, P. Leder, and S. Richard, "Arginine methylation inhibits the binding of proline-rich ligands to Src homology 3, but not WW, domains," *The Journal of Biological Chemistry*, vol. 275, no. 21, pp. 16030–16036, 2000.

[22] I. Babic, A. Jakymiw, and D. J. Fujita, "The RNA binding protein Sam68 is acetylated in tumor cell lines, and its acetylation correlates with enhanced RNA binding activity," *Oncogene*, vol. 23, no. 21, pp. 3781–3789, 2004.

[23] I. Babic, E. Cherry, and D. J. Fujita, "SUMO modification of Sam68 enhances its ability to repress cyclin D1 expression and inhibits its ability to induce apoptosis," *Oncogene*, vol. 25, no. 36, pp. 4955–4964, 2006.

[24] R. Francis, E. Maine, and T. Schedl, "Analysis of the multiple roles of gld-1 in germline development: interactions with the sex determination cascade and the glp-1 signaling pathway," *Genetics*, vol. 139, no. 2, pp. 607–630, 1995.

[25] K. Liu, L. Li, P. E. Nisson, C. Gruber, J. Jessee, and S. N. Cohen, "Neoplastic transformation and tumorigenesis associated with Sam68 protein deficiency in cultured murine fibroblasts," *Journal of Biological Chemistry*, vol. 275, no. 51, pp. 40195–40201, 2000.

[26] Q.-H. Li, I. Haga, T. Shimizu, M. Itoh, T. Kurosaki, and J.-I. Fujisawa, "Retardation of the G2–M phase progression on gene disruption of RNA binding protein Sam68 in the DT-40 cell line," *FEBS Letters*, vol. 525, no. 1–3, pp. 145–150, 2002.

[27] I. Barlat, F. Maurier, M. Duchesne, E. Guitard, B. Tocque, and F. Schweighoffer, "A role for Sam68 in cell cycle progression

Appendix

antagonized by a spliced variant within the KH domain," *The Journal of Biological Chemistry*, vol. 272, no. 6, pp. 3129–3132, 1997.

[28] S. Richard, N. Torabi, G. V. Franco et al., "Ablation of the Sam68 RNA binding protein protects mice from age-related bone loss," *PLoS Genetics*, vol. 1, no. 6, article e74, 2005.

[29] S. Richard, G. Vogel, M.-É. Huot, T. Guo, W. J. Muller, and K. E. Lukong, "Sam68 haploinsufficiency delays onset of mammary tumorigenesis and metastasis," *Oncogene*, vol. 27, no. 4, pp. 548–556, 2008.

[30] E. Bianchi, F. Barbagallo, C. Valeri et al., "Ablation of the Sam68 gene impairs female fertility and gonadotropin-dependent follicle development," *Human Molecular Genetics*, vol. 19, no. 24, Article ID ddq422, pp. 4886–4894, 2010.

[31] M. P. Paronetto, V. Messina, M. Barchi, R. Geremia, S. Richard, and C. Sette, "Sam68 marks the transcriptionally active stages of spermatogenesis and modulates alternative splicing in male germ cells," *Nucleic Acids Research*, vol. 39, no. 12, pp. 4961–4974, 2011.

[32] M. P. Paronetto, V. Messina, E. Bianchi et al., "Sam68 regulates translation of target mRNAs in male germ cells, necessary for mouse spermatogenesis," *Journal of Cell Biology*, vol. 185, no. 2, pp. 235–249, 2009.

[33] M. P. Paronetto, F. Zalfa, F. Botti, R. Geremia, C. Bagni, and C. Sette, "The nuclear RNA-binding protein Sam68 translocates to the cytoplasm and associates with the polysemes in mouse spermatocytes," *Molecular Biology of the Cell*, vol. 17, no. 1, pp. 14–24, 2006.

[34] T. Iijima, K. Wu, H. Witte et al., "SAM68 regulates neuronal activity-dependent alternative splicing of neurexin-1," *Cell*, vol. 147, no. 7, pp. 1601–1614, 2011.

[35] M.-É. Huot, G. Vogel, A. Zabarauskas et al., "The Sam68 STAR RNA-binding protein regulates mTOR alternative splicing during adipogenesis," *Molecular Cell*, vol. 46, no. 2, pp. 187–199, 2012.

[36] K. E. Lukong and S. Richard, "Targeting the RNA-binding protein Sam68 as a treatment for cancer?" *Future Oncology*, vol. 3, no. 5, pp. 539–544, 2007.

[37] W. Hong, R. J. Resnick, C. Rakowski, D. Shalloway, S. J. Taylor, and G. A. Blobel, "Physical and functional interaction between the transcriptional cofactor CBP and the KH domain protein Sam68," *Molecular Cancer Research*, vol. 1, no. 1, pp. 48–55, 2002.

[38] P. Rajan, L. Gaughan, C. Dalgliesh et al., "The RNA-binding and adaptor protein Sam68 modulates signal-dependent splicing and transcriptional activity of the androgen receptor," *Journal of Pathology*, vol. 215, no. 1, pp. 67–77, 2008.

[39] L. Song, L. Wang, Y. Li et al., "Sam68 up-regulation correlates with, and its down-regulation inhibits, proliferation and tumourigenicity of breast cancer cells," *Journal of Pathology*, vol. 222, no. 3, pp. 227–237, 2010.

[40] K. Fu, X. Sun, W. Zheng et al., "Sam68 modulates the promoter specificity of NF-κB and mediates expression of CD25 in activated T cells," *Nature Communications*, vol. 4, article 1909, 2013.

[41] S. Najib, C. Martín-Romero, C. González-Yanes, and V. Sánchez-Margalet, "Role of Sam68 as an adaptor protein in signal transduction," *Cellular and Molecular Life Sciences*, vol. 62, no. 1, pp. 36–43, 2005.

[42] J. J. Derry, S. Richard, H. V. Carvajal et al., "Sik (BRK) phosphorylates sam68 in the nucleus and negatively regulates its RNA binding ability," *Molecular and Cellular Biology*, vol. 20, no. 16, pp. 6114–6126, 2000.

[43] A. H. Andreotti, S. C. Bunnell, S. Feng, L. J. Berg, and S. L. Schreiber, "Regulatory intramolecular association in a tyrosine kinase of the tec family," *Nature*, vol. 385, no. 6611, pp. 93–97, 1997.

[44] C. Sette, M. P. Paronetto, M. Barchi, A. Bevilacqua, R. Geremia, and P. Rossi, "Tr-kit-induced resumption of the cell cycle in mouse eggs requires activation of a Src-like kinase," *The EMBO Journal*, vol. 21, no. 20, pp. 5386–5395, 2002.

[45] M. P. Paronetto, D. Farini, I. Sammarco et al., "Expression of a truncated form of the c-Kit tyrosine kinase receptor and activation of Src kinase in human prostatic cancer," *The American Journal of Pathology*, vol. 164, no. 4, pp. 1243–1251, 2004.

[46] R. Busà, M. P. Paronetto, D. Farini et al., "The RNA-binding protein Sam68 contributes to proliferation and survival of human prostate cancer cells," *Oncogene*, vol. 26, no. 30, pp. 4372–4382, 2007.

[47] K. E. Lukong, D. Larocque, A. L. Tyner, and S. Richard, "Tyrosine phosphorylation of Sam68 by breast tumor kinase regulates intranuclear localization and cell cycle progression," *The Journal of Biological Chemistry*, vol. 280, no. 46, pp. 38639–38647, 2005.

[48] J. H. Ostrander, A. R. Daniel, and C. A. Lange, "Brk/PTK6 signaling in normal and cancer cell models," *Current Opinion in Pharmacology*, vol. 10, no. 6, pp. 662–669, 2010.

[49] K. T. Barker, L. E. Jackson, and M. R. Crompton, "BRK tyrosine kinase expression in a high proportion of human breast carcinomas," *Oncogene*, vol. 15, no. 7, pp. 799–805, 1997.

[50] J. J. Derry, G. S. Prins, V. Ray, and A. L. Tyner, "Altered localization and activity of the intracellular tyrosine kinase BRK/Sik in prostate tumor cells," *Oncogene*, vol. 22, no. 27, pp. 4212–4220, 2003.

[51] M.-É. Huot, G. Vogel, and S. Richard, "Identification of a Sam68 ribonucleoprotein complex regulated by epidermal growth factor," *The Journal of Biological Chemistry*, vol. 284, no. 46, pp. 31903–31913, 2009.

[52] P. Rajan, C. Dalgliesh, C. F. Bourgeois et al., "Proteomic identification of heterogeneous nuclear ribonucleoprotein L as a novel component of SLM/Sam68 nuclear bodies," *BMC Cell Biology*, vol. 10, article 82, 2009.

[53] M.-É. Huot, C. M. Brown, N. Lamarche-Vane, and S. Richard, "An adaptor role for cytoplasmic Sam68 in modulating src activity during cell polarization," *Molecular and Cellular Biology*, vol. 29, no. 7, pp. 1933–1943, 2009.

[54] R. I. Nicholson, J. M. W. Gee, and M. E. Harper, "EGFR and cancer prognosis," *European Journal of Cancer*, vol. 37, no. 4, pp. S9–S15, 2001.

[55] W. T. Liao, J. L. Liu, Z. G. Wang et al., "High expression level and nuclear localization of Sam68 are associated with progression and poor prognosis in colorectal cancer," *BMC Gastroenterology*, vol. 13, article 126, 2013.

[56] Z. Zhang, Y. Xu, N. Sun, M. Zhang, J. Xie, and Z. Jiang, "High Sam68 expression predicts poor prognosis in non-small cell lung cancer," *Clinical and Translational Oncology*, vol. 16, no. 10, pp. 886–891, 2014.

[57] Z. Zhang, J. Li, H. Zheng et al., "Expression and cytoplasmic localization of SAM68 is a significant and independent prognostic marker for renal cell carcinoma," *Cancer Epidemiology Biomarkers and Prevention*, vol. 18, no. 10, pp. 2685–2693, 2009.

[58] Z. Li, C.-P. Yu, Y. Zhong et al., "Sam68 expression and cytoplasmic localization is correlated with lymph node metastasis

Appendix

as well as prognosis in patients with early-stage cervical cancer," *Annals of Oncology*, vol. 23, no. 3, pp. 638–646, 2012.

[59] J.-P. Yang, T. R. Reddy, K. T. Truong, M. Suhasini, and F. Wong-Staal, "Functional interaction of Sam68 and heterogeneous nuclear ribonucleoprotein K," *Oncogene*, vol. 21, no. 47, pp. 7187–7194, 2002.

[60] S. J. Taylor, R. J. Resnick, and D. Shalloway, "Sam68 exerts separable effects on cell cycle progression and apoptosis," *BMC Cell Biology*, vol. 5, article 5, 2004.

[61] N. Cheung, L. C. Chan, A. Thompson, M. L. Cleary, and C. W. E. So, "Protein arginine-methyltransferase-dependent oncogenesis," *Nature Cell Biology*, vol. 9, no. 10, pp. 1208–1215, 2007.

[62] D. J. Kuhn and Q. P. Dou, "The role of interleukin-2 receptor alpha in cancer," *Frontiers in Bioscience*, vol. 10, pp. 1462–1474, 2005.

[63] S. Pandit, D. Wang, and X.-D. Fu, "Functional integration of transcriptional and RNA processing machineries," *Current Opinion in Cell Biology*, vol. 20, no. 3, pp. 260–265, 2008.

[64] H. P. Phatnani and A. L. Greenleaf, "Phosphorylation and functions of the RNA polymerase II CTD," *Genes and Development*, vol. 20, no. 21, pp. 2922–2936, 2006.

[65] E. Batsché, M. Yaniv, and C. Muchardt, "The human SWI/SNF subunit Brm is a regulator of alternative splicing," *Nature Structural & Molecular Biology*, vol. 13, no. 1, pp. 22–29, 2006.

[66] P. Bielli, R. Busà, S. M. Di Stasi et al., "The transcription factor FBI-1 inhibits SAM68-mediated BCL-X alternative splicing and apoptosis," *EMBO Reports*, vol. 15, no. 4, pp. 419–427, 2014.

[67] M. Cappellari, P. Bielli, M. P. Paronetto et al., "The transcriptional co-activator SND1 is a novel regulator of alternative splicing in prostate cancer cells," *Oncogene*, vol. 33, no. 29, pp. 3794–3802, 2014.

[68] M. Zöller, "CD44: can a cancer-initiating cell profit from an abundantly expressed molecule?" *Nature Reviews Cancer*, vol. 11, no. 4, pp. 254–267, 2011.

[69] Q. Lin, S. J. Taylor, and D. Shalloway, "Specificity and determinants of Sam68 RNA binding. Implications for the biological function of K homology domains," *The Journal of Biological Chemistry*, vol. 272, no. 43, pp. 27274–27280, 1997.

[70] M. Itoh, I. Haga, Q.-H. Li, and J.-I. Fujisawa, "Identification of cellular mRNA targets for RNA-binding protein Sam68," *Nucleic Acids Research*, vol. 30, no. 24, pp. 5452–5464, 2002.

[71] N. Matter, P. Herrlich, and H. König, "Signal-dependent regulation of splicing via phosphorylation of Sam68," *Nature*, vol. 420, no. 6916, pp. 691–695, 2002.

[72] L. L. Wang, S. Richard, and A. S. Shaw, "P62 association with RNA is regulated by tyrosine phosphorylation," *Journal of Biological Chemistry*, vol. 270, no. 5, pp. 2010–2013, 1995.

[73] N. H. Meyer, K. Tripsianes, M. Vincendeau et al., "Structural basis for homodimerization of the Src-associated during mitosis, 68-kDa protein (Sam68) Qua1 domain," *The Journal of Biological Chemistry*, vol. 285, no. 37, pp. 28893–28901, 2010.

[74] M. P. Paronetto, M. Cappellari, R. Busà et al., "Alternative splicing of the cyclin D1 proto-oncogene is regulated by the RNA-binding protein Sam68," *Cancer Research*, vol. 70, no. 1, pp. 229–239, 2010.

[75] C. Valacca, S. Bonomi, E. Buratti et al., "Sam68 regulates EMT through alternative splicing-activated nonsense-mediated mRNA decay of the SF2/ASF proto-oncogene," *Journal of Cell Biology*, vol. 191, no. 1, pp. 87–99, 2010.

[76] D. Hanahan and R. A. Weinberg, "Hallmarks of cancer: the next generation," *Cell*, vol. 144, no. 5, pp. 646–674, 2011.

[77] D. Naor, S. Nedvetzki, I. Golan, L. Melnik, and Y. Faitelson, "CD44 in cancer," *Critical Reviews in Clinical Laboratory Sciences*, vol. 39, no. 6, pp. 527–579, 2002.

[78] P. Y. Godge and L. S. Poonja, "Quantitative assessment of expression of cell adhesion molecule (CD44) splice variants: CD44 standard (CD44s) and v5, v6 isoforms in oral leukoplakias: an immunohistochemical study," *Indian Journal of Dental Research*, vol. 22, no. 3, pp. 493–494, 2011.

[79] J. Zeilstra, S. P. J. Joosten, H. van Andel et al., "Stem cell CD44v isoforms promote intestinal cancer formation in Apc(min) mice downstream of Wnt signaling," *Oncogene*, vol. 33, no. 5, pp. 665–670, 2014.

[80] W. Müller, A. Schneiders, K.-H. Heider, S. Meier, G. Hommel, and H. E. Gabbert, "Expression and prognostic value of the CD44 splicing variants v5 and v6 in gastric cancer," *The Journal of Pathology*, vol. 183, no. 2, pp. 222–227, 1997.

[81] Y. Chen, Z. Fu, S. Xu, Y. Xu, and P. Xu, "The prognostic value of CD44 expression in gastric cancer: a meta-analysis," *Biomedicine & Pharmacotherapy*, vol. 68, no. 6, pp. 693–697, 2014.

[82] S.-T. Wu, G.-H. Sun, D.-S. Hsieh et al., "Correlation of CD44v5 expression with invasiveness and prognosis in renal cell carcinoma," *Journal of the Formosan Medical Association*, vol. 102, no. 4, pp. 229–233, 2003.

[83] N. Matter, M. Marx, S. Weg-Remers, H. Ponta, P. Herrlich, and H. König, "Heterogeneous ribonucleoprotein A1 is part of an exon-specific splice-silencing complex controlled by oncogenic signaling pathways," *Journal of Biological Chemistry*, vol. 275, no. 45, pp. 35353–35360, 2000.

[84] A. G. Matera and Z. Wang, "A day in the life of the spliceosome," *Nature Reviews Molecular Cell Biology*, vol. 15, no. 2, pp. 108–121, 2014.

[85] A. Tisserant and H. König, "Signal-regulated pre-mRNA occupancy by the general splicing factor U2AF," *PLoS ONE*, vol. 3, no. 1, Article ID e1418, 2008.

[86] C. Cheng and P. A. Sharp, "Regulation of CD44 alternative splicing by SRm160 and its potential role in tumor cell invasion," *Molecular and Cellular Biology*, vol. 26, no. 1, pp. 362–370, 2006.

[87] C. J. David and J. L. Manley, "Alternative pre-mRNA splicing regulation in cancer: pathways and programs unhinged," *Genes and Development*, vol. 24, no. 21, pp. 2343–2364, 2010.

[88] A. Montecucco and G. Biamonti, "Cellular response to etoposide treatment," *Cancer Letters*, vol. 252, no. 1, pp. 9–18, 2007.

[89] G. Biamonti and J. F. Caceres, "Cellular stress and RNA splicing," *Trends in Biochemical Sciences*, vol. 34, no. 3, pp. 146–153, 2009.

[90] M. J. Muñoz, M. S. P. Santangelo, M. P. Paronetto et al., "DNA damage regulates alternative splicing through inhibition of RNA polymerase II elongation," *Cell*, vol. 137, no. 4, pp. 708–720, 2009.

[91] M. Dutertre, G. Sanchez, M.-C. de Cian et al., "Cotranscriptional exon skipping in the genotoxic stress response," *Nature Structural and Molecular Biology*, vol. 17, no. 11, pp. 1358–1366, 2010.

[92] M. P. Paronetto, B. Miñana, and J. Valcárcel, "The Ewing sarcoma protein regulates DNA damage-induced alternative splicing," *Molecular Cell*, vol. 43, no. 3, pp. 353–368, 2011.

[93] R. Busà and C. Sette, "An emerging role for nuclear RNA-mediated responses to genotoxic stress," *RNA Biology*, vol. 7, no. 4, pp. 390–396, 2010.

Appendix

[94] S. Solier, A. Lansiaux, E. Logette et al., "Topoisomerase I and II inhibitors control caspase-2 pre-messenger RNA splicing in human cells," *Molecular Cancer Research*, vol. 2, no. 1, pp. 53–61, 2004.

[95] D. S. Chandler, R. K. Singh, L. C. Caldwell, J. L. Bitler, and G. Lozano, "Genotoxic stress induces coordinately regulated alternative splicing of the p53 modulators MDM2 and MDM4," *Cancer Research*, vol. 66, no. 19, pp. 9502–9508, 2006.

[96] Y. Wang, J. L. Dean, E. K. A. Millar et al., "Cyclin D1b is aberrantly regulated in response to therapeutic challenge and promotes resistance to estrogen antagonists," *Cancer Research*, vol. 68, no. 14, pp. 5628–5638, 2008.

[97] K. E. Knudsen, J. A. Diehl, C. A. Haiman, and E. S. Knudsen, "Cyclin D1: polymorphism, aberrant splicing and cancer risk," *Oncogene*, vol. 25, no. 11, pp. 1620–1628, 2006.

[98] E. A. Musgrove, C. E. Caldon, J. Barraclough, A. Stone, and R. L. Sutherland, "Cyclin D as a therapeutic target in cancer," *Nature Reviews Cancer*, vol. 11, no. 8, pp. 558–572, 2011.

[99] K. Miura, W. Fujibuchi, and M. Unno, "Splice isoforms as therapeutic targets for colorectal cancer," *Carcinogenesis*, vol. 33, no. 12, pp. 2311–2319, 2012.

[100] D. C. Betticher, N. Thatcher, H. J. Altermatt, P. Hoban, W. D. J. Ryder, and J. Heighway, "Alternate splicing produces a novel cyclin D1 transcript," *Oncogene*, vol. 11, no. 5, pp. 1005–1011, 1995.

[101] Z. Li, X. Jiao, C. Wang et al., "Alternative cyclin D1 splice forms differentially regulate the DNA damage response," *Cancer Research*, vol. 70, no. 21, pp. 8802–8811, 2010.

[102] G. Biamonti, S. Bonomi, S. Gallo, and C. Ghigna, "Making alternative splicing decisions during epithelial-to-mesenchymal transition (EMT)," *Cellular and Molecular Life Sciences*, vol. 69, no. 15, pp. 2515–2526, 2012.

[103] J. P. Thiery, H. Acloque, R. Y. J. Huang, and M. A. Nieto, "Epithelial-mesenchymal transitions in development and disease," *Cell*, vol. 139, no. 5, pp. 871–890, 2009.

[104] K. Polyak and R. A. Weinberg, "Transitions between epithelial and mesenchymal states: acquisition of malignant and stem cell traits," *Nature Reviews Cancer*, vol. 9, no. 4, pp. 265–273, 2009.

[105] L. E. Maquat, W. Y. Tarn, and O. Isken, "The pioneer round of translation: features and functions," *Cell*, vol. 142, no. 3, pp. 368–374, 2010.

[106] R. Karni, E. De Stanchina, S. W. Lowe, R. Sinha, D. Mu, and A. R. Krainer, "The gene encoding the splicing factor SF2/ASF is a proto-oncogene," *Nature Structural and Molecular Biology*, vol. 14, no. 3, pp. 185–193, 2007.

[107] C. Ghigna, S. Giordano, H. Shen et al., "Cell motility is controlled by SF2/ASF through alternative splicing of the Ron protooncogene," *Molecular Cell*, vol. 20, no. 6, pp. 881–890, 2005.

[108] L. H. Boise, M. González-García, C. E. Postema et al., "bcl-x, a bcl-2-related gene that functions as a dominant regulator of apoptotic cell death," *Cell*, vol. 74, no. 4, pp. 597–608, 1993.

[109] D. R. Mercatante, C. D. Bortner, J. A. Cidlowski, and R. Kole, "Modification of alternative splicing of Bcl-x Pre-mRNA in prostate and breast cancer cells. Analysis of apoptosis and cell death," *Journal of Biological Chemistry*, vol. 276, no. 19, pp. 16411–16417, 2001.

[110] D. R. Mercatante, J. L. Mohler, and R. Kole, "Cellular response to an antisense-mediated shift of Bcl-x pre-mRNA splicing and antineoplastic agents," *Journal of Biological Chemistry*, vol. 277, no. 51, pp. 49374–49382, 2002.

[111] J. A. Bauman, S.-D. Li, A. Yang, L. Huang, and R. Kole, "Anti-tumor activity of splice-switching oligonucleotides," *Nucleic Acids Research*, vol. 38, no. 22, pp. 8348–8356, 2010.

[112] S. Bonomi, S. Gallo, M. Catillo, D. Pignataro, G. Biamonti, and C. Ghigna, "Oncogenic alternative splicing switches: role in cancer progression and prospects for therapy," *International Journal of Cell Biology*, vol. 2013, Article ID 962038, 17 pages, 2013.

[113] D. Garneau, T. Revil, J.-F. Fisette, and B. Chabot, "Heterogeneous nuclear ribonucleoprotein F/H proteins modulate the alternative splicing of the apoptotic mediator Bcl-x," *Journal of Biological Chemistry*, vol. 280, no. 24, pp. 22641–22650, 2005.

[114] A. Massiello, J. R. Roesser, and C. E. Chalfant, "SAP155 Binds to ceramide-responsive RNA cis-element 1 and regulates the alternative 5′ splice site selection of Bcl-x pre-mRNA," *The FASEB Journal*, vol. 20, no. 10, pp. 1680–1682, 2006.

[115] P. Cloutier, J. Toutant, L. Shkreta, S. Goekjian, T. Revil, and B. Chabot, "Antagonistic effects of the SRp30c protein and cryptic 5′ splice sites on the alternative splicing of the apoptotic regulator Bcl-x," *The Journal of Biological Chemistry*, vol. 283, no. 31, pp. 21315–21324, 2008.

[116] A. Zhou, A. C. Ou, A. Cho, E. J. Benz Jr., and S.-C. Huang, "Novel splicing factor RBM25 modulates Bcl-x Pre-mRNA 5′ splice site selection," *Molecular and Cellular Biology*, vol. 28, no. 19, pp. 5924–5936, 2008.

[117] T. Revil, J. Pelletier, J. Toutant, A. Cloutier, and B. Chabot, "Heterogeneous nuclear ribonucleoprotein K represses the production of pro-apoptotic Bcl-xS splice isoform," *Journal of Biological Chemistry*, vol. 284, no. 32, pp. 21458–21467, 2009.

[118] M. J. Moore, Q. Wang, C. J. Kennedy, and P. A. Silver, "An alternative splicing network links cell-cycle control to apoptosis," *Cell*, vol. 142, no. 4, pp. 625–636, 2010.

[119] P. Bielli, M. Bordi, V. di Biasio, and C. Sette, "Regulation of BCL-X splicing reveals a role for the polypyrimidine tract binding protein (PTBP1/hnRNP I) in alternative 5′ splice site selection," *Nucleic Acids Research*, vol. 42, no. 19, pp. 12070–12081, 2014.

[120] C. Brignatz, M. P. Paronetto, S. Opi et al., "Alternative splicing modulates autoinhibition and SH3 accessibility in the Src kinase Fyn," *Molecular and Cellular Biology*, vol. 29, no. 24, pp. 6438–6448, 2009.

[121] R. B. Irby and T. J. Yeatman, "Role of Src expression and activation in human cancer," *Oncogene*, vol. 19, no. 49, pp. 5636–5642, 2000.

[122] Z.-Y. Cheny, L. Cai, J. Zhu et al., "Fyn requires hnRNPA2B1 and Sam68 to synergistically regulate apoptosis in pancreatic cancer," *Carcinogenesis*, vol. 32, no. 10, pp. 1419–1426, 2011.

[123] S. Rosenberger, J. De.-Castro Arce, L. Langbein, R. D. M. Steenbergenc, and F. Rösla, "Alternative splicing of human papillomavirus type-16 E6/E6* early mRNA is coupled to EGF signaling via Erk1/2 activation," *Proceedings of the National Academy of Sciences of the United States of America*, vol. 107, no. 15, pp. 7006–7011, 2010.

[124] H. zur Hausen, "Papillomaviruses and cancer: from basic studies to clinical application," *Nature Reviews Cancer*, vol. 2, no. 5, pp. 342–350, 2002.

[125] S. Sengupta, T. R. Peterson, and D. M. Sabatini, "Regulation of the mTOR complex 1 pathway by nutrients, growth factors, and stress," *Molecular Cell*, vol. 40, no. 2, pp. 310–322, 2010.

[126] S. Wullschleger, R. Loewith, and M. N. Hall, "TOR signaling in growth and metabolism," *Cell*, vol. 124, no. 3, pp. 471–484, 2006.

[127] J. Paez and W. R. Sellers, "PI3K/PTEN/AKT pathway. A critical mediator of oncogenic signaling," *Cancer Treatment and Research*, vol. 115, pp. 145–167, 2003.

Appendix

[128] K. V. Prasanth and D. L. Spector, "Eukaryotic regulatory RNAs: an answer to the 'genome complexity' conundrum," *Genes and Development*, vol. 21, no. 1, pp. 11–42, 2007.

[129] I. Ulitsky and D. P. Bartel, "LincRNAs: genomics, evolution, and mechanisms," *Cell*, vol. 154, no. 1, pp. 26–46, 2013.

[130] T. R. Cech and J. A. Steitz, "The noncoding RNA revolution—trashing old rules to forge new ones," *Cell*, vol. 157, no. 1, pp. 77–94, 2014.

[131] V. Messina, O. Meikar, M. P. Paronetto et al., "The RNA binding protein SAM68 transiently localizes in the chromatoid body of male germ cells and influences expression of select microRNAs," *PLoS ONE*, vol. 7, no. 6, Article ID e39729, 2012.

[132] J. Winter, S. Jung, S. Keller, R. I. Gregory, and S. Diederichs, "Many roads to maturity: microRNA biogenesis pathways and their regulation," *Nature Cell Biology*, vol. 11, no. 3, pp. 228–234, 2009.

[133] Y. Lee, C. Ahn, J. Han et al., "The nuclear RNase III Drosha initiates microRNA processing," *Nature*, vol. 425, no. 6956, pp. 415–419, 2003.

[134] E. Bernstein, A. A. Caudy, S. M. Hammond, and G. J. Hannon, "Role for a bidentate ribonuclease in the initiation step of RNA interference," *Nature*, vol. 409, no. 6818, pp. 363–366, 2001.

[135] Y. Wang, G. Lacroix, J. Haines, E. Doukhanine, G. Almazan, and S. Richard, "The QKI-6 RNA binding protein localizes with the MBP mRNAs in stress granules of glial cells," *PLoS ONE*, vol. 5, no. 9, Article ID e12824, 2010.

[136] C. DeOcesano-Pereira, M. S. Amaral, K. S. Parreira et al., "Long non-coding RNA *INXS* is a critical mediator of *BCL-XS* induced apoptosis," *Nucleic Acids Research*, vol. 42, no. 13, pp. 8343–8355, 2014.

Appendix

nature COMMUNICATIONS

ARTICLE

Received 29 Jun 2015 | Accepted 27 Aug 2015 | Published 8 Oct 2015

DOI: 10.1038/ncomms9479 OPEN

The alternative splicing factor Nova2 regulates vascular development and lumen formation

Costanza Giampietro[1,2,*], Gianluca Deflorian[1,*], Stefania Gallo[3,4,*], Anna Di Matteo[3,5], Davide Pradella[3,5], Serena Bonomi[3], Elisa Belloni[3], Daniel Nyqvist[6], Valeria Quaranta[3], Stefano Confalonieri[1,7], Giovanni Bertalot[7], Fabrizio Orsenigo[1], Federica Pisati[1], Elisabetta Ferrero[8], Giuseppe Biamonti[3], Evelien Fredrickx[9], Carla Taveggia[9], Chris D.R. Wyatt[10,11], Manuel Irimia[10,11], Pier Paolo Di Fiore[1,7,12], Benjamin J. Blencowe[13], Elisabetta Dejana[1,2,14,**] & Claudia Ghigna[3,**]

Vascular lumen formation is a fundamental step during angiogenesis; yet, the molecular mechanisms underlying this process are poorly understood. Recent studies have shown that neural and vascular systems share common anatomical, functional and molecular similarities. Here we show that the organization of endothelial lumen is controlled at the post-transcriptional level by the alternative splicing (AS) regulator Nova2, which was previously considered to be neural cell-specific. Nova2 is expressed during angiogenesis and its depletion disrupts vascular lumen formation *in vivo*. Similarly, Nova2 depletion in cultured endothelial cells (ECs) impairs the apical distribution and the downstream signalling of the Par polarity complex, resulting in altered EC polarity, a process required for vascular lumen formation. These defects are linked to AS changes of Nova2 target exons affecting the Par complex and its regulators. Collectively, our results reveal that Nova2 functions as an AS regulator in angiogenesis and is a novel member of the 'angioneurins' family.

[1] FIRC Institute of Molecular Oncology, Via Adamello 16, Milan 20139, Italy. [2] Department of Biosciences, Milan University, Via Celoria 26, Milan 20133, Italy. [3] Istituto di Genetica Molecolare, Consiglio Nazionale delle Ricerche, via Abbiategrasso 207, Pavia 27100, Italy. [4] IUSS—Istituto Universitario di Studi Superiori, Piazza della Vittoria 15, Pavia 27100, Italy. [5] Dipartimento di Biologia e Biotecnologie, 'Lazzaro Spallanzani' - Università degli Studi di Pavia, via Ferrata 9, Pavia 27100, Italy. [6] Division of Vascular Biology, Department of Medical Biochemistry and Biophysics, Karolinska Institutet, Stockholm 171 77, Sweden. [7] Dipartimento di Oncologia Sperimentale, Istituto Europeo di Oncologia, Milan 20141, Italy. [8] Department of Oncology, San Raffaele Scientific Institute, via Olgettina 58, Milan 20132, Italy. [9] Division of Neuroscience and INSPE at San Raffaele Scientific Institute, via Olgettina 58, Milan 20132, Italy. [10] EMBL/CRG Research Unit in Systems Biology, Centre for Genomic Regulation (CRG), Barcelona 08003, Spain. [11] Universitat Pompeu Fabra (UPF), Barcelona 08003, Spain. [12] Dipartimento di Scienze della Salute, University of Milan, Milan 20122, Italy. [13] Donnelly Centre for Cellular and Biomolecular Research, University of Toronto, 160 College Street, Toronto, Ontario, Canada M5S 3E1. [14] Rudbeck Laboratory and Science for Life Laboratory, Department of Immunology, Genetics and Pathology, Uppsala University, Dag Hammarksjöldsv 20, Uppsala 751 85, Sweden. * These authors contributed equally to this work. ** These authors jointly supervised this work. Correspondence and requests for materials should be addressed to E.D. (email: elisabetta.dejana@ifom.eu) or to C.G. (email: arneri@igm.cnr.it).

Appendix

In adulthood most blood vessels remain quiescent; however, in conditions of active physiological tissue growth, such as during embryogenesis or tissue repair, endothelial cells (ECs) migrate and proliferate to form new vessels. This process, known as angiogenesis, is also critical for the pathogenesis of several disorders and to support cancer development and progression[1]. Although angiogenesis does not initiate malignancy, it promotes tumour growth by allowing oxygen and nutrients to reach proliferating cancer cells. Targeting angiogenesis represents a particularly promising anticancer therapeutic approach, and several strategies have been attempted so far[2].

Recent studies have highlighted significant anatomic, structural and molecular similarities between the vascular and the nervous systems[3]. Both systems possess specialized structures—tip cells at the forefront of endothelial sprouts and axonal growth cones—that, through filopodial extensions, probe the environment for guidance cues. Molecules regulating these processes have been termed 'angioneurins'[3]. The prototypic angioneurin is the vascular endothelial growth factor (VEGF), which was originally discovered as a key angiogenic factor, but subsequently shown to be important also in the development of the nervous system[4]. Since blood vessels and nerves are functionally interdependent, the malfunctioning of this 'neurovascular link' can lead to several vascular and neuronal disorders[3].

Until now, the many molecular pathways regulating vascular development and angiogenesis have been suggested to act primarily through the regulation of transcription. However, recent studies indicate that post-transcriptional and epigenetic programmes cooperate to confer tissue-specific vascular properties.

Alternative splicing (AS) is a molecular process that generates multiple, distinct mature mRNAs from a primary transcript (pre-mRNA), leading to the production of protein isoforms with different structural and functional properties. Since more than 90% of human multiexonic genes undergo AS[5,6], this process represents a major mechanism underlying the expansion of the proteome from a limited repertoire of genes[7,8]. AS and transcription predominantly regulate different subsets of genes to generate the molecular and cellular complexity of different cell and tissue types[9–11]. AS thus provides a versatile, additional layer of regulation to both establish and maintain fundamental properties of different cell and tissue types. Despite the importance of AS, the functional roles of the vast majority of AS events is not well understood.

While there are several examples of splicing variants with a role in angiogenesis[12–15], the molecular mechanisms responsible for their production are still unknown. Here we describe a novel role for Nova2, previously described as neural cell-specific[16], as a key AS regulator of angiogenesis. Both its expression and the levels of AS of its target exons are regulated during this process. Through gain- and loss-of-function approaches in ECs, we show that Nova2 regulates AS of factors belonging to the Par polarity complex and its regulators. Consequently, vascular lumen formation defects are developed in zebrafish on *nova2* morpholino-mediated knockdown or clustered regularly interspaced short palindromic repeat (CRISPR)-induced genetic mutation. Collectively, our results provide evidence that Nova2 is a new member of the 'angioneurins' family, and further highlight an important biological role for post-transcriptional regulation of exon networks that contribute to both vascular and neuronal functions.

Results

Nova2 expression and function are regulated in ECs. To identify splicing regulatory factors (SRFs) involved in endothelial growth and quiescence, we studied ECs under sparse and confluent conditions. By mining previously published Affymetrix gene expression data[17] comparing mouse ECs grown at different densities, we identified *Nova2* as an SRF that is significantly upregulated in confluent versus sparse ECs (fold change = 2.3; P value < 0.05, Dunnett test). This result was surprising since Nova2 was considered previously to be neural cell-specific[16].

Nova2 and its paralogue Nova1 are among the best-studied mammalian tissue-specific SRFs. Both proteins bind RNA through KH domains that recognize clusters of YCAY repeats within the pre-mRNA targets[16]. These factors, with indistinguishable biochemical properties but mutually exclusive expression within the central nervous system (CNS)[18], regulate AS programmes involved in neuronal development and synapse activity[16].

Validating the microarray results, we confirmed Nova2 upregulation in confluent versus sparse ECs using reverse transcription–quantitative PCR (RT–qPCR; Fig. 1a). By comparing *VE-cadherin*-null ECs (VEC-null) with the same cells reconstituted with *VE-cadherin* (VEC-positive)[17] we also found that *Nova2* upregulation in confluent versus sparse ECs does not require VE-cadherin expression (Supplementary Fig. 1A). On the contrary, we found that *Nova1* is expressed to a negligible level in ECs, while both factors are expressed in E15.5 mouse whole brain that we used as positive control (Fig. 1a), consistent with recently published results[19,20]. Moreover, expression of the Muscleblind family of tissue-specific AS regulators (*Mbnl1*, *Mbnl2* and *Mbnl3*) was not modified by confluence in ECs (Fig. 1a). We further confirmed the upregulation of Nova2 in confluent ECs at the protein level by immunoblotting (Fig. 1b). Comparable results were obtained by using another EC line (adult ECs from the mouse lung) under sparse and confluent conditions (Supplementary Fig. 1B). Notably, as in the case of mouse cortex (Fig. 1b) and in human neuroblastoma SH-SY5Y cells (Supplementary Fig. 1C), in ECs the anti-Nova2-specific antibody recognized two immunoreactive bands at 50–55 and 70–80 kDa, as previously reported[18]. In agreement with available RNA sequencing (RNAseq) data (Supplementary Fig. 1D), we found that *Nova2* is also expressed in primary human umbilical vein endothelial cells (HUVECs) and that its levels decreased when HUVECs were grown as sparse (Fig. 1c). Moreover, *Nova2* expression increased during endothelial differentiation of mouse embryonic stem (ES) cells (Fig. 1d), or in adult ECs as compared with embryo or fetal ECs (Fig. 1e). Importantly, Nova2 expression correlated with AS changes of its known target *Ank3*: (i) in sparse versus confluent ECs, (ii) during endothelial differentiation of ES cells and (iii) in ECs of different origin (Fig. 1f) and AS of this target parallels that observed in brain of *Nova2*-null mice[21]. Taken together, these data suggest that Nova2 expression and function may play a role in vascular maturation.

To confirm the vascular expression of Nova2 in a more physiological context, we analysed the postnatal mouse retina, which develops a stereotypical vascular pattern following a well-defined sequence of events[22]. In the retina, we found that Nova2-positive nuclei were reduced but still present in the ECs at the sprouting front as compared with the central part of the retina where the majority of ECs of the mature vessels (arteries and veins) and capillaries were Nova2-positive (Fig. 2a,b and Supplementary Fig. 2A). In addition, we found the specific nuclear expression of Nova2 in ECs present in the vessels of different tissues, such as normal human thyroid, skin, bladder, colon and prostate (Fig. 2c and Supplementary Fig. 2B).

Collectively, these data indicate that Nova2 is not exclusively expressed in cells of the nervous system, but it is also present in ECs of different types of vessels.

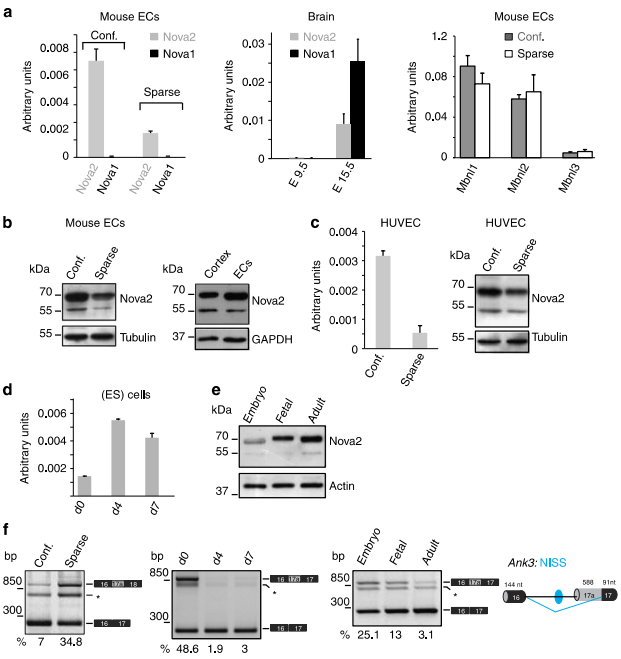

Figure 1 | Nova2 expression levels and AS of its target are regulated in ECs. (**a**) RT–qPCR analysis of *Nova2* and *Nova1* mRNA expression levels in mouse ECs grown as confluent or sparse (left), in E9.5 and E15.5 mouse whole brain (centre), and RT–qPCR analysis of Muscleblind family members (*Mbnl1*, *Mbnl2* and *Mbnl3*) in mouse ECs grown at different densities (right). (**b**) Immunoblotting analysis of Nova2 levels in mouse confluent and sparse ECs (left panel; Tubulin as the loading control) and in confluent ECs and the mouse brain cortex (right panel; GAPDH as loading control). (**c**) Nova2 mRNA and protein expression levels in HUVECs grown at different densities. (**d**) RT–qPCR analysis of *Nova2* during endothelial differentiation of mouse ES cells at the indicated times. (**e**) Immunoblotting analysis of Nova2 in mouse EC lines derived from whole embryo, fetal heart and adult lung; Actin as the loading control. In all histograms, error bars indicate ± s.d. calculated from three independent experiments ($n = 3$). (**f**) RT-PCR analysis of AS of a known Nova2 target (*Ankyrin3/Ank3*) in mouse ECs (confluent and sparse; left), during endothelial differentiation of mouse ES cells (centre) and in mouse ECs of different origins (right). The schematic representation of the mouse gene structure (AS exon in grey; constitutive exons in black), the YCAY cluster predicted to function as Nova2 silencer (blue dot) and the Nova2-regulated exon-skipping event (blue bars) are also shown. NISS, Nova intronic splicing silencer. The percentage of exon inclusion is shown. Asterisk indicates a nonspecific PCR product.

Nova2 regulates the endothelial apical–basal polarity. An important functional similarity in the development of the vascular and nervous systems is the establishment of the apical–basal polarity, as this is a crucial event for the organization of the vascular lumen and for axon guidance[23,24] respectively. Notably, the partitioning-defective (Par) polarity complex is a key determinant of cell polarity in both systems[23,24]. The specific localization and activity of the Par polarity complex involve the association of four key components: Par3, Par6, the small GTPase Cdc42 and the atypical protein kinase C (PKCζ). In addition, the small GTPases Rac1 and Rap1 are important regulators of the Par complex during organization of the vascular lumen[23,25].

To investigate the role of Nova2 in the endothelium as a possible regulator of vascular development, we generated stable *Nova2* knockdown ECs (Fig. 3a). Intriguingly, we found that depletion of *Nova2* expression impairs EC polarity. As shown in Fig. 3b, in two-dimensional (2D) cultures, *Nova2* knockdown altered the subcellular localization of the apical surface marker podocalyxin (Podxl) that was distributed all over the cell membrane and also to the basal surface. These findings prompted us to examine whether silencing of *Nova2* alters the junctional staining and/or activity of components of the Par polarity complex. *Nova2*-depleted ECs displayed impaired junctional distribution of Par3, a multiscaffold protein that promotes the assembly of the Par complex (Fig. 3c). Interestingly, *Nova2* knockdown in ECs caused reduced levels of active (GTP-bound) Cdc42 (Fig. 3d), whose association with the Par complex is induced during EC lumen formation[26]. Accordingly, we

Appendix

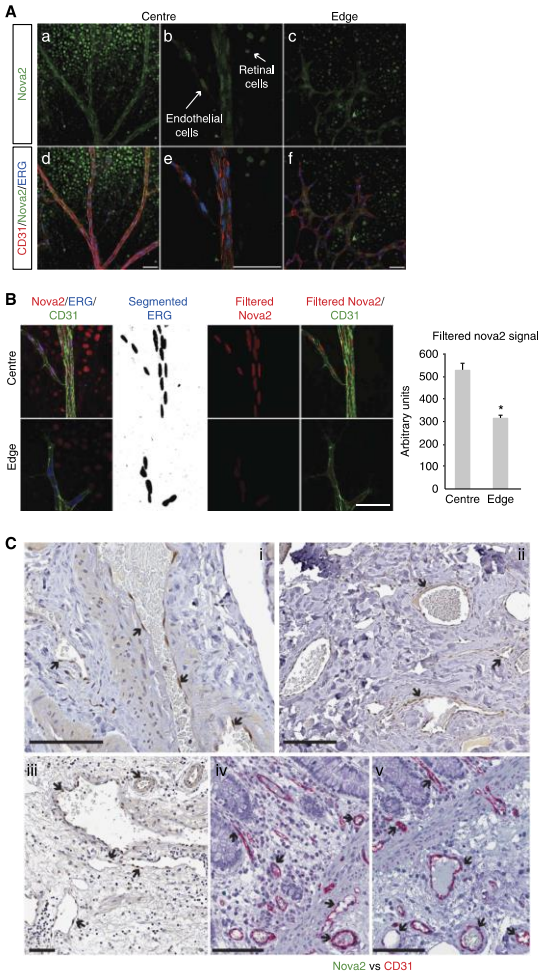

Figure 2 | Nova2 is expressed in the vascular endothelium *in vivo*. (**a**) Immunofluorescence analysis of Nova2 (green), the endothelial markers CD31 (red) and ERG (blue, transcription factor) in whole-mounted postnatal (P6) mouse retina. Optical sections captured using confocal microscopy display large vessels in the central retina region (a,b,d,e) and sprouting ECs in the leading edge of the growing vasculature (c,f). Arrows indicate neural cells of the retina and ECs of vessels expressing Nova2 (scale bar, 50 μm). (**b**) Quantification of Nova2 signal. ERG staining has been segmented with threshold 350–4,096, and segmented images have been filtered to remove speckles and outliers (radius 25). Segmentation results have been used to filter Nova2 staining to isolate EC nuclear staining (scale bar, 50 μm). Chart shows average signals (error bars indicate mean ± s.d.; asterisks P value < 0.05, two-tailed t-test assuming unequal variances; $n = 2$). (**c**) IHC of Nova2 in normal human thyroid (i), skin (ii) and bladder (iii) and IHC of Nova2 and the endothelial marker CD31 in normal human colon (iv, v). Arrows indicate Nova2 nuclear staining of ECs in the blood vessels (scale bar, 100 μm).

Appendix

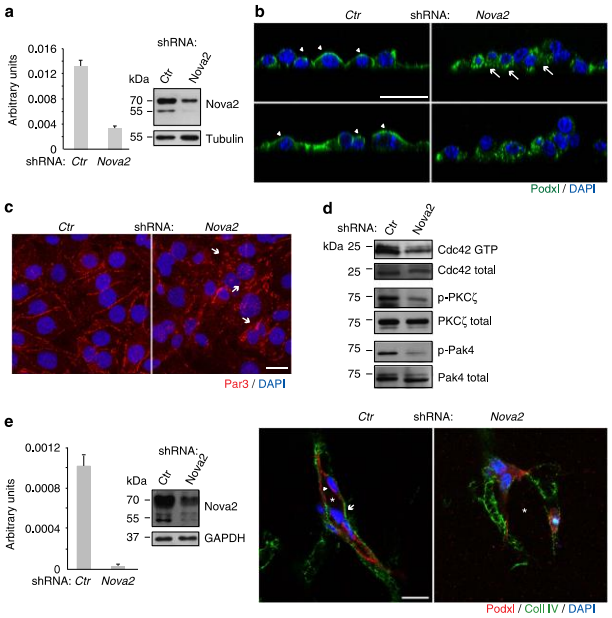

Figure 3 | Nova2 is required for the EC polarization. (**a**) *Nova2* mRNA levels in knockdown mouse ECs (grown as confluent). The Nova2 protein level was analysed by immunoblotting using an anti-Nova2 antibody (Tubulin as loading control). (**b**) Immunofluorescence (IF) analysis of Podocalyxin (Podxl, green) and DAPI (blue) in 2D culture of control (*Ctr*) and *Nova2*-depleted ECs. Podxl is often distributed to the basal (arrows) instead of the apical surface (arrowheads) in *Nova2*-silenced ECs (confocal sections, *z* axis; scale bar, 25 μm). (**c**) IF analysis of Par3 (red) and DAPI (blue) in *Ctr* or *Nova2* knockdown ECs. Arrows indicate altered and fragmented junctional staining of Par3 (bar 20 μm). (**d**) *In vitro* pull down of GTP-bound Cdc42 in *Ctr* and *Nova2*-silenced ECs. Immunoblotting for the phosphorylation status of PKCζ and Pak4 is also shown. (**e**) Left: *Nova2* mRNA levels in knockdown HUVECs. The Nova2 protein level was analysed by immunoblotting using an anti-Nova2 antibody (GAPDH as the loading control). Right: in 3D collagen gel, control HUVECs form vascular structures with a central lumen (asterisk) and apical Podxl and basal collagen IV (Coll IV) proper localization (arrowheads and arrows, respectively), whereas *Nova2*-silenced HUVECs are not correctly polarized (scale bar, 20 μm). Error bars indicate mean ± s.d. calculated from three independent experiments ($n = 3$).

determined that phosphorylation of PKCζ, a Cdc42-GTP-activated protein[27], is also reduced in *Nova2*-depleted ECs (Fig. 3d). Moreover, *Nova2* knockdown ECs were characterized by reduced levels of phosphorylated Pak4 (p21-activated kinase; Fig. 3d), one of the main Cdc42 downstream effectors[28].

EC polarization correlates with lumen formation[25,29]. Thus, to test whether Nova2 is required for the formation of the endothelial lumen, we have carried out its knockdown in primary HUVECs that, when are cultured in three-dimensional (3D) collagen gel, rapidly organize into a network of hollow structures[30]. As shown in Fig. 3e, control HUVEC cells forming vascular-like structures were correctly polarized with Podxl and collagen IV localized to the apical and basal surfaces, respectively. On the contrary, knockdown of *Nova2* resulted in the formation of capillary-like tubular networks with irregular lumen and a non-polarized distribution of endothelial Podxl and collagen IV. These results strongly suggest that Nova2 splicing factor is crucial for EC morphogenesis.

Recently, the Par polarity complex has been shown to regulate endothelial cell-cell contacts and affect migratory behaviour[25,31]. In agreement with these observations we found that silencing of *Nova2* affected junctional clustering of VEC and β-catenin since the architecture of cell–cell boundaries was partially disorganized in *Nova2* knockdown ECs (Supplementary Fig. 3A). Cell polarity is also established during directional cell migration, where cytoskeletal, adhesive and signalling molecules are distributed asymmetrically. We found that *Nova2* knockdown affected the collective behaviour of migrating ECs. During wound closure, migrating ECs depleted of *Nova2* have in part lost their contacts with neighbouring cells positioned at the back (Supplementary Fig. 3B). The leading edge was more tortuous compared with control ECs (Supplementary Fig. 3B). Finally, given the junctional alterations induced by Nova2 knockdown, we tested whether endothelial permeability was also modified. We found that the permeability of confluent endothelial monolayers was indeed increased upon *Nova2* depletion (Supplementary Fig. 3C).

Appendix

To comprehensively identify AS events regulated by Nova2 in the endothelium, we performed high-throughput RNAseq of two biological replicates of *Nova2* knockdown and control ECs. We used *vast-tools*[32] to identify and quantify all major types of AS events. *vast-tools* maps RNAseq reads to comprehensive sets of annotated and novel splice junctions to derive confident estimates of the percentage of alternative sequence inclusion in a given sample. We identified 365 AS events affected by Nova2 depletion, including 188 (51.5%) cassette exons (Supplementary Fig. 4, Supplementary Table 1 and see Supplementary Methods for details). Gene Ontology (GO) analyses of AS events predicted to generate alternative protein isoforms (41% of all AS events and 64% of cassette exons; Supplementary Fig. 5) showed a significant enrichment for genes involved in cytoskeleton and cell adhesion (including tight and adherens junctions, and integrin binding), consistent with the phenotypes described above (Supplementary Table 2). In addition, the strongest enriched functional terms corresponded to chromatin remodelling and regulators, suggesting a multilayered impact of Nova2 regulation on endothelial formation. Finally, we also observed multiple GO terms related to neuronal differentiation and function (for example, neurogenesis, synapsis, axon part and calcium transport), similar to those reported for Nova-regulated genes in the brain[16]. Indeed, comparison of differentially included cassette exons in genes expressed in both neurons and ECs (see Supplementary Methods) revealed a highly significant overlap between alternative exons predicted to be regulated by Nova proteins in the brain[33] and those showing changes in inclusion levels upon *Nova2* knockdown in the endothelium ($P = 1.93e^{-11}$, hypergeometric test; Supplementary Fig. 6; Supplementary Table 3), despite the very different approaches used in the two studies (see Supplementary Materials for details).

These newly identified Nova2 targets expanded the list of previously known targets involved in apical–basal polarity, actin polymerization dynamics and cytoskeletal remodelling, important processes associated with cell polarity, cell shape, motility and adhesion (Supplementary Tables 4 and 5). Thus, to confirm a possible molecular link between these AS events and the phenotypes described above, we analysed AS changes in selected targets using RNA extracted from *Nova2* knockdown ECs (Fig. 4a). Reduced Nova2 expression in ECs resulted in altered AS of transcripts encoding *Par3*, and regulators of Par activity or localization, including *Magi1*, which recruits Rap1 at junctions[34], *Rap1GAP* (Rap1 inhibitor)[35], *Pix-α*, *Dock6*, *Dock9* and *DBS* (Cdc42 activators)[36–38] (Fig. 4a and Supplementary Fig. 7). Importantly, these AS changes parallel to those observed in the brain of *Nova2*-null mice[16,33], or in two stages of brain development (Supplementary Fig. 8A) characterized by different Nova2 expression levels (Fig. 1a). We confirmed the Nova2-dependent AS of target transcripts in RNA samples extracted from *Nova2*-overexpressing ECs (Fig. 4a, Supplementary Fig. 7 and Supplementary Fig. 8B). Notably, the direction of the observed AS changes is consistent with the position of Nova2-binding sites (YCAY; Fig. 4a and Supplementary Fig. 7), as previously reported[16].

Our data suggest that in cultured ECs Nova2 establishes EC polarity by controlling Par3 localization and by regulating the activity of Cdc42. To begin to address the functional relevance of the AS events regulated by Nova2 in ECs, we focused on the Cdc42 activator Pix-α (ref. 36). Our results indicate that Nova2 promotes the production of a specific Pix-α AS isoform lacking exon 17 (Pix-α-Δ17; Fig. 4a). Intriguingly, we found that Pix-α-Δ17 is more efficient than the Pix-α isoform containing exon 17 (Pix-α-FL) in rescuing the defect of Cdc42 activity caused by *Nova2* knockdown (Fig. 4b).

Collectively, these results provide evidence that Nova2 is required for EC polarity and that it acts by inducing AS of a set of key effectors of cell polarity.

Nova2 promotes vascular lumen formation *in vivo*. Since EC polarity regulates vascular lumen formation, we tested whether vascular development was affected in the absence of Nova2. To this end, we investigated the role of Nova2 in the embryos and larvae of zebrafish, which constitutes a unique and powerful model to study vertebrate vascular development[39]. Importantly, the Nova2 RNA-binding domain is 94% identical between zebrafish and human[40], and we found that a zebrafish *Nova2* orthologous gene (*nova2*) is expressed in the vasculature during development in addition to CNS (Fig. 5a). To assess the role of *nova2* in zebrafish, we performed a morpholino-mediated knockdown of its expression. To specifically visualize the developing blood vessels, we injected morpholino oligos into transgenic embryos expressing the enhanced green fluorescent protein (*EGFP*) gene under the control of the endothelial-specific promoter *fli1a* (*Tg(fli1a:EGFP)y1*)[41]. We used a morpholino targeting the start codon of zebrafish *nova2* (MO-nova2) to block translation of both maternal and zygotic *nova2* mRNAs. While embryos injected with a control morpholino displayed a normal morphology, more than 90% of *nova2* morphant embryos showed defects at the level of the forming blood vessels. Moreover, during early embryogenesis the pattern of some intersomitic vessels (ISVs) displayed extra-branching formation and a delay in the connection with the dorsal longitudinal anastomotic vessel (Fig. 5b). Confocal microscopy analysis confirmed that *nova2* knockdown resulted in altered lumen size of both cephalic vessels and of main trunk blood vessels (Fig. 5b,c). To visualize and further characterize the phenotype at the level of the dorsal aorta and posterior cardinal vein, we performed a morphological analysis using transversal paraffin sections stained with haematoxylin–eosin of embryos at different developmental stages (Fig. 5d). The analysis showed that in most of *nova2* morphants the lumen of the dorsal aorta had a larger diameter if compared with controls, through all developmental stages analysed. The lumen of the posterior cardinal vein appeared irregular along the length of the trunk, with areas of enlargement but also few restrictions (Fig. 5d). Furthermore, starting from 2 days of development, even ISVs display an enlarged lumen (Supplementary Fig. 9A). To better characterize the phenotype of *nova2* morphants at the level of ISVs during the angiogenic process, we performed an *in vivo* time lapse imaging assay. As shown in Supplementary Movies 1–3 in *nova2* morphant embryos the apical cells of some ISVs develop many more filopodia and could barely reach the dorsal longitudinal anastomotic vessel. Importantly, co-injection of *nova2* mutants with a morpholino-resistant zebrafish *nova2* mRNA rescued, in more than 60% of the injected embryos, the morphological phenotype of the vessels, confirming the specificity of the effects (Fig. 5b–d and Supplementary Movies 1–3). The abnormal phenotype of blood vessels observed in *nova2* morphants was not due to haemodynamic problems, since at 48 h post fertilization (hpf) the heart appeared normal for size, shape and beat (Supplementary Movies 4 and 5). In addition, EC proliferation and apoptosis were not significantly modified in the morphants (Supplementary Fig. 9B,C). Collectively, these data indicate that *in vivo* nova2 is required for proper vascular morphogenesis and for the formation of a correct vascular lumen.

Since Par complex members and regulators identified as Nova2 targets have putative orthologues in zebrafish, we analysed their AS using RNA extracted from *ctr* and *nova2* morphants. Of the investigated pre-mRNAs (Fig. 4a), four (*Rap1GAP*, *Pix-α*, *DBS*

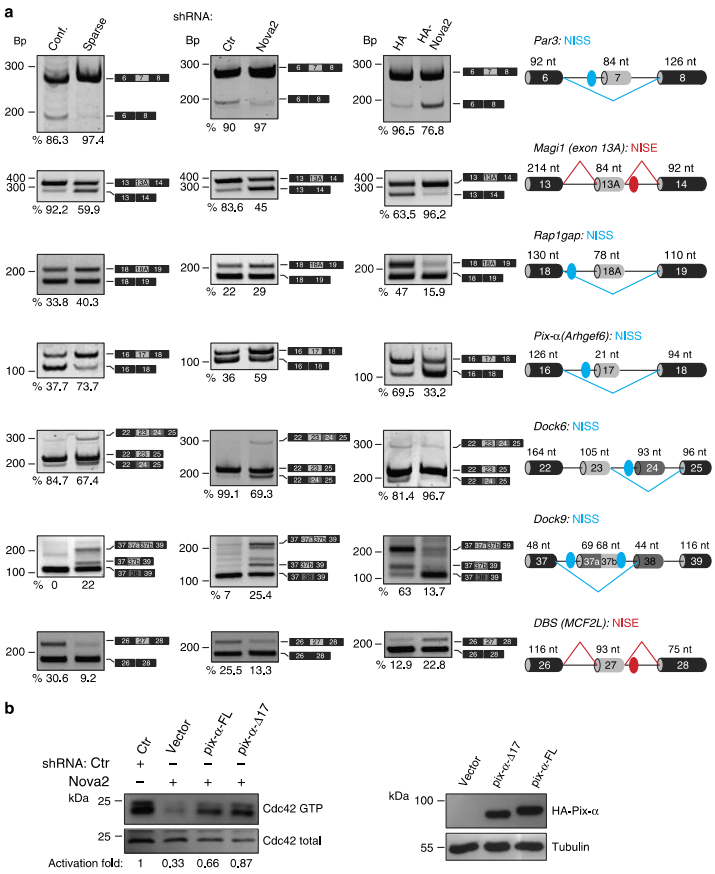

Figure 4 | AS changes in Nova2 overexpression and knockdown ECs. (**a**) AS of the indicated Nova2 targets as determined using RT–PCR in confluent and sparse mouse ECs (left), in confluent *Nova2* knockdown ECs (middle) and in sparse ECs overexpressing HA-tagged Nova2 (right). For each gene, the schematic representations of the genomic region containing the AS exon, the transcripts generated from skipping or inclusion of the AS exon and the calculated percentage of exon inclusion are indicated. For *Dock6*, the percentage indicates the ratio between the isoform containing exon 23 (skipping exon 24) and total, whereas for *Dock9* the percentage is the ratio between the isoform containing exon 37a plus 37b and total. Grey boxes, AS exons; black boxes, constitutive exons; blue/red dots indicate YCAY clusters predicted to function as Nova silencer/enhancer. Blue/red bars indicate Nova-silenced/enhanced exon inclusion. NISS, Nova intronic splicing silencer; NISE, Nova intronic splicing enhancer. (**b**) *In vitro* pull down of GTP-bound Cdc42 in *Nova2*-silenced ECs transfected with the indicated vectors driving the expression of HA-tagged Pix-α deleted of exon 17 (Pix-α-Δ17), Pix-α containing exon 17 (Pix-α-FL) or transfected with the empty vector (vector). The Cdc42 activation fold, calculated as the ratio between GTP-bound Cdc42 and total, is shown (*Ctr* sample used as a reference value). Pix-α isoform expression was analysed by using anti-HA and Tubulin antibodies.

and *Dock6*) are alternatively spliced in zebrafish (Fig. 5e). Interestingly, in all cases nova2 knockdown alters exon inclusion levels (Fig. 5e) in the direction predicted by the position of putative Nova-binding motifs[21] (Supplementary Fig. 10). Importantly, aberrant AS events of *nova2* morphants were rescued by co-injection of *nova2* mRNA (Fig. 5e). Of note, we

found that some nova2 targets (see, for instance, *Rap1gap* and *Pix-α*, Supplementary Fig. 9C) are not expressed at the same level in the different types of vessels suggesting that the effects of the knockdown of *nova2* may have different morphological and functional consequences along the vascular tree.

To assess the apical–basal cell polarity in *nova2* morphant embryos, we analysed the localization of Podocalyxin (Podxl2). As shown in Fig. 6a, in *ctr* embryos Podxl2 is localized at the apical region of the ECs forming ISVs, while in *nova2* morphants Podxl2 is mislocalized in ECs of the ISVs. Moreover, this defect

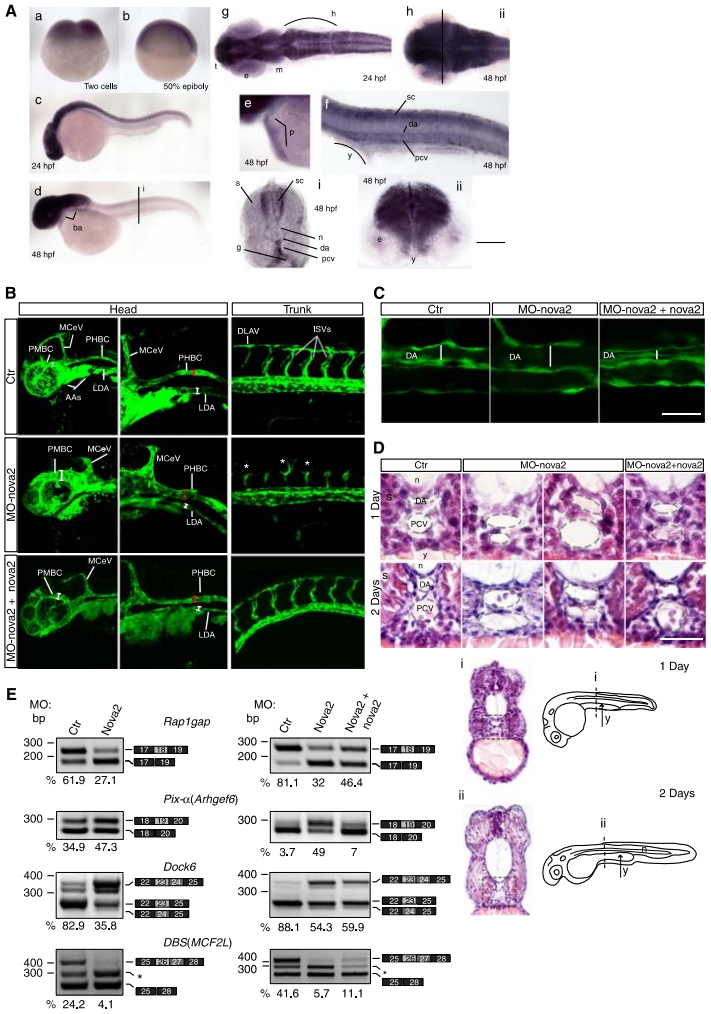

Appendix

persisted at late developmental stage (Supplementary Fig. 9A). Likewise, altered Podxl2 localization was also observed in dorsal aorta of *nova2* morphants (Fig. 6a), suggesting an altered establishment of apical–basal polarity. Again, co-injection of *nova2* mRNA rescued Podxl2 localization in ECs (Fig. 6a).

Since Nova2 is expressed in neurons as well as in ECs, and these cells influence their reciprocal differentiation and development[42], it was important to address whether the vascular phenotype of *nova2* morphants was due to alterations in the nervous or vascular systems. To do this, we used a morpholino-resistant zebrafish *nova2* cDNA, fused with the red fluorescent protein mCherry, under the control of the vasculature-specific *fli1a* promoter (Fig. 6b). The vascular defects in *nova2* morphants were restored by the mosaic transient expression in the vascular endothelium of morpholino-resistant *nova2* cDNA (Fig. 6b–d). Moreover, by generating a zebrafish transgenic line, which stably expresses morpholino-resistant *nova2-mCherry* in the vascular endothelium, we found that injection of MO-nova2 did not significantly alter blood vasculature morphology (Fig. 6e), indicating that the vascular phenotype of *nova2* morphants is cell autonomous.

To independently validate our findings, we used CRISPRs genome engineering[43] to generate genetic *nova2* mutant fish (Supplementary Fig. 11A and see Methods for details). The characterization of *nova2* mutants strongly supported our results and conclusions obtained using MO-mediated *nova2* knockdown (Supplementary Fig. 11). In particular, *nova2* homozygous mutants displayed overlapping defects with *nova2* morphants, such as shortening of the anteroposterior body axis, reduced head size, curved trunk and slight pericardial oedema (Supplementary Fig. 11B). Moreover, we observed that *nova2* mutants do not develop the swim bladder and display a strong haemorrhagic phenotype visible both at the level of the head and trunk (Supplementary Fig. 11C,D). Notably, similar to Nova knockout mice[44,45], zebrafish *nova2* mutant embryos displayed paralysis. In particular, they have severe difficulty in swimming (probably because of motor–neuronal dysfunction) and died 7–10 days post fertilization, whereas there was no abnormal phenotype in *nova2* heterozygote mutant embryos. Confocal microscopic analyses performed on the *nova2* mutants transgenic for *kdr:EGFP* showed that many blood vessels had an enlarged lumen size, both in the head and in the trunk (Supplementary Fig. 11E), as observed in *nova2* morphant embryos. Similar findings were obtained by histological analysis (Supplementary Fig. 11F). Finally, *nova2* mutants displayed AS changes (Supplementary Fig. 11G) that are comparable to those in *nova2* morphants.

Collectively, our results show that Nova2 controls the development of the vascular system *in vivo* by modulating endothelial polarity and lumen formation.

Discussion

Here we report that AS regulation orchestrates some important aspects of EC biology. In particular, our data demonstrate that the AS factor Nova2, known to be neural cell-specific[16], is also expressed in the vascular endothelium and plays a relevant role in vascular morphogenesis.

In spite of its importance, our current understanding of the mechanisms underlying vascular tubulogenesis is only beginning to be unravelled[23,25,29]. We have shown that Nova2 acts as a post-transcriptional regulator of the molecular mechanisms involved in the organization of the vascular lumen. In zebrafish, depletion and genetic knockout of *nova2* prevents proper formation of the lumen of blood vessels and also results in defects in EC polarization. Interestingly, in avascular organisms, such as *Drosophila melanogaster*, the Nova homologue (Pasilla, *ps*), is not expressed in the brain, but instead is expressed at high levels in salivary glands and several other non-neuronal tissues[46,47]. Notably, *ps* mutants have altered apical secretion and are characterized by developmental defects of the salivary gland including regions of lumen alteration[46]. This type of morphology, with a severely altered lumen, is somehow reminiscent of the morphology of the zebrafish vasculature observed on *nova2* depletion. Recently, several regulators of salivary gland lumen formation (such as Cdc42, Pak proteins and cadherins) have been identified in *Drosophila*[48]. Intriguingly, they are also implicated in vascular lumenogenesis[23] and, more importantly, regulators of their activity and localization are known Nova2 AS targets[33].

Our data show that, in cultured ECs, Nova2 establishes EC polarity by controlling Par3 localization, the activity of Cdc42 and the phosphorylated state of PKCζ. Notably, signalling downstream of Cdc42 is impaired in the absence of Nova2, as the active form of PKCζ and Pak4 are reduced in Nova2-depleted ECs. Interestingly, Pak4 phosphorylation correlates with EC lumen formation and RNA interference-mediated suppression of *Pak4* strongly inhibits these processes[26]. Similarly, depletion of *Nova2* impairs the establishment of EC polarity and the organization of the vascular lumen. These defects are associated with aberrant AS of pre-mRNAs encoding factors belonging to the Par polarity complex and its regulators.

Par complex and downstream effectors play important roles in regulating cell–cell adhesions[25], in controlling the organization of the microtubule cytoskeleton[49], and in promoting directional, collective cell migration[31]. Strikingly, we found that downregulation of *Nova2* affected the architecture of cell–cell boundaries and the behaviour of migrating ECs. In particular, in wound closure *Nova2*-depleted ECs failed to move in a cohesive manner with the lack of coordination in the direction of cell movement suggesting that, in addition to its role on lumen

Figure 5 | Nova2 is required for vascular lumen formation in zebrafish. (**a**) *In situ* hybridization of different zebrafish developmental stages showed *Nova2* expression in the pericardium (p in e), in the trunk vessels (f,i) of 48 hpf embryos and in the CNS of 24 (g) and 48 hpf embryos (h,ii; scale bars, 250 μm in a,b; 125 μm in c,d,g,h); 50 μm in e,f; 25 μm for vibratome sections i,ii). (**b**) Lateral views of the head and trunk of 28 hpf *Tg(fli1a:EGFP)y1* embryos, expressing the EGFP under the endothelial-specific promoter *fli1a*, injected with control (*ctr*) or morpholino against *nova2* (MO-nova2). *Nova2* knockdown results in lumen defects of lateral dorsal aorta (LDA), middle cerebral vein (MCeV) and primordial hindbrain channels (PHBC; compare red and/or white bars length between *ctr* and *nova2* morphants). The ISVs display extra-branching formation (*) and a delay in the connection with the dorsal longitudinal anastomotic vessel (DLAV). Co-injection of a morpholino-resistant zebrafish *nova2* RNA (MO-nova2 + nova2) rescues the vascular defects. (**c**) Confocal analysis of the blood vessels in the trunk region of 28-hpf embryos (lateral views); *nova2* morphants display enlarged lumen (white bars) of the dorsal aorta (scale bar, 50 μm). (**d**) High magnifications of paraffin 10 μm transversal sections, stained with haematoxylin–eosin, of the trunk region of 1- and 2-day embryos (dashed black squares in i,ii) highlighted alterations of the lumen size of the dorsal aorta and PCV in more than 90% of *nova2* morphants. Abnormal phenotype was rescued by co-injection of *nova2* mRNA (scale bar, 50 μm). e, eye; g, gut; h, hindbrain; m, midbrain; n, notochord; s, somite; sc, spinal cord; t, telencephalon; y, yolk; AAs, mandibular arches; PMBC, primordial midbrain channel. (**e**) *Nova2* knockdown alters the AS of its targets (24 hpf) that is corrected by the co-injection of *nova2* mRNA (28 hpf). The percentage of exon inclusion is indicated (grey, AS exon); *Dock6* as in Fig. 4, *DBS* is the ratio 26 + 27/total. Asterisk, novel *DBS* AS variant containing 75 nt (exon 27b: ACGCAGGTCCTCACATCACTCTCACCCGAGTGAGATGGCTGAGCACTTC TAGTCTGTTGCAGACTAAACGCAGAG) of intron 27.

Appendix

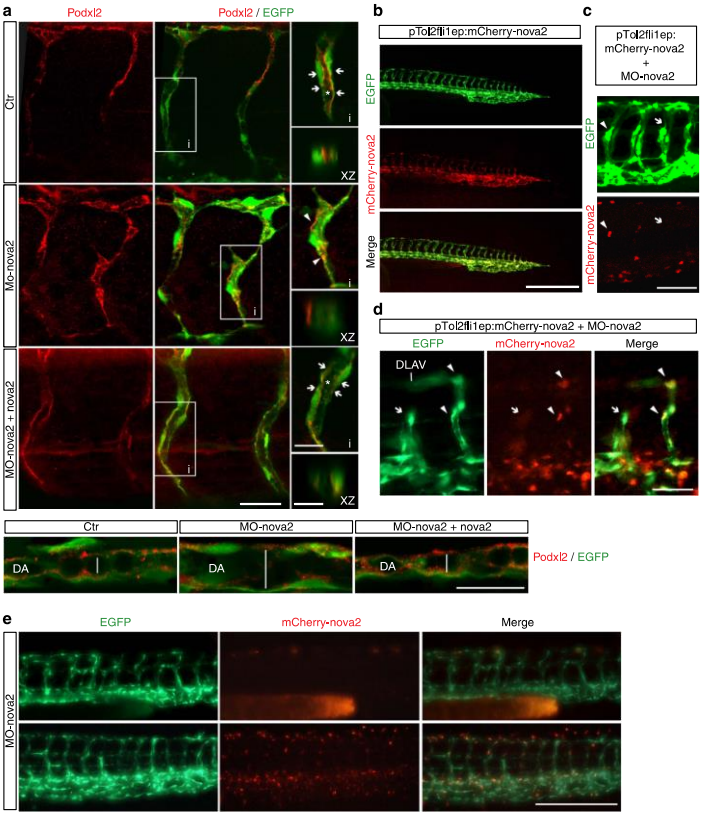

Figure 6 | Endothelial Nova2 is essential for EC polarization. (**a**) *Tg(fli1a:EGFP)y1* zebrafish embryos were treated with control (*ctr*) or *nova2* morpholino (MO-nova2) oligos and analysed with anti-Podocalyxin antibody (Podxl2, red) in the ISVs (upper panel). Co-injection of a morpholino-resistant zebrafish *nova2* mRNA was able to rescue the apical-membrane staining (arrow) of Podxl2 in *nova2* morphant (MO-nova2 + nova2; scale bar, 20 μm). Areas (i) are magnified on the right (scale bar, 10 μm). This is also visualized in the optical transverse sections (XZ, scale bar, 5 μm). Asterisk, lumen; arrowheads indicate Podxl2 mislocalization. Lower panel: Podxl2 localization in the dorsal aorta (scale bar, 50 μm). (**b**) Lateral view of the *Tg(fli1a:EGFP)y1* embryo with EGFP under the control of the endothelial-specific promoter *fli1a*. The same transgenic zebrafish embryos were co-injected at one-cell stage with a vector (pTol2fli1ep:mCherry-nova2) driving the expression of a morpholino-resistant zebrafish *nova2* mRNA fused to mCherry fluorescent protein under the *fli1a* promoter. In this case individual ECs were mosaically labelled with mCherry-nova2 expression (nova2, red) in the nucleus of some cells of the trunk blood vessels (scale bar, 250 μm). (**c**) Endothelial-autonomous rescue of *nova2* morphants. PTol2fli1ep:mCherry-nova2 plasmid was co-injected with the *nova2* morpholino oligo (MO-nova2) in one-cell stage *Tg(fli1a:EGFP)y1* embryos (bar 40 μm; arrowheads and arrows indicate vessels positive and negative for nova2, respectively). (**d**) ISV of the trunk expressing nova2 (arrowheads) showed a normal pattern and developed a correct lumen, whereas an adjacent ISV (arrows), negative for nova2 expression, was not formed properly, so that it failed to reach DLAV (scale bar, 30 μm). (**e**) Lateral view of 28-hpf transgenic embryos injected with the MO-nova2. Embryo showed in the upper row expresses in the vessel endothelium only GFP, whereas the embryo showed in the lower row expresses also a morpholino-resistant *nova2* cDNA fused with mCherry. The presence of *nova2* in the vessel endothelium is sufficient to preserve vessel morphology of *nova2* morphant embryos (scale bar, 50 μm).

Appendix

formation, Nova2 expression might also control adhesion signals and the directional migration of ECs.

Our current lack of knowledge of the functional implications of most AS events makes it difficult to interpret the global impact of the AS changes we have identified. Moreover, it is plausible that additional AS events are regulated by Nova2 in ECs. Nevertheless, we found that the alteration in Cdc42 activity in *Nova2* knockdown ECs is preferentially reverted by overexpression of a specific AS isoform of Pix-α (Pix-α-Δ17) regulated by Nova2, indicating that AS of this gene plays an important role in Cdc42 activation.

We found Nova2-dependent AS regulation of zebrafish orthologous genes encoding polarity regulators. Among these, there are well-characterized activators (*Pix-α*, *Dock6* and *DBS*) of Cdc42, which—in turn—plays an essential role in controlling lumen formation *in vitro* and *in vivo*[26,48,50–52].

Remarkably, Nova2-regulated pre-mRNA targets encode proteins that interact with each other[16], suggesting that Nova2 regulates a network of apical–basal polarity regulators and that AS plays an important role in affecting physical interactions between these factors during the organization of the vascular lumen. Hence, the phenotypic changes that we observed on *Nova2* knockdown are likely the integrated effects of several AS changes that may act in a coordinated and non-redundant manner.

On the basis of the fact that Nova2 affects both neural and vascular cell processes, we suggest that Nova2 is a novel member of the 'angioneurins' family[3,4]. Interestingly, Nova2 is the only member of the angioneurin family defined so far that functions as post-transcriptional regulator. Malfunctioning or imbalance in angioneurin signalling contributes to various neurological disorders, indicating that non-neuronal defects contribute to these diseases[3]. In line with this, in Alzheimer's disease patients' vascular dysfunction can be observed before the onset of the disease, suggesting that vascular alterations might causally contribute to disease initiation or progression[53]. Notably, significant AS changes associated with decreased Nova activity were reported in Alzheimer's patients[54]. Since Nova2 is an autoimmune target in a severe neurodegenerative disorder paraneoplastic opsoclonus myoclonus ataxia (POMA)[55], an obvious question is whether POMA patients, in addition to displaying neurological symptoms, also develop vascular abnormalities.

Methods

Cell culture. ECs were isolated by dissection and dissociation with collagenase type I (Roche, 1.5 mg ml^{-1}), DNase (Roche, 25 μg ml^{-1}) at 37 °C for 1 h and by passing through a 40-μm cell strainer. ECs were immortalized by infecting them with a retrovirus expressing the polyoma middle-sized T antigen. VEC-null and VEC-positive were grown as sparse or confluent by placing 500,000 cells in 100- and 35-mm Petri dishes, respectively.

Culture medium of mouse ECs, VEC-null and VEC-positive ECs was DMEM (GIBCO) with 20% fetal bovine serum (FBS; HyClone), glutamine (2 mM, Sigma-Aldrich), penicillin/streptomycin (100 U l^{-1}, Sigma-Aldrich), sodium pyruvate (1 mM, Sigma-Aldrich), heparin (100 μg ml^{-1}, from porcine intestinal mucosa; Sigma-Aldrich) and EC growth supplement (5 μg ml^{-1}, made from calf brain; complete culture medium). HUVECs were isolated from umbilical vein by treatment with Collagenase (Roche, 0.1%, for 30 min at 37 °C) and were cultured in MCDB 131 with EC supplements.

Mouse ES cell culture. To obtain endothelial differentiation of mouse ES cells, cells were mildly trypsinized and suspended in Iscove's modified Dulbecco medium with 15% FBS, 100 U ml^{-1} penicillin, 100 μg ml^{-1} streptomycin, 450 μM monothioglycerol, 10 μg ml^{-1} insulin, 50 ng ml^{-1} human recombinant VEGF-A165 (Peprotech Inc.), 2 U ml^{-1} human recombinant erythropoietin (Cilag AG) and 100 ng ml^{-1} human basic fibroblast growth factor (bFGF) (Genzyme). Cells were seeded in Petri dishes and cultured for 4 or 7 days at 37 °C with 5% CO_2 and 95% relative humidity.

Lentivirus production and transduction. GIPZ Lentiviral Nova2 short-hairpin RNAs (shRNAs) were obtained from Open Biosystems, while pLenti-GIII-CMV-humanNova2-HA from THP Medical Products. HEK293T (American Type Culture Collection, CRL-1573) cells were seeded in DMEM-HIGH supplemented with 10% FBS without antibiotics in 60-mm Petri dishes (one Petri per infection). The day after, cells at 60–70% confluence were transfected (calcium phosphate transfection method) using these quantities of DNA: 5 μg of packaging plasmid, 5 μg of envelope plasmid and 20 μg of Nova2 vectors. After 18 h, the medium was replaced with growth medium DMEM supplemented with 20% FBS and 1% penicillin/streptomycin. Cells were incubated for 24 h and the medium containing the lentiviral particles was harvested, filtered using a 0.45-μm filter unit and used to infect the cells.

For viral transduction, mouse EC cells were seeded in 100-mm Petri dishes and were infected at 70% of confluence. Cells were incubated overnight with the viral supernatant supplemented with 0.2 mM proline and polybrene (final concentration 8 μg ml^{-1}; Sigma). After 48 h puromycin selection (3 μg ml^{-1}) was started and it was continued until all non-infected control cells died (typically, 5 days).

2D culture. Mouse ECs transduced with lentiviral vectors carrying shRNA for Nova2 were seeded in 35-mm Petri dishes coated with Gelatin (Difco) 0.1% and cultured for 72 h. The splitting ratio was such that confluence was reached overnight after seeding. For immunofluorescence, ECs were fixed with 4% paraformaldehyde (PFA) and then permeabilized with 0.5% Triton X-100 for 10 min. Blocking (1 h), primary (overnight) and secondary (1 h) antibodies were diluted in PBS with 2% BSA. The following primary antibodies were used: anti-Par3 (1:100 Millipore), anti-Podocalyxin (1:100 R&D), anti-VE-cadherin (1:100 C-19, sc-6458, goat, Santa Cruz Biotechnology) and anti-β-catenin (1:50 BD Transduction Laboratories). Secondary antibodies for immunofluorescence were donkey antibodies to the appropriate species conjugated with Alexa Fluor 488, 555 or 647 (dilution 1:200 or 1:400).

For imaging, charge-coupled device camera on epifluorescence microscope (Leica) or Leica TCS SP2 confocal microscopy were used. ImageJ (NIH) was employed for data analysis. Figures were assembled using Adobe Photoshop and Adobe Illustrator. Only adjustments of brightness and contrast were used in the preparation of the figures. For comparison purposes, different sample images of the same antigen were acquired under constant acquisition settings.

Immunoblot analysis. Cells were lysed in Laemmli buffer and proteins were separated using SDS–PAGE and analysed with western blotting. The following primary antibodies were used: anti-Nova2 (1:200 Santa Cruz Biotechnology, C-16), anti-GAPDH (1:5,000 Abcam; 1:50,000 AbFrontier), anti-Tubulin (1:100,000 Sigma-Aldrich), anti-total-Pak4 (1:1,000 Cell Signaling), anti-phospho-Pak4 (1:1,000 Cell Signaling), anti-haemagglutinin (HA; 1:1,000 Covance), anti-total-PKCζ (1:1,000 Abcam), anti-phospho-PKCζ (1:1,000 Cell Signaling) and anti-Actin (1:500 Santa Cruz Biotechnology). The following secondary antibodies linked to horseradish peroxidase (Jackson ImmunoResearch) were used: anti-Mouse (1:10,000), anti-Goat (1:5,000) and anti-Rabbit (1:10,000). Immunostained bands were detected using the chemiluminescent method (Pierce).

Retinal immunohistochemistry. All animal work using mice was conducted in accordance with the Swedish Animal Welfare Board at the Karolinska Institutet, Stockholm, Sweden. Eyes retrieved from pups at P6 were fixed in cold 100% MeOH and stored at − 20 °C before dissection. After dissection, retinas were incubated in 5% donkey sera, 1% BSA and 0.5% Triton X-100 in PBS overnight and then incubated with antibodies towards Nova2 (Santa Cruz Biotechnology, C-16), PECAM (BD Bioscience, MEC13.3) and ERG (Abcam, ab92513) overnight. For secondary detection, retinas were incubated with fluorescently conjugated antibodies (Jackson ImmunoResearch) and mounted flat with ProLong Gold (Invitrogen).

Immunohistochemistry. All procedures involving human samples were approved by the Istituto Europeo di Oncologia (IEO) Ethical Committee. When possible, a written informed consent for research use of biological samples was obtained from all patients, and the research project was approved by the Institutional IEO Ethical Committee. Immunohistochemistry (IHC) was performed using 3-μm sections from formalin-fixed and paraffin-embedded tissue samples. Samples were rehydrated through xylene and graded alcohols. Antigen retrieval was accomplished using 10 mM sodium citrate, 0.05% Tween20, pH 6.0. Samples were then incubated with 3% H_2O_2 for 5 min, followed by 30 min of blocking in 2% BSA and 0.05% Tween20, and then by the incubation with goat anti-Nova2 (1:100 Santa Cruz Biotechnology, C-16) overnight at 4 °C in 2% BSA and 0.02% Tween20. Immunocomplexes were visualized with LSAB + System-HRP, DAKO (K0690) and acquired with the Aperio ScanScope system. Slides were counterstained with haematoxylin for histological evaluation. Double IHC was performed as follows: antigen retrieval was accomplished using 1 mM EDTA, 0.05% Tween. Samples were then incubated with 3% H_2O_2 for 5 min, followed by 30 min of blocking in 2% BSA and 0.02% Tween20, and then were incubated with a mix of goat anti-Nova2 (1:200) and mouse anti-CD31 (1:60 DAKO, Clone JC70A) in 2% BSA and 0.02% Tween20 for 2 h at room temperature. Immunocomplexes were visualized with an

Appendix

anti-goat horseradish peroxidase (HRP) detection system (Goat-on-Rodent HRP-Polymer, Biocare Medical), for 30 min at RT, followed by incubation with a Goat Anti-Mouse AP Polymer detection system (MACH 2 Mouse AP-Polymer Biocare Medical) for 30 min at RT. CD31 was visualized in red using the Vulcan Fast Red Chromogen (Biocare Medical) and Nova2 was visualized in green using the Vina Green Chromogen Kit (Biocare Medical) according to the manufacturer's protocol.

Migration assay. To analyse cell migration, the wound-healing technique was used. Briefly, confluent EC monolayers on a tissue culture dish were wounded by manually scratching with a pipette tip after an overnight starving, washed with starving medium and incubated at 37 °C for 8 h in complete media containing Mitomycin C (4 $\mu g\,ml^{-1}$). The wound-induced cell migration was followed by staining with fluorescent phalloidin (10 μM, Sigma).

Paracellular flux. Mouse ECs were seeded on 0.4-μm pore size Transwell Permeable Supports (Corning) cultured in complete culture medium before assaying permeability. Next, fluorescein isothiocyanate dextran (70 kDa; Sigma) was added to the medium of the transwell apical compartment. At different times of incubation, a 50-μl aliquot of the medium was collected from the basal compartment, and the paracellular tracer flux was measured as the amount of fluorescein isothiocyanate dextran in the medium using a fluorometer.

3D culture in collagen gels. HUVECs were transduced with GIPZ lentiviral vectors (Open Biosystems) carrying shRNA for Nova2 or control shRNA. Control and *Nova2* knockdown HUVECs were cultured in 3D collagen gel. The final cell density in collagen (3.5 $mg\,ml^{-1}$ final concentration collagen type1 from rat tail, High Concentration, BD Biosciences) was 5×10^5 $cells\,ml^{-1}$. Culture medium was 199 with 1% FCS, Insulin-Transferrin-Selenium supplement (Life Technologies), 50 $ng\,ml^{-1}$ phorbol myristate acetate, 50 $\mu g\,ml^{-1}$ ascorbic acid, 40 $ng\,ml^{-1}$ VEGF and 40 $ng\,ml^{-1}$ bFGF. For confocal microscopy, 190 μl cell suspension in collagen was used for each microwell (μ-slide 80826, Ibidi, Germany). 3D cultures were fixed with 3% PAF for 35 min, quenched with 75 mM NH_4Cl and 20 mM glycine in PBS, pH 8, for 10 min and blocked with 0.7% FSG and 0.3% Triton X-100 PBS (blocking buffer) for 30 min. Primary and secondary antibodies were incubated overnight at 4°C. Primary antibody contained 5% donkey serum. Washes in blocking buffer were performed over the course of a day at room temperature. For immunofluorescence, the following primary antibodies were used: anti-Podocalyxin (R&D, 1:400) and anti-Coll IV (AbD Serotech, 1:200). Secondary antibodies for immunofluorescence were donkey antibodies to the appropriate species conjugated with Alexa Fluor 488, 555 or 647 (dilution 1:200 or 1:400).

Plasmids. Mouse Pix-α-FL fused to HA-tag was amplified with primers SG57-F and SG56-R (Supplementary Table 9) and was cloned in pcDNA3.1(+) vector (Invitrogen), whereas Pix-α-Δ17 was generated by PCR-mediated mutagenesis of Pix-α-FL (using primers SG55-F/-R and SG56-F/-R). All constructs were verified by sequencing.

RNA extraction and RT–PCR. Total RNA was isolated using the RNeasy Mini Kit (QIAGEN) according to the manufacturer's instructions. After treatment with DNase (Ambion), 2–3 μg of RNA was retro-transcribed with mix of $d(T)_{18}$ oligos and random hexamers or gene-specific primers (Supplementary Table 10) and Superscript III RT (Invitrogen). An aliquot (1/20th) of RT was then PCR-amplified. For qPCR, an aliquot of the RT reaction was analysed with QuantiTect SYBR Green PCR (QIAGEN) by using LyghtCycler 480 (Roche). Target transcript levels were normalized to those of reference gene. The expression of each gene was measured in at least three independent experiments. All primers are listed in Supplementary Tables 6 and 7. AS bands were quantified using densitometric analysis.

Pull down of GTP-bound Cdc42. Nova2-depleted and control mouse ECs cultured in 100-mm Petri dishes were analysed for Cdc42 activity by using the Cdc42 Activation Assay Kit (Abcam) according to the manufacturer's instructions. For experiments with *Pix-α* minigenes, cells were transfected with Lipofectamine 3000 (Invitrogen) and grown to reach confluence before the beginning of the pull down.

Zebrafish strains and maintenance. Zebrafish (*Danio rerio*) from wild-type *AB* and transgenic *Tg(fli1a:EGFP)y1* (ref. 41) strains were maintained and bred according to the national guidelines (Italian decree '4 march 2014, n.26'). All experimental procedures were approved by the FIRC Institute of Molecular Oncology Institutional Animal Care and Use Committee.

***In situ* hybridization on zebrafish embryos and sections.** Zebrafish *nova2* cDNA was amplified using PCR (primers CG13F and CG13R in Supplementary Table 9) and cloned into pCRII-TOPO vector (Invitrogen). The antisense RNA probe was generated using T7 RNA Polymerase and digoxigenin-labelled UTPs (kit from Roche) and was purified with the RNeasy Mini Kit (QIAGEN) according to the manufacturer's instructions. Whole embryos of different developmental stages were fixed overnight in 4% PFA, washed in PBS and pre-incubated for 2 h at 63 °C in hybridization buffer. Next, the *nova2* probe was added to the mix and incubated overnight at 63 °C. Embryos were then washed in SSC buffer and pre-incubated for 2 h in blocking medium at room temperature. A ratio of 1:2,000 anti-DIG antibody conjugated with alkaline phosphatase (Roche) was added and incubated overnight at 4 °C. After several PBS washes, embryos were incubated in NBT/BCIP staining buffer. Stained embryos were then equilibrated in glycerol 85% in PBS overnight at 4 °C and were observed with a stereomicroscope equipped with optic fibres. To prepare 50-μm transversal sections of 48- hpf embryos, previously stained by *in situ* hybridization, we cut them in PBS with a vibratome after inclusion in 5% low-melting agarose. Sections obtained were equilibrated and mounted in glycerol 85% in PBS on glass slides and observed under a Nikon Upright microscope. All images were acquired with high-resolution digital cameras (Nikon).

To detect the mRNA expression of *Rap1gap* and *Pix-α/Arhgef6* genes and GFP, we use 5-μm paraffin sections of the head of 48-hpf *Tg(fli1a:EGFP)y1* embryos fixed overnight with 4% PFA in PBS. To orientate embryos in the proper way before including in paraffin and cutting microtome sections, we have pre-included them in 1% low-melting agarose (in PBS) under a dissecting microscope with optic fibers, using plastic base moulds of 7 mm of diameter. Paraffin was removed with xylene and sections were rehydrated through graded EtOH washes, permeabilized with Proteinase-K and HCl 2 N and were incubated overnight at 64 °C in hybridization mix with DIG-labelled LNA probes for *Rap1gap* (5′-TTCACCTCTT CACAGACAAGCT-3′) and *Pix-α/Arhgef6* (5′-TAGACGTAGAGGTGTTGG ACT-3′) (designed and produced by Exiqon). Sections were then treated overnight at 4 °C with an anti-DIG antibody (1:2,000 Roche) conjugated with AP and stained with NBT/BCIP. After several washes in PBS, embryo sections were incubated overnight at 4 °C with mouse anti-GFP antibody (Upstate, 1:200) and labelled using the *Vina Green Chromogen kit* (Biocare Medical).

Zebrafish haematoxylin–eosin staining and immunofluorescence. Agarose was used to embed 24- and 48-h zebrafish embryos before including in paraffin and cutting microtome 10-μm sections. Sections were stained with haematoxylin– eosin to assess the histological features. For immunofluorescence, paraffin was removed with xylene and the sections were rehydrated in graded alcohol. Antigen retrieval was carried out using preheated target retrieval solution (pH 6.0) for 45 min. Tissue sections were blocked with FBS serum in PBS for 90 min and incubated overnight with the following primary antibodies: GFP (1:100 Millipore), Phosphohistone H3 (PHH3, 1:100 Millipore), Caspase3 (1:100 Cell Signaling) and Podocalyxin (Podxl2 1:200, kindly provided by Heinz-Georg Belting). Alexa Fluor-conjugated antibodies were used for the immunodetection, and all sections were counterstained with 4,6-diamidino-2-phenylindole (DAPI) and visualized using a Confocal microscope (Leica SP2).

Morpholino injections and RT–PCR of zebrafish embryo. Zebrafish embryos at one- to two-cell stage were injected with 6.7 ng of an ATG-morpholino antisense oligonucleotide (Supplementary Table 8), designed to block translation of the zebrafish *nova2* gene (ENSDARG00000017673). To analyse the kinetics and the pattern of formation of the ISVs, we mounted in 1.2% low-melting agarose in E3 water *Tg(fli1a:EGFP)y1*-dechorionated embryos at 22 hpf, previously anaesthetized using 15 $mg\,l^{-1}$ of tricaine (Sigma). Image acquisition was performed overnight every 10 min with a ×40 water immersion objective on a Leica TCS SP2 confocal microscope. Confocal stacks from each time point were processed for maximum intensity projections and, subsequently, movies were generated with the Leica LCS software. To observe and evaluate the shape and function of the heart, we mounted under a stereomicroscope 48-hpf dechorionated embryos in 3% methyl-cellulose in E3 water, previously anaesthetized using 15 $mg\,l^{-1}$ of tricaine (Sigma). Using high-resolution digital camera (Nikon), we acquired 13-s movies from both control and *nova2* morphant embryos. Total RNA was extracted from 24-hpf pooled embryos with TRIzol reagent (Invitrogen), purified with the RNeasy Mini Kit (QIAGEN) and retro-transcribed with $d(T)_{18}$ oligo or gene-specific primer and Superscript III RT (Invitrogen) and then analysed in PCR for AS modification of *nova2* targets. To rescue morphological and vascular defects due to the knockdown of *nova2*, we amplified with primers CG30F/CG13R (Supplementary Table 9) by using RT generated from *Tg(fli1a:EGFP)y1* embryos, a morpholino-resistant zebrafish *nova2* cDNA, with six mismatches in the pairing region with the morpholino, which, however, do not alter the amino-acid sequence of the translated protein. We cloned this cDNA in pCRII-TOPO vector (Invitrogen) and we transcribed *in vitro* the capped mRNA using SP6 mMessage mMachine kit (Ambion). Co-injection in one- to two-cell stage embryos of 6.7 ng of MO-nova2 and 160 pg of each *nova2* mRNAs was performed. The molecular and morphological changes of *nova2* morphants were scored at 28 hpf.

Generation of new fish line for endothelial-specific rescue. To drive Nova2 expression selectively in the zebrafish vascular endothelium, we cloned the morpholino-resistant zebrafish *nova2* cDNA into the pTolfli1epCherryDest vector[56] in frame with mCherry at the N terminus under the endothelial *fli1a* enhancer/promoter flanked by Tol2 transposable elements (*pTolfli1:nova2-CherryDest*). Fertilized eggs from *casper* x *Tg(fli1a:EGFP)y1* mutant/transgenic line were injected

Appendix

with 2 nl of a mixture containing 25 ng μl^{-1} of the circular plasmid *pTolfli1:nova2-CherryDest* and 25 ng μl^{-1} of T2 transposase mRNA. Injected embryos were selected for simultaneous expression of GFP and mCherry in the vessels, raised to adulthood and crossed with *casper* × *Tg(fli1a:EGFP)y1* fish. F1 embryos were observed under a fluorescent dissecting microscope from days 1 to 5 after fertilization to select carrier fish of the new mutant/double transgenic line *casper* × *Tg(fli1a:EGFP)y1* + *Tg(fli1:nova2-mCherry)*.

To assay the capability of *nova2* mRNA to rescue *nova2* morphant phenotype specifically in the vessel endothelium, we performed two experiments. Co-injection of 6.7 ng of MO-nova2, 50 pg of the rescuing DNA construct *pTolfli1:nova2-CherryDest* and 120 pg of Tol2 transposase mRNA was performed directly into the cytoplasm of one-cell stage *casper* × *Tg(fli1a:EGFP)y1* embryos. The phenotype of the vessels of the resulting 'mosaic' embryos was scored at 28 hpf. Alternatively, injection of 6.7 ng of MO-nova2 was performed into one-cell stage *casper* × *Tg(fli1a:EGFP)y1* + *Tg(fli1:nova2-mCherry)* embryos. The phenotype of all the vessels of the resulting embryos was scored at 28 hpf.

Immunofluorescence staining of zebrafish embryos. Zebrafish embryos from the *Tg(fli1a:EGFP)y1* strain at 48 hpf were dechorionated and fixed in 2% PFA in PBS, overnight at 4 °C. Embryos were then washed four times for 5 min in PBST (PBS + 0.1% Tween20). Permeabilization in PSBT + 0.5% Triton X-100 was performed for 30 min at room temperature. Embryos were then blocked in a solution of PBST + 0.5% Triton X-100, 10% normal goat serum and 1% BSA for 2 h at room temperature. Embryos were incubated with primary antibodies in blocking solution overnight at 4 °C. Successively, embryos were washed six times in PBST over 4 h at room temperature and then incubated with secondary antibodies in blocking solution, overnight at 4 °C. Embryos were washed finally six times in PBST over 4 h at room temperature and equilibrated in glycerol 85% in PBS. The following antibodies were used: mouse anti-GFP (1:2,000 Millipore); rabbit anti-podocalyxin (1:150 kindly provided by Heinz-Georg Belting); rabbit anti-mouse Alexa-488-conjugated IgG (1:400); and goat anti-rabbit Alexa 546-conjugated IgG (1:400). For the microscope analysis, we mounted on slides the trunk and tail regions dissected from five to six embryos of each samples. Images were taken with a Leica TCS SP2 confocal microscope, using oil-immersion objective × 40.

Generation of nova2 zebrafish mutant by CRISPR/Cas9. To identify the best target site and to design the single guide RNA (gRNA), we submitted to the ZiFiT targeter website (http://zifit.partners.org/ZiFiT) the sequence of the first exon of the zebrafish *nova2* gene. Oligonucleotides corresponding to the target region (see Supplementary Fig. 11A and Supplementary Table 11) were annealed and cloned into the pDR274 gRNA expression vector (Addgene, 42250) immediately upstream of the crRNA:trascRNA backbone. The *nova2* genomic target sequence starts with two GG nucleotides at the 5′ end for efficient transcription from the T7 promoter and ends with the protospacer-adjacent motif. The correct position of the target sequence into the pDR274 plasmid was verified through sequencing, using M13-Rev primer (Supplementary Table 11). The *nova2* gRNA was *in vitro* transcribed and purified from DraI-digested plasmid as template, using the Maxiscript T7 Kit (Life Technologies). Capped and polyadenylated *Cas9* mRNA was *in vitro* transcribed and purified from 1 μg of PmeI-digested pMLM3613 Cas9 expression vector (Addgene, 42251) as a template, using the mMessage mMachine T7 ULTRA kit (Life Technologies).

A volume of 2 nl of a solution containing ~13 ng μl^{-1} of *nova2* gRNA and ~300 ng μl^{-1} of *Cas9* mRNA was co-injected in one-cell stage zebrafish embryos. On the next day, only embryos with a normal morphological phenotype were allowed to grow. To evaluate the efficiency of Cas9 nuclease activity, genomic DNA was extracted from 48-hpf single injected embryos and the *nova2*-targeted genomic locus was amplified from genomic DNA of each embryo (primers n2-locus-F and n2-locus-R in Supplementary Table 11). PCR products were then processed for the T7 Endonuclease I (T7EI) assay. PCR products were denaturated at 95 °C and rapidly re-annealed using a PCR thermocycler. PCR products were then incubated for 20 min with T7EI enzyme at room temperature, and the digestion products were visualized on 2% agarose gels. We found that 95% of the injected embryos had mutations at the level of the *nova2* target site.

To analyse the kinds of mutations obtained at the level of the *nova2* locus, we sequenced PCR products, cloned into pCRII-TOPO plasmid using the TOPO TA cloning kit (Life Technologies), amplified from genomic DNA extracted from fin-fragments of 2-month fishes. Among these fishes, we isolated those carrying the mutation also in the germline and subsequently we selected from their progeny fishes with nonsense or missense mutations in the *nova2* locus. A male carrying a nonsense mutation was crossed with a female from the *Tg(kdrl:EGFP)* line to generate a double *EGFP* transgenic-*nova2* mutant line expressing the EGFP reporter in vascular ECs and allowing to characterize the vascular phenotype of *nova2* mutants.

o-dianisidine staining. For histochemical staining of haemoglobin, 72 hpf live embryos were incubated with o-dianisidine staining solution (40% ethanol, 0.01 M sodium acetate, 0.65% H_2O_2, 0.6 mg ml^{-1} o-dianisidine (Sigma, D-9143) for 15 min. Embryos were then washed with PBS, post-fixed in 4% PFA in PBS overnight at 4 °C and stored in 85% glycerol for microscope analysis.

RNAseq and splicing analysis. RNAseq was conducted on two control and two *Nova2*-depleted ECs. Samples were sequenced on Illumina HiSeq2500 (average of ~93 million, 100-nucleotide (nt) paired-end reads for each run). We employed *vast-tools*[32] to identify and quantify all major types of AS events, including single and multiple cassette exons and microexons, alternative 5′ and 3′ splice sites and alternatively retained introns, from each RNAseq sample. *vast-tools* map reads to comprehensive sets of exon–exon junctions (EEJs) and exon–intron junctions (EIJs) to derive alternative sequence inclusion levels (PSIs, 'Percent Spliced In', for exons; PIR, 'Percent Intron Retention', for introns)[57]. We then compared the two replicates of *Nova2* knockdown ECs versus control ECs. Differentially regulated AS events were defined as those showing an absolute ΔPSI ≥ 15 between knockdown and control means and a ΔPSI ≥ 5 between the ranges of the two groups. Only AS events with a minimum read coverage in all four samples were compared, which was defined as:

- For cassette exons (except for those quantified using the microexon pipeline, see Irimia *et al.*[32] for details): (i) ≥ 10 reads mapping to the sum of exclusion EEJs or (ii) ≥ 10 reads mapping to one of the two inclusion EEJs and ≥ 5 to the other inclusion EEJ.
- For microexons: (i) ≥ 10 reads mapping to the sum of exclusion EEJs or (ii) ≥ 10 reads mapping to the sum of inclusion EEJs.
- For intron retention: (i) ≥ 10 reads mapping to the sum of skipping EEJs or (ii) ≥ 10 reads mapping to one of the two inclusion EIJs and ≥ 5 to the other inclusion EIJ.
- For alternative 3′ and 5′ splice sites: ≥ 10 reads mapping to the sum of all EEJs involved in the specific event.

Additional filtering was used to remove intron retention events with a binomial *P* value score above 0.05 in any of the four samples[57].

This resulted in 365 differentially regulated AS events (Supplementary Fig. 4 and Supplementary Table 1), which were subdivided according to the predicted impact of *Nova2* knockdown on the coding sequence (Supplementary Fig. 5A): (i) AS events predicted to generate protein isoforms both when Nova2 is present or depleted (150, 41.1%); (ii) AS events predicted to trigger nonsense-mediated decay (NMD) or create a truncated protein when Nova2 is present (135, 37.0%); (iii) AS events predicted to trigger NMD or to create a truncated protein when Nova2 is absent (33, 9.0%); (iv) AS events in noncoding regions (40, 11.0%); and (v) AS events not able to be categorized into previous categories (7, 2%).

GO analysis was performed for each of the subdivided groups using ClueGO[58]. The background reference was based on multiexonic genes with the same minimum read coverage in the endothelium used above. Two categories had significant enrichment (P value < 0.05), those generating protein isoforms ((i) 49 terms enriched in 150 genes; Supplementary Fig. 5B) and those predicted to trigger NMD/disrupted proteins when Nova2 is included ((ii) 15 terms enriched in 135 genes; Supplementary Fig. 5C). Detail of *P* values (as calculated by ClueGO) are found in Supplementary Table 2.

To compare AS events that show differential inclusion on *Nova2* knockdown in ECs to those regulated by Nova proteins in neural cells, we used the 325 cassette exons previously predicted to be Nova targets in the brain[33] (Supplementary Table 3). Nearly all (319/325) exons could be matched to *vast-tools* AS event IDs based on the exact splice site coordinates and official gene symbols. Of these, 195/319 (61%) had enough read coverage to confidently derive inclusion estimates (PSIs) in all four EC RNAseq samples. From these, 28/195 (14.4%) exons showed a ΔPSI ≥ 10 on *Nova2* knockdown in ECs in the same direction as previously predicted for Nova proteins in the brain, compared with only 2/195 (1%) in the opposite direction (Supplementary Fig. 6). This overlap between Nova-regulated exons in endothelial and neural cells is highly significant ($P = 1.93e^{-11}$, hypergeometric test; background event set corresponded to 14,970 cassette exons with a minimal read coverage in the endothelium as described above and in genes with a cRPKM > 2 in neurons[19]). Moreover, several methodological differences suggest that the actual overlapping of Nova2 regulation between endothelial and neural cells may be even higher. First, predictions of Zhang *et al.*[33] include Nova1 and Nova2 targets, which may not be fully redundant. Second, exons described in Zhang *et al.* are predicted to be Nova protein targets based on Nova binding and presence of binding sites, among others. However, only half of the full set of Nova targets shows measurable differences in PSI in Nova knockout mice[33]. Finally, Nova2 proteins may use different cofactors that may be differentially expressed between endothelial and neural cells.

References

1. Chung, A. S. & Ferrara, N. Developmental and pathological angiogenesis. *Annu. Rev. Cell Dev. Biol.* **27,** 563–584 (2011).
2. Potente, M., Gerhardt, H. & Carmeliet, P. Basic and therapeutic aspects of angiogenesis. *Cell* **146,** 873–887 (2011).
3. Zacchigna, S., Lambrechts, D. & Carmeliet, P. Neurovascular signalling defects in neurodegeneration. *Nat. Rev. Neurosci.* **9,** 169–181 (2008).
4. Segura, I., De Smet, F., Hohensinner, P. J., Ruiz de Almodovar, C. & Carmeliet, P. The neurovascular link in health and disease: an update. *Trends Mol. Med.* **15,** 439–451 (2009).

Appendix

5. Pan, Q., Shai, O., Lee, L. J., Frey, B. J. & Blencowe, B. J. Deep surveying of alternative splicing complexity in the human transcriptome by high-throughput sequencing. *Nat. Genet.* **40,** 1413–1415 (2008).
6. Wang, E. T. *et al.* Alternative isoform regulation in human tissue transcriptomes. *Nature* **456,** 470–476 (2008).
7. Chen, M. & Manley, J. L. Mechanisms of alternative splicing regulation: insights from molecular and genomics approaches. *Nat. Rev. Mol. Cell Biol.* **10,** 741–754 (2009).
8. Nilsen, T. W. & Graveley, B. R. Expansion of the eukaryotic proteome by alternative splicing. *Nature* **463,** 457–463 (2010).
9. Blencowe, B. J. Alternative splicing: new insights from global analyses. *Cell* **126,** 37–47 (2006).
10. Le, K. *et al.* Detecting tissue-specific regulation of alternative splicing as a qualitative change in microarray data. *Nucleic Acids Res.* **32,** e180 (2004).
11. Pan, Q. *et al.* Revealing global regulatory features of mammalian alternative splicing using a quantitative microarray platform. *Mol. Cell* **16,** 929–941 (2004).
12. Palumbo, A. *et al.* A chemically modified antibody mediates complete eradication of tumours by selective disruption of tumour blood vessels. *Br. J. Cancer* **104,** 1106–1115 (2011).
13. Neri, D. & Bicknell, R. Tumour vascular targeting. *Nat. Rev. Cancer* **5,** 436–446 (2005).
14. Bazigou, E. *et al.* Integrin-alpha9 is required for fibronectin matrix assembly during lymphatic valve morphogenesis. *Dev. Cell* **17,** 175–186 (2009).
15. Bazigou, E. *et al.* Genes regulating lymphangiogenesis control venous valve formation and maintenance in mice. *J. Clin. Invest.* **121,** 2984–2992 (2011).
16. Ule, J. *et al.* Nova regulates brain-specific splicing to shape the synapse. *Nat. Genet.* **37,** 844–852 (2005).
17. Taddei, A. *et al.* Endothelial adherens junctions control tight junctions by ve-cadherin-mediated upregulation of claudin-5. *Nat. Cell Biol.* **10,** 923–934 (2008).
18. Yang, Y. Y., Yin, G. L. & Darnell, R. B. The neuronal rna-binding protein nova-2 is implicated as the autoantigen targeted in poma patients with dementia. *Proc. Natl Acad. Sci. USA* **95,** 13254–13259 (1998).
19. Zhang, Y. *et al.* An rna-sequencing transcriptome and splicing database of glia, neurons, and vascular cells of the cerebral cortex. *J. Neurosci.* **34,** 11929–11947 (2014).
20. Yan, Q. *et al.* Systematic discovery of regulated and conserved alternative exons in the mammalian brain reveals nmd modulating chromatin regulators. *Proc. Natl Acad. Sci. USA* **112,** 3445–3450 (2015).
21. Ule, J. *et al.* An rna map predicting nova-dependent splicing regulation. *Nature* **444,** 580–586 (2006).
22. Hellström, M. *et al.* Dll4 signalling through notch1 regulates formation of tip cells during angiogenesis. *Nature* **445,** 776–780 (2007).
23. Iruela-Arispe, M. L. & Davis, G. E. Cellular and molecular mechanisms of vascular lumen formation. *Dev. Cell* **16,** 222–231 (2009).
24. Solecki, D. J., Govek, E., Tomoda, T. & Hatten, M. E. Neuronal polarity in CNS development. *Genes Dev.* **20,** 2639–2647 (2006).
25. Lampugnani, M. G. *et al.* Ccm1 regulates vascular-lumen organization by inducing endothelial polarity. *J. Cell Sci.* **123,** 1073–1080 (2010).
26. Koh, W., Mahan, R. D. & Davis, G. E. Cdc42- and rac1-mediated endothelial lumen formation requires pak2, pak4 and par3, and pkc-dependent signaling. *J. Cell Sci.* **121,** 989–1001 (2008).
27. Yamanaka, T. *et al.* Par-6 regulates apkc activity in a novel way and mediates cell-cell contact-induced formation of the epithelial junctional complex. *Genes Cells* **6,** 721–731 (2001).
28. Jaffer, Z. M. & Chernoff, J. P21-activated kinases: three more join the pak. *Int. J. Biochem. Cell Biol.* **34,** 713–717 (2002).
29. Strilić, B. *et al.* The molecular basis of vascular lumen formation in the developing mouse aorta. *Dev. Cell* **17,** 505–515 (2009).
30. Bayless, K. J. & Davis, G. E. The cdc42 and rac1 gtpases are required for capillary lumen formation in three-dimensional extracellular matrices. *J. Cell Sci.* **115,** 1123–1136 (2002).
31. Oubaha, M. *et al.* Formation of a pkcζ/β-catenin complex in endothelial cells promotes angiopoietin-1-induced collective directional migration and angiogenic sprouting. *Blood* **120,** 3371–3381 (2012).
32. Irimia, M. *et al.* A highly conserved program of neuronal microexons is misregulated in autistic brains. *Cell* **159,** 1511–1523 (2014).
33. Zhang, C. *et al.* Integrative modeling defines the nova splicing-regulatory network and its combinatorial controls. *Science* **329,** 439–443 (2010).
34. Sakurai, A. *et al.* Magi-1 is required for rap1 activation upon cell-cell contact and for enhancement of vascular endothelial cadherin-mediated cell adhesion. *Mol. Biol. Cell* **17,** 966–976 (2006).
35. Tsygankova, O. M., Wang, H. & Meinkoth, J. L. Tumor cell migration and invasion are enhanced by depletion of rap1 gtpase-activating protein (rap1gap). *J. Biol. Chem.* **288,** 24636–24646 (2013).
36. Baird, D., Feng, Q. & Cerione, R. A. The cool-2/alpha-pix protein mediates a cdc42-rac signaling cascade. *Curr. Biol.* **15,** 1–10 (2005).
37. Liu, Z., Adams, H. C. 3. & Whitehead, I. P. The rho-specific guanine nucleotide exchange factor dbs regulates breast cancer cell migration. *J. Biol. Chem.* **284,** 15771–15780 (2009).
38. Miyamoto, Y., Yamauchi, J., Sanbe, A. & Tanoue, A. Dock6, a dock-c subfamily guanine nucleotide exchanger, has the dual specificity for rac1 and cdc42 and regulates neurite outgrowth. *Exp. Cell Res.* **313,** 791–804 (2007).
39. Montero-Balaguer, M. *et al.* Stable vascular connections and remodeling require full expression of ve-cadherin in zebrafish embryos. *PLoS ONE* **4,** e5772 (2009).
40. Jelen, N., Ule, J., Zivin, M. & Darnell, R. B. Evolution of nova-dependent splicing regulation in the brain. *PLoS Genet.* **3,** 1838–1847 (2007).
41. Lawson, N. D. & Weinstein, B. M. In vivo imaging of embryonic vascular development using transgenic zebrafish. *Dev. Biol.* **248,** 307–318 (2002).
42. Quaegebeur, A., Lange, C. & Carmeliet, P. The neurovascular link in health and disease: molecular mechanisms and therapeutic implications. *Neuron* **71,** 406–424 (2011).
43. Hwang, W. Y. *et al.* Efficient genome editing in zebrafish using a CRISPR-Cas system. *Nat. Biotechnol.* **31,** 227–229 (2013).
44. Jensen, K. B. *et al.* Nova-1 regulates neuron-specific alternative splicing and is essential for neuronal viability. *Neuron* **25,** 359–371 (2000).
45. Ruggiu, M. *et al.* Rescuing Z+ agrin splicing in Nova null mice restores synapse formation and unmasks a physiologic defect in motor neuron firing. *Proc. Natl Acad. Sci. USA* **106,** 3513–3518 (2009).
46. Seshaiah, P., Miller, B., Myat, M. M. & Andrew, D. J. Pasilla, the drosophila homologue of the human nova-1 and nova-2 proteins, is required for normal secretion in the salivary gland. *Dev. Biol.* **239,** 309–322 (2001).
47. Irimia, M. *et al.* Stepwise assembly of the nova-regulated alternative splicing network in the vertebrate brain. *Proc. Natl Acad. Sci. USA* **108,** 5319–5324 (2011).
48. Pirraglia, C., Walters, J. & Myat, M. M. Pak1 control of e-cadherin endocytosis regulates salivary gland lumen size and shape. *Development* **137,** 4177–4189 (2010).
49. Ramahi, J. S. & Solecki, D. J. The par polarity complex and cerebellar granule neuron migration. *Adv. Exp. Med. Biol.* **800,** 113–131 (2014).
50. Martin-Belmonte, F. *et al.* Pten-mediated apical segregation of phosphoinositides controls epithelial morphogenesis through cdc42. *Cell* **128,** 383–397 (2007).
51. Choi, S. Y. *et al.* Cdc42 deficiency causes ciliary abnormalities and cystic kidneys. *J. Am. Soc. Nephrol.* **24,** 1435–1450 (2013).
52. Jin, Y. *et al.* Deletion of cdc42 enhances adam17-mediated vascular endothelial growth factor receptor 2 shedding and impairs vascular endothelial cell survival and vasculogenesis. *Mol. Cell Biol.* **33,** 4181–4197 (2013).
53. Zlokovic, B. V. The blood-brain barrier in health and chronic neurodegenerative disorders. *Neuron* **57,** 178–201 (2008).
54. Tollervey, J. R. *et al.* Analysis of alternative splicing associated with aging and neurodegeneration in the human brain. *Genome Res.* **21,** 1572–1582 (2011).
55. Ule, J. *et al.* Clip identifies nova-regulated rna networks in the brain. *Science* **302,** 1212–1215 (2003).
56. Villefranc, J. A., Amigo, J. & Lawson, N. D. Gateway compatible vectors for analysis of gene function in the zebrafish. *Dev. Dyn.* **236,** 3077–3087 (2007).
57. Braunschweig, U. *et al.* Widespread intron retention in mammals functionally tunes transcriptomes. *Genome Res.* **24,** 1774–1786 (2014).
58. Bindea, G. *et al.* ClueGO: a Cytoscape plug-in to decipher functionally grouped gene ontology and pathway annotation networks. *Bioinformatics* **25,** 1091–1093 (2009).

Acknowledgements

We thank Professor Natan Lawson for pTolfli1epCherryDest plasmid; Dr Heinz-Georg Belting and Professor Markus Affolter for antibody against zebrafish Podxl2; Dr Davide Gabellini for helpful discussion; Dr Maria Paola Paronetto for critical reading of the manuscript; the IFOM (FIRC Institute of Molecular Oncology) Zebrafish Facility; DNA Sequencing Facility Unit—Cogentech c/o IFOM-IEO Campus; Professor Giuseppe Viale (IEO) for providing normal human tissues; Progetto d'Interesse Invecchiamento (CNR-MIUR). Dax Torti of the Donnelly Sequencing Centre is gratefully acknowledged for sequencing samples. This work was supported by grants from the Associazione Italiana per la Ricerca sul Cancro (AIRC, project 11913), the Association for International Cancer Research (AICR-UK, project 11–0622), Fondazione Banca del Monte di Lombardia to C.G.3 and grants from the Associazione Italiana per la Ricerca sul Cancro (AIRC, project 14471), 'Special Program Molecular Clinical Oncology 5 × 1000'—AGIMM (AIRC-Gruppo Italiano Malattie Mieloproliferative), the European Research Council (project EU-ERC 268870), the European Community (ITN VESSEL 317250), CARIPLO Foundation (project 2012-0678) and Telethon (project GGP14149) to E.D. Work in P.P.D.F. laboratory was supported by grants from the Associazione Italiana per la Ricerca sul Cancro (AIRC IG 14404 and MCO 10.000), MIUR (the Italian Ministry of University and Scientific Research), the Italian Ministry of Health and the Monzino Foundation. D.N. was supported by grants from the Swedish Research Council and the Swedish Society of Medical Research. C.D.R.W. is supported by a 'La Caixa/Severo

Appendix

Ochoa' pre-doctoral fellowship. B.J.B. is supported by operating grants from the Canadian Institutes for Health Research and holds the Banbury Chair in Medical Research at the University of Toronto. S.G. is awarded a Fondazione Adriano Buzzati Traverso postdoctoral fellowship.

Author contributions

C.G.[1,2] and S.G. designed and performed *in vitro* experiments; G.D., V.Q., E.B. and F.P. performed *in vivo* experiments in zebrafish embryos; D.N. performed analysis in mouse retina; S.C. and G.B.[6] performed the IHC analysis and discussed the results with PPDF; S.B., A.D.M., G.B.[3], D.P., E.F.[8], C.T., F.O. and E.F.[7] performed the experiments and discussed the results; C.D.R.W., M.I. and B.J.B. performed bioinformatic analysis and discussed the results; C.G.[3] and E.D. conceived and designed the study and wrote the manuscript.

Additional information

Accession codes. RNASeq reads are available in the NCBI Sequence Read Archive, under Bioproject code PRJNA293346.

Supplementary Information accompanies this paper at http://www.nature.com/naturecommunications

Competing financial interests: The authors declare no competing financial interests.

Reprints and permission information is available online at http://npg.nature.com/reprintsandpermissions/

How to cite this article: Giampietro, C. *et al.* The alternative splicing factor Nova2 regulates vascular development and lumen formation. *Nat. Commun.* 6:8479 doi: 10.1038/ncomms9479 (2015).

Appendix

Global Journal of Human Genetics & Gene Therapy, 2014, *2*, 1-19

Alternative Pre-mRNA Processing in Cancer Progression: Clinical Significance and Therapeutic Implications

Maria Paola Paronetto[1,2,*], Stefania Gallo[3], Anna di Matteo[3] and Claudia Ghigna[3,*]

[1]*Department of Health Sciences, University of Rome "Foro Italico", 00135 Rome, Italy*

[2]*Laboratory of Cellular and Molecular Neurobiology, Fondazione Santa Lucia IRCSS, 00143 Rome, Italy*

[3]*Istituto di Genetica Molecolare, Consiglio Nazionale delle Ricerche (IGM-CNR), 27100 Pavia, Italy*

Abstract: Alternative pre-mRNA processing is a fundamental step in the regulation of gene expression in eukaryotic cells. The combinatorial assortment of exons in the coding sequence, as well as in the untranslated regions, determines in time and space when a specific protein isoform becomes available to the cell, thus allowing fine regulation of gene expression and expansion of the coding potential of the genome.

Alternative splicing errors, generated by mutations in *cis*-acting regulatory elements or in genes encoding splicing factors, dramatically alter gene regulatory networks and contribute to the combined disruption of tumor suppressor genes and activation of oncogenes, thus causing pathological consequences driving the malignant phenotype. In this regard, recent studies have highlighted that changes in splicing fidelity contribute to every aspect of cancer cell biology. This plastic nature of splicing regulation is emerged as promising source of novel and more specific diagnostic and prognostic markers for human cancer. Notably, its potential for anti-cancer therapy is shown by several clinical trials of splicing regulatory drugs.

In this review, we discuss the current molecular understanding of the alternative splicing alterations contributing to oncogenic transformation and the resistance to traditional chemotherapeutic treatments. The abnormal expression of splicing factors and their regulators will be reviewed in detail. Finally, novel therapeutic approaches that take advantage of antisense oligonucleotides (ASOs) and small molecules able to bind spliceosomal components and splicing regulators will be also discussed.

Keywords: Alternative splicing, cancer, cancer-associated alternative splicing isoforms, anti-cancer therapy.

1. INTRODUCTION

The expression of the eukaryotic 'interrupted' genes is known to be a complex process involving different steps. During transcription by RNA polymerase II, the precursor messenger RNA (pre-mRNA) undergoes 5'end capping, splicing (namely the removal of introns) and cleavage/polyadenylation at its 3'end to generate the mature mRNA that can be exported to the cytoplasm for translation. In particular, introns are excised by a macromolecular complex named spliceosome, which is composed of a specific set of small nuclear ribonucleic particles (RNA-protein complexes known as snRNPs U1, U2, U4, U5 and U6) and many constitutive and auxiliary proteins [1]. For at least 90% of human genes, the removal of introns can be differentially regulated through the alternative splicing reaction in which the choice and usage of 5' and 3' splice sites within the pre-mRNA are finely modulated to produce multiple mRNAs encoding for different protein isoforms [2, 3]. This fundamental step in the regulation of gene expression is the primary source for increasing the functional diversity of the human proteome as it allows to generate an excess of 100,000 different protein isoforms from a relatively small number of ~20,000 protein-coding genes. On the contrary, alternative splicing is far less common in lower organisms suggesting that this process evolved to drive the evolution of complex, multicellular organisms [4, 5].

Similar to other levels of gene expression regulation, the different types of alternative splicing (exon skipping, intron retention, mutually exclusive exons, alternative 5' splice sites and alternative 3' splice site schematically reported in Figure **1**) are achieved by the interaction of *trans*-acting proteins with *cis*-acting sequences. In particular, alternatively spliced exons are often characterized by short and degenerate (or sub-optimal) splice sites that reflect their reduced affinity for the splicing machinery (the spliceosome). The recognition of alternative exons is thus modulated by an additional layer of information provided by regulatory sequences, located both in exons and in the flanking introns, that promote (enhancers) or inhibit (silencers) exon recognition [6] (Figure **2**). Generally, enhancer sequences are recognized by members of the arginine/serine dipeptide repeats (SR)-protein

*Address correspondence to these authors at the Department of Health Sciences, University of Rome "Foro Italico", 00135 Rome, Italy; Tel: +39 06 36733576; Fax: +39 06 32650767; E-mail: mariapaola.paronetto@uniroma4.it

Istituto di Genetica Molecolare, Consiglio Nazionale delle Ricerche (IGM-CNR), 27100 Pavia, Italy; Tel: +39 0382 546324; Fax: +39 0382 422286;
E-mail: arneri@igm.cnr.it

E-ISSN: 2311-0309/14

Appendix

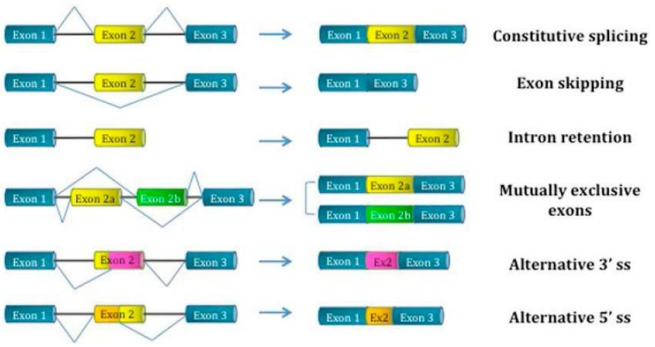

Figure 1: Different types of alternative splicing mechanisms. While constitutive exons are always present in the mature mRNA molecule, alternatively spliced mRNAs result from skipping of an exon cassette (that is sometimes included or excluded from the mRNA), intron retention, usage of alternative 3′- (acceptor) or 5′- (donor) splice sites (ss) and from selection of mutually exclusive exons (in which the mature mRNA contains only one of several possible exon choices). These mechanisms can affect different regions of the pre-mRNA and, at the protein level, drastically change the amino acid sequence by deletions or insertion of domains, frame-shifts or stop codons. Exons (boxes); introns (lines).

family, while the vast group of heterogeneous nuclear ribonucleoproteins (hnRNPs) are able to interact with splicing silencers [6]. The combinatorial control of these splicing factors (often with antagonistic roles) and multiple regulatory *cis*-acting elements is the basis of the extreme accuracy and flexibility of alternative splicing regulation (Figure **2**).

Recently, microarrays and high-throughput sequencing analyses have enabled genome-wide identification of alternative splicing events in diverse biological contexts and conditions, showing that this mechanism is involved in all major aspects of eukaryotic cell biology, including cell proliferation, differentiation, migration, communication, cell death, sex determination, synaptic function and in the response to physiological stimuli [7]. Moreover, alternative splicing is more prominent in complex tissues and in organs characterized by highly plastic and specialized cells, such as the testis and brain [8]. The relevance of tissue-specific alternative splicing is emphasized by the fact that splicing defects play a causative role in several neurodegenerative diseases [9, 10]. In particular, in line with its central role in regulation of gene expression, up to 50–60% of point mutations responsible for genetic diseases in humans cause aberrant splicing [11].

In recent years, the significance of alternative splicing for tumor progression has become more and more evident [12-15]. Cancer is a heterogeneous and complex disease, predominantly driven by genomic alterations, including inherited genetic mutations and acquired genomic aberrations. In a combinatorial fashion, all these effects trigger a generalized mis-regulation of gene expression, thus causing changes in protein functions. Recently, the emphasis is given to the many circuits of epigenetic, transcriptional and post-transcriptional programs that operate in normal cells and that are deregulated and reprogrammed to confer hallmark capabilities to cancer cells [16]. The great plasticity offered by alternative splicing to modify the proteome makes it a precious tool used by cancer cells to produce oncogenic proteins involved in tumor establishment, progression and in resistance to therapeutic treatments. Interestingly, several cancer-related associated genes are controlled by alternative splicing; these genes encode for proteins implicated in all major aspects of cancer cell biology [17-21]. Indeed, computational analyses have demonstrated that for many of these genes the expression ratio between various splice variants significantly differs between cancer and normal cells [22, 23]. Notably, specific splice variants have been shown to be up-regulated in tumors compared with normal tissues [21, 24]. In general, cancer cells preferentially express isoforms that are produced in a regulated manner during development and are normally not present in adult normal tissues [14, 25]. Additionally, some splicing

Appendix

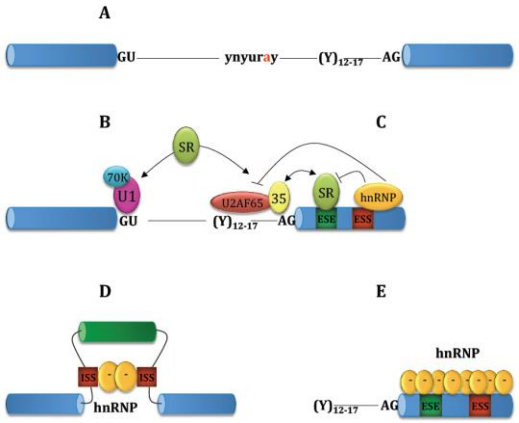

Figure 2: Models for alternative splicing activation and repression. (**A**) The splicing reaction is directed by short consensus sequences (core splicing signals) located within the introns and at the exon-intron boundaries. The 5' splice site (donor) contains a conserved GU dinucleotide marking the beginning of the intron. The 3' splice site (acceptor) comprises: i) a conserved sequence at the intron/exon junction with the intron 3'-end AG dinucleotide, ii) an upstream polypyrimidine tract of variable length and iii) the branch point, typically located 18–40 nucleotides upstream of the 3' splice site and containing an adenosine that is the only conserved residue from yeast to human. The recognition of alternative exons is modulated by auxiliary cis-acting elements, called splicing enhancers that promote exon inclusion, and silencers that stimulate exon skipping. Enhancers (ESEs, Exonic Splicing Enhancers and ISEs, Intronic Splicing Enhancers) represent binding sites for members of the SR protein family, whereas silencers (ESSs, Exonic Splicing Silencers and ISSs, Intronic Splicing Silencers) are known to recruit hnRNP factors. Several models explain activator and repressors activity of SR and hnRNPs proteins. (**B**) SR factors bound to ESEs can activate splicing by promoting the recruitment of spliceosomal components, such as U2AF and snRNP U1 ("recruitment model"). (**C**) In the "direct competition model", hnRNP factors can sterically block the binding of snRNPs to core splicing signals, as well as those of SR regulators to enhancers. This mechanism occurs when silencer and enhancer elements are very close and even overlapping. (**D**) Splicing factors are also able to interact with the flanking regions of an alternative exon and dimerize, thus masking the alternative exon in a loop and inhibiting its recognition by splicing machinery ("looping out model"). (**E**) Another possible mechanism involves the initial binding of a splicing repressor to a high-affinity site, followed by its polymerization along the pre-mRNA. The effect of multimerization is the inhibition of spliceosome assembly as well as the displacement of splicing activators bound to a distant enhancer ("multimerization and cooperative binding").

variants appear to arise *de novo* in cancer, since they are detected exclusively in cancerous samples and not in normal tissues [21, 25, 26]. These results suggest that cancer-associated splicing isoforms could play a direct role in tumor progression and might represent potential sources of new diagnostic, prognostic and predictive biomarkers for human cancer. In addition, determining the function(s) of cancer-specific splice variants will be equally important for a better comprehension of the malignant transformation.

In some cases the generation of novel cancer-specific isoforms is due to mutations at 3' and 5' splice sites, alternative promoter usage, alternative polyadenylation, all of them altering coding regions and, consequently, the function of the resulting proteins. However, changes in the expression and/or activity of splicing regulators (SR and hnRNP factors) also play a major role in altering the fidelity of the splicing reaction in cancer cells. In particular, post-translational modifications can profoundly affect the activity of these splicing factors [27] and in this respect extracellular stimuli can be communicated to the splicing machinery and to specific RNA-binding proteins that ultimately control exon definition events [28].

All these findings indicate that deregulation of alternative splicing must be added to the growing list of cancer hallmarks [29]. Importantly, aberrant alternative splicing could represent a sort of "Achilles heel" for treatments targeting cancer cells in a specific manner without (or with modest) effects on normal tissues [30]. The scope of this review is to provide brief overview

Appendix

into the regulation of splicing during tumorigenesis by focusing on a number of alternative splicing events with known functional implication in cancer development, progression and on their potential for anti-cancer therapy.

2. ABERRANT REGULATION OF SPLICING FACTORS IN ONCOGENIC TRANSFORMATION

2.1. Spliceosomal Components as Drivers of Cancer: Spliceosomal Mutations in Hematological Disorders

Exome sequencing recently discovered mutations in genes encoding spliceosomal components both in myeloid and lymphoid malignancies [31]. Hematopoietic malignancies mostly result from somatic mutations in hematopoietic stem cells (HSCs) in the bone marrow, leading to malignant cells that grow uncontrollably. The cell type affected and the type of mutation are thought to control the type of hematopoietic malignancy that develops. Remarkably, a substantial proportion of patients affected by myelodysplastic syndromes (MDS), chronic myelomonocytoic leukemia (CMML) or chronic lymphocytic leukemia (CLL) harbor mutations, especially missense mutations, in genes encoding spliceosomal proteins, such as *U2AF35, SF3B1*, *SRSF2* and *ZRSR2* [31, 32]. The recurrence of these mutations in myeloid and lymphoid hematopoietic malignancies strongly suggests that these mutations represent general drivers for the observed cancer progression. Most importantly, there are already also some indications as to what could be the effects of these mutations on the functionality of some of these genes.

For example, the spliceosomal component U2AF consists of two subunits of 65 and 35 kDa, U2AF65 and U2AF35 [33]. U2AF65 binds to the polypyrimidine (Py) tract upstream from the 3' splice site and plays a key role in assisting U2 snRNP recruitment [34]. On the other hand, U2AF35 directly binds the 3' splice site, thus facilitating and stabilizing U2AF65 binding [35]. Moreover, U2AF35 binding to 3' splice-site is critical for introns with weak Py tracts [36]. Notably, the mutations identified in MDS patients affect Serine 34 and Glutamine 157 within zinc finger domains of U2AF35 protein, which may be crucial for RNA binding activity [32, 37].

On the contrary, the missense mutations identified in the gene encoding SF3B1 protein (also known as SF3B155 or SAP155) in patients with MDS and CLL seem to be less deleterious than expected, and the mutant SF3B1 protein should retain its structural integrity. Intriguingly, most mutations in SF3B1 (in both MDS and CLL) recur at amino acid residues within HEAT repeats 4-9. The C-terminal region of SF3B1 contains 22 tandem repeats of the HEAT motif [38]. A single HEAT motif consists of approximately 40 amino acids forming two antiparallel α-helices, and tandem repeats of the motif are present in a variety of proteins, such as protein phosphatase 2A, importin-β and eukaryotic initiation factor 4G [39-41]. These mutations could therefore alter the functionality of SF3B1 during spliceosome assembly. During the first steps of spliceosome assembly, in fact, the U2 snRNA engages base-pairing interaction with the branchpoint site and this interaction is stabilized by heteromeric protein complexes of the U2 snRNP, namely SF3A and SF3B [42], and also by the arginine-serine-rich domain of the U2AF65 protein [43]. SF3b is a 450 kDa complex that comprises seven subunits: SF3B1, SF3B2, SF3B3, SF3B4, SF3B5, SF3B14 and PHF5A. It is currently unknown whether *SF3B1* mutations influence splicing itself or interactions with the spliceosomal components, or even interactions with the transcriptional complex. In addition to myeloid and lymphoid neoplasms, *SF3B1* mutations have been also identified in uveal melanoma [44, 45], the most frequent malignant tumor of the eye, and in pancreatic ductal carcinoma [46]. Thus, identification of *SF3B1* as an oncogenic target in multiple cancers may pave the way to potential targeted therapy.

Finally, mutations in the *SRSF2* gene have also been reported in several hematologic malignancies, particularly in MDS and related diseases [37]. The *SRSF2* gene encodes a member of SR family [47] and SRSF2 (also known as SC35) has been reported to be critical for constitutive/alternative mRNA splicing and for the coupling between transcription and splicing [47, 48]. Depletion of *SRSF2* gene leads to genomic instability [49] and might possibly explain the worse outcome in MDS patients with *SRSF2* mutations. Interestingly, there are some clinical links between *SRSF2* mutations and other recurring mutations in hematologic malignancies associated to a clinical phenotype. For example, it was noted that *SRSF2* mutations seem to be mutually exclusive with mutations in *EZH2* gene, a poor prognostic marker [50, 51]. Moreover, *SRSF2* mutations showed better outcomes in CMML patients with concomitant *RUNX1* mutations [51].

The most common mutation identified in *SRSF2* gene in CMML patients occurs in the Proline 95 of the

Appendix

protein, between the RNA recognition motif (RRM) and the arginine/serine rich RS domain [52].

Finally, SRSF2 and its phosphorylated form P-SRSF2 have been found up-regulated in non small cell lung carcinoma (NSCLC) and their over-expression correlate with more aggressive clinico-pathological features in adenocarcinoma [53]. In addition, the SR phosphorylating kinases SRPK1 and SRPK2 are also up-regulated in lung tumors [53], opening the possibility for SRPK inhibitors as anti-cancer agents.

2.2. De-Regulation of other Splicing Factors in Cancer

SR Proteins

Several laboratories have independently reported the involvement of a specific member of SR family, SRSF1 (or SF2/ASF), in cancer progression. In particular, SRSF1 plays a role in the development of mammary tumors in humans and mice [54, 55]. In this respect, genomic amplification of *SRSF1* has been observed in breast tumors [55] and even a slight over-expression of *SRSF1* is sufficient to transform immortal rodent fibroblasts, which form sarcomas in nude mice [55].

Regarding the functional bases of this effect, it has to be noted that the first RRM domain and nuclear functions of SRSF1 are required to promote proliferation and to delay apoptosis in SRSF1-transduced MCF10 cells [56]. Thus, SRSF1 mediated oncogenic transformation is driven by the splicing activity of SRSF1, through the regulation of specific alternative splicing events, like the alternative splicing of the tumor suppressor *BIN1*, the kinases *MNK2* and *S6K1* and the apoptotic gene *BIM* (also known as *BCL2L11*) [55]. In particular, the resulting *BIN1* isoforms lack tumor-suppressor activity, while the generated *MNK2* and *S6K1* isoforms promote activation of these enzymes independently of upstream signaling activity [55], thus promoting oncogenic transformation. Importantly, it has been recently shown that the *SRSF1* gene is a direct target of the transcription factor and oncoprotein MYC [57]. These two oncogenes are significantly co-expressed in lung carcinomas, where MYC activates *SRSF1* expression by direct binding to two non-canonical E-boxes in its promoter [57]. On the other hand, MYC knockdown leads to the down-regulation of SRSF1 expression in lung-cancer cell lines [56]. In either case, the resulting alterations in SRSF1 protein are sufficient to modulate alternative splicing of a subset of transcripts.

SRSF1, as well as its regulator, the kinase SRPK1, were found to be de-regulated upon Wnt inactivation in colorectal carcinoma cells [58]. SRPK1 was also found up-regulated in both adenoma samples and cancer samples, thus leading to the aberrant regulation of the alternative splicing of *SLC39A14* gene [58], a metal ion transporter with the capacity to transport divalent cations, such as zinc, iron, and cadmium. The two mutually exclusive isoforms of *SLC39A14* gene differ in the cation-binding domain, thus conferring different capacities to bind cadmium (Cd2+) and causing an increased Cd2+ uptake in colorectal tumors [58]. Notably, Cd2+ is a potent carcinogen whose uptake in the body can cause damage to multiple tissue [59].

In addition, it has to be noted that SRPK1 up-regulation is a common cancer related event; as this factor has been shown to be up-regulated in pancreatic, breast and colon carcinomas [60], but reduced in neuroblastoma [61]. In tumor cells, SRSF1 is phosphorylated by SRPK1 and is localized in the nucleus [62].

These observations could well pave the way for potential therapeutic intervention. For example, silencing of *SRSF1* in pancreatic ductal adenocarcinoma (PDAC) [63], as well as in leukemia cells [64], increased the sensitivity of the cells to chemotherapeutic treatments, by enhancing the cytostatic effect of the drugs and promoting apoptosis.

In addition to *SRSF1* and *SRSF2*, other genes encoding SR proteins have been suggested to play a role in cancer although less is known about their role and significance. For example, *SRSF3* (*SRp20*) was indicated as a proto-oncogene that regulates cell proliferation and its increased expression is associated with cancer progression [65]. Moreover, the *SRSF3* gene is amplified in some cancers and loss of SRSF3 expression in different cancer cell lines has been shown to increases apoptosis and decrease proliferation [66].

The gene encoding the SR-like protein TRA2β is also amplified in several human cancers [66], which may account for the up-regulation of TRA2β protein observed in breast, cervical, ovarian and colon cancers [67-70]. Interestingly, knockdown of TRA2β in colon cancer cells reduced cell viability and increased the level of apoptosis [69]. Three TRA2β-target alternative exons have been identified in genes known to play important roles in cancer: the gene encoding the nuclear autoantigenic sperm protein (*NASP*), highly

Appendix

expressed in all dividing cells including embryonic and malignant tissues [71], *CD44,* which encodes a transmembrane protein involved in cellular motility, modulation of intracellular signaling cascades and metastasis [72], and *HIPK3* (homeodomain interacting protein kinase-3), which encodes a serine/threonine kinase involved in transcriptional regulation and negative control of apoptosis [73, 74].

Collectively, these reports suggest that over-expression of SR proteins contribute to cancer progression *via* multiple mechanisms.

hnRNPs

The heterogeneous nuclear ribonucleoproteins (hnRNPs) are a family of RNA-binding proteins (RBPs) that share common structural domains and play essential roles in DNA repair, telomere biogenesis, cell signaling and regulation of gene expression at both the transcriptional and translational levels [75]. Individual hnRNPs have been described to play roles in tumor development and progression through the inhibition of apoptosis, angiogenesis and cell invasion.

Interestingly, hnRNP promoter regions often contain upstream binding elements for oncogenes such as *E2F*, *AP1*, and *c-MYC*, suggesting that hnRNP genes may be regulated by oncogenes [76, 77]. Conversely, the opposite has also been shown to be the case and hnRNPs can regulate the expression of oncogenes. For instance, several hnRNPs have been shown to regulate *c-MYC* expression. In particular, hnRNP K has been reported to increase transcriptional activation of the *c-MYC* gene [78] and furthermore IRES (internal ribosome entry site)-mediated translation of *c-MYC* mRNA is increased by hnRNP C [79], hnRNP K [80], [81] and hnRNP I (also known as polypyrimidine tract binding protein, PTB) [82]. Furthermore, transcriptional activation of other oncogenes such c-Src and eIF4E is also induced by hnRNP K [83, 84].

Aberrant expression of hnRNPs has been described in different type of cancers. hnRNP A1, A2/B1, C1/C2, and K are all up-regulated in lung cancer cell lines and biopsies [85, 86]. Furthermore, hnRNP A1 was found to be over-expressed in colorectal cancers due to a single nucleotide polymorphism (SNP) in the 5' upstream promoter region of the gene, thus possibly contributing to the oncogenic transformation of colon epithelial cells [87]. Three hnRNPs, PTB, hnRNP A1 and hnRNP A2, have been described to regulate the mutually exclusive alternative splicing of the *PKM* pre-mRNA, switching from inclusion of exon 9, which leads to the PKM1 isoform, to exon 10, leading to the PKM2 isoform. PKM2 is the embryonic pyruvate kinase isoform that is re-expressed in cancer and was proposed to be involved in the “Warburg effect” [88] (see also section 3). PTB, hnRNP A1 and A2 bind repressively to sequences flanking exon 9 of *PKM* gene, thus resulting in exon 10 inclusion [76, 89]. Remarkably, the oncogenic transcription factor c-MYC was shown to up-regulate the transcription of PTB, hnRNP A1 and hnRNP A2, ensuring a high PKM2/PKM1 ratio in cancer cells [76].

EWSR1 and the FET Family

In addition to these general hnRNP proteins, a separate chapter should be devoted at discussing the role played by the FET (**F**US Fused in Liposarcoma, **E**WS Ewing Sarcoma, **T**AF15 TATA Box-Binding Protein-Associated Factor 15) family of DNA and RNA binding proteins, that structurally belong to the hnRNP family (FUS is also named hnRNP P2; [90]). This protein family is famous because of the characteristic chromosomal translocation driving tumors. Ewing sarcoma is a highly aggressive primary tumor of bone and soft-tissue affecting predominantly children and young adults, displaying an undifferentiated small round cell phenotype. At the genetic level, Ewing sarcoma is characterized originally by the t(11;22)(q24;q12) chromosome translocation, landmark of Ewing sarcoma and related subtypes of primitive neuroectodermal tumors [91]. This translocation alters the open reading frame of the *EWSR1* gene on chromosome 22 by substituting a sequence encoding a putative RNA binding domain with that of the DNA-binding domain of *FLI-1*, the human homologue of murine *Fli-1* [92].

The other genes of the FET family have also been found in oncogenic translocations, following a common scheme. *FUS* can form fusion with several partners, including *ATF1*, *ERG*, and *CHOP*, respectively associated with Ewing sarcoma, fibromyxoid sarcoma, and myxoid liposarcoma [93]. *TAF15* can form fusion with *NR4A3* gene in extraskeletal myxoid chondrosarcoma [93]. As a consequence, the resulting translocations behave as aberrant transcription factor oncogenes that deregulate gene expression and trigger a specific oncogenic program. Ewing sarcoma typically arises in the bone, but a small portion of patients displays extraosseous primary tumors in soft-tissues with a high propensity to metastasize in lung, bone and bone marrow [94]. Much knowledge about the function of EWS and its family comes from studies on the

Appendix

oncogenic fusions. By contrast, besides the oncogenic translocations, not much is known on the independent role of the canonical EWS protein in cancer [95].

Interestingly, inactivation of *Ews* in mouse embryonic fibroblasts resulted in hypersensitivity to ionizing radiation and caused premature cellular senescence, while *Ews* deficiency in mice leads to developmental defects in meiosis and pre-B cell formation [96]. A physiological function for EWS in response to genomic alterations is also consistent with two genetic screens that identified *EWSR1* as a gene required for resistance to ionizing radiations [97], and to the topoisomerase I inhibitor camptothecin [98]. Moreover, it was recently documented that EWS regulates the alternative splicing of a subset of genes involved in the DNA damage response, such as *CHEK2* and *ABL1* [99]. Improper responses to different types of DNA lesions may lead to accumulation of mutations in the genome, which then accelerate the cancer progression by changing the transcriptional profile of the cell to support its escape from the tight regulation of cell cycle progression. Finally, considering the reported role of EWS in genome stability, it is possible that the protein is also essential to preserve the genome integrity and protect cells from neoplastic transformation [95]. Thus, since translocations typically disrupt the RNA binding domain of EWS, it would be interesting to determine whether part of the oncogenic potential of the EWS/FLI1 fusions is due to loss of functions of the EWS tumor suppressor activity.

Remarkably, a mononucleotide $(T/U)_{16}$ tract located in the 3' untranslated region (3'UTR) of the *EWSR1* gene has recently been described as a novel microsatellite instability (MSI) target locus of sensitivity in DNA mismatch repair (MMR) deficient cancers. Moreover, re-localization of EWS protein from the nucleus to the cytoplasm has been described in MMR-deficient cancers, pointing to *EWSR1* gene as a MSI target in MMR-deficient cancers [100].

SAM68

In addition to SR and hnRNP family members, several other type of RNA binding proteins have been implicated in cancer progression. In particular, SAM68 (Src associated in mitosis of 68kDa) was originally identified as the first mitotic substrate of the oncogenic tyrosine kinase Src in fibroblasts [101, 102]. SAM68 belongs to the signal transduction and activation of RNA (STAR) family of RBPs [103]. Although initial studies using non-transformed murine fibroblasts pointed to a tumor suppressor function for SAM68 [101, 102], direct investigation of the expression and function in cancer cells have recently suggested a pro-oncogenic role of SAM68 protein [104]. In fact, unlike other tumor suppressor genes, knockout of *Sam68* in mice does not sensitize to tumor formation *in vivo* [105]. Conversely *Sam68* heterozygote mice showed delayed onset of breast tumors and reduced number of lung metastases [106]. These results suggest that high levels of SAM68 are required for cell transformation highlighting a role for SAM68 as a proto-oncogene.

Regarding the functional bases of these effects, SAM68 has been shown to modulate the alternative splicing process of cancer relevant genes, such as *BCL2L1*, *CD44*, *CCND1* and *SRSF1* [107-109]. Interestingly, immunohistochemical analyses of biopsies from prostate cancer patients have indicated that SAM68 is frequently up-regulated in prostate cancer [110, 111]. The expression of SAM68 was also increased in breast cancer and renal carcinomas, where it correlated with poor prognosis [112, 113].

Notably, in advanced stages of these tumors, SAM68 was shown to be localized both in the nucleus and in the cytoplasm [112, 113]. Since SAM68 was previously shown to localize in the cytoplasm of male germ cells [114] and neurons [115] and to associate with the translation initiation complex [116] and with polysomes [114, 115], it is possible that, in addition to its well documented ability to modulate cancer-specific splicing events, SAM68 plays additional functions in the cytoplasm of highly malignant cancer cells by regulating translation of selected mRNAs, thus contributing to neoplastic transformation.

3. THERAPEUTIC POTENTIAL OF CANCER-ASSOCIATED ALTERNATIVE SPLICING ISOFORMS

3.1. Oligonucleotides-Based Approaches

Cancer chemotherapy is based on the concept that anticancer drugs will preferentially kill quickly dividing tumor cells, rather than normal cells. Unfortunately, one of the problems of several pharmacological treatments for solid tumors is the reduced selectivity. This observation limits the overall dose of drug that can be administered because of intolerable toxicities to normal tissues. For this reason, the development of more selective anticancer drugs that better distinguish between tumor and normal cells is the imperative goal of current anticancer research.

Today, the possibility to relate alternative splicing cancer-specific isoforms in a patient to the diagnosis

Appendix

and to the outcome of the therapy paves the way to the personalized oncology. Important prerequisites for these strategies to work are the following:

i) the function of the splicing isoform should be well established in processes relevant to cancer biology,

ii) the isoform should be absent in normal tissues to avoid any side effects,

iii) the strategy chosen and the delivery should be highly efficient.

Therapeutic approaches that target specific variants are proving to be effective in the clinic. For instance, specific antibodies directed against the CD44-v6 splice isoform are used in radiotherapy, highlighting the crucial need to discover other promising targets for cancer treatment [117]. Here, therefore, we will discuss some significant examples that could represent the first basis for future pre-clinical studies.

A number of therapeutic approaches aimed at targeting specific splicing isoforms are based on oligonucleotides acting at the RNA level through different mechanisms. SiRNAs (short interfering RNA) and ASOs (Antisense Oligonucleotides) are designed to bind and lead to down-regulation of specific "dangerous" isoforms [118]. These strategies can either elicit the degradation of particular mRNAs or alter the alternative splicing patterns of specific genes and restore the expression of the "physiological" (or non pathological) splicing variant. Moreover, ASOs can prevent ribosomal assembly, and hence mRNA translation. In addition, new generations of ASOs contain chemical modifications (such as *2'-O*-methyl, *2*'-fluoro and *2'-O*-methoxyethyl) that increase their half-life and protect them from nuclease degradation, while the replacement of the sugar phosphate backbone (LNA, Locked Nucleic Acids; PNA, Peptide Nucleic Acids and PMO, phosphorodiamidate morpholino) can be used to increase their selectivity and specificity [118].

Compared to siRNA-based therapy, one of the advantages of ASOs is that targeting an exon-intron junction may sterically block the access to splicing machinery, redirecting splicing reaction to an adjacent splicing site. In addition, ASOs can also target splicing enhancer or silencer elements, masking the sequence to *trans*-acting regulatory factors and promoting inclusion or skipping of specific exons.

Bcl-X

The use of ASOs is particularly interesting when the two splicing isoforms have opposite function, as in the case of *Bcl-x* gene, a member of the Bcl-2 family that directs mitochondrial breakdown during apoptosis [119]. In this case, two Bcl-X isoforms result from the selection of alternative 5' splice sites in exon 2: a long anti-apoptotic form (Bcl-XL) that promotes cell survival and a short isoform that associates with the mitochondrial membrane and promotes apoptosis (Bcl-XS) [120]. Notably, high Bcl-XL/Bcl-XS ratios are observed in a variety of cancer types [120-122] and, more importantly, this ratio has a significant role in determining the sensitivity of the cells to a wide variety of apoptotic agents and may have significance in drugs resistance and chemotherapeutic responsiveness [123].

Considering the importance of this alternative splicing event for cancer cells, several approaches have been investigated in order to shift splicing of *Bcl-x* to the Bcl-XS isoform and to induce apoptosis in cancer cells [124]. Recently, a modified ASO, targeting the downstream 5' alternative splice site of exon 2 in *Bcl-x* pre-mRNA, was tested in a mice model of metastatic melanoma, an aggressive malignancy that shows poor prognosis when associated with increased expression of Bcl-XL splice variant [125]. This treatment, in addition to modifying *Bcl-x* splicing so as to increase the pro-apoptotic Bcl-XS variant, was associated with a significant reduction of tumour burden in rapidly growing and highly tumorigenic lung metastases [125].

MCL-1

Apoptosis regulator MCL-1 (myeloid cell leukemia-1) is another member of the BCL-2 family that is over-expressed in many cancer tissues and cancer cell lines [126, 127]. In addition, its up-regulation has been associated with poor prognosis in breast cancer [128] and, similarly to *Bcl-x*, this gene also appears to be an important factor involved in resistance to cancer therapies [129, 130]. Through alternative splicing of exon 2 the *MCL-1* gene produces two protein isoforms: the full-length anti-apoptotic MCL-1L and a short pro-apoptotic MCL-1S. MCL-1S induces apoptosis and it dimerizes with MCL-1L directing it to proteosomal degradation and abolishing its anti-apoptotic function [131]. In particular, MCL-1L antagonizes apoptosis by preventing mitochondrial outer membrane permeabilization, thus sequestering pro-apoptotic factors in mitochondria, whereas MCL-1S allows the release of factors that cause mitochondrial outer

Appendix

membrane permeabilization [132]. Recently, Shieh and collaborators have used antisense morpholino oligonucleotides to induce skipping of exon 2 and production of the pro-apoptotic MCL-1S isoform [133]. Importantly, this treatment was also able to significantly increase apoptosis in two different tumor cell lines: the skin basal cell carcinoma (BCC) and the human gastric adenocarcinoma (AGS) cell lines [133].

Caspase-9

Caspases are a family of cysteine proteases with a central role in the execution-phase of apoptosis. The initiator *caspase-9* is activated after release of cytochrome c from mitochondria and multiple transcript variants of this gene are generated through alternative splicing [134]. In particular, two alternative splicing variants of caspase-9 with opposite function exist: inclusion of exon 3, 4, 5, and 6 cassette produces the pro-apoptotic caspase-9a, while skipping of this cassette generates the anti-apoptotic caspase-9b. The caspase-9a/9b ratio is altered in non-small cell lung cancer (NSCLC) and is involved in the resistance to chemotherapy [135, 136]. In addition to SRSF1 [137], also the member of the hnRNP family hnRNP-L has been recently linked to *caspase-9* splicing regulation [135]. Interestingly, by interacting with an ESS element in exon 3, hnRNP-L induces down-regulation of the caspase-9a/9b ratio only in tumor cells but not in normal cells, suggesting the existence of a post-translational modification specific for non-transformed cells [135]. In particular, the phosphorylation state of hnRNP-L in Serine 52 has been indicated as the critical event for the control of the alternative splicing of caspase-9. Importantly, as a consequence of the changes in *caspase-9* pre-mRNA processing, down-regulation of hnRNP-L in a mouse xenograft model was able to determine complete loss of tumorigenic capacity [135].

HER4

Alternative splicing regulation of apoptosis in cancer cells was investigated for HER4/ErbB-4, a member the epidermal growth factor receptor (EGFR) family that presents oncogenic and tumor-suppressive functions in cancer development and progression [138]. Alternative splicing has been reported to generate several HER4 isoforms with different activation mechanisms and several *in vivo* functions. In particular, the CYT1 isoform containing exon 26 retains the cytoplasmic PI3 (phosphatydilinositol 3-kinase) binding domain, while the isoform CYT2 deleted of exon 26 lacks the cytoplasmic domain interacting with PI3K [139]. CYT1, but not CYT2, is capable to enhance the resistance to starvation and etoposide inhibiting apoptosis *via* the PI3K/AKT pathway. Accordingly, over-expression of CYT1 in medulloblastoma cells confers protection from apoptosis [140] and high CYT1/CYT2 ratio is associated with increased aggressiveness and poor survival [140, 141]. Recently, a LNA-based oligoribonucleotide directed against the 5' splice site of exon 26 (SSOe26) of the *HER4* pre-mRNA was used to prevent spice site recognition and stimulate skipping of exon 26, thus decreasing CYT1/CYT2 ratio. Importantly, SSOe26 was able to reduce cancer cell proliferation *in vitro* and decrease the growth of the xenografted tumor [142].

PKM

As mentioned before, a peculiar feature of tumor cells is an increased utilization of glucose and its conversion to lactate, with a consequential metabolic switch from oxidative to aerobic glycolysis. This metabolic switch (known as "Warburg effect") depends on the expression of PKM2 splicing isoform of the pyruvate kinase M (PKM), the enzyme that catalyzes the final step of glycolysis [88]. Mutually exclusive inclusion of exons 9 and 10 of the *PKM* gene generates the M1 and M2 isoforms, respectively. Since the switch from PKM1 to PKM2 promotes aerobic glycolysis and provides a selective advantage for tumor formation, directing the alternative splicing reaction toward the production of PKM1 isoform may represent a promising anticancer strategy. Recently, ASO technology was used to correct aberrant alternative splicing and induce down-regulation of PKM2 isoform (but not up-regulation of PKM1) [143]. Importantly, ASO treatment was also sufficient to induce apoptosis of glioblastoma cell lines [143]. This approach potentially represents an effective therapeutic strategy in glioblastoma since these tumor cells are able to take up chemically modified ASOs *in vivo* without the support of delivery agents [144]. Moreover, it is more efficient than previously tested siRNA strategy to knockdown *PKM2* [145].

STAT5B

Prostate cancer is one of the most frequent causes of death in male population [146] and STAT5B, a member of the STAT (Signal Transducer and Activator of Transcription) family, was described to be closely associated with the progression of this type of tumor [147]. Also in this case, alternative splicing has been shown to play an important role in regulating STAT5B activities. The full isoform of STAT5B acts as a proto-oncogene and promotes tumor progression, whereas

Appendix

retention of intron 18 generates a truncated STAT5ΔB isoform lacking the transactivation domain [147]. In particular, STAT5ΔB is a dominant-negative form of STAT5B with tumor suppressor activity [147]. Recently, a mixture of modified ASOs, with complimentary sequence to the 5' exon-intron boundary of exon 18 and to the 3' intron-exon boundary of exon 19, was used to reduce cell proliferation and survival of prostate cancer cells [148]. Considering that several members of the STAT family generate dominant-negative isoforms through alternative splicing regulation, it would be highly valuable to anticancer research the possibility to modulate their actions and specifically switch their functions from tumor activating to tumor suppressing molecules.

KLF6

Krüppel-like zinc finger family of transcription factors (KLFs) are DNA-binding proteins that regulate gene expression and are involved in cancer development and progression [149]. Alternative splicing of the *KLF6* gene produces four alternatively spliced isoforms displaying different properties [150]. The KLF6-SV1 isoform is generated from the use of an alternative 5' splice site within exon 2 and from the exclusion of exon 3. Compared to the full length form of KLF6, the KLF6-SV1 isoform contains a different C-terminal domain lacking the zinc finger-binding domains, whereas it retains the N-terminal activation domains [150]. KLF6-SV1, by antagonizing the tumor suppressor function of KLF6, stimulates cancer cells proliferation, invasion and metastasis and inhibits apoptosis [150, 151]. Moreover, it is associated to bad prognosis in prostate, lung, and ovarian cancer [149]. Interestingly, while down-regulation of the full length KLF6 was described to stimulate tumor formation in nude mice, specific silencing of the KLF6-SV1 variant was able to trigger apoptosis in cell culture and to synergize with chemotherapeutic agents (such as cisplatin), thus inducing tumor regression *in vivo* [150-152].

Telomerase

Cancer cells are able to overcome the senescence program through lengthening of chromosomal telomeres, operated by the telomerase, a ribonucleoprotein in which the reverse-transcriptase activity of the protein component (hTERT) catalyzes telomere elongation using the RNA template component (hTR) [153]. Telomerase is a promising target in anticancer therapy since it is absent in the majority of somatic tissues while it is present in 85% of human cancer cells [154]. Telomerase production is regulated at both transcriptional and post-transcriptional levels: the approximately 20 mRNAs transcribed in one cancer cell ensure the production of few active enzyme molecules being processed thanks to alternative splicing in order to generate a number of inactive isoforms [155]. Notably, skipping of exons 7 and 8 generates the minus beta variant, the major splicing isoform of hTERT transcripts in cancer cells. This specific alternative splicing event introduces a premature stop in exon 10 that leads the mRNA to degradation by the nonsense-mediated mRNA decay (NMD) pathway [156]. Recently, some intronic regulatory sequences have been described to be involved in the generation of this splice variant and an antisense oligonucleotide, blocking the activity of one of these elements, was used to increase the expression of the non-functional minus beta isoform suggesting that perturbation of the this splicing event might subtract a portion of active enzyme to cancer cells [157].

RON

An increasing body of data implicates alternative splicing as a mechanism to control Epithelial-Mesenchymal-Transition (EMT), a key process in embryonic development and metastasis formation during malignant progression [15]. During EMT, differentiated epithelial cells undergo several molecular and morphological changes through which they assume an elongated fibroblast-like shape, lose their intercellular junctions and acquire invasive properties (mesenchymal phenotype) [158, 159]. The first example of the implication of alternative splicing during EMT was provided by the analysis of the *RON* proto-oncogene that encodes for a tyrosine-kinase receptor involved in the control of cell dissociation, migration and invasion of extracellular matrices [160]. *RON* pre-mRNA undergoes several alternative splicing events that generate different isoforms with distinct activities [161]. In particular, ΔRON is a constitutively active isoform deleted of 49 amino acids in the extracellular domain that originates from skipping of exon 11 [162]. Notably, ΔRON accumulates during tumor progression of epithelial cancers and its over-expression confers invasive properties to recipient cells [162-164], suggesting the possibility that *RON* splicing could contribute to the metastatic process. At the functional level, the SRSF1 splicing factor directly binds to an ESE element in exon 12 and promotes the production of ΔRON isoform. Interestingly, interference on the expression levels of SFSR1 correlates with changes in the ΔRON production and more importantly affects

Appendix

activation of EMT program [164]. Thus, the correction of pathological *ΔRON* splicing event could represent a potential target for the development of new anti-metastatic therapeutic strategies.

In this regard, a bifunctional oligonucleotide TOES (Targeted Oligonucleotide Enhancers of Splicing) was used to efficiently correct *ΔRON* splicing and increase exon 11 inclusion. TOES are antisense RNA molecules complementary to a target region, with a terminal non-complementary tail bearing an enhancer of splicing [165]. Several TOES were used to correct aberrant splicing events of genes involved in Duchenne muscular dystrophy and spinal muscular atrophy [166, 167] and for the first time in the case of the *RON* gene to correct splicing in cancer cells. In particular, the TOES oligo enhancing *RON* exon 11 is complementary to the initial portion of this exon and contains a tail of GGA repeats, that are a binding site for a positive splicing regulator which in turn is able to stimulate spliceosome recruitment on exon 11 to trigger its inclusion in the mature transcript.

3.1. Small Molecules Targeting Splicing Components

In addition to ASOs and siRNAs, small molecules targeting the spliceosome or *trans*-acting splicing regulatory factors also provide potential targets for the development of new therapeutic strategies [168, 169].

The identification in the fermentation broth of *Pseudomonas* spp. and *Streptomyces* spp. of molecules capable of disrupting the activity of the spliceosome, has created novel and interesting perspectives for the development of new drugs [169, 170]. Several of these natural products are able to bind the spliceosomal SF3B subunit and show antitumor activity suggesting the relevance of the spliceosome as a therapeutic target. Starting from these natural products, synthetic analogues have been obtained, with less complex structure, and therefore with minor synthesis costs and higher stability, solubility and activity.

Spliceostatin

One of the first drugs identified for the potent cytostatic activity and subsequently discovered to specifically target the spliceosome is spliceostatin A (SSA). SSA is a methyl-ketal derivative of FR901464, a metabolite from the bacterium *Pseudomonas*, which was originally isolated as a transcriptional activator, with a potent cytotoxic activity against a number of different human cancer cell lines [171]. Recent studies have shed light on how SSA and its synthetic analogues work in splicing inhibition. SSA binds tightly to SF3B, thus destabilizing U2 snRNP–pre-mRNA complexes and preventing subsequent events in spliceosome assembly [172]. In particular, SSA prevents SF3B1-pre-mRNA interactions and induces base pairing of U2 snRNA with decoy sequences upstream to the branch point sequence [173]. Thus, the splicing inhibitory effect of the drug results in intron retention or exon skipping, leading to unprocessed or incorrectly processed mRNAs and arrest of the cell cycle in phases G1 and G2/M [174].

E7107

E7107, a synthetic derivative of pladienolide D isolated from *Streptomyces platensis*, is another inhibitor of the spliceosome. Notably, E7107 showed potent and selective antitumor activity in human tumor xenograft models, without important toxicity and for these reasons it rapidly entered clinical trials [175, 176].

Meayamycin B

Recently, it has been reported that it is possible to correct the splicing of *MCL-1* decreasing the anti-apoptotic isoform by targeting SF3B1, one of the regulators of the MCL-1L/MCL-1S ratio [177]. In particular, meayamycin B, a potent inhibitor of SF3B1, was successfully used to promote the production of MCL-1S protein and, when this drug was used in combination with Bcl-XL inhibitor (ABT-737), it triggered apoptosis in cells resistant to ABT-737 [178].

Amiloride

Screening of small molecules modulating RNA splicing in a human hepatocellular carcinoma cell line (Huh-7) has identified amiloride as a new compound able to affect the phosphorylation status of SRSF1 and the expression level of SRSF3 [179]. Amiloride treatment decreased the activity of AKT, ERK1/2 and PP1, while it increased the activity of p38 and JNK. Interestingly, all these kinases and phosphatases are known to affect phosphorylation of splicing factors [26]. In particular, amiloride was shown to modulate alternative splicing of various cancer genes [179, 180]. It acts by "normalizing" the splicing of *Bcl-x*, *HIPK3*, *APAF1* (apoptotic peptidase activating factor 1) and *RON* transcripts towards less malignant patterns, thus increasing the production of pro-apoptotic Bcl-XS, HIPK3 and APAF1 variants and decreasing (at low concentration) ΔRON isoform [179, 180]. Moreover,

Appendix

invasion and migration defects, cell cycle disruption and lethal DNA degradation have been detected in treated cells. Thus, although clinical trials for the treatment of cancer with amiloride have not started yet, the data described above suggest a possible new anticancer therapeutic perspective for this drug [181]. In this regard, amiloride has been recently described as a novel adjuvant of radiotherapy in human glioblastomas by reinforcing the antiproliferative effect of ionizing radiation [180].

NB-506 and TG003

Phosphorylation of SR proteins is one of the key determinants regulating pre-mRNA splicing *via* modulation of their protein-protein and protein-RNA interactions [182]. In the past, several kinases involved in SR protein phosphorylation have been identified and characterized [13, 27]. Remarkably, phosphorylation of SR proteins is required for spliceosome assembly, whereas dephosphorylation is critical for the splicing reaction to occur. For this reason, inhibiting SR protein phosphorylation/dephosphorylation can be used as a tool to specifically inhibit their activity.

NB-506, for example, is a glycosylated indolocarbazole derivative that completely inhibits the ability of topoisomerase I to phosphorylate SRSF1, while it does not demonstrate any activity against other kinases known to phosphorylate SRSF1, such as SRPK1 and CDC2 kinase [183]. NB-506 displays antitumor properties and modulates gene expression by interfering with the spliceosome assembly, thus changing the splicing pattern of protein-encoding genes [183]. Notably, Edotecarin, a derivative of NB-506, is currently under trial in patients with advanced solid tumors [184-186]. In addition to NB-506, pharmacological inhibition of Clk kinases by the benzothiazole compound TG003 affects the regulation of alternative splicing mediated by phosphorylation of SR proteins *in vitro* and *in vivo* [187]. Remarkably, treatment with the splicing modulator TG003, as well as disruption of the splicing machinery by small interfering RNA targeting multiple spliceosome-associated proteins, causes the accumulation of p53 protein and an increase in p53 transcriptional activity [188].

IDCs

Finally, indole derivatives compounds (IDC) represent a new class of splicing inhibitors that display a selective activity against exonic splicing enhancers (ESE)-dependent activity of individual SR proteins [189]. Rather than general inhibitors of splicing, these molecules are highly selective for splicing events that are mediated by different classes of ESE sequences, and their selectivity is thought to depend on their interaction with individual SR protein [190]. Although little is known about their mechanism of action, some of them have antiproliferative activity with a tolerable toxicity [190]. Interestingly, an indole derivative (IDC92) has been used to switch *ΔRON* splicing toward the production of the non-pathological isoform and to reduce the invasive phenotype of tumor cells [191]. Since IDC92 did not perturb the splicing of other SRSF1 targets [191], it would be interesting to further investigate it *in vivo*.

SRPIN340

Vascular endothelial growth factor (VEGF) is a key regulatory component in physiological and pathological angiogenesis and the inhibition of VEGF has been shown to be effective in cancer [192]. Pro-angiogenic and anti-angiogenic VEGF isoforms are generated either by proximal or distal splice site selection in the terminal exon, which is regulated by SRSF1 and SRSF6 [193]. The inhibitor of SRPK1/2 kinase, SRPIN340, resulted in significant inhibition of angiogenesis and increased normal vascularization, by regulating SR protein phosphorylation and activity [194].

CONCLUDING REMARKS

Before translation to clinic practice, both the approaches (ASO and small molecules) need further improvement and *in vivo* testing.

First of all, oligonucleotides-mediated therapy research has to solve the problem of delivery, since several physical barriers have to be passed and the half-life of the oligos has to be increased. Nevertheless, in this respect significant progress has been recently reported in models of muscular dystrophies [195-197]. Several small molecules seem more effective and some clinical trials are opened (Clinicaltrial.gov). Even though much progress has been made, various challenges have to be overcome. Indeed, because of their lack of specificity in modulating pre-mRNA splicing, these compounds display their activity also toward normal cells, thus limiting the applicability. A rational targeted design of compounds that can modulate splice site selection on specific genes may pave the way towards new therapeutic approaches with anti-cancer purposes. Thus, better understanding of the mechanism of action of these molecules is needed to allow for the rational design of more selective and

Appendix

less toxic compounds. Finally, simpler and cheaper synthesis systems have to be developed in order to produce the quantity of drugs needed for a wide distribution to patients.

ACKNOWLEDGEMENTS

We thank Claudio Sette, Emanuele Buratti and Davide Gabellini for helpful comments on the manuscript. This work was supported by grants from the Associazione Italiana per la Ricerca sul Cancro (AIRC) (MFAG 11913), the Association for International Cancer Research (AICR-UK 11-0622) to C.G. and grants from the Associazione Italiana Ricerca sul Cancro (AIRC) (MFAG 11658) and from the University of Rome "Foro Italico" (RIC052013) to M.P.P. Conflict of interest statement: None declared.

REFERENCES

[1] Wahl MC, Will CL, Lührmann R. The spliceosome: design principles of a dynamic rnp machine. Cell 2009; 136(4): 701-18. http://dx.doi.org/10.1016/j.cell.2009.02.009

[2] Wang ET, Sandberg R, Luo S, Khrebtukova I, Zhang L, Mayr C, *et al*. Alternative isoform regulation in human tissue transcriptomes. Nature 2008; 456(7221): 470-6. http://dx.doi.org/10.1038/nature07509

[3] Pan Q, Shai O, Lee LJ, Frey BJ, Blencowe BJ. Deep surveying of alternative splicing complexity in the human transcriptome by high-throughput sequencing. Nat Genet 2008; 40(12): 1413-5. http://dx.doi.org/10.1038/ng.259

[4] Stolc V, Gauhar Z, Mason C, Halasz G, van Batenburg MF, Rifkin SA, *et al*. A gene expression map for the euchromatic genome of drosophila melanogaster. Science 2004; 306(5696): 655-60. http://dx.doi.org/10.1126/science.1101312

[5] Hillier LW, Reinke V, Green P, Hirst M, Marra MA, Waterston RH. Massively parallel sequencing of the polyadenylated transcriptome of c. elegans. Genome Res 2009; 19(4): 657-66. http://dx.doi.org/10.1101/gr.088112.108

[6] Barash Y, Calarco JA, Gao W, Pan Q, Wang X, Shai O, *et al*. Deciphering the splicing code. Nature 2010; 465(7294): 53-9. http://dx.doi.org/10.1038/nature09000

[7] Black DL. Mechanisms of alternative pre-messenger rna splicing. Annu Rev Biochem 2003; 72: 291-336.

[8] Blencowe BJ. Alternative splicing: new insights from global analyses. Cell 2006; 126(1): 37-47. http://dx.doi.org/10.1016/j.cell.2006.06.023

[9] Tazi J, Bakkour N, Stamm S. Alternative splicing and disease. Biochim Biophys Acta 2009; 1792(1): 14-26. http://dx.doi.org/10.1016/j.bbadis.2008.09.017

[10] Licatalosi DD, Darnell RB. Splicing regulation in neurologic disease. Neuron 2006; 52(1): 93-101. http://dx.doi.org/10.1016/j.neuron.2006.09.017

[11] Cartegni L, Chew SL, Krainer AR. Listening to silence and understanding nonsense: exonic mutations that affect splicing. Nat Rev Genet 2002; 3(4): 285-98. http://dx.doi.org/10.1038/nrg775

[12] David CJ, Manley JL. Alternative pre-mrna splicing regulation in cancer: pathways and programs unhinged. Genes Dev 2010; 24(21): 2343-64. http://dx.doi.org/10.1101/gad.1973010

[13] Ghigna C, Valacca C, Biamonti G. Alternative splicing and tumor progression. Curr Genomics 2008; 9(8): 556-70. http://dx.doi.org/10.2174/138920208786847971

[14] Pal S, Gupta R, Davuluri RV. Alternative transcription and alternative splicing in cancer. Pharmacol Ther. 2012; 136(3): 283-94. http://dx.doi.org/10.1016/j.pharmthera.2012.08.005

[15] Biamonti G, Bonomi S, Gallo S, Ghigna C. Making alternative splicing decisions during epithelial-to-mesenchymal transition(emt). Cell Mol Life Sci 2012; 69(15): 2515-26. http://dx.doi.org/10.1007/s00018-012-0931-7

[16] Hanahan D, Weinberg RA. Hallmarks of cancer: the next generation. Cell 2011; 144(5): 646-74. http://dx.doi.org/10.1016/j.cell.2011.02.013

[17] Ghigna C, Riva S, Biamonti G. Alternative splicing of tumor suppressors and oncogenes. Cancer Treat Res 2013; 158: 95-117.

[18] Skotheim RI, Nees M. Alternative splicing in cancer: noise, functional, or systematic? Int J Biochem Cell Biol 2007; 39(7-8): 1432-49. http://dx.doi.org/10.1016/j.biocel.2007.02.016

[19] Germann S, Gratadou L, Dutertre M, Auboeuf D. Splicing programs and cancer. J Nucleic Acids 2012; 2012: 269570.

[20] Lenzken SC, Loffreda A, Barabino SML. Rna splicing: a new player in the dna damage response. Int J Cell Biol 2013; 2013: 153634.

[21] Eswaran J, Cyanam D, Mudvari P, Reddy SDN, Pakala SB, Nair SS, *et al*. Transcriptomic landscape of breast cancers through mrna sequencing. Sci Rep 2012; 2: 264.

[22] Venables JP, Klinck R, Koh C, Gervais-Bird J, Bramard A, Inkel L, *et al*. Cancer-associated regulation of alternative splicing. Nat Struct Mol Biol 2009; 16(6): 670-6. http://dx.doi.org/10.1038/nsmb.1608

[23] Körner M, Miller LJ. Alternative splicing of pre-mrna in cancer: focus on g protein-coupled peptide hormone receptors. Am J Pathol 2009; 175(2): 461-72. http://dx.doi.org/10.2353/ajpath.2009.081135

[24] Omenn GS. Plasma proteomics, the human proteome project, and cancer-associated alternative splice variant proteins. Biochim Biophys Acta 2013; pii: S1570-9639(13): pp.00374-9.

[25] He C, Zhou F, Zuo Z, Cheng H, Zhou R. A global view of cancer-specific transcript variants by subtractive transcriptome-wide analysis. PLoS One 2009; 4(3): e4732. http://dx.doi.org/10.1371/journal.pone.0004732

[26] Xu Q, Lee C. Discovery of novel splice forms and functional analysis of cancer-specific alternative splicing in human expressed sequences. Nucleic Acids Res 2003; 31(19): 5635-43. http://dx.doi.org/10.1093/nar/gkg786

[27] Naro C, Sette C. Phosphorylation-mediated regulation of alternative splicing in cancer. Int J Cell Biol 2013; 2013: 151839.

[28] Siegfried Z, Bonomi S, Ghigna C, Karni R. Regulation of the ras-mapk and pi3k-mtor signalling pathways by alternative splicing in cancer. Int J Cell Biol 2013; 2013: 568931.

[29] Ladomery M. Aberrant alternative splicing is another hallmark of cancer. Int J Cell Biol. 2013; 2013: 463786.

[30] Wang G, Cooper TA. Splicing in disease: disruption of the splicing code and the decoding machinery. Nat Rev Genet 2007; 8(10): 749-61. http://dx.doi.org/10.1038/nrg2164

[31] Quesada V, Conde L, Villamor N, Ordóñez GR, Jares P, Bassaganyas L, *et al*. Exome sequencing identifies recurrent mutations of the splicing factor sf3b1 gene in chronic

Appendix

lymphocytic leukemia. Nat Genet 2012; 44(1): 47-52. http://dx.doi.org/10.1038/ng.1032

[32] Graubert TA, Shen D, Ding L, Okeyo-Owuor T, Lunn CL, Shao J, *et al.* Recurrent mutations in the u2af1 splicing factor in myelodysplastic syndromes. Nat Genet 2012; 44(1): 53-7. http://dx.doi.org/10.1038/ng.1031

[33] Zamore PD, Green MR. Identification, purification, and biochemical characterization of u2 small nuclear ribonucleoprotein auxiliary factor. Proc Natl Acad Sci U S A 1989; 86(23): 9243-7. http://dx.doi.org/10.1073/pnas.86.23.9243

[34] Zamore PD, Patton JG, Green MR. Cloning and domain structure of the mammalian splicing factor u2af. Nature 1992; 355(6361): 609-14. http://dx.doi.org/10.1038/355609a0

[35] Merendino L, Guth S, Bilbao D, Martínez C, Valcárcel J. Inhibition of msl-2 splicing by sex-lethal reveals interaction between u2af35 and the 3' splice site ag. Nature 1999; 402(6763): 838-41. http://dx.doi.org/10.1038/45602

[36] Wu S, Romfo CM, Nilsen TW, Green MR. Functional recognition of the 3' splice site ag by the splicing factor u2af35. Nature 1999; 402(6763): 832-5. http://dx.doi.org/10.1038/45590

[37] Yoshida K, Sanada M, Shiraishi Y, Nowak D, Nagata Y, Yamamoto R, *et al.* Frequent pathway mutations of splicing machinery in myelodysplasia. Nature 2011; 478(7367): 64-9. http://dx.doi.org/10.1038/nature10496

[38] Wang C, Chua K, Seghezzi W, Lees E, Gozani O, Reed R. Phosphorylation of spliceosomal protein sap 155 coupled with splicing catalysis. Genes Dev 1998; 12(10): 1409-14. http://dx.doi.org/10.1101/gad.12.10.1409

[39] Marcotrigiano J, Lomakin IB, Sonenberg N, Pestova TV, Hellen CU, Burley SK. A conserved heat domain within eif4g directs assembly of the translation initiation machinery. Mol Cell 2001; 7(1): 193-203. http://dx.doi.org/10.1016/S1097-2765(01)00167-8

[40] Groves MR, Hanlon N, Turowski P, Hemmings BA, Barford D. The structure of the protein phosphatase 2a pr65/a subunit reveals the conformation of its 15 tandemly repeated heat motifs. Cell 1999; 96(1): 99-110. http://dx.doi.org/10.1016/S0092-8674(00)80963-0

[41] Cingolani G, Petosa C, Weis K, Müller CW. Structure of importin-beta bound to the ibb domain of importin-alpha. Nature 1999; 399(6733): 221-9. http://dx.doi.org/10.1038/20367

[42] Gozani O, Feld R, Reed R. Evidence that sequence-independent binding of highly conserved u2 snrnp proteins upstream of the branch site is required for assembly of spliceosomal complex a. Genes Dev 1996; 10(2): 233-43. http://dx.doi.org/10.1101/gad.10.2.233

[43] Valcárcel J, Gaur RK, Singh R, Green MR. Interaction of u2af65 rs region with pre-mrna branch point and promotion of base pairing with u2 snrna [corrected]. Science 1996; 273(5282): 1706-9. http://dx.doi.org/10.1126/science.273.5282.1706

[44] Martin M, Maßhöfer L, Temming P, Rahmann S, Metz C, Bornfeld N, *et al.* Exome sequencing identifies recurrent somatic mutations in eif1ax and sf3b1 in uveal melanoma with disomy 3. Nat Genet 2013; 45(8): 933-6. http://dx.doi.org/10.1038/ng.2674

[45] Harbour JW, Roberson EDO, Anbunathan H, Onken MD, Worley LA, Bowcock AM. Recurrent mutations at codon 625 of the splicing factor sf3b1 in uveal melanoma. Nat Genet 2013; 45(2): 133-5. http://dx.doi.org/10.1038/ng.2523

[46] Biankin AV, Waddell N, Kassahn KS, Gingras M, Muthuswamy LB, Johns AL, *et al.* Pancreatic cancer genomes reveal aberrations in axon guidance pathway genes. Nature 2012; 491(7424): 399-405. http://dx.doi.org/10.1038/nature11547

[47] Graveley BR. Sorting out the complexity of sr protein functions. RNA 2000; 6(9): 1197-211. http://dx.doi.org/10.1017/S1355838200000960

[48] Lin S, Coutinho-Mansfield G, Wang D, Pandit S, Fu X. The splicing factor sc35 has an active role in transcriptional elongation. Nat Struct Mol Biol 2008; 15(8): 819-26. http://dx.doi.org/10.1038/nsmb.1461

[49] Xiao R, Sun Y, Ding J, Lin S, Rose DW, Rosenfeld MG, *et al.* Splicing regulator sc35 is essential for genomic stability and cell proliferation during mammalian organogenesis. Mol Cell Biol 2007; 27(15): 5393-402. http://dx.doi.org/10.1128/MCB.00288-07

[50] Schnittger S, Bacher U, Haferlach C, Kern W, Alpermann T, Haferlach T. Clinical impact of flt3 mutation load in acute promyelocytic leukemia with t(15;17)/pml-rara. Haematologica 2011; 96(12): 1799-807. http://dx.doi.org/10.3324/haematol.2011.049007

[51] Meggendorfer M, Roller A, Haferlach T, Eder C, Dicker F, Grossmann V, *et al.* Srsf2 mutations in 275 cases with chronic myelomonocytic leukemia(cmml). Blood 2012; 120(15): 3080-8. http://dx.doi.org/10.1182/blood-2012-01-404863

[52] Visconte V, Makishima H, Maciejewski JP, Tiu RV. Emerging roles of the spliceosomal machinery in myelodysplastic syndromes and other hematological disorders. Leukemia 2012; 26(12): 2447-54. http://dx.doi.org/10.1038/leu.2012.130

[53] Gout S, Brambilla E, Boudria A, Drissi R, Lantuejoul S, Gazzeri S, *et al.* Abnormal expression of the pre-mrna splicing regulators srsf1, srsf2, srpk1 and srpk2 in non small cell lung carcinoma. PLoS One 2012; 7(10): e46539. http://dx.doi.org/10.1371/journal.pone.0046539

[54] Stickeler E, Kittrell F, Medina D, Berget SM. Stage-specific changes in sr splicing factors and alternative splicing in mammary tumorigenesis. Oncogene 1999; 18(24): 3574-82. http://dx.doi.org/10.1038/sj.onc.1202671

[55] Karni R, de Stanchina E, Lowe SW, Sinha R, Mu D, Krainer AR. The gene encoding the splicing factor sf2/asf is a proto-oncogene. Nat Struct Mol Biol 2007; 14(3): 185-93. http://dx.doi.org/10.1038/nsmb1209

[56] Anczuków O, Rosenberg AZ, Akerman M, Das S, Zhan L, Karni R, *et al.* The splicing factor srsf1 regulates apoptosis and proliferation to promote mammary epithelial cell transformation. Nat Struct Mol Biol 2012; 19(2): 220-8. http://dx.doi.org/10.1038/nsmb.2207

[57] Das S, Anczuków O, Akerman M, Krainer AR. Oncogenic splicing factor srsf1 is a critical transcriptional target of myc. Cell Rep 2012; 1(2): 110-7. http://dx.doi.org/10.1016/j.celrep.2011.12.001

[58] Thorsen K, Mansilla F, Schepeler T, Øster B, Rasmussen MH, Dyrskjøt L, *et al.* Alternative splicing of slc39a14 in colorectal cancer is regulated by the wnt pathway. Mol Cell Proteomics 2011; 10(1): M110.002998.

[59] Waalkes MP. Cadmium carcinogenesis. Mutat Res 2003; 533(1-2): 107-20. http://dx.doi.org/10.1016/j.mrfmmm.2003.07.011

[60] Hayes GM, Carrigan PE, Miller LJ. Serine-arginine protein kinase 1 overexpression is associated with tumorigenic imbalance in mitogen-activated protein kinase pathways in breast, colonic, and pancreatic carcinomas. Cancer Res 2007; 67(5): 2072-80. http://dx.doi.org/10.1158/0008-5472.CAN-06-2969

[61] Krishnakumar S, Mohan A, Kandalam M, Ramkumar HL, Venkatesan N, Das RR. Srpk1: a cisplatin sensitive protein expressed in retinoblastoma. Pediatr Blood Cancer 2008; 50(2): 402-6. http://dx.doi.org/10.1002/pbc.21088

Appendix

[62] Sanford JR, Ellis JD, Cazalla D, Cáceres JF. Reversible phosphorylation differentially affects nuclear and cytoplasmic functions of splicing factor 2/alternative splicing factor. Proc Natl Acad Sci U S A 2005; 102(42): 15042-7. http://dx.doi.org/10.1073/pnas.0507827102

[63] Adesso L, Calabretta S, Barbagallo F, Capurso G, Pilozzi E, Geremia R, *et al*. Gemcitabine triggers a pro-survival response in pancreatic cancer cells through activation of the mnk2/eif4e pathway. Oncogene 2013; 32(23): 2848-57. http://dx.doi.org/10.1038/onc.2012.306

[64] Zou L, Zhang H, Du C, Liu X, Zhu S, Zhang W, *et al*. Correlation of srsf1 and prmt1 expression with clinical status of pediatric acute lymphoblastic leukemia. J Hematol Oncol 2012; 5: 42. http://dx.doi.org/10.1186/1756-8722-5-42

[65] Jia R, Li C, McCoy JP, Deng C, Zheng Z. Srp20 is a proto-oncogene critical for cell proliferation and tumor induction and maintenance. Int J Biol Sci 2010; 6(7): 806-26. http://dx.doi.org/10.7150/ijbs.6.806

[66] Cerami E, Gao J, Dogrusoz U, Gross BE, Sumer SO, Aksoy BA, *et al*. The cbio cancer genomics portal: an open platform for exploring multidimensional cancer genomics data. Cancer Discov 2012; 2(5): 401-4. http://dx.doi.org/10.1158/2159-8290.CD-12-0095

[67] Watermann DO, Tang Y, Zur Hausen A, Jäger M, Stamm S, Stickeler E. Splicing factor tra2-beta1 is specifically induced in breast cancer and regulates alternative splicing of the cd44 gene. Cancer Res 2006; 66(9): 4774-80. http://dx.doi.org/10.1158/0008-5472.CAN-04-3294

[68] Takeo K, Kawai T, Nishida K, Masuda K, Teshima-Kondo S, Tanahashi T, *et al*. Oxidative stress-induced alternative splicing of transformer 2beta(sfrs10) and cd44 pre-mrnas in gastric epithelial cells. Am J Physiol Cell Physiol 2009; 297(2): C330-8. http://dx.doi.org/10.1152/ajpcell.00009.2009

[69] Kajita K, Kuwano Y, Kitamura N, Satake Y, Nishida K, Kurokawa K,*et al*. Ets1 and heat shock factor 1 regulate transcription of the transformer 2β gene in human colon cancer cells. J Gastroenterol. 2013; 48(11): pp.1222-33. http://dx.doi.org/10.1007/s00535-012-0745-2

[70] Fischer D, Noack K, Runnebaum IB, Watermann DO, Kieback DG, Stamm S, *et al*. Expression of splicing factors in human ovarian cancer. Oncol Rep 2004; 11(5): 1085-90.

[71] Perou CM, Sørlie T, Eisen MB, van de Rijn M, Jeffrey SS, Rees CA, *et al*. Molecular portraits of human breast tumours. Nature 2000; 406(6797): 747-52. http://dx.doi.org/10.1038/35021093

[72] Naor D, Nedvetzki S, Golan I, Melnik L, Faitelson Y. Cd44 in cancer. Crit Rev Clin Lab Sci 2002; 39(6): 527-79. http://dx.doi.org/10.1080/10408360290795574

[73] Venables JP, Bourgeois CF, Dalgliesh C, Kister L, Stevenin J, Elliott DJ. Up-regulation of the ubiquitous alternative splicing factor tra2beta causes inclusion of a germ cell-specific exon. Hum Mol Genet 2005; 14(16): 2289-303. http://dx.doi.org/10.1093/hmg/ddi233

[74] Best A, Dagliesh C, Ehrmann I, Kheirollahi-Kouhestani M, Tyson-Capper A, Elliott DJ. Expression of tra2 β in cancer cells as a potential contributory factor to neoplasia and metastasis. Int J Cell Biol 2013; 2013: 843781.

[75] Han SP, Tang YH, Smith R. Functional diversity of the hnrnps: past, present and perspectives. Biochem J 2010; 430(3): 379-92. http://dx.doi.org/10.1042/BJ20100396

[76] David CJ, Chen M, Assanah M, Canoll P, Manley JL. Hnrnp proteins controlled by c-myc deregulate pyruvate kinase mrna splicing in cancer. Nature 2010; 463(7279): 364-8. http://dx.doi.org/10.1038/nature08697

[77] Carpenter B, MacKay C, Alnabulsi A, MacKay M, Telfer C, Melvin WT, *et al*. The roles of heterogeneous nuclear ribonucleoproteins in tumour development and progression. Biochim Biophys Acta 2006; 1765(2): 85-100.

[78] Takimoto M, Tomonaga T, Matunis M, Avigan M, Krutzsch H, Dreyfuss G, *et al*. Specific binding of heterogeneous ribonucleoprotein particle protein k to the human c-myc promoter, *in vitro*. J Biol Chem 1993; 268(24): 18249-58.

[79] Kim JH, Paek KY, Choi K, Kim T, Hahm B, Kim K, *et al*. Heterogeneous nuclear ribonucleoprotein c modulates translation of c-myc mrna in a cell cycle phase-dependent manner. Mol Cell Biol 2003; 23(2): 708-20. http://dx.doi.org/10.1128/MCB.23.2.708-720.2003

[80] Evans JR, Mitchell SA, Spriggs KA, Ostrowski J, Bomsztyk K, Ostarek D, *et al*. Members of the poly(rc) binding protein family stimulate the activity of the c-myc internal ribosome entry segment *in vitro* and *in vivo*. Oncogene 2003; 22(39): 8012-20. http://dx.doi.org/10.1038/sj.onc.1206645

[81] Jo OD, Martin J, Bernath A, Masri J, Lichtenstein A, Gera J. Heterogeneous nuclear ribonucleoprotein a1 regulates cyclin d1 and c-myc internal ribosome entry site function through akt signaling. J Biol Chem 2008; 283(34): 23274-87. http://dx.doi.org/10.1074/jbc.M801185200

[82] Cobbold LC, Wilson LA, Sawicka K, King HA, Kondrashov AV, Spriggs KA, *et al*. Upregulated c-myc expression in multiple myeloma by internal ribosome entry results from increased interactions with and expression of ptb-1 and yb-1. Oncogene 2010; 29(19): 2884-91. http://dx.doi.org/10.1038/onc.2010.31

[83] Ritchie SA, Pasha MK, Batten DJP, Sharma RK, Olson DJH, Ross ARS, *et al*. Identification of the src pyrimidine-binding protein(spy) as hnrnp k: implications in the regulation of src1a transcription. Nucleic Acids Res 2003; 31(5): 1502-13. http://dx.doi.org/10.1093/nar/gkg246

[84] Lukong KE, Larocque D, Tyner AL, Richard S. Tyrosine phosphorylation of sam68 by breast tumor kinase regulates intranuclear localization and cell cycle progression. J Biol Chem 2005; 280(46): 38639-47. http://dx.doi.org/10.1074/jbc.M505802200

[85] Pino I, Pío R, Toledo G, Zabalegui N, Vicent S, Rey N, *et al*. Altered patterns of expression of members of the heterogeneous nuclear ribonucleoprotein(hnrnp) family in lung cancer. Lung Cancer 2003; 41(2): 131-43. http://dx.doi.org/10.1016/S0169-5002(03)00193-4

[86] Ghigna C, Moroni M, Porta C, Riva S, Biamonti G. Altered expression of heterogenous nuclear ribonucleoproteins and sr factors in human colon adenocarcinomas. Cancer Res 1998; 58(24): 5818-24.

[87] Ushigome M, Ubagai T, Fukuda H, Tsuchiya N, Sugimura T, Takatsuka J, *et al*. Up-regulation of hnrnp a1 gene in sporadic human colorectal cancers. Int J Oncol 2005; 26(3): 635-40.

[88] Christofk HR, Vander Heiden MG, Harris MH, Ramanathan A, Gerszten RE, Wei R, *et al*. The m2 splice isoform of pyruvate kinase is important for cancer metabolism and tumour growth. Nature 2008; 452(7184): 230-3. http://dx.doi.org/10.1038/nature06734

[89] Clower CV, Chatterjee D, Wang Z, Cantley LC, Vander Heiden MG, Krainer AR. The alternative splicing repressors hnrnp a1/a2 and ptb influence pyruvate kinase isoform expression and cell metabolism. Proc Natl Acad Sci U S A 2010; 107(5): 1894-9. http://dx.doi.org/10.1073/pnas.0914845107

[90] Calvio C, Neubauer G, Mann M, Lamond AI. Identification of hnrnp p2 as tls/fus using electrospray mass spectrometry. RNA 1995; 1(7): 724-33.

Appendix

[91] Aurias A, Rimbaut C, Buffe D, Zucker JM, Mazabraud A. Translocation involving chromosome 22 in ewing's sarcoma. a cytogenetic study of four fresh tumors. Cancer Genet Cytogenet 1984; 12(1): 21-5. http://dx.doi.org/10.1016/0165-4608(84)90003-7

[92] Delattre O, Zucman J, Plougastel B, Desmaze C, Melot T, Peter M, *et al*. Gene fusion with an ets dna-binding domain caused by chromosome translocation in human tumours. Nature 1992; 359(6391): 162-5. http://dx.doi.org/10.1038/359162a0

[93] Riggi N, Cironi L, Suvà M, Stamenkovic I. Sarcomas: genetics, signalling, and cellular origins. part 1: the fellowship of tet. J Pathol 2007; 213(1): 4-20. http://dx.doi.org/10.1002/path.2209

[94] Sankar S, Lessnick SL. Promiscuous partnerships in ewing's sarcoma. Cancer Genet 2011; 204(7): 351-65. http://dx.doi.org/10.1016/j.cancergen.2011.07.008

[95] Paronetto MP. Ewing sarcoma protein: a key player in human cancer. Int J Cell Biol 2013; 2013: 642853.

[96] Li H, Watford W, Li C, Parmelee A, Bryant MA, Deng C, *et al*. Ewing sarcoma gene ews is essential for meiosis and b lymphocyte development. J Clin Invest 2007; 117(5): 1314-23. http://dx.doi.org/10.1172/JCI31222

[97] Hurov KE, Cotta-Ramusino C, Elledge SJ. A genetic screen identifies the triple t complex required for dna damage signaling and atm and atr stability. Genes Dev 2010; 24(17): 1939-50. http://dx.doi.org/10.1101/gad.1934210

[98] O'Connell BC, Adamson B, Lydeard JR, Sowa ME, Ciccia A, Bredemeyer AL, *et al*. A genome-wide camptothecin sensitivity screen identifies a mammalian mms22l-nfkbil2 complex required for genomic stability. Mol Cell 2010; 40(4): 645-57. http://dx.doi.org/10.1016/j.molcel.2010.10.022

[99] Paronetto MP, Miñana B, Valcárcel J. The ewing sarcoma protein regulates dna damage-induced alternative splicing. Mol Cell 2011; 43(3): 353-68. http://dx.doi.org/10.1016/j.molcel.2011.05.035

[100] Kishore S, Piscuoglio S, Kovac M, Gylling A, Wenzel F, Trapani F, Altermatt HJ, Mele V, Marra G, Peltomäki P, Terracciano L, Zavolan M, Heinimann K. 3'utr poly(t/u) tract deletions and altered expression of ewsr1 are a hallmark of mismatch repair deficient cancers. Cancer Res 2013. http://dx.doi.org/10.1158/0008-5472.CAN-13-2100

[101] Taylor SJ, Shalloway D. An rna-binding protein associated with src through its sh2 and sh3 domains in mitosis. Nature 1994; 368(6474): 867-71. http://dx.doi.org/10.1038/368867a0

[102] Fumagalli S, Totty NF, Hsuan JJ, Courtneidge SA. A target for src in mitosis. Nature 1994; 368(6474): 871-4. http://dx.doi.org/10.1038/368871a0

[103] Vernet C, Artzt K. Star, a gene family involved in signal transduction and activation of rna. Trends Genet 1997; 13(12): 479-84. http://dx.doi.org/10.1016/S0168-9525(97)01269-9

[104] Bielli P, Busà R, Paronetto MP, Sette C. The rna-binding protein sam68 is a multifunctional player in human cancer. Endocr Relat Cancer 2011; 18(4): R91-R102. http://dx.doi.org/10.1530/ERC-11-0041

[105] Richard S, Torabi N, Franco GV, Tremblay GA, Chen T, Vogel G, *et al*. Ablation of the sam68 rna binding protein protects mice from age-related bone loss. PLoS Genet 2005; 1(6): e74. http://dx.doi.org/10.1371/journal.pgen.0010074

[106] Richard S, Vogel G, Huot M, Guo T, Muller WJ, Lukong KE. Sam68 haploinsufficiency delays onset of mammary tumorigenesis and metastasis. Oncogene 2008; 27(4): 548-56. http://dx.doi.org/10.1038/sj.onc.1210652

[107] Valacca C, Bonomi S, Buratti E, Pedrotti S, Baralle FE, Sette C, *et al*. Sam68 regulates emt through alternative splicing-activated nonsense-mediated mrna decay of the sf2/asf proto-oncogene. J Cell Biol 2010; 191(1): 87-99. http://dx.doi.org/10.1083/jcb.201001073

[108] Paronetto MP, Achsel T, Massiello A, Chalfant CE, Sette C. The rna-binding protein sam68 modulates the alternative splicing of bcl-x. J Cell Biol 2007; 176(7): 929-39. http://dx.doi.org/10.1083/jcb.200701005

[109] Matter N, Herrlich P, König H. Signal-dependent regulation of splicing *via* phosphorylation of sam68. Nature 2002; 420(6916): 691-5. http://dx.doi.org/10.1038/nature01153

[110] Rajan P, Gaughan L, Dalgliesh C, El-Sherif A, Robson CN, Leung HY, *et al*. The rna-binding and adaptor protein sam68 modulates signal-dependent splicing and transcriptional activity of the androgen receptor. J Pathol 2008; 215(1): 67-77. http://dx.doi.org/10.1002/path.2324

[111] Busà R, Paronetto MP, Farini D, Pierantozzi E, Botti F, Angelini DF, *et al*. The rna-binding protein sam68 contributes to proliferation and survival of human prostate cancer cells. Oncogene 2007; 26(30): 4372-82. http://dx.doi.org/10.1038/sj.onc.1210224

[112] Zhang Z, Li J, Zheng H, Yu C, Chen J, Liu Z, *et al*. Expression and cytoplasmic localization of sam68 is a significant and independent prognostic marker for renal cell carcinoma. Cancer Epidemiol Biomarkers Prev 2009; 18(10): 2685-93. http://dx.doi.org/10.1158/1055-9965.EPI-09-0097

[113] Song L, Wang L, Li Y, Xiong H, Wu J, Li J, *et al*. Sam68 up-regulation correlates with, and its down-regulation inhibits, proliferation and tumourigenicity of breast cancer cells. J Pathol 2010; 222(3): 227-37. http://dx.doi.org/10.1002/path.2751

[114] Paronetto MP, Zalfa F, Botti F, Geremia R, Bagni C, Sette C. The nuclear rna-binding protein sam68 translocates to the cytoplasm and associates with the polysomes in mouse spermatocytes. Mol Biol Cell 2006; 17(1): 14-24. http://dx.doi.org/10.1091/mbc.E05-06-0548

[115] Grange J, Boyer V, Fabian-Fine R, Fredj NB, Sadoul R, Goldberg Y. Somatodendritic localization and mrna association of the splicing regulatory protein sam68 in the hippocampus and cortex. J Neurosci Res 2004; 75(5): 654-66. http://dx.doi.org/10.1002/jnr.20003

[116] Paronetto MP, Messina V, Bianchi E, Barchi M, Vogel G, Moretti C, *et al*. Sam68 regulates translation of target mrnas in male germ cells, necessary for mouse spermatogenesis. J Cell Biol 2009; 185(2): 235-49. http://dx.doi.org/10.1083/jcb.200811138

[117] Orian-Rousseau V. Cd44, a therapeutic target for metastasising tumours. Eur J Cancer 2010; 46(7): 1271-7. http://dx.doi.org/10.1016/j.ejca.2010.02.024

[118] Watts JK, Corey DR. Silencing disease genes in the laboratory and the clinic. J Pathol 2012; 226(2): 365-79. http://dx.doi.org/10.1002/path.2993

[119] Wang X. The expanding role of mitochondria in apoptosis. Genes Dev 2001; 15(22): 2922-33.

[120] Xerri L, Parc P, Brousset P, Schlaifer D, Hassoun J, Reed JC, *et al*. Predominant expression of the long isoform of bcl-x(bcl-xl) in human lymphomas. Br J Haematol 1996; 92(4): 900-6. http://dx.doi.org/10.1046/j.1365-2141.1996.423958.x

Appendix

[121] Takehara T, Liu X, Fujimoto J, Friedman SL, Takahashi H. Expression and role of bcl-xl in human hepatocellular carcinomas. Hepatology 2001; 34(1): 55-61. http://dx.doi.org/10.1053/jhep.2001.25387

[122] Olopade OI, Adeyanju MO, Safa AR, Hagos F, Mick R, Thompson CB, *et al.* Overexpression of bcl-x protein in primary breast cancer is associated with high tumor grade and nodal metastases. Cancer J Sci Am 1997; 3(4): 230-7.

[123] Zhu H, Guo W, Zhang L, Davis JJ, Teraishi F, Wu S, *et al.* Bcl-xl small interfering rna suppresses the proliferation of 5-fluorouracil-resistant human colon cancer cells. Mol Cancer Ther 2005; 4(3): 451-6.

[124] Mercatante DR, Bortner CD, Cidlowski JA, Kole R. Modification of alternative splicing of bcl-x pre-mrna in prostate and breast cancer cells. analysis of apoptosis and cell death. J Biol Chem 2001; 276(19): 16411-7. http://dx.doi.org/10.1074/jbc.M009256200

[125] Bauman JA, Li S, Yang A, Huang L, Kole R. Anti-tumor activity of splice-switching oligonucleotides. Nucleic Acids Res 2010; 38(22): 8348-56. http://dx.doi.org/10.1093/nar/gkq731

[126] Placzek WJ, Wei J, Kitada S, Zhai D, Reed JC, Pellecchia M. A survey of the anti-apoptotic bcl-2 subfamily expression in cancer types provides a platform to predict the efficacy of bcl-2 antagonists in cancer therapy. Cell Death Dis 2010; 1: e40.

[127] Akgul C. Mcl-1 is a potential therapeutic target in multiple types of cancer. Cell Mol Life Sci 2009; 66(8): 1326-36. http://dx.doi.org/10.1007/s00018-008-8637-6

[128] Ding Q, He X, Xia W, Hsu J, Chen C, Li L, *et al.* Myeloid cell leukemia-1 inversely correlates with glycogen synthase kinase-3beta activity and associates with poor prognosis in human breast cancer. Cancer Res 2007; 67(10): 4564-71. http://dx.doi.org/10.1158/0008-5472.CAN-06-1788

[129] Nguyen M, Marcellus RC, Roulston A, Watson M, Serfass L, Murthy Madiraju SR, *et al.* Small molecule obatoclax(gx15-070) antagonizes mcl-1 and overcomes mcl-1-mediated resistance to apoptosis. Proc Natl Acad Sci U S A 2007; 104(49): 19512-7. http://dx.doi.org/10.1073/pnas.0709443104

[130] Mitchell C, Yacoub A, Hossein H, Martin AP, Bareford MD, Eulitt P, *et al.* Inhibition of mcl-1 in breast cancer cells promotes cell death *in vitro* and *in vivo*. Cancer Biol Ther 2010; 10(9): 903-17. http://dx.doi.org/10.4161/cbt.10.9.13273

[131] Bae J, Leo CP, Hsu SY, Hsueh AJ. Mcl-1s, a splicing variant of the antiapoptotic bcl-2 family member mcl-1, encodes a proapoptotic protein possessing only the bh3 domain. J Biol Chem 2000; 275(33): 25255-61. http://dx.doi.org/10.1074/jbc.M909826199

[132] Llambi F, Green DR. Apoptosis and oncogenesis: give and take in the bcl-2 family. Curr Opin Genet Dev 2011; 21(1): 12-20. http://dx.doi.org/10.1016/j.gde.2010.12.001

[133] Shieh J, Liu K, Huang S, Chen Y, Hsieh T. Modification of alternative splicing of mcl-1 pre-mrna using antisense morpholino oligonucleotides induces apoptosis in basal cell carcinoma cells. J Invest Dermatol 2009; 129(10): 2497-506. http://dx.doi.org/10.1038/jid.2009.83

[134] Seol DW, Billiar TR. A caspase-9 variant missing the catalytic site is an endogenous inhibitor of apoptosis. J Biol Chem 1999; 274(4): 2072-6. http://dx.doi.org/10.1074/jbc.274.4.2072

[135] Goehe RW, Shultz JC, Murudkar C, Usanovic S, Lamour NF, Massey DH, *et al.* Hnrnp l regulates the tumorigenic capacity of lung cancer xenografts in mice *via* caspase-9 pre-mrna processing. J Clin Invest 2010; 120(11): 3923-39. http://dx.doi.org/10.1172/JCI43552

[136] Shultz JC, Goehe RW, Murudkar CS, Wijesinghe DS, Mayton EK, Massiello A, *et al.* Srsf1 regulates the alternative splicing of caspase 9 *via* a novel intronic splicing enhancer affecting the chemotherapeutic sensitivity of non-small cell lung cancer cells. Mol Cancer Res 2011; 9(7): 889-900. http://dx.doi.org/10.1158/1541-7786.MCR-11-0061

[137] Massiello A, Chalfant CE. Srp30a(asf/sf2) regulates the alternative splicing of caspase-9 pre-mrna and is required for ceramide-responsiveness. J Lipid Res 2006; 47(5): 892-7. http://dx.doi.org/10.1194/jlr.C600003-JLR200

[138] Hynes NE, MacDonald G. Erbb receptors and signaling pathways in cancer. Curr Opin Cell 2009; 21(2): 177-84. http://dx.doi.org/10.1016/j.ceb.2008.12.010

[139] Elenius K, Choi CJ, Paul S, Santiestevan E, Nishi E, Klagsbrun M. Characterization of a naturally occurring erbb4 isoform that does not bind or activate phosphatidyl inositol 3-kinase. Oncogene 1999; 18(16): 2607-15. http://dx.doi.org/10.1038/sj.onc.1202612

[140] Ferretti E, Di Marcotullio L, Gessi M, Mattei T, Greco A, Po A, *et al*. Alternative splicing of the erbb-4 cytoplasmic domain and its regulation by hedgehog signaling identify distinct medulloblastoma subsets. Oncogene 2006; 25(55): 7267-73. http://dx.doi.org/10.1038/sj.onc.1209716

[141] Paatero I, Lassus H, Junttila TT, Kaskinen M, Bützow R, Elenius K. Cyt-1 isoform of erbb4 is an independent prognostic factor in serous ovarian cancer and selectively promotes ovarian cancer cell growth *in vitro*. Gynecol Oncol 2013; 129(1): 179-87. http://dx.doi.org/10.1016/j.ygyno.2012.12.044

[142] Nielsen TO, Sorensen S, Dagnæs-Hansen F, Kjems J, Sorensen BS. Directing her4 mrna expression towards the cyt2 isoform by antisense oligonucleotide decreases growth of breast cancer cells *in vitro* and *in vivo*. Br J Cancer 2013; 108(11): 2291-8. http://dx.doi.org/10.1038/bjc.2013.247

[143] Wang Z, Jeon HY, Rigo F, Bennett CF, Krainer AR. Manipulation of pk-m mutually exclusive alternative splicing by antisense oligonucleotides. Open Biol 2012; 2(10): 120133. http://dx.doi.org/10.1098/rsob.120133

[144] Hua Y, Sahashi K, Hung G, Rigo F, Passini MA, Bennett CF, *et al.* Antisense correction of smn2 splicing in the cns rescues necrosis in a type iii sma mouse model. Genes Dev 2010; 24(15): 1634-44. http://dx.doi.org/10.1101/gad.1941310

[145] Goldberg MS, Sharp PA. Pyruvate kinase m2-specific sirna induces apoptosis and tumor regression. J Exp Med 2012; 209(2): 217-24. http://dx.doi.org/10.1084/jem.20111487

[146] Shafi AA, Yen AE, Weigel NL. Androgen receptors in hormone-dependent and castration-resistant prostate cancer. Pharmacol Ther 2013; 140(3): 223-38. http://dx.doi.org/10.1016/j.pharmthera.2013.07.003

[147] Kazansky AV, Spencer DM, Greenberg NM. Activation of signal transducer and activator of transcription 5 is required for progression of autochthonous prostate cancer: evidence from the transgenic adenocarcinoma of the mouse prostate system. Cancer Res 2003; 63(24): 8757-62.

[148] Shchelkunova A, Ermolinsky B, Boyle M, Mendez I, Lehker M, Martirosyan KS, *et al.* Tuning of alternative splicing--switch from proto-oncogene to tumor suppressor. Int J Biol Sci 2013; 9(1): 45-54. http://dx.doi.org/10.7150/ijbs.5194

[149] DiFeo A, Martignetti JA, Narla G. The role of klf6 and its splice variants in cancer therapy. Drug Resist Updat 2009; 12(1-2): 1-7. http://dx.doi.org/10.1016/j.drup.2008.11.001

Appendix

[150] Narla G, DiFeo A, Yao S, Banno A, Hod E, Reeves HL, *et al.* Targeted inhibition of the klf6 splice variant, klf6 sv1, suppresses prostate cancer cell growth and spread. Cancer Res 2005; 65(13): 5761-8. http://dx.doi.org/10.1158/0008-5472.CAN-05-0217

[151] Narla G, DiFeo A, Fernandez Y, Dhanasekaran S, Huang F, Sangodkar J, *et al*. Klf6-sv1 overexpression accelerates human and mouse prostate cancer progression and metastasis. J Clin Invest 2008; 118(8): 2711-21. http://dx.doi.org/10.1172/JCI34780

[152] Chen H, Chen L, Sun L, Zhen H, Li X, Zhang Q. A small interfering rna targeting the klf6 splice variant, klf6-sv1, as gene therapy for gastric cancer. Gastric Cancer. 2011; 14(4): 339-52.

[153] Rubtsova MP, Vasilkova DP, Malyavko AN, Naraikina YV, Zvereva MI, Dontsova OA. Telomere lengthening and other functions of telomerase. Acta Naturae 2012; 4(2): 44-61.

[154] Tian X, Chen B, Liu X. Telomere and telomerase as targets for cancer therapy. Appl Biochem Biotechnol 2010; 160(5): 1460-72.

[155] Yi X, White DM, Aisner DL, Baur JA, Wright WE, Shay JW. An alternate splicing variant of the human telomerase catalytic subunit inhibits telomerase activity. Neoplasia 2000; 2(5): 433-40. http://dx.doi.org/10.1038/sj.neo.7900113

[156] Isken O, Maquat LE. The multiple lives of nmd factors: balancing roles in gene and genome regulation. Nat Rev Genet 2008; 9(9): 699-712. http://dx.doi.org/10.1038/nrg2402

[157] Wong MS, Chen L, Foster C, Kainthla R, Shay JW, Wright WE. Regulation of telomerase alternative splicing: a target for chemotherapy. Cell Rep 2013; 3(4):1028-35.

[158] Thiery JP, Acloque H, Huang RYJ, Nieto MA. Epithelial-mesenchymal transitions in development and disease. Cell 2009; 139(5): 871-90.

[159] Polyak K, Weinberg RA. Transitions between epithelial and mesenchymal states: acquisition of malignant and stem cell traits. Nat Rev Cancer 2009; 9(4): 265-73. http://dx.doi.org/10.1038/nrc2620

[160] Yao H, Zhou Y, Zhang R, Wang M. Msp-ron signalling in cancer: pathogenesis and therapeutic potential. Nat Rev Cancer 2013; 13(7): 466-81. http://dx.doi.org/10.1038/nrc3545

[161] Lu Y, Yao HP, Wang MH. Multiple variants of the ron receptor tyrosine kinase: biochemical properties, tumorigenic activities, and potential drug targets. Cancer Lett 2007; 257(2): 157-64.

[162] Collesi C, Santoro MM, Gaudino G, Comoglio PM. A splicing variant of the ron transcript induces constitutive tyrosine kinase activity and an invasive phenotype. Mol Cell Biol 1996; 16(10): 5518-26.

[163] Zhou Y, He C, Chen Y, Wang D, Wang M. Altered expression of the ron receptor tyrosine kinase in primary human colorectal adenocarcinomas: generation of different splicing ron variants and their oncogenic potential. Oncogene 2003; 22(2): 186-97. http://dx.doi.org/10.1038/sj.onc.1206075

[164] Ghigna C, Giordano S, Shen H, Benvenuto F, Castiglioni F, Comoglio PM, *et al.* Cell motility is controlled by sf2/asf through alternative splicing of the ron protooncogene. Mol Cell 2005; 20(6): 881-90. http://dx.doi.org/10.1016/j.molcel.2005.10.026

[165] Owen N, Zhou H, Malygin AA, Sangha J, Smith LD, Muntoni F, *et al.* Design principles for bifunctional targeted oligonucleotide enhancers of splicing. Nucleic Acids Res 2011; 39(16): 7194-208. http://dx.doi.org/10.1093/nar/gkr152

[166] Monani UR. Spinal muscular atrophy: a deficiency in a ubiquitous protein; a motor neuron-specific disease. Neuron 2005; 48(6): 885-96. http://dx.doi.org/10.1016/j.neuron.2005.12.001

[167] Kinali M, Arechavala-Gomeza V, Feng L, Cirak S, Hunt D, Adkin C, *et al.* Local restoration of dystrophin expression with the morpholino oligomer avi-4658 in duchenne muscular dystrophy: a single-blind, placebo-controlled, dose-escalation, proof-of-concept study. Lancet Neurol 2009; 8(10): 918-28. http://dx.doi.org/10.1016/S1474-4422(09)70211-X

[168] Bonomi S, Gallo S, Catillo M, Pignataro D, Biamonti G, Ghigna C. Oncogenic alternative splicing switches: role in cancer progression and prospects for therapy. Int J Cell Biol 2013; 2013: 962038. http://dx.doi.org/10.1038/nrd3823

[169] Bonnal S, Vigevani L, Valcárcel J. The spliceosome as a target of novel antitumour drugs. Nat Rev Drug Discov 2012; 11(11): 847-59.

[170] Webb TR, Joyner AS, Potter PM. The development and application of small molecule modulators of sf3b as therapeutic agents for cancer. Drug Discov Today 2013; 18(1-2): 43-9. http://dx.doi.org/10.1016/j.drudis.2012.07.013

[171] Nakajima H, Hori Y, Terano H, Okuhara M, Manda T, Matsumoto S, *et al*. New antitumor substances, fr901463, fr901464 and fr901465. ii. activities against experimental tumors in mice and mechanism of action. J Antibiot (Tokyo) 1996; 49(12): 1204-11. http://dx.doi.org/10.7164/antibiotics.49.1204

[172] Kaida D, Motoyoshi H, Tashiro E, Nojima T, Hagiwara M, Ishigami K, *et al*. Spliceostatin a targets sf3b and inhibits both splicing and nuclear retention of pre-mrna. Nat Chem Biol 2007; 3(9): 576-83. http://dx.doi.org/10.1038/nchembio.2007.18

[173] Corrionero A, Miñana B, Valcárcel J. Reduced fidelity of branch point recognition and alternative splicing induced by the anti-tumor drug spliceostatin a. Genes Dev 2011; 25(5): 445-59. http://dx.doi.org/10.1101/gad.2014311

[174] Kaida D, Schneider-Poetsch T, Yoshida M. Splicing in oncogenesis and tumor suppression. Cancer Sci 2012; 103(9): 1611-6. http://dx.doi.org/10.1111/j.1349-7006.2012.02356.x

[175] Fan L, Lagisetti C, Edwards CC, Webb TR, Potter PM. Sudemycins, novel small molecule analogues of fr901464, induce alternative gene splicing. ACS Chem Biol 2011; 6(6): 582-9. http://dx.doi.org/10.1021/cb100356k

[176] Eskens FALM, Ramos FJ, Burger H, O'Brien JP, Piera A, de Jonge MJA, *et al.* Phase i, pharmacokinetic and pharmacodynamic study of the first-in-class spliceosome inhibitor e7107 in patients with advanced solid tumors. Clin Cancer Res 2013; 19(22): 6296-304. http://dx.doi.org/10.1158/1078-0432.CCR-13-0485

[177] Moore MJ, Wang Q, Kennedy CJ, Silver PA. An alternative splicing network links cell-cycle control to apoptosis. Cell 2010; 142(4): 625-36. http://dx.doi.org/10.1016/j.cell.2010.07.019

[178] Gao Y, Koide K. Chemical perturbation of mcl-1 pre-mrna splicing to induce apoptosis in cancer cells. ACS Chem Biol 2013; 8(5): 895-900. http://dx.doi.org/10.1021/cb300602j

[179] Chang J, Yang D, Chang W, Chow L, Chan W, Lin H, *et al.* Small molecule amiloride modulates oncogenic rna alternative splicing to devitalize human cancer cells. PLoS One 2011; 6(6): e18643. http://dx.doi.org/10.1371/journal.pone.0018643

[180] Tang J, Chang H, Chang J. Modulating roles of amiloride in irradiation-induced antiproliferative effects in glioblastoma multiforme cells involving akt phosphorylation and the

Appendix

alternative splicing of apoptotic genes. DNA Cell Biol 2013; 32(9): 504-10.
http://dx.doi.org/10.1089/dna.2013.1998

[181] Chang W, Liu T, Yang W, Lee C, Lin Y, Chen T, *et al.* Amiloride modulates alternative splicing in leukemic cells and resensitizes bcr-ablt315i mutant cells to imatinib. Cancer Res 2011; 71(2): 383-92.
http://dx.doi.org/10.1158/0008-5472.CAN-10-1037

[182] Cáceres JF, Misteli T, Screaton GR, Spector DL, Krainer AR. Role of the modular domains of sr proteins in subnuclear localization and alternative splicing specificity. J Cell Biol 1997; 138(2): 225-38.
http://dx.doi.org/10.1083/jcb.138.2.225

[183] Pilch B, Allemand E, Facompré M, Bailly C, Riou JF, Soret J, *et al.* Specific inhibition of serine- and arginine-rich splicing factors phosphorylation, spliceosome assembly, and splicing by the antitumor drug nb-506. Cancer Res 2001; 61(18): 6876-84.

[184] Saif MW, Sellers S, Diasio RB, Douillard J. A phase i dose-escalation study of edotecarin(j-107088) combined with infusional 5-fluorouracil and leucovorin in patients with advanced/metastatic solid tumors. Anticancer Drugs 2010; 21(7): 716-23.

[185] Saif MW, Diasio RB. Edotecarin: a novel topoisomerase i inhibitor. Clin Colorectal Cancer 2005; 5(1): 27-36.
http://dx.doi.org/10.3816/CCC.2005.n.014

[186] Hurwitz HI, Cohen RB, McGovren JP, Hirawat S, Petros WP, Natsumeda Y, *et al.* A phase i study of the safety and pharmacokinetics of edotecarin(j-107088), a novel topoisomerase i inhibitor, in patients with advanced solid tumors. Cancer Chemother Pharmacol 2007; 59(1): 139-47.
http://dx.doi.org/10.1007/s00280-006-0267-9

[187] Muraki M, Ohkawara B, Hosoya T, Onogi H, Koizumi J, Koizumi T, *et al.* Manipulation of alternative splicing by a newly developed inhibitor of clks. J Biol Chem 2004; 279(23): 24246-54.
http://dx.doi.org/10.1074/jbc.M314298200

[188] Allende-Vega N, Dayal S, Agarwala U, Sparks A, Bourdon J, Saville MK. P53 is activated in response to disruption of the pre-mrna splicing machinery. Oncogene 2013; 32(1): 1-14.
http://dx.doi.org/10.1038/onc.2012.38

[189] Tazi J, Durand S, Jeanteur P. The spliceosome: a novel multi-faceted target for therapy. Trends Biochem Sci 2005; 30(8): 469-78.
http://dx.doi.org/10.1016/j.tibs.2005.06.002

[190] Soret J, Bakkour N, Maire S, Durand S, Zekri L, Gabut M, *et al.* Selective modification of alternative splicing by indole derivatives that target serine-arginine-rich protein splicing factors. Proc Natl Acad Sci U S A 2005; 102(24): 8764-9.
http://dx.doi.org/10.1073/pnas.0409829102

[191] Ghigna C, De Toledo M, Bonomi S, Valacca C, Gallo S, Apicella M, *et al.* Pro-metastatic splicing of ron proto-oncogene mrna can be reversed: therapeutic potential of bifunctional oligonucleotides and indole derivatives. RNA Biol 2010; 7(4): 495-503.
http://dx.doi.org/10.4161/rna.7.4.12744

[192] Potente M, Gerhardt H, Carmeliet P. Basic and therapeutic aspects of angiogenesis. Cell 2011; 146(6): 873-87.
http://dx.doi.org/10.1016/j.cell.2011.08.039

[193] Nowak DG, Woolard J, Amin EM, Konopatskaya O, Saleem MA, Churchill AJ, *et al.* Expression of pro- and anti-angiogenic isoforms of vegf is differentially regulated by splicing and growth factors. J Cell Sci 2008; 121(Pt 20): 3487-95.
http://dx.doi.org/10.1242/jcs.016410

[194] Nowak DG, Amin EM, Rennel ES, Hoareau-Aveilla C, Gammons M, Damodoran G, *et al.* Regulation of vascular endothelial growth factor(vegf) splicing from pro-angiogenic to anti-angiogenic isoforms: a novel therapeutic strategy for angiogenesis. J Biol Chem 2010; 285(8): 5532-40.
http://dx.doi.org/10.1074/jbc.M109.074930

[195] Sahashi K, Ling KKY, Hua Y, Wilkinson JE, Nomakuchi T, Rigo F, *et al.* Pathological impact of smn2 mis-splicing in adult sma mice. EMBO Mol Med 2013; 5(10): 1586-601.
http://dx.doi.org/10.1002/emmm.201302567

[196] Sahashi K, Hua Y, Ling KKY, Hung G, Rigo F, Horev G, *et al.* Tsunami: an antisense method to phenocopy splicing-associated diseases in animals. Genes Dev 2012; 26(16): 1874-84.
http://dx.doi.org/10.1101/gad.197418.112

[197] Hua Y, Sahashi K, Rigo F, Hung G, Horev G, Bennett CF, *et al.* Peripheral smn restoration is essential for long-term rescue of a severe spinal muscular atrophy mouse model. Nature 2011; 478(7367): 123-6.
http://dx.doi.org/10.1038/nature10485

Received on 27-11-2013 Accepted on 10-12-2013 Published on 25-03-2014

DOI: http://dx.doi.org/10.14205/2311-0309.2014.02.01.1

Acknowledgments

I am grateful to the University of Pavia and to the CNR Institute for enabling me to carry out the work object of this PhD thesis.

Firstly, I would like to express my sincere gratitude to my advisor Dr. Claudia Ghigna for the continuous support of my Ph.D study and related research, for her patience, motivation, and immense knowledge. I would like to thank Prof. Torroni as mentor of my PhD studies.

Besides my advisors, I would like to thank all the rest of my thesis committee, first of all Prof. Buratti and Prof. Paronetto, for their insightful suggestions and comments on this thesis.

My sincere thanks also goes to Dr. Landthaler, who provided me an opportunity to join his team of talented scientists, even if for a short period, and to Dr. Dejana, Dr. De Florian and Dr. Giampietro who gave me access to their laboratories and research facilities and whose collaboration has been essential for my studies and researches.

I thank my fellow lab-mates for the stimulating discussions, for all the advice on both research as well as on my career and for encouraging me throughout this experience.

I recognize that this research would not have been possible without the financial assistance of AIRC and AICR grants and I express my gratitude to those agencies.